Year 2013

UNIVERSITY OF CERGY-PONTOISE/UNIVERSITY OF YEUNGNAM

THESIS

For the degrees of

DOCTEUR DE L'UNIVERSITÉ DE CERGY-PONTOISE

Ecole doctorale n° 417: Sciences et Ingénierie
Spécialité: Génie Électrique et Électronique

and

DOCTOR OF YEUNGNAM UNIVERSITY

Graduate School of Yeungnam University
Department of Electrical Engineering
Major: Energy and Electromagnetic Environment

Presented and defended by

Herie PARK

May 15th 2013

Dynamic Thermal Modeling
of Electrical Appliances for Energy Management
# of Low Energy Buildings

Board of Jury

Previewers	:	Professor Gilles FRAISSE	Savoie University
		Professor Sang-Tae CHOI	Gyeongju University
Examiners	:	Professor Benoît ROBYNS	HEI de Lille
		Professor Corinne ALONSO	Toulouse University
		Doctor Marie RUELLAN	Cergy-Pontoise University
		Professor Rachid BENNACER	ENS Cachan
Co-Supervisors	:	Professor Eric MONMASSON	Cergy-Pontoise University
		Professor Kwang-Sik LEE	Yeungnam University
Invited Member	:	Professor Hee-Young LEE	Yeungnam University

This thesis is dedicated to my parents Insoo Park and Jung-Young Park for their endless love and unlimited support throughout my life.

ACKNOWLEDGEMENTS

ABSTRACT

This work proposes a dynamic thermal model of electrical appliances within low energy buildings. It aims to evaluate the influence of thermal gains of these appliances on the buildings and persuades the necessity of dynamic thermal modeling of electrical appliances for the energy management of low energy buildings and the thermal comfort of inhabitants.

Since electrical appliances are one of the internal heat sources of a building, the building which thermally interacts with the appliances has to be modeled. Accordingly, a test room which represents a small scale laboratory set-up of a low energy building is first modeled based on the first thermodynamics principle and the thermal-electrical analogy. Then, in order to establish the thermal modeling of electrical appliances, the appliances are classified into four categories from thermal and electrical points of view. After that, a generic physically driven thermal model of the appliances is derived. It is established based also on the first thermodynamics principle. Along with this modeling, the used experimental protocol and the used identification procedure are presented to estimate the thermal parameters of the appliances. In order to analyze the relevance of the proposed generic model applied to practical cases, several electrical appliances which are widely used in residential buildings, namely a monitor, a computer, a refrigerator, a portable electric convection heater, and a microwave are chosen to study and validate the proposed generic model and the measurement and identification protocols. Finally, the proposed dynamic thermal model of electrical appliances is integrated into a residential building model which was developed and validated by the French Technical Research Center for Buildings (Centre Scientifique et Technique du Bâtiment: CSTB) on a real building. This coupled model of the appliances and the building is implemented in a building energy simulation tool SIMBAD, which is a specific toolbox of Matlab/Simulink®. Through the simulation, thermal behavior and heating energy use of the building are observed during a winter period. In addition, thermal discomfort owing to usages of electrical appliances during a summer period is also studied and quantified.

This work therefore provides the quantitative results of thermal effect of differently characterized electrical appliances within a low energy building and leads to observe their thermal dynamics and interactions. Consequently, it permits the energy management of low energy buildings and the thermal comfort of inhabitants in accordance with the usages of electrical appliances.

Keywords: Low energy building, Internal heat gains, Thermal model of electrical appliances, Thermal-electrical analogy, Thermal network, Linear parametric model, Building energy simulation tool, Building energy management, Thermal comfort.

RÉSUMÉ

Ce travail propose un modèle thermique dynamique des appareils électriques dans les bâtiments basse consommation. L'objectif de ce travail est d'étudier l'influence des gains thermiques de ces appareils sur le bâtiment. Cette étude insiste sur la nécessité d'établir un modèle thermique dynamique des appareils électriques pour une meilleure gestion de l'énergie du bâtiment et le confort thermique de ses habitants.

Comme il existe des interactions thermiques entre le bâtiment et les appareils électriques, sources de chaleur internes au bâtiment, il est nécessaire de modéliser le bâtiment. Le bâtiment basse consommation est modélisé dans un premier temps par un modèle simple reposant sur l'étude d'une pièce quasi-adiabatique. Ensuite, dans le but d'établir le modèle des appareils électriques, ceux-ci sont classés en quatre catégories selon leurs propriétés thermiques et électriques. A partir de cette classification et du premier principe de la thermodynamique, un modèle physique générique est établi. Le protocole expérimental et la procédure d'identification des paramètres thermiques des appareils sont ensuite présentés. Afin d'analyser la pertinence du modèle générique appliqué à des cas pratiques, plusieurs appareils électriques utilisés fréquemment dans les résidences – un écran, un ordinateur, un réfrigérateur, un radiateur électrique à convection et un micro-onde – sont choisis pour étudier et valider ce modèle ainsi que les protocoles d'expérimentation et d'identification. Enfin, le modèle proposé est intégré dans le modèle d'un bâtiment résidentiel développé et validé par le Centre Scientifique et Technique du Bâtiment (CSTB). Ce modèle couplé des appareils et du bâtiment est implémenté dans SIMBAD, un outil de simulation du bâtiment. A travers cette simulation, le comportement thermique du bâtiment et la quantité d'énergie nécessaire à son chauffage sur une période hivernale, ainsi que l'inconfort thermique dû aux appareils électriques durant l'été, sont observés.

Ce travail fournit des résultats quantitatifs de l'effet thermique de différents appareils électriques caractérisés dans un bâtiment basse consommation et permet d'observer leur dynamique thermique et leurs interactions. Finalement, cette étude apporte une contribution aux études de gestion de l'énergie des bâtiments à basse consommation énergétique et du confort thermique des habitants.

Mots-clés: Bâtiment basse consommation, apport énergétique interne, modèle thermique des appareils électriques, analogie thermique-électrique, modèle paramétrique linéaire, outil de simulation du bâtiment, gestion énergétique du bâtiment, confort thermique.

요 약

　　본 논문에서는 친환경 저에너지 건축물에서의 가전제품의 동적 열모델을 제안한다. 연구 목적은 가전제품을 통한 열획득이 건축물에 미치는 영향을 구명(究明)하고, 가전제품의 동적 열모델링이 친환경 저에너지 건축물의 에너지 최적 관리와 사용자의 열쾌적성 확보를 위하여 필수적인 요소임을 증명하기 위함이다.

　　본 연구는 먼저 열역학 제 1 법칙 및 열전기유사성으로부터 가전제품과 열적 상호작용을 맺고 있는 친환경 저에너지 건축물 실험실을 모델링하는 것으로부터 시작한다. 다음으로, 가전제품을 열적 · 전기적인 네 가지 유형으로 분류한 후, 각각의 경우에 상응하는 가전제품의 동적 열모델을 구성한다. 그 모델의 매개변수를 추정하기 위한 방법으로 선형 파라메트릭 모델을 응용한다. 제시한 방법을 가정 내에서 널리 사용하고 있는 가전제품인 모니터, 컴퓨터, 냉장고, 간이 전기히터, 전자레인지의 동적 열모델링에 실제적으로 적용하고, 각각의 모델을 실험과 시뮬레이션을 통하여 검증한다. 나아가, 제안한 가전제품의 동적 열모델을 프랑스 건축물기술연구센터 (Centre Scientifique et Technique du Bâtiment: CSTB)가 개발하고 검증한 실제 가정용 건축물 모델에 통합시킨 후, 건축물 에너지 시뮬레이션 도구인 SIMBAD 를 활용하여 가전제품의 사용에 따른 동 · 하절기 건축물의 열적 거동과 난방에너지 소비량 및 주거자의 열쾌적성을 평가하고 수치화한다.

　　본 연구를 통하여 가전제품이 친환경 저에너지 건축물에 미치는 열적 효과에 관한 수치화된 결과가 과학적으로 검증되며, 가전제품과 건축물 간의 열역학 관계 및 상호작용이 이론적으로 밝혀진다. 연구 결과는 가전제품의 사용에 따른 건축물의 에너지 최적 관리와 주거자의 열쾌적성 관리를 위한 심화 자료로 활용될 것으로 기대된다.

핵심어: 친환경 저에너지 건축물, 건축물 내부 획득열, 가전제품의 열적 모델, 열전기유사성, 선형 파라메트릭 모델, 건축물 에너지 시뮬레이션 프로그램, 건축물의 에너지 최적 관리, 열쾌적성.

Table of Contents

LIST OF FIGURES

LIST OF TABLES

NOTATIONS

*	Measured value
a_i, b_i, c_i, d_i, f_i	i^{th} constant coefficients of the corresponding polynomials
$A(q), B(q), C(q), D(q), F(q)$	Predefined polynomials of a parametric model
$A_{leakage}$	Effective air leakage area
$A_{sun,n}$	Equivalent n^{th} effective surface capturing the solar irradiation
$c_{p,air}$	Specific heat of air
$c_{p,i}$	Specific heat of ith wall
$c_{p,water}$	Specific heat of water
C_{ap}	Thermal capacitance of an electrical appliance
C_e	Thermal capacitances of external mass of a building
C_i	Thermal capacitances of internal mass of a building
C_i	Thermal capacitance of ith wall
C_{i_w}	Sum of the thermal capacitance of internal air mass and the half of the thermal capacitance of the wall
C_{i_wi}	Thermal capacitance of internal air mass of a building
C_{stack}	Stack coefficient
C_{th}	Global thermal capacitance of a test room
C_w	Thermal capacitance of a wall
C_{w_e}	Sum of the thermal capacitances of the half of the wall and the external air mass of a building
C_{wi_e}	Sum of the thermal capacitances of the wall and the external air mass of a building
C_{wind}	Wind coefficient
$D_{appliance}$	Duration while the electrical appliances are used
$D_{discomfort}$	Duration while the indoor temperature exceeds 26 °C
D_{flow}	Flow rate of the mass which goes inside/outside an electrical appliance
e_i	Thickness of ith wall
$E_{1,heater}$	Energy use of the heater in the living room
$E_{2,appliance}$	Energy use of the selected electrical appliances in the living room
$E_{2,heater}$	Energy use of the heater in the living room
E_{elec}	Electrical energy

h_{ap}	Thermal convective coefficient of air near an electrical appliance
h_e	External convective heat transfer coefficient
h_i	Internal convective heat transfer coefficient
H_t	Total transmission coefficient of a building
I_{sun}	Solar irradiation
J_N	Loss function
κ	Ratio of contact surface area to surface area of an electrical appliance
l_{ap}	Thickness of an electrical appliance material
n_a, n_b, n_c, n_d, n_f	order of the corresponding polynomials
N_{change}	Number of air change per hour
$P_{appliance,l}$	Power dissipated by the lth electrical appliance
P_{elec}	Supplied power into an electrical appliance
P_{lamp}	Heat flux due to lamps
P_{mech}	Mechanical power
$\dot{Q}_{ap}$	Heat flux of an electrical appliance
$\dot{Q}_{ap\_cond}$	Conductive heat flux
$\dot{Q}_{ap\_conv}$	Convective heat flux
$\dot{Q}_{ap\_open}$	Mass flux of an electrical appliance
$\dot{Q}_{ap\_rad}$	Radiative heat flux
$\dot{Q}_{appliance}$	Internal heat gain by heat dissipation of electrical appliances
$\dot{Q}_{envelope}$	Heat loss through a test room's envelopes
$\dot{Q}_{heat}$	Heat flux across the boundary of an electrical appliance
$\dot{Q}_{heating}$	Heat gain contributed by electricity and fuels for heating a building
$\dot{Q}_{hotwater}$	Heat loss by hot water consumption
$\dot{Q}_{in}$	Heat gain of a building
$\dot{Q}_{infiltration}$	Heat loss by infiltration
$\dot{Q}_{metabolism}$	Free internal heat gain of metabolism of occupants
$\dot{Q}_{open}$	Mass flux across the boundary of an electrical appliance
$\dot{Q}_{out}$	Heat loss of a building
$\dot{Q}_{recovery}$	Recovered heat flux
$\dot{Q}_{sun}$	Free internal heat gain of solar energy
$\dot{Q}_{transmission}$	Transmission heat loss through building envelopes

$\dot{Q}_{ventilation}$	Heat loss by ventilation
Q_{ap}	Quantity of heat of an electrical appliance
R_{ap}	Global thermal resistance of an electrical appliance
R_{ap_cond}	Thermal conductive resistance of an electrical appliance
R_{ap_conv}	Thermal convective resistance of an electrical appliance
R_{ap_open}	Equivalent resistance of mass flux
R_{ap_rad}	Thermal radiative resistance of an electrical appliance
R_e	Convective resistances of an external wall
R_i	Convective resistances of an internal wall
R_{i_w}	Sum of the convective resistance of the internal wall and the half of the conductive resistance of a wall
R_{i_wi}	Convective resistance of an internal wall
R_t	total thermal resistance
R_{th}	Global thermal resistance of a room
R_{w_e}	Sum of the half of the conductive resistance of the wall and the convective resistance of the external wall
R_{wi_e}	Sum of the conductive resistance of the wall and the convective resistance of the external wall
sim	Simulated value
$sim1$	Simulated value by *ARX* model
$sim2$	Simulated value by *ARMAX* model
S	Sum of the squared difference
S_{ap}	Frontier surface area of an electrical appliance material
S_{flow}	Surface area of the pipe where the mass goes inside/outside an electrical appliance
S_{panel}	Surface of a solar panel
t	Time
T_e	Outdoor air temperature
T_{e_mass}	Temperature of external mass of a building
T_i	Indoor temperature
T_{in}	Indoor temperature of a building
T_{out}	Outdoor temperature of a building
T_S	Sampling period
T_w	Wall temperature
T_{we}	Outdoor wall temperature

T_{wi}	Indoor wall temperature
U_{ap}	Energy of an electrical appliance
U_{in}	Energy entering into a building
U_{out}	Energy going out a envelope
U_{stored}	Energy stored in a building
v_{flow}	Velocity of the mass which goes inside/outside an electrical appliance
v_{wind}	Local wind speed
$\dot{V}_{escape}$	Escaped water flow rate through pipes
$\dot{V}_{infiltration}$	Air flow rate due to an infiltration through unsealed surfaces and thermal bridges
$\dot{V}_{ventilation}$	Air flow rate through a ventilation equipment
V_{room}	Volume of a test room
V_{tank}	Storage volume of a tank
V_{zone}	Volume of a building zone
W_{ap}	Work of an appliance
X	Vector of unknown parameters
X_L	Lower bound of unknown parameters
X_U	Upper bound of unknown parameters
$y_{generated}$	Generated data y
$y_{measured}$	Measured data y
$y_{predicted}$	Predicted data y
η	Efficiency of mechanical part of an electrical appliance
$\eta_{recovery}$	Re-circulated air rate
θ	Parameter vector
θ_N	Optimal set of parameters
λ_{ap}	Thermal conductivity of an electrical appliance material
λ_i	i^{th} wall layer thermal conductance
ξ	Ratio between the temperature of external mass and the exterior temperature of a building
ρ_{air}	Air density
ρ_i	Density of ith wall
ρ_{water}	Water density
τ_{ap}	Global time constant of an electrical appliance
τ_{th}	Global time constant of a room

$\Phi_{ap,Active}$ — Heat fluxes while the electrical appliance is activated

$\Phi_{ap,Inactive}$ — Heat fluxes while the electrical appliance is inactivated

$\Phi_{metabolism,k}$ — Mean of metabolic rate of the kth occupant

ABBREVIATIONS

APE	Absolute Percentage Error
ARMAX	Auto-Regressive Moving Average with eXogenous input
ARX	Regressive with eXogenous input
ASHRAE	American Society of Heating, Refrigerating and Air-Conditioning Engineers
BBC	Bâtiment de Basse Consommation (Fr), Low Energy Building (Eng)
BEMS	Building Energy Management Systems
BJ	Box-Jenkins
BLAST	Building Loads Analysis and System Thermodynamics
CEN	Committee European de Normalization
CFD	Computational Fluid Dynamics
CHP	Combined Heat and Power
CHS	Closed-Heating System
CHTC	Convective Heat Transfer Coefficients
CS	Closed system
CSTB	Centre Scientifique et Technique du Bâtiment (Fr), French Technical Research Center for Building (Eng)
CTF	Conduction Transfer Function
CWS	Closed-Working System
DD	Degree-Day
DHW	Domestic Hot Water
DOE	Department of Energy
ECBCS	Energy Conservation in Buildings and Community Systems
EMF	Electromotive Force
EPBD	Energy Performance of Buildings Directive
ESP-r	Environmental System Performance
ESRU	Energy Systems Research Unit
EU	European Union
GHG	Greenhouse Gas
HS	Heating System
HVAC	Heating, Ventilation, Air Conditioning
IAQ	Indoor Air Quality

IEA	International Energy Agency
IS	Isolated System
ISO	International Standardization Organization
KERI	Korea Electrotechnology Researching Institute
LBNL	Lawrence Berkley National Laboratory
MAE	Mean of the sum of Absolute Error
MAPE	Mean Absolute Percentage Error
MDD	Modified Degree-Day
MISO	Multi-Input Single-Output
NNARX	Neural Network Auto-Regressive, with eXogenous Input
NZR SEM 16	NZR Standby-Energy-Monitor 16
OE	Output Error
OHS	Open-Heating System
OS	Open system
OWS	Open-Working System
pbARMAX	physics-based *ARMAX*
PEM	Prediction Error Methods
PLEAIDE	Passive Low Energy Innovative Architectural Design
RF	Response Factor
SEL	Solar Energy Laboratory
SHC	Solar Heating and Cooling
SIMBAD	SIMulator of Building And Devices
SPARK	Simulation Problem Analysis and Research Kernel
SSE	Sum of Squared Errors
TDR	Thermal Discomfort Rate
TRNSYS	TRaNsient SYStems simulation
VBDD	Variable Base Degree-Day
WS	Working System

Chapter 1

INTRODUCTION

1.1 BACKGROUND

As improving the quality of human life, energy consumption has continuously increased. It brings out global concerns about climate change and resource depletion over the past few decades. The Commission of European Communities states that energy consumption accounts for 80 % of all greenhouse gas (GHG) emission in the European Union (EU) and that their CO_2 emission will annually increase by 5 % until 2030. Moreover, the energy import dependence of EU will be up to 50-65 % of total EU energy consumption in 2030 [1]. It may lead not only environmental problems but also economical and political problems. Since these problems are concerning all the countries, common efforts and differentiated responsibilities of the entire world are needed.

The primary energy[1] is used in four sectors: Buildings, Industry, Transport, and Others. The building sector accounts for 30-40 % of the primary energy consumption in the most countries [2]. If the energy consumption at the level of building constructions is also considered, the proportion of the building energy consumption will grow up to 50 % because manufacturing and transporting materials also demand energy consumption [3]. It shows that the building sector becomes the largest consumer of energy and that the buildings produce a large quantity of CO_2. Hence, it is important to raise energy efficiency of buildings to solve the above-mentioned problems.

---

[1] "Primary energy should be used to designate those sources that only involve extraction or capture, with or without separation from contiguous material, cleaning or grading, before the energy embodied in that source can be converted into heat or mechanical work. And secondary energy should be used to designate all sources of energy that results from transformation of primary sources", UN, Concepts and Methods in Energy Statistics, New York, 1982.
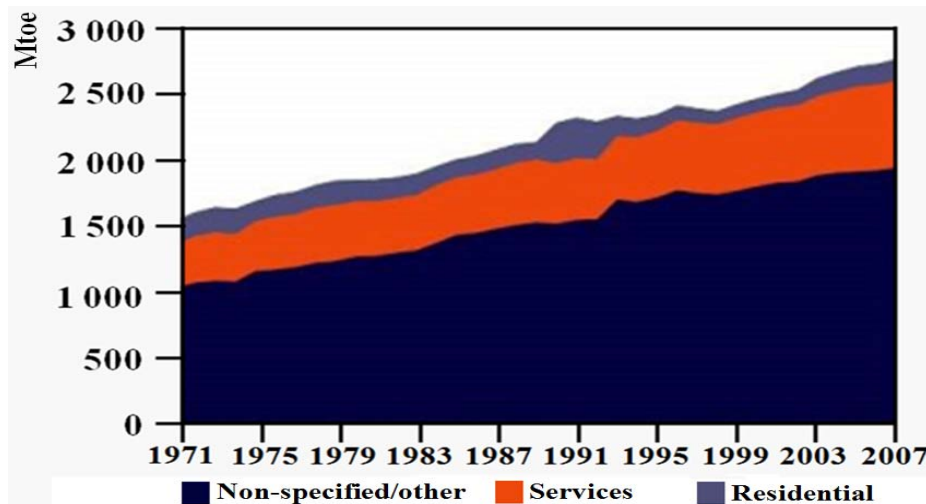
Figure 1. 1 Energy consumption of buildings [4]

Figure 1. 1 illustrates energy consumption of buildings. Between 1971 and 2007, total energy consumption in the building sector grew up by 1.6 % per year from 1535 to 2759 Mtoe[2] [4]. As following the trend, the quantity of energy consumption in buildings will continuously increase.

In order to reduce the environmental impact of buildings and realize high energy efficiency of buildings, many countries strengthen their building regulations and codes [5]. Especially, EU has launched the Energy Performance of Buildings Directive (EPBD) to lead all EU State Members to tighten their building energy regulations and to introduce energy certification schemes [6,7]. In addition, global scale standards by ISO[3] and CEN[4], assessment tools and certifications for sustainable building, such as BREEAM [8], LEED [9], CASBEE [10], Passivhaus [11], Minérgie [12], Effinérgie [13], etc. have been being developed [14,15].

A building achieving high energy efficiency using local carbonless-renewable energy is called 'Low energy building'. The similar terms are 'Green energy building', 'Eco-building', 'Zero-energy building', 'Energy-positive building', 'Autonomous building', 'Zero-carbon building', 'Passive house', '3-Litre house', etc [16]. Even though they have different names emphasizing their energy demand levels, their CO_2 emission levels or their technical application problems, the goal is the same as reducing their environmental impacts.

In the field of buildings, the energy is used for space heating/cooling, lighting, equipments/appliances operating, and water heating. The energy demands for heating and cooling system is more than a third of the energy used in both residential and non-residential (or commercial) buildings [17]. However, these demands decrease in low energy buildings of which thermal insulation/inertia levels are high. The well-insulation leads to reduce unwanted heat loss in the winter and to prevent overheating in the summer. Besides, the high thermal inertia plays a role of heat storage in order to level out the indoor temperature variations and

---

[2] Mtoe: Million Tonnes of Oil Equivalent
[3] ISO: International Standardization Organization
[4] CEN: Committee European de Normalisation

helps to improve indoor thermal comfort and to reduce heating and cooling cost of the building [18].

Under these conditions, a quantity of the heat exchange between inside and outside the building becomes reduced. Moreover, the internal heat gains which are obtained by solar irradiation, metabolism, and electrical appliances remain longer in low energy buildings than in conventional buildings. It means that the free auxiliary heat gain can be considered as one another effective heat source in low energy buildings, further in energy-positive buildings. Thus, the free heat gains influence the indoor temperature, the thermal comfort of occupants, and consequently the global energy management of buildings [19].

To achieve high energy efficiency of buildings, building energy simulation tools have been also developed during the past few decades [20]. According to the directory of U.S. Department of energy (DOE), there are more than 400 building software tools. They are based on fundamental laws of energy, heat, and mass transfer and mainly used for predicting energy performance of buildings, improving energy efficiency of building systems, load calculations, and retrofit analysis [21].

In order to evaluate and improve these building energy simulation tools, several investigations have also been undertaken [22,23,24,25]. Especially, the International Energy Agency (IEA) has sponsored several research programs, such as Solar Heating and Cooling (SHC) and Energy Conservation in Buildings and Community Systems (ECBCS). In these programs, there are some tasks which are related to the test and the validation of building energy simulation tools [26,27,28,29,30]. Such a study is helpful to assess, compare and improve the accuracy of the different simulation tools.

With the help of the validated building simulation tools, the energy performance of buildings can then be evaluated before the buildings are constructed. The simulation tools require information of building structures and envelopes, HVAC[5] systems, electrical appliances, occupancy profiles, and weather forecasts for energy analysis purposes. Among these inputs, the internal heat gains obtained by solar irradiation, electrical appliance's operation, and occupant's behavior in a building are considered as important factors, especially for heating/cooling load calculations.

However, it is not easy to predict these internal heat gains of buildings because they are not deterministic and their models are not very well-known. Therefore, rough information, such as the past weather information and simply estimated profiles of electrical load usages and occupant's behaviors have been used for the simulations. As a result, it has led unwanted retrofit errors between the simulation and the validation of the energy analysis of buildings [31]. In order to obtain more accurate and reliable results of the simulations, more accurate models are needed.

In addition, as the simulation tools are coupled with control design tool, it requires more accurate and reliable analysis. As a consequence, the simulation time interval tends to be shorter,

---

[5] HVAC: Heating, Ventilation, Air Conditioning

even less than an hour. In such intra-hour simulations it needs to model building systems more accurately in order to capture the rapid dynamics which could be neglected in simulations taken with long term intervals. Thus a shorter simulation time-step requires a detailed modeling of the internal heat gains. Accordingly, there are many investigations on the modeling of solar irradiations, both deterministic and stochastic models of usage profiles on lighting equipment, HVAC installation, electrical load, and occupant's behaviors have gradually increased. However, only a few works on thermal modeling of electrical appliances have been conducted until now [32,33].

There are two main reasons that the heat gain of electrical appliances has not been accurately modeled before. Firstly, the heat dissipation of electrical appliances within a conventional building was too small to compensate the heat loss through building envelopes. It means the quantity of heat gain of electrical appliances is relatively small comparing to the heat loss through the building envelopes and it is therefore ignored. Secondly, the operation time and the thermal dynamics of the electrical appliances are relatively short and too fast to be considered as of great impact in the simulations where long time-steps are used.

However, in a low energy building where the insulation is reinforced, the heat gain of the electrical appliances becomes important as explained above. In addition, despite of increasing more energy-efficient appliances, their power densities have been increasing too, as the usage of various appliances have increased and that the quality of human life has been improved. Figure 1. 2 shows the growth in electrical appliance usage in IEA 19 countries[6]. According to the IEA report, the energy demand for electrical appliances has significantly increased, more than 57 % from 1990 to 2005. In the late 1990s, electrical appliances overtook water heating as the second most energy-consuming category, accounting for 21 % of total household energy consumption [34].
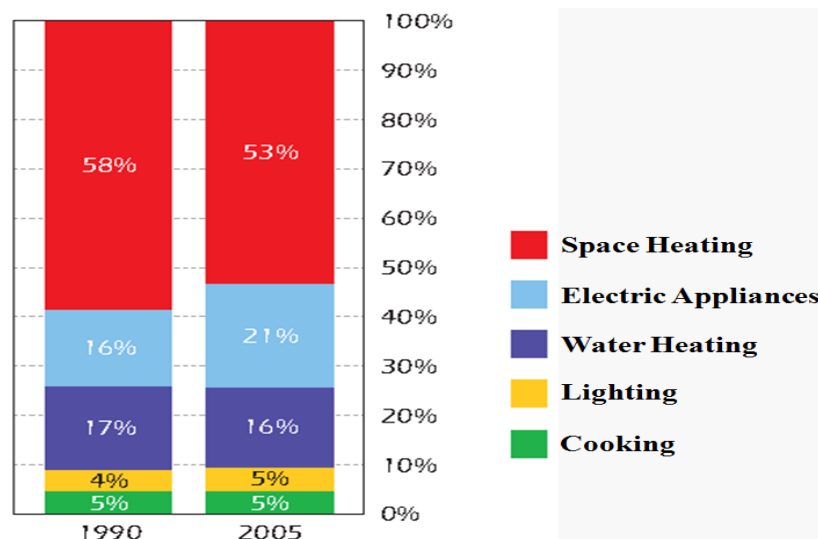
Figure 1. 2 Growth in appliance use in 19 countries [34]

[6] IEA19 countries : Australia, Austria, Canada, Denmark, Finland, France, Germany, Ireland, Italy, Japan, Republic of Korea, Netherlands, New Zealand, Norway, Spain, Sweden, Switzerland, United Kingdom, United States

As seen above, thermal effect of electrical appliances in tomorrow's buildings cannot be neglected any more. Moreover, since the simulation time interval tends to be shorter, the detailed modeling of building systems, which includes accurate models of electrical appliances, is also strongly required.

1.2 MOTIVATION

This thesis focuses on the thermal modeling of internal heat gains produced by electrical appliances in well-insulated buildings, such as low energy buildings, zero-energy buildings, and further energy positive buildings. To accomplish this aim, the following steps are included in this thesis:

1) State-of-the-art thermal modeling of building systems
2) Thermal modeling of well-insulated building
3) Thermal modeling of electrical appliances
4) Simulation of coupled models of a building and electrical appliances

Through this thesis work, the author's contributions are:
✓   A thermal model of well-insulated buildings,
✓   A generic thermal model of electrical appliances,
✓   The identification of the thermal parameters of these models,
✓   The integration of the obtained models of electrical appliances into the building model and the quantification of the thermal effect of electrical appliances in low energy buildings.

1.3 OUTLINE OF THE THESIS

In this introductive chapter, we presented increasing energy consumption of buildings and their environmental impact. We focused on the solutions to achieve low energy buildings concerning building regulations and codes, thermal insulation of buildings, and application of building energy simulation tools. In accordance with this, we highlighted the internal heat gains of buildings which influence the thermal behavior and the energy consumption of the buildings. We subsequently introduced the need for modeling accurately electrical appliances.

In chapter 2, we accordingly bring out the relevant problematic issues and their scientific solutions by literature reviews. Firstly, the possible methodologies for thermal modeling of building systems, including a building and its sub-systems are presented. Secondly, the parameter identification methods adapted to the building models are introduced with a number of examples. It aims to describe the thermal behavior of building systems according to physical laws, physical properties and characteristics, or a mathematical relationship between input and output of the systems. Thirdly, the state-of-the-art building simulation tools are reviewed. Several references of comparative studies on the simulation tools are given and the uncertain

factors of simulation tools are also discussed. Based on these literature reviews, the main interests of this thesis are once again highlighted.

In order to quantify and model the heat gains of electrical appliances, a test room has to be firstly modeled. As a consequence, Chapter 3 presents the experimental set-up and the modeling methodology for a single quasi-adiabatic room. The room represents a small scale laboratory set-up of a low energy building, in which the electrical appliances have been tested. The energy balance of a conventional building, a low energy building, and a chosen quasi-adiabatic test room is first overviewed. Then, the experimental set-up and the procedures for characterizing the test room are presented. Lumped *RC* parameter circuits are suggested as the models of the test room using thermal-electrical analogy. Thereafter, thermal parameters of the model components are estimated by experimental results and parameter identification methods. The proposed model structures and their parameters of the test room are implemented on Matlab/Simulink® and then simulated. The simulation results are compared to the measured data in order to validate the models and verify their accuracy.

Chapter 4 proposes a methodology to establish a thermal model of electrical appliances and to identify its corresponding thermal parameters. In order to present a generic model of all kinds of electrical appliances, electrical appliances are firstly classified into four categories according to thermal and electrical points of view. Based on this classification, a generic thermal model of electrical appliances is established. Then, parameter identification methods for estimating the parameters of the obtained generic model are described. In sequence, the generic thermal model of electrical appliances is integrated into a building model. Afterward, several practical case studies are conducted in order to illustrate the relevance of the proposed generic model in accordance with the presented identification procedure.

After modeling electrical appliances, the corresponding models are integrated into a building simulation tool in order to observe their thermal influences within a low energy building. To this purpose, Chapter 5 treats the coupled model of a residential building and electrical appliances developed in SIMBAD simulation tool. It first describes the chosen building model and gives the basic information of its thermal behavior under different conditions of HVAC systems. After that, several types of electrical appliances are integrated into the building model, and thermal behavior and heating energy consumption of the building are observed during a winter period. According to the scheduling of electrical appliances, the change of energy demand of the considered building is extracted and analyzed. In addition, thermal discomfort owing to usages of electrical appliances during a summer period is also studied and quantified.

Finally, this thesis work is resumed as listing its highlighted issues and the proposed solutions in General Conclusions. The scientific prospects and the critical comments of this work are supplementary at the end of this dissertation.

Chapter 2

STATE-OF-THE-ART LITERATURE

2.1 BACKGROUND

Nowadays, improving building energy performance becomes one of the main issues of the world. Similar terms of low energy buildings such as green energy building, energy positive building, and zero-carbon building are focused on achieving the low environmental impacts of building constructions. It is especially important to reduce the amount of energy consumption and CO_2 emission. Toward this common purpose, many of researchers have been involved in works related to the improvement of the energy efficiency of buildings and the renewable energy technologies integrated to the buildings into building structures.

As one of the ways to enhance building energy performance, thermal analyses of building systems have been carried out. The building system includes envelopes of a building and its inner sub-systems, such as HVAC and electrical equipment. In order to conduct the analysis of a building system, three main processes are needed [35]: Firstly, it requires modeling the building system based on physical laws and phenomena that lead to the thermal behavior within the building. Secondly, thermal parameters of the building system have to be identified. These parameters are known by the physical properties and characteristics of the building system. If the prior physical knowledge of the building system is not precisely determined, the parameters can be estimated by measurements and identification methods. Thirdly, the model has to be validated by comparing theoretical and empirical results. According to these results, the thermal behavior within the building can be understood and further predicted.

Figure 2. 1 Dynamic interactions of building components

For obtaining a complete understanding of thermal behavior of a building system, the characteristics of the following components of the building have to be known:

- Exterior conditions: orientation, location, climate, etc.
- Physical properties: structure, materials, thermal capacitance, thermal resistance, etc.
- Energy efficiency of inner sub-systems: HVAC, lighting, electrical appliances, renewable energy source installation, etc.
- Occupancy

These characteristics are dynamically interacting with each other (Figure 2. 1). It requires a more detailed study of the above characteristics of the building system in order to assess its energy performance [36]. In order to obtain a more accurate data, each component of the building system has to be rigorously studied. Furthermore, since the thermal characteristics of the building system are closely related to the energy consumption, thermal modeling of each component of the building system is the most important task to do for analyzing the building energy performance.

In order to achieve low energy consumption of buildings, their thermal insulation has been reinforced. In a well-insulated environment, even small quantity of heat gains due to solar radiation, occupant's metabolism and heat dissipation of electrical appliances impacts thermal behavior within the building. To evaluate the thermal influence of those auxiliary heat gains in low energy buildings, accurate thermal models of this kind of buildings and their internal gains are therefore mandatorily developed.

Until now, there have been many investigations on the solar irradiation modeling. Both deterministic and stochastic models of occupant's behavior and lighting/equipment usages, metabolic heat by occupants in buildings have also been given [37,38]. However, these investigation have been conducted in conventional buildings. Moreover, there are also very few works on **modeling of heat gains of electrical appliances** [19,32], since the heat flux dissipated by electrical appliances within a standard building is usually considered as too small to compensate the heat loss through the building structures and envelopes. However, as stated above, in low energy buildings, the heat gain of electrical appliances may impact more the thermal behavior of these buildings. Despite of the increase of the distribution rate of more efficient electrical appliances in low energy buildings, their energy consumption has increased as the usages of various appliances are growing.

This chapter reviews the literature on which are related to our thesis work that investigates the influence of electrical appliances on the thermal behavior of tomorrow's buildings. By reviewing them, we will catch some ideas and responses on how an electrical appliance can be thermally modeled and how the corresponding model can be adapted to well-insulated building models.

The proposed literature review is organized in three parts:

- Modeling methods of building system
- Parameter identification methods adapted to the thermal modeling of buildings
- Building simulation tools

2.2 THERMAL MODELING OF BUILDING AND ITS SUB-SYSTEMS

Thermal analysis of building systems permits the determination of thermal quantities for the systems and understanding of their thermal behavior. The most interesting thermal quantities in thermal analysis are temperature and heat flux [35]. As using the obtained information of these quantities, energy demand of buildings and thermal comfort of occupants can be evaluated. In order to obtain accurate results of the analysis, which brings more precise advancements and quantifications, it is necessary to adapt a suitable thermal modeling method for each system.

2.2.1 Analysis Methods

In this sub-section, we mention two fundamental analysis methods for thermal modeling of building systems as follows [39,40]: steady-state analysis and transient-state analysis. **Figure 2. 2** shows a classification of building thermal analysis methods. According to this classification, we enter into details.

```
                                    ┌──────────────────────────────┐
                                ┌───│      Degree-Day Method        │
                                │   └──────────────────────────────┘
                                │   ┌──────────────────────────────┐
                                ├───│   Modified Degree-Day Method  │
                                │   └──────────────────────────────┘
                 ┌────────────┐ │   ┌──────────────────────────────┐
              ┌──│Steady-State│─┼───│ Variable-Base Degree-Day Method│
              │  │  Analysis  │ │   └──────────────────────────────┘
              │  └────────────┘ │   ┌──────────────────────────────┐
              │                 ├───│          Bin Method           │
              │                 │   └──────────────────────────────┘
              │                 │   ┌──────────────────────────────┐
┌───────────┐ │                 └───│      Modified Bin Method      │
│Thermal     │ │                     └──────────────────────────────┘
│Analysis of │─┤                     ┌──────────────────────────────┐
│Building    │ │                 ┌───│      Numerical Method         │
│Systems     │ │                 │   └──────────────────────────────┘
└───────────┘ │  ┌────────────┐ │   ┌──────────────────────────────┐
              │  │Transient-  │ ├───│      Harmonic Method          │
              └──│State       │─┼───└──────────────────────────────┘
                 │Analysis    │ │   ┌──────────────────────────────┐
                 └────────────┘ ├───│    Response Factor Method     │
                                │   └──────────────────────────────┘
                                │   ┌──────────────────────────────┐
                                └───│    Thermal Network Method     │
                                    └──────────────────────────────┘
```
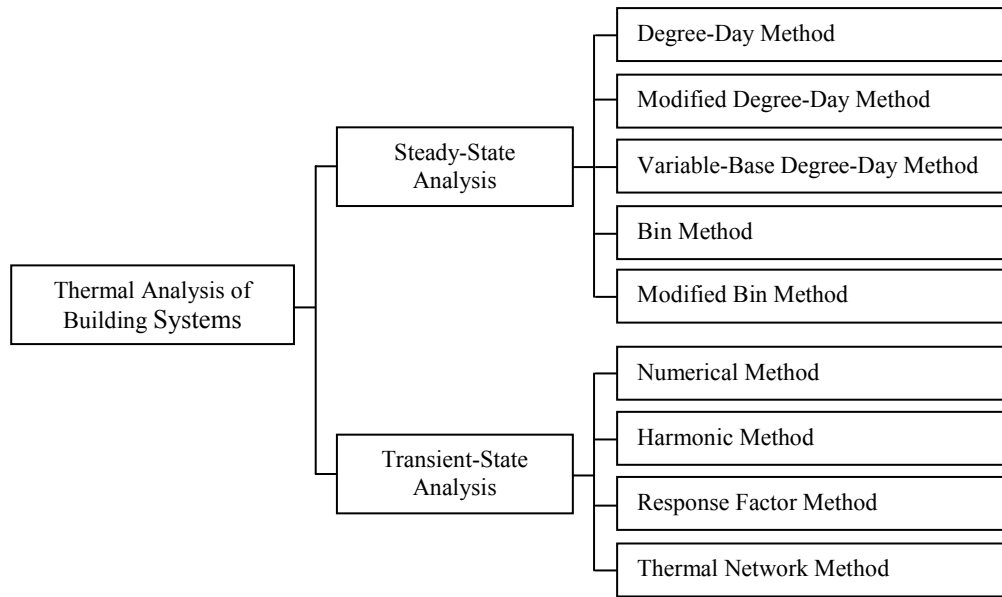
Figure 2. 2 A classification of building thermal analysis methods [39]

2.2.1.1   *Steady-state Methods*

The steady-state method is called "hand" calculations. It simplifies but neglects some important thermal behaviors of a building, such as heat storage, thermal delay, additional heat sources, and temperature variations. Since this method is relatively simple and thus quickly performed, it is useful when computational resources are limited. Moreover, it is practical for simple calculations of cooling/heating loads or thermal conductivity of building components.

Until the mid-1960s, there were only few manual calculation methods such as Degree-Day method and Bin method for heating/cooling load calculations. Due to their simplicity, they are popular until now and is suited for obtaining rough order magnitude approximations. However, there is a 10~40 % error margin with their utilization.

Al-Homoud (2001) [41] summarized several available energy analysis techniques for alternative building design strategies, standard compliance, and economic methods. According to him, the simplified manual analysis can be distinguished into five approaches: Degree-day method, Modified degree-day method, Variable-base degree-day method, Bin method, and Modified bin method.

Briefly, the Degree-Day (DD) method considers that heat loss and gain are proportional to the equivalent heat-loss coefficient of the building's envelope. This approach is widely used to estimate heating and cooling energy demands of small buildings. The assumption of the calculation procedure is that the average heat gain during a long-term is balanced to the heat loss by the mean daily inside temperature (e.g. 18.3 °C or 65 °F), called a balance point temperature. Energy consumption of buildings is proportional to the difference between the balance point temperature and the mean daily temperature. Analogically, the cooling and heating energy demands are calculated. In order to reduce the inaccuracy of the DD procedure,

an empirical correction factor is used by the Modified Degree-Day (MDD) method. The correction factor is a function of designed outdoor temperature. It corrects the heating effect of the building. Further, the Variable Base Degree-Day (VBDD) method uses the variable balance temperature for the calculation instead of the fixed balance temperature. It takes into account different building conditions and hourly weather information. Moreover, the VBDD method is extended into the estimation of the annual heating and cooling energy demand by using temperature samples called "bins". This approach is called Bin method. Furthermore, the Modified Bin method even accounts for the impact of solar gain and wind effect on the building energy consumption.

The above methods are not used for modeling of building systems with precision, but are available for sizing the building sub-systems, such as heating/cooling systems and predicting energy demand of the conventional buildings.

2.2.1.2 Transient-state Methods

The transient-state method, called "dynamic" analysis, requires various information and computational calculations in order to provide more detailed and accurate results. This method treats dynamic thermal behavior of building systems, including steady and transient-states. It allows the analysis of temporal and spatial performances within building systems. For example, the gradient of temperature and the diffusion of heat flux inside the building can be described by this method. Furthermore, it is possible to analyze the whole building system that contains the building envelopes and its sub-systems.

According to Wang and Chen (2003) [42], there are four types of methods for predicting space heating loads as transient analysis: numerical methods, harmonic methods, response factor methods, and conduction transfer function methods. The numerical methods are based on Fourier's heat conduction equation, approximating the derivatives in space and time using finite difference or finite element methods. The accuracy of results, cost of calculations, and model stability are related to the number of nodes, the time-step of simulation and selected solution methods. Since numerical methods are treated in arithmetic expression, the advantage is conceptually a simple calculation. Moreover, it is able to consider both linear and nonlinear boundary conditions.

The harmonic method is used to analyze the heat transfer of building components [43]. It approximates the heat flux due to weather conditions expressed by a periodic function and solves the heat conduction equation of the building. Mackey and Wright calculated heat gains through homogeneous and multi-layer walls using the periodic outdoor air temperature and the constant room air temperature variables [44, 45]. Van Gorcum obtained the wall thermal impedance using the oscillations of the periodic temperature [46].

The Response Factor (RF) method is a convenient method to describe the dynamic thermal characteristics of a building based on a set of heat balance equations [47, 48, 49]. It is used for cooling/heating load calculations. It calculates the heat gain or loss through building components (e.g. envelopes and windows) by reducing the heat excitation. There are three steps

in this method: i) Resolving the excitation function into a time series, ii) Calculating the response of each component, iii) Super-positioning the responses of each component. For example, any heat flux enters into a building can be formulated by the time series function. Then, the thermal response of the building is expressed by the values of the unit response factor in time. Gathering the excitation functions and their response factors, the influence of each excitation is clearly shown within the final results. Specifically, DOE-2 [49], one of the building simulation tools calculates the heat transfer through building components using this method.

Additionally, the conduction transfer function (CTF) method is widely used for solving heat diffusion equation of building systems [50,51]. The heat flux is expressed by a linear equation in terms of the temperature, the time interval, and the CTF coefficients. For the calculation, Laplace transform [52], state-space models [53], and frequency-domain regression methods [54,55] are used [56]. Moreover, this method has been applied to several building energy simulation tools, such as DOE-2 [49], HVACSIM+ [57], TRNSYS [58], BLAST [59], and EnergyPlus [60].

As one another method to analyze transient state of thermal building systems, the thermal network was proposed in the mid-1980s. This method is based on the energy balance equation and the analogy between thermal and electrical systems. It is possible to describe heat transfer phenomena of building systems and heat gain/loss corresponding to solar radiation, occupants, infiltration/ventilation, and equipment by electrical components and sources. The analysis has good accuracy and robustness, as well as simplicity.

The heat dissipation of electrical appliances that we want to study in this thesis work is considered as one of the heat sources within buildings. In order to investigate the thermal influence of electrical appliance within low energy buildings, it is also necessary to model an integrated building system. The system contains the thermal model of electrical appliances and the well-insulated building model. From now on, we are therefore focusing on the thermal network modeling approach for the reason of its simplicity and its accuracy to compose both the heat source and the structure of the building at the same time.

2.2.2 Thermal Network Modeling Approach

From the mid-1980s, the thermal network method using the thermal-electrical analogy has been used in order to simplify the building modeling. The thermal network method is based on the energy balance equation. The heat transfer phenomena of building systems are described by their corresponding electrical components. The supplementary heat gain/loss due to solar radiation, metabolic heat of occupants, infiltration/ventilation, and electrical equipment and appliances can be expressed by current sources. It permits the analysis of thermal behavior of building systems during steady and transient-states. Table 2. 1 shows the thermal-electrical analogy.

Briefly, the thermal models of building systems are represented by electrical circuits, including electrical components and electrical sources. The thermal dynamics of the building

systems are analyzed in accordance with the electrical dynamics of the corresponding electric circuits.

Table 2. 1 Thermal-electrical analogy

		Thermal system		Electrical system	
		Parameter	Unit	Parameter	Unit
Source		Temperature T	[K]	Voltage V	[V]
		Heat flux Φ	[W],[J/s]	Current I	[A],[C/s]
Element		Conductivity k	[W/K·mm]	Conductivity σ	[A/V·mm]
		Thermal resistance R_{ther}	[K/W]	Electrical resistance R_{elec}	[Ω],[V/A]
		Thermal capacitance C_{ther}	[J/K]	Electrical capacitance C_{elec}	[F],[C/V]

The relevant literature on the modeling of building components and heat sources by using the thermal network modeling method is mainly viewed as follows. Firstly, the examples of the thermal modeling of building envelopes are introduced. It contains the modeling of both simple-layer and multi-layers walls. In accordance with the building energy balance equation, the heat fluxes that pass through the envelopes are also deduced. Secondly, the examples of the thermal modeling of heat sources that influences inside and outside buildings are reviewed.

2.2.2.1   Building Envelopes Modeling

Roux (1984) [61] presented building envelope models using the thermal-electrical analogy, in which the models were proved by the finite-difference method. The exchange of heat flux through the models by conduction, convection, and radiation was investigated. According to Roux, each heat transfer phenomenon is distinguished as follows: the conduction through a homogeneous uni-directional wall, the convection between exterior/interior wall and its environment, the long and short wave solar radiation through a wall and a window, and the long and short waves radiation amongst walls. From the physical laws and the heat balance equation, the thermal network modeling of the above phenomena is deduced. Each heat transfer phenomenon is represented by appropriate electrical components (resistor and capacitor). This study also showed how those components are simplified and linearized. Several simulation tools were used in order to compare the proposed building models.

Along with this, Ren and Wright (1998) [62] presented a thermal model of a multi-layer wall of building by using the *RC* components in order to describe the thermal dynamics of a slab

thermal storage system within a room. An example of a multi-layer wall is shown in Figure 2. 3. Its thermal network model is represented in Figure 2. 4.
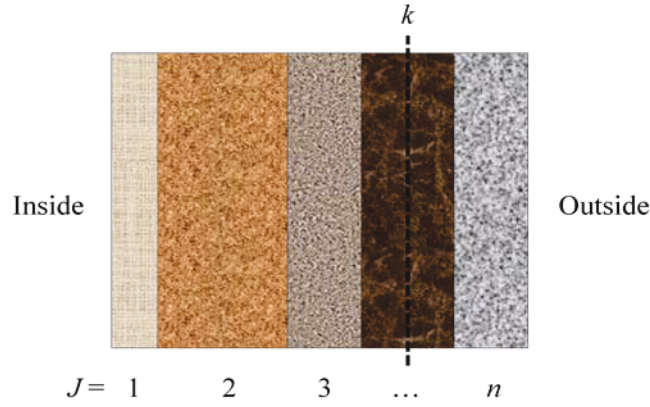
Figure 2. 3 A multi-layer wall of a building
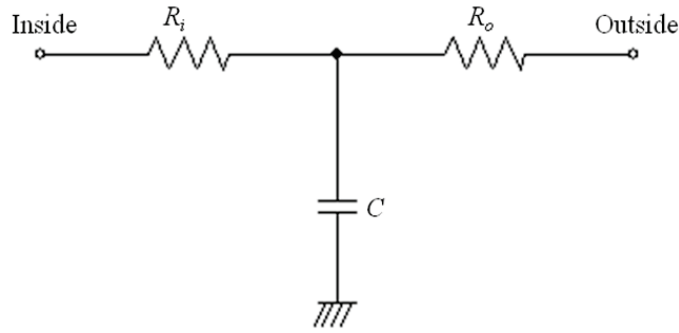
Figure 2. 4 A lumped *RC* parameter model of a building wall corresponding to Figure 2. 3

R_i and R_o are the thermal resistances of the mass node to the disturbances from the inside and the outside of the wall, respectively. C is the total heat capacitance of the wall. These parameters are mathematically defined as follows:

$$R_i = R_{si} + \sum_{j=1}^{k-1} R_j + \frac{R_k}{2} \tag{2.1}$$

$$R_o = \frac{R_k}{2} + \sum_{j=k+1}^{n} R_j + R_{so} \tag{2.2}$$

$$C = \sum_{j=1}^{n} C_j \tag{2.3}$$

where R_{si} and R_{so} are the resistances of the inside and outside surfaces of the wall. R_j and R_k are the thermal resistances of layers of the wall j and k. C_j is the thermal capacity of jth layer of the wall.

The model can be more accurate by increasing the model order. Gouda et al. (2002) [63] showed the multi-order models from *2R1C* to *21R20C*. The multi-layer building element was

shown in Figure 2.3, and is also represented by a second order lumped *RC* parameter model, as shown in Figure 2. 5.
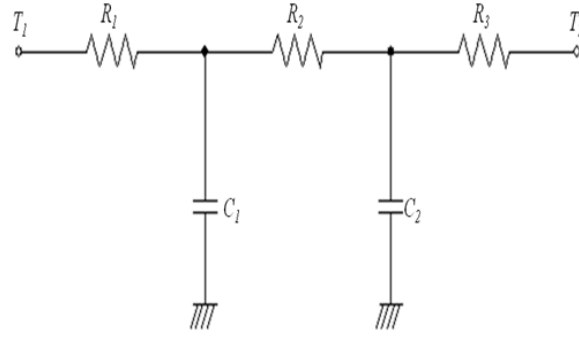
Figure 2. 5 A second-order lumped parameter model of building element

Figure 2. 6 indicates a benchmarked high-order lumped parameter model. However, since relatively low-order linear systems can capture the essential dynamics of observed behavior, simplified or reduced-order *RC* network models are also widely used. Gouda et al. presented a method for reducing orders of lumped thermal circuit model of the building with a small loss of accuracy and tested the proposed method both on high and low thermal capacity modeling problems. At the same time, they stated that the simplified lumped model has a better accuracy, when the building model has a high value of thermal capacitance.

Furthermore, Fraisse et al. (2002) [64] proposed the global analogical *RC* network models of a building. The wall which is made of 8 cm exterior insulating material and 16 cm concrete material were modeled by *1R2C*, *3R2C,* and *3R4C* models. The models were compared and were evaluated in time and frequency domains. Among them, the *3R4C* model is more accurate because it considers the thermal inertia of the interior surface of the wall. The *3R4C* model was then applied to the zone model that has windows, a ceiling, a floor, internal walls, and partition walls within TRNSYS [58], one of the most widely used building simulation tools. The simulation results and the experimental results were compared to each other and the proposed models were verified. They found that the developed models are simple and accurate.
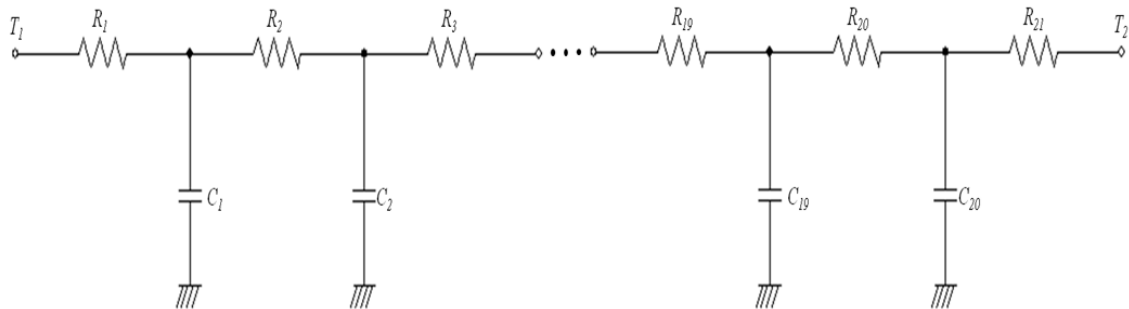
Figure 2. 6 A high-order lumped parameter model of building element

Aforementioned investigations yield that the advantage of the thermal network method, adapted to the modeling of building envelopes, is simplicity and high accuracy of the model of which order is even reduced. As the model is simpler, coding and computing time are also reduced and that the analytical solution is easily obtainable and readily verifiable.

The modeling approach for the building envelopes using the thermal network method has been well adapted for the conventional buildings. The cases of low energy buildings for which thermal insulation and mass distribution are strengthened were also studied. Parnis (2012) [65] presented a thermal model of a single zone of a low energy house in Sydney using electric circuits. Each of layers of the envelopes of the house was modeled by *RC* components. For improving the accuracy of the modeling of heat diffusion through the envelopes, Parnis increased the number of the *RC* components according to error evaluation with the variations of temperature and heat flux. Then, each modeled layer was represented by a Thevenin impedance. For example, a concrete layer of the floor of the room was modeled by a *15R15C* with 1 % of error. Then, the corresponding model was represented by a Thevenin impedance Z_{th}. This work improved the accuracy and simplicity of the thermal analysis comparing with the reference model.

Another interesting part of the thermal network model is the active elements, namely the heat sources and the temperature potentials. The heat sources are represented by the current source of electrical circuits. Each node of thermal masses of the building implies temperature potentials. The exterior temperature of the building can be expressed by a voltage source. The temperatures of the building envelopes or their inside/outside temperatures also correspond to the voltage source of the electrical circuits. The next sub-section introduces the examples of the modeling of active elements of building systems.

2.2.2.2 Active Elements Modeling

There are various studies on multiple *RC* models with multiple heat sources. Ghiaus et al. (2010) and Hazyuk et al. (2012) [66,67] recently showed a building thermal model using lumped parameters and various heat sources. The model is illustrated in Figure 2. 7. They demonstrated a thermal lumped parameter model for the load calculation of buildings. This model includes the contributions of outdoor air temperature, solar radiation, and internal heat gain. They applied an unconstrained optimal control algorithm to this model for reducing heating energy consumption at a set-point temperature.

They designed heat sources which influence thermal condition of a building. The models of solar radiation on envelopes of the building $\dot{Q}_s$ and radiative heat gain of a water-based heating system $\dot{Q}_g$ were especially proposed.

<u>a/ Solar radiation on envelopes of the building $\dot{Q}_s$</u>

They designed a heat source model of solar radiation on envelopes of the building model $\dot{Q}_s$. The quantity of the incident solar radiation on the surfaces of the building envelopes is not directly measured. Since the only information about diffuse radiation I_d and beam radiation I_b are available, it needs to determine the radiation on each surface of the envelopes, multiply it by the corresponding surface area, and add the results for all sides of the envelopes.
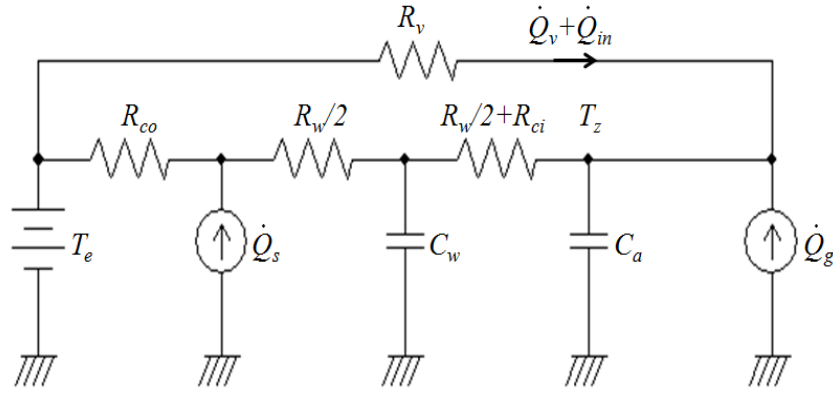
T_z: zone temperature, T_e: outdoor temperature, $\dot{Q}_s$: solar radiation on walls, $\dot{Q}_v$, $\dot{Q}_{in}$: ventilation and infiltration heat flux, $\dot{Q}_g$: free gains from occupants, electrical devices and direct solar gains, and auxiliary heat flux by heating system, R_{co}: outdoor convection thermal resistance, R_{ci}: indoor convection thermal resistance, R_w: wall conduction resistance, R_v: resistance equivalent to ventilation and infiltration, C_w: equivalent wall thermal capacitance, C_a: equivalent thermal capacity of the zone

Figure 2. 7 Reduced building model with multiple sources

Considering an isotropic model of the sky, the incident solar radiation on a tilted surface described in Figure 2. 8 is calculated by [67]:

$$I_T = I_b R_b + I_d \frac{1 + \cos(\beta)}{2} + (I_b + I_d)\rho_g \frac{1 - \cos(\beta)}{2} \tag{2.4}$$

where the ground albedo ρ_g is usually 0.2^7 [68,69], the ratio of beam radiation on a tilted surface to that on a horizontal surface R_b is calculated by:

$$R_b = \frac{\cos(\alpha_T)}{\cos(\alpha)} \tag{2.5}$$

The angles α and α_T are the incidence angles of the beam radiation on the horizontal and tilted surfaces, respectively. The details are as follows:

$$\begin{aligned}
\cos(\alpha) &= \sin(\delta)\sin(\varphi) + \cos(\delta)\cos(\varphi)\cos(\omega) \\
\cos(\alpha_T) &= \sin(\delta)\sin(\varphi)\cos(\beta) - \sin(\delta)\cos(\varphi)\sin(\beta)\cos(\gamma) + \cos(\delta)\cos(\varphi)\cos(\beta)\cos(\omega) \\
&\quad + \cos(\delta)\sin(\varphi)\sin(\beta)\cos(\gamma)\cos(\omega) + \cos(\delta)\sin(\beta)\sin(\gamma)\sin(\omega)
\end{aligned} \tag{2.6}$$

where δ is the solar declination[8] in the nth day of the year, φ is the geographical latitude of the location of the building (positive for north hemisphere), γ is the azimuth angle of the surface

---

[7] According to Psiloglou et Kambezidis, for most calculations, when ground-albedo measurements are not available, it has been customary to use the average value of 0.2, which describes the reflective properties of bare ground, free of snow.

[8] Solar declination: the angle between the sun's rays and the earth's equatorial plane,

$\delta = 23.45^{\circ} \sin\left(\left(\frac{360}{365.25}\right) \cdot \text{day}\right)$

(zero for south facing, negative for west facing and positive for east facing), ω is the solar hour angle[9] and β is the angle between the tilted surface and the horizontal plane.
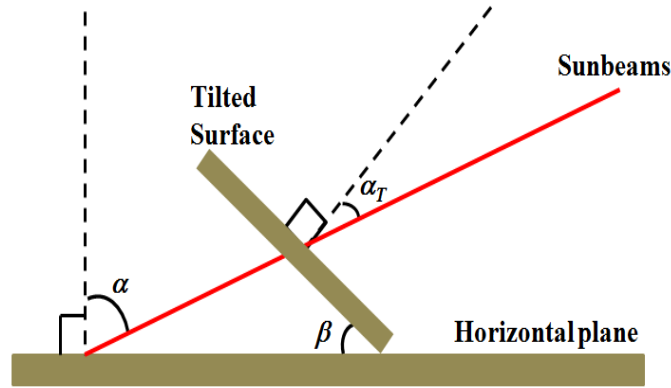
Figure 2. 8 Incident solar radiation on a tilted surface

Considering that all surfaces of the envelopes are perpendicular to the horizontal plane (the roof is not a part of the envelope, but it completely shades the ceiling so it is not exposed to solar radiation), the incidence angle of beam radiation on the walls is

$$\cos(\alpha_T) = -\sin(\delta)\cos(\phi)\cos(\gamma) + \cos(\delta)\sin(\phi)\cos(\gamma)\cos(\omega) + \cos(\delta)\sin(\gamma)\sin(\omega) \qquad (2.7)$$

Then, the total solar radiation on a wall is

$$I_T = I_b\left(R_b + \frac{\rho_g}{2}\right) + I_d\frac{1 + \rho_g}{2} \qquad (2.8)$$

Once the total solar radiation is calculated for each building side and multiplied by the corresponding surface area, the heat flux of solar radiation of the building is obtained by:

$$\dot{Q}_s = \sum_{k=1}^{4} I_{Tk}S_k \qquad (2.9)$$

where k is the number of the side surface of the building envelopes.

b/ Heat gain of the radiative heat flux of a water-based heating system $\dot{Q}_g$

As one of the other heat sources in the building model, Hazyuk et al. propose the internal heat gain by the radiative heat flux of a water-based heating system $\dot{Q}_g$. It represents the radiative and convective heat fluxes. Firstly, the radiative heat flux density $\dot{q}_r$ is driven as follows.

---

[9] Solar hour angle: the angle of the sun *along* the arc traversed by the sun across the sky, $\omega = 15(\text{LST} - 12)$, where LST is the Local Solar Time.

$$\dot{q}_r = \varepsilon\sigma\left(T_{hot}{}^4 - T_{cold}{}^4\right) \qquad (2.10)$$

where T_{hot} is the hot surface temperature and T_{cold} is the cold surface temperature. ε is the emissivity, and σ is the Stephan-Boltzmann radiation constant ($=5.67 \times 10^{-8}$ W/m^2 K^4),

Equation (2.10) can be linearized as follows:

$$\dot{q}_r = \varepsilon\sigma\left(T_{hot} + T_{cold}\right)\left(T_{hot}{}^2 + T_{cold}{}^2\right)\left(T_{hot} - T_{cold}\right) = h_r\left(T_{hot} - T_{cold}\right) \qquad (2.11)$$

The linearization of this relation is based on the following consideration: in buildings, the hot surface is the radiator and its temperature varies between 20 and 60 °C. The temperature of the cold surfaces varies roughly between 15 and 20 °C. As in the eq.(2.11) temperature is on the absolute scale, T [K]$=273+\theta_{surface}$ [°C], its usual variations are relatively small compared to its absolute value. Thus, these variations do not have a significant relative impact on the first two parentheses and therefore they are approximated by a constant heat transfer coefficient, h_r, by taking the mean temperature of the surfaces.

Secondly, the convective heat flux density for a vertical surface of the heater $\dot{q}_c$ can be expressed as follows. However, it is available for the heater which is taller than 30 cm [67].

$$\dot{q}_c = 1.78\left(T_{surf} - T_{air}\right)^{1/4}\left(T_{surf} - T_{air}\right) = h_c\left(T_{surf} - T_{air}\right) \qquad (2.12)$$

Here, the first parenthesis is also considered approximately constant and equal to the convective heat transfer coefficient, h_c. By making the hypothesis that radiative and convective heat transfer coefficients are constant, the total heat flux density is obtained by summing the Equations (2.11) and (2.12):

$$\dot{q}_T = \dot{q}_c + \dot{q}_r = (h_c + h_r)\left(T_{hot} - T_{cold}\right) = h_T\left(T_{hot} - T_{cold}\right) \qquad (2.13)$$

The total heat flux delivered by radiators is obtained by multiplying the total heat flux density, $\dot{q}_T$, by the radiator's surface area S_{rad} as follows:

$$\dot{Q}_g = S_{rad}\dot{q}_T \qquad (2.14)$$

Along the same line, Dong (2010) [30] presented an integrated building with HVAC systems using the *RC* network. In this study, Dong described sub-models of the building: the heat flux due to infiltration and window opening $\dot{Q}_{inf}$, the energy flux of tank-less water heater Q_{hw} and the energy flux of cooling equipment Q_{fcu}.

<u>c/ Heat flux due to infiltration and window opening $\dot{Q}_{inf}$</u>

The heat flux due to infiltration and window opening $\dot{Q}_{inf}$ is calculated as below.

$$\dot{Q}_{in} = \rho_{air} c_{air} V_{inf} \frac{dT}{dt} \tag{2.15}$$

where, ρ_{air} is the density of the air [kg/m^3], c_{air} is the specific heat of the air [J/(kg·°C)] and V_{inf} is the volume of the air goes inside/outside of the building [m^3].

<u>d/ Energy flux of a tank-less water Q_{hw}</u>

The total heat flux of the tank-less water $\dot{Q}_{hw}$ is calculated by

$$Q_{hw} = m_w c_{pw} (T_{hw,s} - T_{hw,r}) \tag{2.16}$$

where $T_{hw,s}$ and $T_{hw,r}$ are the supply and return water temperature of tank-less water heater [°C], respectively. m_w [kg] is the total water flow rate and c_{pw} [J/(kg·°C)] is the specific heat of the water.

<u>e/ Cooling energy flux due to cooling equipment Q_{fcu}</u>

The cooling heat flux from cooling equipment using a multi-spit fan coil unit $\dot{Q}_{fcu}$ is represented by:

$$Q_{fcu} = m_{fcu} c_{air} (T_{air,s} - T_{air,r}) \tag{2.17}$$

where m_{fcu} is the air mass flow rate [m^3/s], $T_{air,s}$ is the supply air temperature [°C], $T_{air,r}$ is the room air temperature [°C].

The above heat sources are represented by current sources according to the thermal-electrical analogy in *RC* networks based on their physical modeling. However, they are also more detailed. García-Sanz et al. (1997) [70] modeled a central heating system for analyzing the thermal condition of buildings and achieving their control strategies. In this research, the heating system was represented by *2R1C* network.

In addition, Bacher and Madsen et al. (2011) [71] suggested several kinds of *RC* thermal network models of a building system that has a heating system. They also proposed parameter identification procedures of the models for analyzing the heat dynamics of the building. Figure 2. 9 (a) and (b) respectively depicts the simplest and the most complex models amongst the proposed models of a building with a heating system modeled by *RC* components.

The simplest model represents the envelope and the interior of the building by *RC* components and the heat sources such as the heater and the solar radiation by current sources.

The complex one describes building components in detail including the sensor, the interior, the medium, and the envelope by RC components. The thermal model of a heater is designed, not only by a current source, but also by $1R1C$ components. This study shows a good example how the thermal networks of a building and its sub-systems are developed from low order to high order models.

(a) The simplest model

(b) The complex model
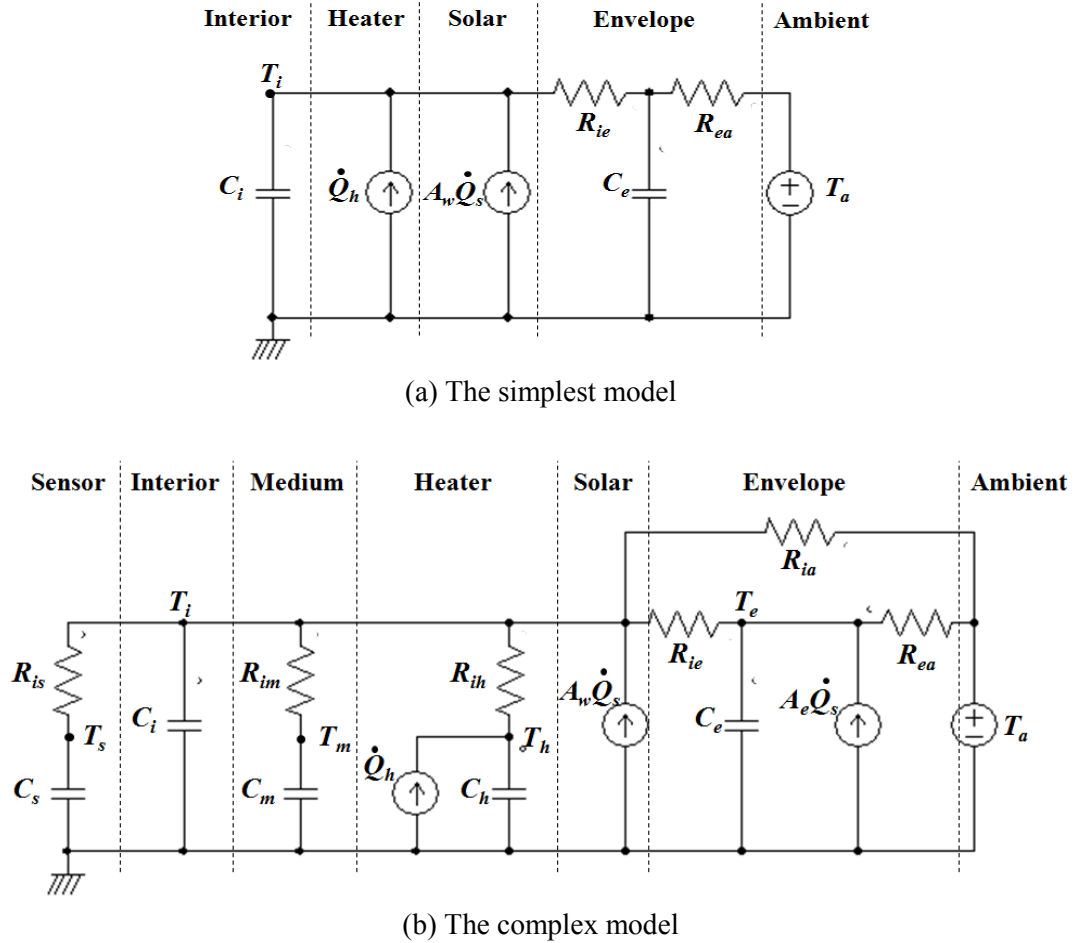
T_s: sensor temperature, T_i: interior temperature, T_m: medium temperature, T_h: heater temperature, T_e: envelope temperature, T_a: ambient temperature, $\dot{Q}_h$: heat flux of the heater, $\dot{Q}_s$: solar radiation on walls and windows, R_{is}: thermal resistance between the interior and the sensor, R_{im}: thermal resistance between the interior and the medium, R_{ih}: thermal resistance between the interior and the heater, R_{ie}: thermal resistance between the interior and the envelope, R_{ia}: thermal resistance between the interior and the ambient, R_{ea}: thermal resistance between the envelope and the ambient, C_s: thermal capacitance of the sensor, C_i: thermal capacitance of the interior, C_m: thermal capacitance of the medium, C_h: thermal capacitance of the heater, C_e: thermal capacitance of the envelope, A_w: surface of the window, A_e: surface of the envelope

Figure 2. 9 The full model with the individual model parts

<u>f/ Heat flux of occupants</u>

There are also some investigations on the modeling of occupant's heat gain. Occupant's heat gain is deduced from the heat balance equation of human body. With indoor conditions, the heat exchange of the body is represented by the following equation [72]:

$$M + S = RL + CL + EL \tag{2.18}$$

where M is the metabolic rate of generation of heat in the body, S is the storage, or the rate of net loss of heat due to lowering of body temperature, counted negative when the body gains heat, RL is the rate of radiative loss of heat to the environment, negative when the walls or other radiative surfaces are warmer than the skin, CL is the rate of convective loss of heat to the environment, negative when the air is warmer than the skin, and EL is the rate of loss of heat by evaporation in the lungs and from the skin.

The most important part as a building system is M, the metabolic rate of generation of heat in body. Even though, metabolic heat production is a rate of production of energy with time and hence has the units of power [W], the value is usually related to surface area of the body or body mass. Thus, the unit is [W/m^2]. Frequently, values of 1.8 m^2 are assumed for the surface area and 70 kg for the mass of a man and 60 kg and 1.6 m^2 for a woman. The unit sometimes used is the "MET", where 1 MET is 50 kcal/m^2/h=58.2 W/m^2 and is said to be the metabolic rate of a seated person at rest [73].

The ISO 8996 standard [74] provides methods and data for estimating the metabolic heat production of humans. It provides the fundamental support to ISO thermal comfort and other standards. Table 2. 2 describes the classification of metabolic rates by activity.

Table 2. 2 Classification of metabolic rates by activity

Class	Mean of metabolic rate [W/m^2]	Metabolic Heat [W]	Example
Resting	65	115	Resting
Low	100	180	Sitting at ease/standing
Moderate	165	295	Sustained hand/arm work
High	230	415	Intense work
Very High	290	520	Very intense to maximum activity

The ISO 7730 standard [75] is used in TRNSYS [58] for calculations of internal heat gain by occupants. Table 2. 3 shows the heat gain for each activity [76].

22

Table 2. 3 Rates of heat gain from occupants of conditioned spaces-ISO7730

Class	Adjusted Total Heat [W]	Sensible Heat [W]	Latent Heat [W]
Seated at rest	100	60	40
Seated, very light writing	120	65	55
Seated, eating	170	75	95
Seated, light work, typing	150	75	75
Standing, light work or working slowly	185	90	95
Light bench work	230	100	130
Walking 1.3m/s, light machine work	305	100	205
Bowling	280	100	180
Moderate dancing	375	120	255
Heavy work, lifting, heavy machine work	470	165	300
Heavy work, athletics	525	185	340

These metabolic heat gains are supplied to the building models and effect the thermal behaviors of the buildings in time. If it is adapted to the *RC* thermal network of building systems, it is represented by current sources. As the metabolic heat in body is also transferred by conduction, convection, and radiation from the body to the clothing, and the environment, it can be modeled by *RC* components. Thellier et al. (2008) [77] derived an equivalent circuit of the heat transfer through clothing of human body in steady-state as shown in Figure 2. 10. Even though the study is made for knowing the influence of the solar radiation to the inhabitant of a building, it is inversely applicable to the environment influenced by metabolic heat of human body. The rates of heat gain of occupants might be represented by a current source. Moreover, the thermal capacitance and resistance of the human body and the clothing will be designed by *RC* components from the basics of the thermal-electrical analogy and the heat balance equation.
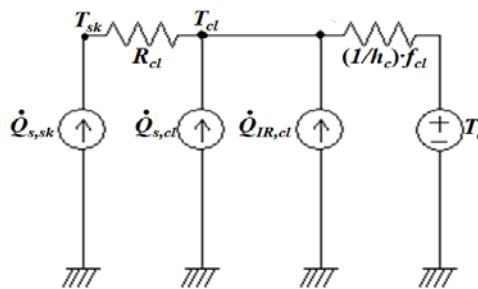
T_{sk}: skin temperature, T_{cl}: clothing temperature, T_a: ambient temperature of the room, $\dot{Q}_{s,sk}$: solar radiation on human skin, $\dot{Q}_{s,cl}$: solar radiation on human clothing, $\dot{Q}_{IR,cl}$: infrared radiation on human clothing, R_{cl}: thermal resistance between the human body and the clothing, h_c: coefficient of convective exchange from the clothing to the air in the room, f_{cl}: ratio of the area of the clothed body to the area of naked skin

Figure 2. 10 Equivalent electric circuit of heat transfers through clothing in steady-state

<u>g/ Heat flux of occupants</u>

As above, we reviewed several representative heat sources of buildings, such as solar radiation, radiant heat gain of an electric heater, heat gains due to infiltration and windows opening, cooling equipment, hot water equipment, and occupant's metabolism. However, there remains yet heat dissipation of lighting equipment and electrical appliances of buildings.

Most of building simulation tools requires heat gains of lighting equipment and electrical appliances within a building in order to calculate heating/cooling loads of the building. The heat gains are not sophisticatedly modeled. Instead, arithmetic aggregations of power consumption profiles of the electrical loads are obtained through the usage profiles of lighting equipment and electrical appliances and their power inputs. These calculated constant values versus time are considered as one of the heat gains of the building.

For examples, a building simulation tool TRNSYS [58] demands the magnitudes of the sensible and latent heat gains of artificial lightings, computers, and other devices with their pre-defined usage schedules. SIMBAD toolbox [78] also needs heat gains of equipment and artificial lighting systems. For equipment, information of heat flux density [W/m^2], convective part of heat emission [%], humidity generation [kg/h/m^2], and CO_2 generation [l/h/m^2] are required. For a lighting system, total lighting power of lamps in luminaire [W], ballast consumption as a percentage of luminaire consumption [%], illuminance efficiency [lm/W], luminaire mean efficiency, and luminaire maintenance factor are the required inputs. Figure 2. 11 shows block diagrams of heat gains of electrical appliance modeled in Simbad toolbox version 5.
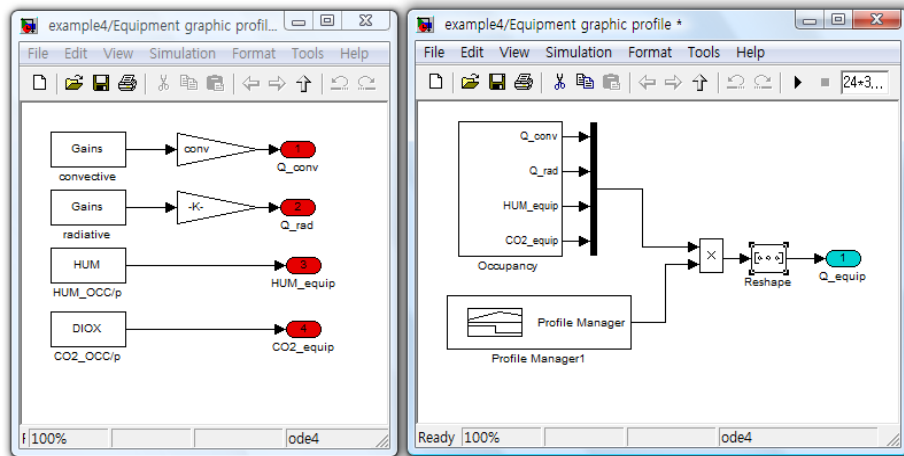
Figure 2. 11 'Equipment graphic profile' block diagram of heat gains of electrical appliances within Simbad toolbox

Thermal gains of electrical appliances have been modeled by the usage profile of the electrical appliances before. However, since the thermal behavior of electrical appliances becomes more important in a well-insulated building, it is necessary to model them more accurately. From this review, we can notice that the *RC* thermal network modeling approach can be available for the modeling of dissipated heat by electrical appliances used in buildings. Moreover, since the electrical appliances have their own thermal characteristics corresponding

to their materials and structures, they can be modeled more sophisticatedly like any other heat sources that we reviewed above.

Once a model has been developed, its parameters should be identified in order to simulate the model and observe the model's behavior. The next section will present the review on the parameter identification methods especially adapted to the thermal models of the building systems.

2.3 THERMAL PARAMETER IDENTIFICATION

2.3.1 System Identification

In a process of system modeling, the system parameter identification is one of the most important steps to describe the system behavior with accurate results. Depending on modeling approaches, different parameter identification methods are used. The modeling approaches are often classified by white-box model, black-box model, and grey-box model (Figure 2. 12). These three approaches and their applications for the modeling of building systems are reminded in the following sub-sections.

White-box Model   Grey-box Model   Black-box Model
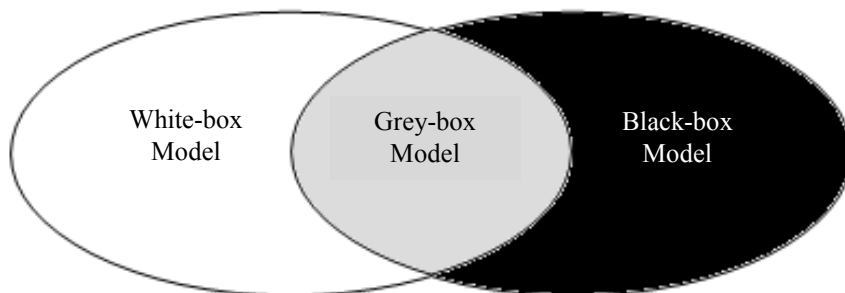
Figure 2. 12 Concept of white-box, black-box, and grey-box models

2.3.2 White-box Model

In a white-box model, both the underlying physical laws and the physical properties are known. From this information, the parameters of the model are easily obtained. The behavior of the system is described by the complete knowledge of the model, such as mathematical formulas, physical structures, and ideal parameter values of the model components. Although this approach is unrealistic since there is no complete ideal knowledge of a system, it is used in a situation where the simulation results are close to the reality.

In building modeling, the white-box models are available for analyzing the building behavior which is changed due to the different building materials or variables which influence the building energy performance [79]. Most of building simulation tools, such as TRNSYS [58],

ESP-r [80], EnergyPlus [81] and PowerDomus [82] are using conservation equations of energy and mass balance and the physical characteristics of the system which are already known.

Since accurate input data are needed for these sophisticated building simulation programs, Kosny et al. (2004) [83] developed an interactive materials database, which is based on experimental data on thermal and air tightness characteristics of building envelopes with advanced analytical methods available for thermal and energy analysis.

In order to achieve a low energy building, the cost analysis by a white-box model was done by Bambrook et al. (2011) [84] and Zemella et al.(2011) [85]. Bambrook et al. varied the insulation thickness of the walls and roof, the window type, the thickness of an internal thermal mass wall, and the night ventilation air change rate towards creating a zero energy house in Sydney. They selected an optimal case with very low space energy requirements and a photovoltaic system, in order to cover the remaining house electrical consumption over a 1-year time interval. In addition, Zemella showed optimization algorithms to be effective in identifying good solutions for the design of efficient buildings. An optimization algorithm called Evolutionary Neural Network was specially developed to be coupled with the simulation tool EnergyPlus. The optimal design of a typical envelope module for an office building was provided.

2.3.3 Black-box Model

In the cases where there is no prior information for a model structure, or interaction between the structure and the input/output of the system, the black-box model is used. It is based on a general model structure in time domain or in frequency domain. Then, the parameters of the model are identified by empirical relationships between the measured inputs and outputs.

However, the structure and the parameters are unsuitable for representing the system at all the times since these are empirically obtained through measurements for a specific condition. This approach is mostly used in order to know the thermal behavior of a whole building system. Despite of insufficient knowledge of the inner process or physical characteristics of the system, inner temperature or humidity within the building system can be at least estimated by this modeling approach.

Over the decades, linear regression methods were used in the process of parameter identification for the black-box models. Givoni (1998) [86] introduced experimental equations deducing maximum indoor temperature of ventilated building from measured data. The measurements were conducted under different conditions of window shading and closing, and ventilations. Based on the model of Givoni [86], Krüger (2004) [87] experimentally developed predictive temperature formulas for three types of occupied/unoccupied dwellings in order to predict their thermal performance. The formulas consist of the average of outdoor temperature during the whole period of a given experimental time series, the average elevation of the maximum indoor temperature and the ratios of the temperature change. The proportional values of these parameters depend on climatic conditions and of the types of houses. The black-box

prediction results were compared with both the measurements and the data obtained by COMFIE simulation tool, which uses a white-box modeling approach. The prediction results had over 0.97 of coefficients of determination (R^2)[10]. Fang and Yang (2008) [88] also introduced a specific model for a given solar heating wall. The model consists of a regression constant, an ambient temperature, a solar radiation, and a parameter design function. The function is used for sensitivity analysis of thermal performance of the model. The model was validated with the high accuracy. Furthermore, Catalina et al. (2008) [89] suggested multiple regression models in order to forecast heating energy demands of dwellings. The TRNSYS software was used in order to realize the dwellings. The input variables of the dwellings are the building shape factor, the building envelope U-value, the window to floor area ratio, the building time constant, and the climate. The outputs are the heating demand of the dwellings. As considering a number of cases, quadratic polynomial models were developed and used for the prediction of heating energy demand. Analyzing 270 different scenarii with a 1.2-5.2 % of errors validated the models.

As one of the black-box modeling approaches, linear parametric models are also used. The linear parametric models represent the relation of inputs and outputs of a system. Based on the measurements, the parameters of the models are obtained by the least square errors minimization. Among the available models, the most representative ones are the Auto-Regressive with eXogenous input (*ARX*) model, the Auto-Regressive Moving Average with eXogenous input (*ARMAX*) model, the Box-Jenkins (*BJ*) model, and the Output Error (*OE*) model. The details of these models will be explained in Chapter 4. There are some studies on these models for predicting thermal behavior of various kinds of buildings, such as a greenhouse, a classroom, an office, and a house. Frausto et al. (2003) [90] presented linear *ARX* models and *ARMAX* models in order to describe the inside air temperature of an unheated, naturally ventilated greenhouse under Western European weather conditions. They searched the model parameters for different seasons. They observed that *ARX* models performed better than the *ARMAX* models in this case. Ríos-Moreno et al. (2007) [91] also presented *ARX* and *ARMAX* models for predicting the inside air temperature of a building, particularly in a classroom. As shown in Figure 2. 13, outdoor temperature, global solar radiation flux, outdoor relative humidity, and air velocity are the input variables. The interior air temperature is the output that is predicted by the *ARX* and *ARMAX* models. The obtained results by *ARMAX* model were compared to the results of *ARX* model. They showed that the *ARX* model gives better prediction accuracy with a coefficient of determination (R^2) than the *ARMAX* model. Mustafaraj et al. (2010) [92] was carried out several parametric identification models to identify the thermal behavior of an office within a commercial building. Using external and internal climate data, recorded over the summer, autumn and winter seasons, the several models (*BJ* model, *OE* model, *ARX* model, and *ARMAX* model) were established and provided reasonably good predictions of room temperature and relative humidity. The *BJ* model outperformed all other models.

---

[10] Coefficient of determination is a square of coefficient of correlation *R*:

$$R = \frac{\frac{1}{n}\sum_{i=1}^{n}(x_i - \bar{x})(y_i - y)}{\sqrt{\sum_{i=1}^{n}(x_i - \bar{x})^2 \sum_{i=1}^{n}(y_i - \bar{y})^2}}$$
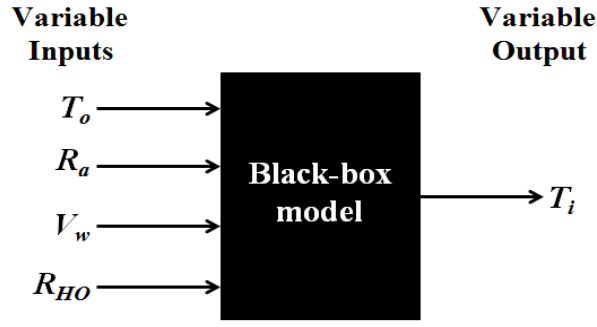
T_o: outdoor air temperature, R_a: global solar radiation flux, V_w: wind speed, R_{HO}: outdoor air relative humidity, T_i: indoor air temperature

Figure 2. 13 A block diagram of black box model used to prediction of indoor temperature [91]

Moreover, there are some studies introducing non-linear parametric models using neural network algorithms added to the linear parametric model. It aims to improve the accuracy of the parameters and the performance of the models. Mechaqrane and Zouak (2004) [93] presented an *ARX* model and a neural network auto-regressive, with exogenous input (*NNARX*) model, in order to predict the indoor temperature of a residential building. The inputs of the model were measured outdoor temperature, electrical heating power, and horizontal solar radiation. They deduced the parameters of each model and calculated the sum of squared errors (SSE) of the models. They showed that the *NNARX* model that captured some non-linearity of the building system overperformed the linear *ARX* model in a prediction error. Patil et al. (2008) [94] modeled a tropical greenhouse system using *ARX*, *ARMAX* and *NNARX* models to predict the indoor temperature of the greenhouse under tropical conditions of Thailand. Eighteen different model structures were selected and assessed by means of the coefficient of determination. The *NNARX* models performed better than the *ARX* and the *ARMAX* models. However, in order to get a good accuracy of the model during a period of a whole year, a retuning process of the models was needed. Lu and Viljanen (2009) [95] additionally applied *ARX* and *NNARX* models to the prediction of indoor temperature and relative humidity of a tested house. They extended the research to the *NNARX* model using a genetic algorithm. The genetic algorithm helped to select the order of the structures and improved the accuracy of the predictions.

As seen above, the black-box modeling permits the formulation of a building model as difference equations in the discrete-time domain, estimating the proper parameters and describing the model's behavior. However, according to Madsen and Holst [96], there are some serious drawbacks of this kind of modeling, especially in discrete-time difference equations. They stated that the formulations and the parameters cannot explain the physical meaning of the modeled system and as a consequence obtained structures are only adapted under the similar conditions where experiments were conducted. Furthermore, it is difficult to convert the discrete-time formulations into reasonable continuous-time models, owing to observational errors and a limitation with the flexibility of the obtained models.

Table 2. 4 Examples of parametric models used for building thermal analysis

Authors	Used parametric models	Applied building	Prediction variables
Frausto et al. [90]	*ARX, ARMAX*	Greenhouse	Indoor temperature
Rios-Moreno et al. [91]	*ARX, ARMAX*	Classroom	Indoor temperature
Mustafaraj et al. [92]	*ARX, ARMAX, BJ, OE*	Office within a commercial building	Indoor temperature, Indoor relative humidity
Mechaqrane and Zouak [93]	*ARX, NNARX*	Residential building	Indoor temperature
Patil et al. [94]	*ARX, ARMAX, NNARX*	Greenhouse	Indoor temperature
Lu and Viljanen [95]	*ARX, NNARX*	Unoccupied residential building	Indoor temperature, Indoor relative humidity

2.3.4   Grey-box Model

A grey-box modeling is the intermediate modeling between the white-box modeling and the black-box modeling. Although the model is relying on physical laws, the parameters of the model are unknown or there are some phenomena that are not easily described. The unknown elements within the model can be approximated by a general model structure that includes physical priors of the system. Therefore, estimated parameters have physical meaning.

Since several decades, many researchers have studied on the identification of thermal parameters of building components such as thermal conductivity, heat capacity, and convective heat transfer coefficient using grey-box models. These parameters can be determined through measurements (in laboratory or in situ) and computational estimations.

There are two measuring methods for thermal conductivity: steady-state test and transient test. The steady-state test simply seeks the temperature and the heat flux of the material. The tested material is put into the known specimens and is supplied heat flux by the specimens. While the temperature is unchanged (during steady-state), the thermal conductivity is obtained. However, high thermal conductivity measurements need a high temperature condition. It requires a long time to reach the steady-state conditions. In order to reduce time and cost of the measurements, transient tests are often used for the high thermal conductivity measurements. The transient test only needs variations of the tested material temperature. Since the property depends on the different conditions such as climatic effects and its age, etc., it needs to test in situ to analyze the building dynamics. Cuomo et al. (2006) [97] conducted the experiments in situ to obtain the thermal resistance of a building envelope. For this, they measured temperature, heat flux, and solar radiant. They calculated the thermal conductivity and heat capacity using an equivalent *RC* circuit of a multi-layered wall and evaluated them by the European standard EN 12494. Penga et Wu (2008) [98] presented three kinds of calculation methods for the building thermal resistance using the measurement data in situ. These methods are: 1) the method of

synthetic temperatures that eliminates the effect of thermal storage and calculates the thermal resistance by using the mean of temperature and heat-flow rates during a certain period, 2) the method of surface temperatures which calculates the total thermal resistance by obtaining interior convective, conductive, and exterior convective thermal resistances and summing them, and 3) the method of frequency responses in order to obtain the thermal resistances by the product of the frequency responses of heat conduction and the resistance of heat diffusion on the inner surface of buildings. They also evaluate the parameters by comparing them with the design value. They also determined the specific heat capacity of insulated materials using the transient method and compared the different values of heat capacity to the measured response.

There are also some investigations on the convective heat transfer coefficients (CHTC) by measurements. The coefficient inside the building depends on the indoor conditions (e.g. temperature distribution, air movement, internal heat gain, etc.). Therefore, the coefficient on the exterior building surface changes due to the climatic conditions, especially to the wind speed and its direction. Jayamasha et al. (1997) [99] introduced an apparatus to measure this coefficient and tested it under actual conditions. They measured wind speed, temperature difference between the tested plate and the ambient air, heat flux and absorbed solar radiation. In addition, they found out a correlation between wind speed and the CHTC. Moreover, Luo et al. (2011) [100] monitored the total heat flux and temperature of a room and estimated the room CHTC by the linear fitting method. They also calculated the thermal resistance and the heat capacity and compared them with ASHRAE[11] data to examine the accuracy.

In addition, there is also literature that presents the computational identification methods. Firstly, the thermal parameters of building envelopes can be obtained with the help of computational calculations. Gouda et al. (2002) [63] suggested reduced order lumped models for multi-layer walls of building. The *RC* parameters of the model were obtained by non-linear constrained optimization. They compared the measured internal air temperature and the simulated one. Wang and Xu (2006) [101] also proposed simple *RC* models for building envelopes. The *RC* parameters were obtained by using Genetic Algorithm optimization.

Secondly, the computational method is also used for a thermal modeling of a building subsystem. Zhang et al. (2006) [102] developed a thermal model of building subsystems in order to control the renewable energy system in the building. They used a simplified zone model that was originally introduced by Crabb et al. [103]. The model has two temperature nodes representing the air and the envelope with two dynamics. The thermal parameters of the structure and several parameters related to the heat gain were identified by a constrained evolutionary strategy. This method searches the values of the parameters that minimize the sum of the squares of the differences between the predicted and measured zone air temperatures. The obtained parameters were adapted to the building zone model for the purpose of the study. Moreover, Dong (2010) [30] presented a thermal model of an integrated building system including a building zone model, a radiant floor heating system model, and a heat pump cooling model. From experimental data on the real systems, the thermal resistances, the capacitances, the coefficients of infiltration and the solar radiation were estimated by interior-reflective Newton method [104], one of the optimization methods and then adapted to the designed

---

[11] ASHRAE: American Society of Heating, Refrigerating and Air-Conditioning Engineers

models. The simulation-based results showed that the heating, cooling, and ventilation energy reduction could reach nearly 50 % for the entire heating/cooling testing periods compared to the conventional scheduled temperature set-point. Platt et al. (2010) [105] presented an adaptive HVAC zone modeling in order to provide control of energy flows within a building. An HVAC zone is modeled by simple *RC* circuit, airflow rate, wall thermal resistor, leakage of the zone, etc., were estimated by genetic algorithm using measured variables that are average zone temperature, outside temperature and supplied air temperature. Computational calculations based on physical laws and measurements are all the more useful that the studied building is complex.

While the above studies presented building systems in continuous-time differential equations, the below studies were carried out in discrete-time difference equations. Madsen and Holst (1995) [96] established a thermal dynamic model to describe indoor temperature variations of a building. The model was first formulated as stochastic linear differential equations in continuous-time, and then converted to discrete-time forms. The discrete-time model permits the use of experimental data that was sampled in discrete-time. A maximum likelihood function was selected to estimate the model parameters from the data. Jiménez and Madsen (2008) [106] introduced several models for describing thermal characteristics of building components. Continuous-time linear models in state space form, discrete time models in state space form, discrete-time transfer function form, and linear regression model in stationary operating conditions were presented. Non-linear models were also investigated. From these model structures, the thermal characteristics such as thermal transmission coefficient and solar transmittance of the tested component were estimated. Jiménez et al. (2008) [107] also presented a method to determine U-value and global solar irradiance on the external surface of building envelopes at steady-state. The building dynamics were modeled by a general structure of the *ARMAX* model, with respect of the heat balance equation. The model parameters were estimated by output error method and prediction error method. Moreover, the obtained parameters were physically interpreted. Bacher and Madsen (2011) [71] subsequently suggested several models of heating system using *RC* components for the heat dynamics of a building. A stochastic linear state-space model was also established. Then, the corresponding coupled data-driven model, represented by the discrete-time measurement equation was used for parameter estimations. The performance of each model was evaluated by likelihood ratio test. Wu and Sun (2012) [108] recently presented a physics-based *ARMAX* (*pbARMAX*) model of temperature in office buildings. The heat balance equations were used to select the structure and the order of the *ARMAX* model. The ensemble parameters of the room, the HVAC system, and the outside air were estimated with the least square method. The performance of *pbARMAX* model was compared to the performances of the different *ARMAX* models and was consistently better than the others.

In this section, we reviewed several parameter identification methods used for white-box, black-box and grey-box models, which are especially adapted to the models of building systems. After the modeling of an electrical appliance and the identification of its model parameters completed, the model is integrated into a building model. The goal is to observe the effect of the electrical appliance on the thermal behavior of the building. For this, we should select a building simulation tool that permits an easy integration of the thermal models for electrical appliances. We will now overview the most popular building simulation tools.

2.4 BUILDING SIMULATION TOOLS

2.4.1 Overview

Since the 1960s, building simulation tools have been developed and upgraded mainly for improving the energy performance of buildings. The directory of U.S. Department of Energy (DOE) advises that there are more than 400 building simulation tools for improving energy efficiency and sustainability, load calculation, renewable energy installation, and retrofit analysis of buildings. The most representative simulation tools are ESP-r, TRNSYS, EnergyPlus, SPARK, DOE-2, and SIMBAD.

Clarke (2001) [109] provided an evaluation of building simulation tools and demonstrated the process of dynamic thermal simulation of buildings. Figure 2. 14 shows the energy flow path that explains dynamic thermal energy interaction between interior and exterior of a building. Each component of a building has thermal nodes and is connected to each other. This overall flow path can be represented by several equations and electric circuits. The simulation tools have been improved in terms of rapidity and accuracy.
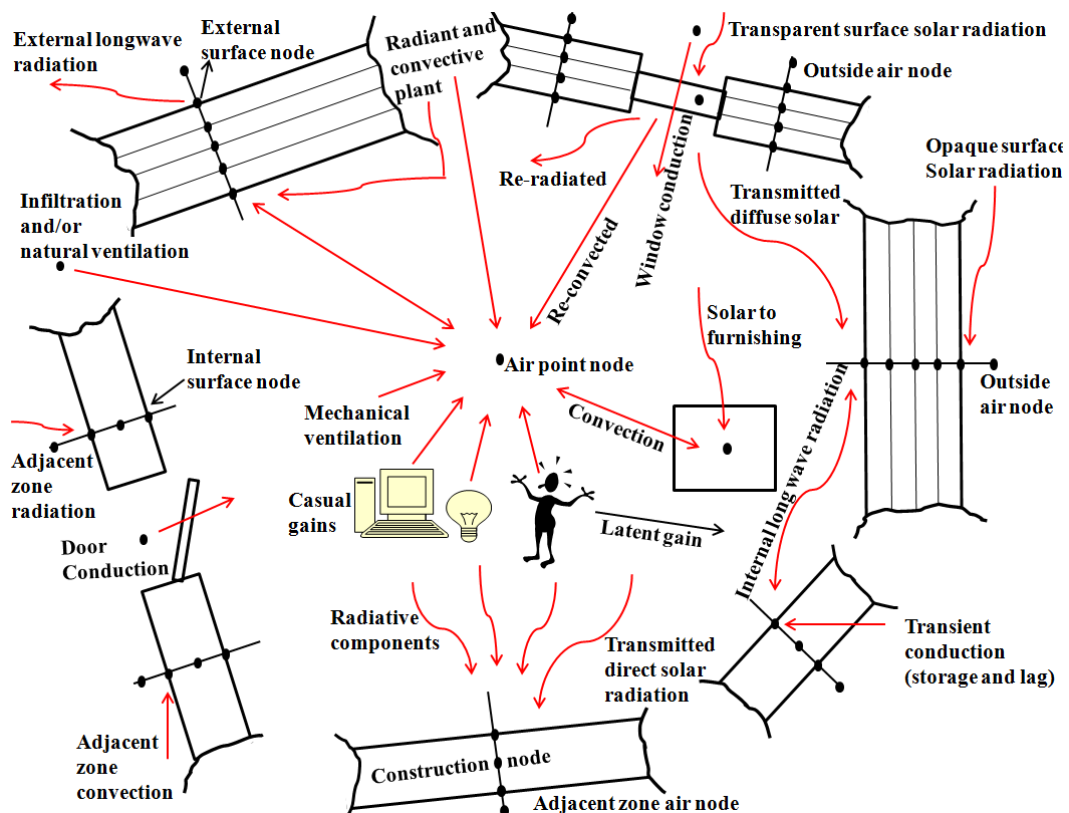
Figure 2. 14 Building energy flowchart [109]

2.4.2 Comparative Study of Simulation Tools

Since each of the building simulation tools has its own language, functions, and calculation methods, it is not easy to select a suitable tool for a given purpose. In order to provide the basic features and capability of the tools to users, several comparative studies on the simulation tools were performed.

Hong and al. (2000) [110] described the state-of-the art building simulation tools. They classified the tools by their applications, availability and furthermore gave the directions on how to choose the suitable tools. According to them, the building simulation tools are applied to the following: 1) building heating/cooling load calculation, 2) energy performance analysis for design and retrofitting, 3) building energy management and control system design, 4) complying with building regulations, codes and standards, 5) cost analysis, 6) studying passive energy saving options, 7) computational fluid dynamics, and so on. The simulation tools have been developed in accordance with their applications. For example, DOE-2 and ESP-r were developed for building energy performance simulations while TRNSYS, HVACSIM+, and SIMBAD were developed for HVAC system simulations. Functionalities of simulation tools have been enhanced for wide use in training.

Crawley et al.(2008) [111] compared twenty major building energy simulation programs: BLAST, BSim, DeST, DOE-2.1E, ECOTECT, Ener-Win, Energy Express, Energy-10, EnergyPlus, eQuest, ESP-r, IDA ICE, IES <VE>, HAP, HEED, PowerDomus, SUNREL, TAS, TRACE, and TRNSYS. Their report detailed up to 14 categories: general modeling features; zone loads; building envelope and day-lighting and solar; infiltration, ventilation and multi-zone airflow; renewable energy systems; electrical systems and equipment; HVAC systems; HVAC equipment; environmental emissions; economic evaluation; climate data availability, results reporting; validation; and user interface, links to other programs, and availability.

Doyle (2008) [112] dealt with several representative simulation tools such as EnergyPlus, ESP-r, TRNSYS, TAS, IES <Virtual Environment (VE)>, national building simulation tools and international comparative projects. Aforementioned tools were analyzed under the following headings: 1) Thermal characteristics and air tightness, 2) Heating installation and hot water supply, 3) Air-conditioning installation, 4) Built-in lighting installation, 5) Position, orientation and outdoor climate, 6) Passive solar systems and solar protection, 7) Natural ventilation, 8) Indoor climatic conditions, 9) Active solar and renewable energy systems, 10) Electricity produced by CHP [12], 11) Natural lighting, 12) Validation. Based on these comparisons, he presented a basic office building energy performance package using the IES <VE> tool and benchmarks the results with other products.

According to the above comparative studies, we briefly describe several selected simulation tools which are EnergyPlus, ESP-r, TRNSYS and SIMBAD.

---

[12] CHP: Combined Heat and Power

ESP-r: In 1974, the Energy Systems Research Unit (ESRU) at the University of Strathclyde in Glasgow developed the Environmental System Performance (ESP-r) tool. The energy and mass flows within a combined building and plant systems are modeled by attributions from basic data of construction, internal heat gain, and ventilation and infiltration of the systems. The project manager of ESP-r deals with the database management, problem description, simulation invocation, and result analysis. It provides the assessment of the thermal, visual, and acoustic performance of buildings and the energy use. Moreover, it is an open source program available to download from the website of the ESRU at University of Strathclyde.

TRNSYS: TRaNsient SYStems simulation (TRNSYS) was developed by the Solar Energy Laboratory (SEL) of the University of Wisconsin-Madison and the Solar Energy Application Lab of the University of Colorado. It was developed for modeling of active solar systems and commercially released in 1975. This tool is primarily used to simulate the transient performance of thermal energy systems. It is based on a modular structure that implements a component-based approach. Each physical component of the systems is represented by a different FORTRAN subroutine. New components are available to be developed in any programming language and modules implemented by using other software such as Matlab/Simulink® and Excel/VBA, and to be directly embedded into a simulation. The components and the building input data are configured into visual interfaces. The simulation engine solves the algebraic and differential equations of the whole energy system according to its specifications.

EnergyPlus: EnergyPlus is a whole building energy simulation tool developed by the U.S. DOE in cooperation with the U.S. Army Construction Engineering Research Laboratory. It is based on the most popular features and capability of BLAST[13] and DOE-2[14]. EnergyPlus models heating, cooling, lighting, ventilation, other energy flows, and water use. It includes many innovative simulation capabilities: intra-hour time steps (15 min default), modular systems and plant integrated with heat balance-based zone simulation, multi-zone air flow, thermal comfort, water use, natural ventilation, and photovoltaic systems [113]. It has three basic components as illustrated in Figure 2. 15: a simulation manager, a heat and mass balance simulation module, and a building systems simulation module. Text files and modules describe a building. The simulation manager controls the entire simulation process, handles communication between the heat balance engine and various building systems simulation modules. It interacts with other simulation tools such as SPARK[15] and TRNSYS. For analysis of the simulation results, it relies on third party user interfaces.

---

[13] BLAST: Building Loads Analysis and System Thermodynamics. It was developed by Building Systems Laboratory of University of Illinois. Its major subprograms are space load prediction, air system simulation, and central plant.

[14] DOE-2 is a widely used and accepted building energy analysis tool. It predicts the energy use and cost for all types of buildings. It uses a description of the building layout, constructions, operating schedules, conditioning systems (lighting, HVAC, etc.) and utility rates provided by the user, along with weather data, to perform an hourly simulation of the building and to estimate utility bills (reference: http://doe2.com/).

[15] SPARK: Simulation Problem Analysis and Research Kernel. It was developed by Lawrence Berkley National Laboratory (LBNL) and Ayres Sowell Associates with support from the U.S. DOE. It is a building simulation tools which is an object-oriented program that allows the user to quickly build models of complex physical processes by connecting equation-based calculation modules from an object library (references: http://gundog.lbl.gov/VS/spark.html,
http://apps1.eere.energy.gov/buildings/tools_directory/software.cfm/ID=111/pagename=alpha_list_sub)
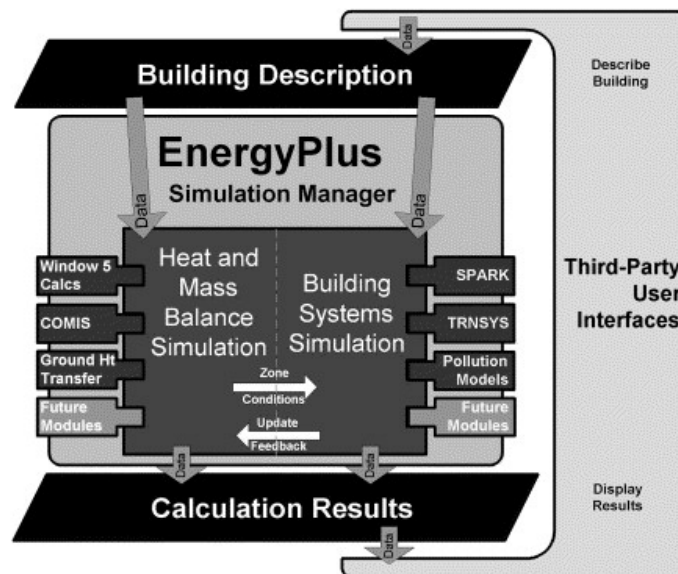
Figure 2. 15 The overall structure of EnergyPlus [114]

SIMBAD: SIMulator of Building And Devices (SIMBAD) was developed by the CSTB[16] in purpose of testing BEMS[17]. The SIMBAD software permits to simulate different types of buildings with heating/cooling/air conditioning equipment. It includes a simulation environment within Matlab/Simulink®, building and climatic equipment models, typical installations with different operating states, and profiles of climate and internal loads [115]. It has three levels of hierarchy in a graphical interface, as illustrated in Figure 2. 16. The basic blocks are in the current library of the software. The first level of the components is called a component-block. Assembled component-blocks is called a macro-block. It corresponds to the complex components of the equipment (e.g. fan-coils, air handling units). A combination of the component-blocks and the macro-blocks is called a system-block. It represents a real system. The realization of block diagram environment is one of the benefits of this tool. It is user-friendly and automatically integrates any improvement in the simulation environment. The graphical interface makes the configuration of the systems easier [78].
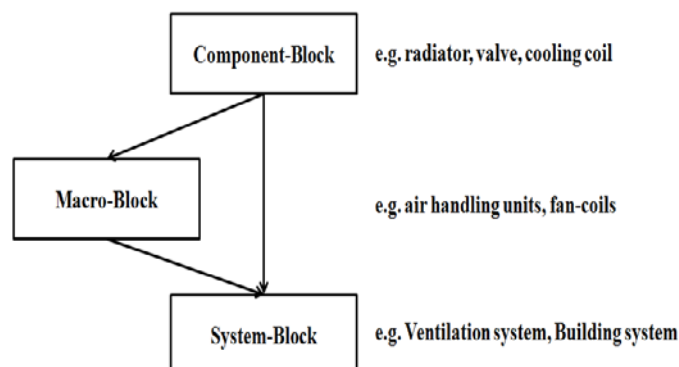
Figure 2. 16 The levels of hierarchy in the block diagram environment [78]

---

[16] CSTB: Centre Scientifique et Technique du Bâtiment (French Scientific and Technical Centre for Building)

[17] BEMS: Building Energy Management Systems

Moreover, the components can be linked to m-files, C language or FORTRAN files. As the demand of the control of the building equipment increases, the building simulation tools tend to be coupled with Matlab/Simulink® for the co-simulation with this software. It makes it easier to adapt the predefined blocks and functions into the building systems designed in SIMBAD. In addition, a simulation time step can be simply modified by users and therefore intra-hour simulation is also available.

In order to integrate the thermal model of electrical appliances that will be presented in this thesis work, we will select the SIMBAD software among the presented simulation tools. There are facilities to adapt the models defined in the interface of Matlab/Simulink® to the building models designed in SIMBAD. By integrating the thermal models of electrical appliances in a building model of SIMBAD, we can then observe the thermal influence of the electrical appliances on the building thermal behavior, the thermal comfort of occupants, and the energy consumption of the building.

Before starting the next chapter, we discuss the uncertainty of input data required to utilize building simulation tools for analyzing the building energy performance.

2.4.3   Uncertainty of Simulation Tools

With the help of the validated building simulation tools, energy performance of a building can be evaluated. It is obvious that the results of the evaluation differ from the combined system of the building and its sub-systems. Among these components of the system, there are internal heat gains caused by solar radiation, electrical appliances and occupant's behavior. These gains have been taken into account for the heating/cooling load calculation. In a low energy building, for which thermal insulation is reinforced, the internal heat gains may become decisive for the building energy consumption and the thermal comfort of the occupants. However, it is not easy to predict these gains because of their uncertainties. Almost all of the simulation tools have used the past weather information and the pre-determined profiles of electric load usages and occupancy.

These uncertainties of heat gains have caused retrofit errors between the simulation and the validation of energy analysis of buildings [23,24]. Along this line, Roulet (2002) [116] showed that the uncertainty caused by internal heat gains propagates larger relative errors when the annual heating energy consumption of a building is calculated. The used calculation methodology was proposed as the European Standard EN 13790 2004 [117]. It includes the calculation of heat losses of the heated building at a constant internal temperature, internal heat gains of the building, and annual heat demand required to maintain specified set point of temperatures. The study states that different users obtain different results by as much as 20 % and that comparisons to the actual buildings lead to a difference in energy use from 50 %to 150 % due to assumptions on occupant behavior and airflow rates. Moreover, a study carried on by Karlsson et al. (2007) [118] states that the annual predicted total energy demand of a Swedish low energy house by using three different simulation tools deviated by approximately 2 %. The energy use deviation due to airflow control was about 10 %, the deviation due to differences in heat exchanger efficiency was about 20 %, and the deviation in annual energy use due to

differences in internal gains was 7 %. In addition, when comparing the predicted energy use during the design process of the low-energy building with actual measurements after the occupants have moved in, the difference reached about 50 %. From these results, they concluded that the differences due to the occupant's behavior were much more important than the differences due to the change of the simulation tool. For this reason it is mandatory to develop more accurate models of the internal heat gains.

In order to reduce the uncertainty of the building simulation, many researchers have specifically carried out non-predictable heat gain models, such as solar radiation models [26,37,67,119], both deterministic and stochastic models of occupant's behavior and lighting usages [38,120,121,122], and fewer works on metabolic heat gains by occupants [71,72] in buildings.

Among the above studies on heat gain models, there are only a few works on the modeling of heat gain of electrical appliances [32,33]. Since the heat gain due to the power dissipation of appliances within a normal building was too small to compensate for the heat losses by the building envelopes, it was not necessary to model them accurately before. However, in a low energy building, the heat gain by appliances becomes more important. In addition, despite the increasing energy-efficiency of appliances, power consumption continues to grow as the usage of various appliances has increased [123]. In this context, it is necessary to introduce a generic thermal model of electrical appliances. By integrating this model to a building model, more rapid thermal dynamics of the building system including building envelopes and its sub-systems will be captured. It can also provide data to the intra-hour simulations expected for more reliable results and accuracy of simulations of the thermal model.

2.5 CONCLUSION

This chapter has made an in-depth presentation of the methodologies on how to thermally model building systems, including buildings and their sub-systems. Whole building system modeling, as well as building sub-system modeling from the external building envelope models to the internal heat gain models, were presented. Most of the examples were carried out applying a thermal network method.

Then, the parameter identification methods adapted for the building models were introduced with a number of examples. In order to describe the thermal behavior of buildings, several modeling approaches were used including white-box, black-box, and grey-box modeling. According to the physical laws, the physical properties and characteristics, or a mathematical relationship between input and output of a building system, the relevant parameters of models were obtained with the help of the measurements and the identification methods.

Finally, the state-of-the-art building simulation tools were presented. Several references of comparative studies on the simulation tools were given. The uncertain factors of simulation tools were also discussed.

Based on the above literature review, several emerging issues are required in order to achieve a more accurate analysis of building energy performance and thermal comfort. The followings are the main interests of this thesis.

- Investigation of thermal effect of electrical appliances in a well-insulated building,
- Development of a generic thermal model of electrical appliances,
- Identification of the parameters of the generic thermal model of several appliances,
- Simulation of whole building model and analysis of the effects of the appliances on the thermal balance of the building and the comfort of the inhabitants

Now that the problematic issues were brought out by literature review, the next step is to present a method on how a generic thermal model of electrical appliances can be developed. The model will influence the thermal behavior of a well-insulated building. In order to quantify and model the heat gain due to electrical appliances, it is necessary to achieve experiments on electrical appliances and to model a test room where the experiments are carried out. As a consequence, the next chapter will present the experimental set-up and the modeling methodology for a single quasi-adiabatic room in which the electrical appliances have been tested.

Chapter 3

THERMAL MODELING OF
A WELL-INSULATED ROOM

3.1 INTRODUCTION

In order to reduce heating energy demand and CO_2 emission of buildings, thermal insulation has been reinforced [124,125]. The well-insulation prevents losing unwanted heat loss of buildings through their structures and envelopes. As a consequence, internal heat gains (auxiliary heat gains, free heat gains) obtained by solar radiation, metabolism, and heat dissipation of home electrical appliances (i.e. a refrigerator, a lamp, a television, etc.) have to be considered for global energy management of low energy buildings, especially in summer or winter period [19].

According to the energy balance of buildings, the thermal characteristics of buildings have an important role in determining the thermal influence of auxiliary heat gains on buildings. In order to evaluate thermal influence of auxiliary heat gains due to home electrical appliances, especially in a low energy building, it is preliminarily necessary to thermally characterize a building and understand its thermal behavior. Once identifying thermal characteristics of the building, it is possible to quantify and model the free heat gain of home electrical appliances. To this purpose, we thereby establish a thermal model of a well-insulation room. It is considered as a small scale laboratory set-up of a low energy building in this chapter.

As seen in the previous chapter, literature introduced a thermal network method using thermal-electrical analogy for thermal modeling of building systems [63,64,101,126,127,128]. Most of these building models are based on the energy balance equation. Using this equation, building thermal parameters which are thermal resistance and thermal capacitance as well as local conditions (outdoor/indoor temperature and internal gains by solar radiation, metabolic

heat and electrical appliances) are converted to the electrical circuit components, such as a resistor, a capacitor, a voltage source, and a current source.

In this chapter, we establish a thermal model for a well-insulated room using the thermal network method. The building energy balance equation is overviewed at the beginning of this chapter. The focus is then narrowed from a conventional building to a chosen quasi-adiabatic test room which represents a small scale laboratory set-up of a low energy building. Then, the experimental set-up and the procedures for characterizing the test room are presented. Lumped *RC* parameter circuits are suggested as the models of the test room using thermal-electrical analogy. Thereafter, thermal parameters of the model components are estimated from experimental results and parameter identification methods. Based on the proposed model structures and their parameters, the thermal behavior of the test room implemented on Matlab/Simulink® is then simulated. The simulation results are compared to the measured data in order to validate the models and verify their accuracy. Finally conclusions are given.

3.2 BUILDING ENERGY BALANCE

3.2.1 Overview

The building energy balance corresponds to the conservation of energy within a building. It is based on the first law of thermodynamics, which states that energy cannot be created or destroyed, only modified in form or transferred from one place to another [129]. The boundary of the building energy balance is the envelope of a building. The energy entering into the building across the envelope U_{in} is equal to the sum of the energy going out through the envelope U_{out}, and the energy stored in the building's thermal mass U_{stored}. It yields:

$$U_{in} = U_{out} + U_{stored} \tag{3.1}$$

where U is the energy [J]. There are various types of energy U_{in}, which are supplied to a building. It can be:

- Electricity,
- Fuels (gas, oil, coal, wood, etc.),
- Solar energy by radiation,
- Heat produced by any types of heater,
- Metabolic heat of habitants and animals,
- Joule heat dissipation of electrical appliances,
- Etc.

Those kinds of energy are finally transformed into heat and transferred by conduction, convection, and radiation. It means that the forms of energy outward the building U_{out} and the stored energy inside the building U_{stored} are heat. The heat balance of the building is then expressed by:

$$\dot{Q}_{in} = \dot{Q}_{out} + \frac{dU_{stored}}{dt} \qquad (3.2)$$

where $\dot{Q}_{in}$ is the heat gain [W], $\dot{Q}_{out}$ is the heat loss [W] of the building and t is the time [sec]. At steady-state, it yields:

$$U_{in} = U_{out} \qquad (3.3)$$

$$\dot{Q}_{in} = \dot{Q}_{out} \qquad (3.4)$$

From this, it is known that in the case where the temperature of a building is constant, the sum of the heat gains into the building is equal to the total heat losses of the building during the considered period. Table 3. 1 shows the major sources of heat gains and losses of buildings.

Table 3. 1 Main sources of heat gains and heat losses of buildings

Heat gain	Heat loss
Contributed heat gain by electricity	Heat transmission through building envelopes
Contributed heat gain by fuels	Heat transmission through floors and ceilings
Contributed heat gain by solar energy	Heat loss by thermal bridge
Thermal radiation by exterior objects	Heat loss by ventilation
Thermal radiation by building components	Thermal storage of building structure and
Metabolic heat gain by occupants	furniture
Joule heat dissipation of electrical appliances	Hot water consumption

Figure 3. 1 depicts a Sankey diagram of a building energy balance [130]. It shows global heat fluxes of a building. As stated above, heat fluxes generated by the operation of heating installation and electrical appliances, solar energy, metabolism, and recovered heat are the heat gains of the building. On the contrary, a part of heat is mainly lost through envelopes, ventilation & infiltration, and hot water consumption. According to the diagram, the demand of local heating energy flux depends on the quantity of the heat gains and losses. For achieving a low energy building, the part of the usable free heat gains has to increase. At the same time, the part of the heat losses has to decrease.

A mathematical expression of the diagram is:

$$\dot{Q}_{heating} + \dot{Q}_{sun} + \dot{Q}_{metabolism} + \dot{Q}_{appliance} + \dot{Q}_{recovery} = \dot{Q}_{transmission} + \dot{Q}_{ventilation} + \dot{Q}_{infiltration} + \dot{Q}_{hotwater} \qquad (3.5)$$
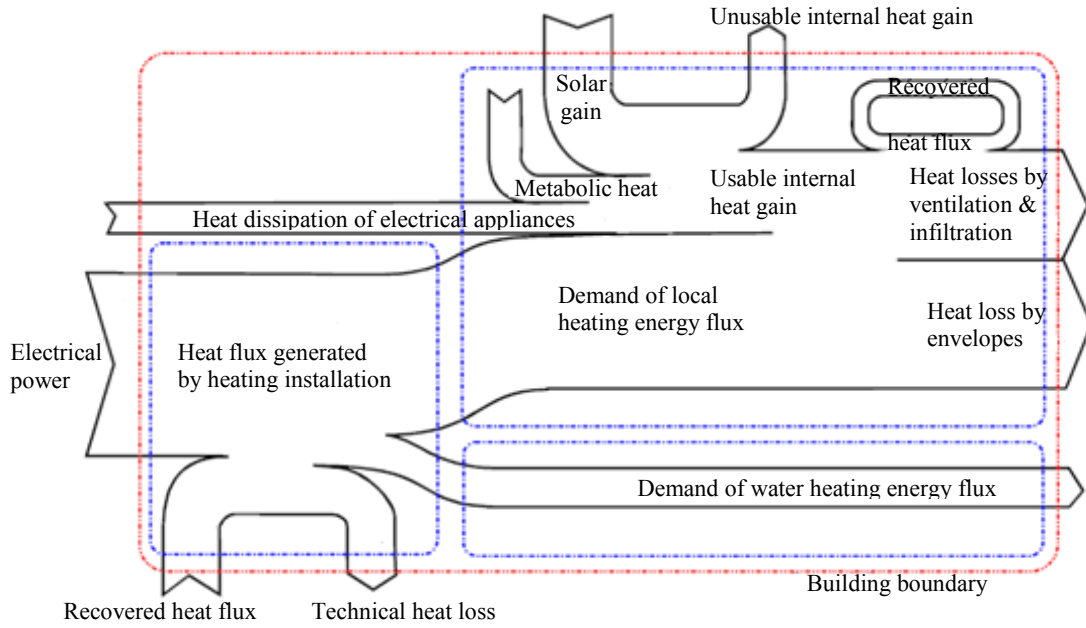
Figure 3. 1 Diagram of global heat fluxes of a building [130]

where

$\dot{Q}_{heating}$ is the heat gain contributed by electricity and fuels for heating a building [W],

$\dot{Q}_{sun}$ is the free internal heat gain of solar energy [W],

$\dot{Q}_{metabolism}$ is the free internal heat gain of metabolism of occupants [W],

$\dot{Q}_{appliance}$ is the internal heat gain by heat dissipation of electrical appliances [W],

$\dot{Q}_{recovery}$ is the recovered heat flux [W],

$\dot{Q}_{transmission}$ is the transmission heat loss through building envelopes (walls, windows, ceilings, floors and doors) [W],

$\dot{Q}_{ventilation}$ is the heat loss by ventilation [W],

$\dot{Q}_{infiltration}$ is the heat loss by infiltration [W],

$\dot{Q}_{hotwater}$ is the heat loss by hot water consumption [W].

The entering fluxes are distinguished into contributed heat gains by electricity or fuels, and free heat gains. The heat gain contributed by electricity or fuels for heating a building, $\dot{Q}_{heating}$ is the difference of the total free heat gains and the heat losses of the building.

The free internal heat gain obtained by solar energy is:

$$\dot{Q}_{sun} = \sum_j \dot{Q}_{sun,j} = \sum_j I_{sun,j} \left(\sum_n A_{sun,n,j} \right) \tag{3.6}$$

where, j is the number of the different orientations of a building, n is the number of surfaces of the building, $\dot{Q}_{sun,j}$ is the solar heat gain for the jth orientation [W]. $I_{sun,j}$ is the solar irradiation for

the jth orientation [W/m^2], $A_{sun,n,j}$ is the equivalent n^{th} effective surface which captures the solar irradiation for the jth orientation [m^2]. It is the product of the real surface, shading factor and transmission coefficient of nth surface. In addition, the amplitude of $\dot{Q}_{sun}$ depends on materials, locality, and weather conditions of the building.

- The free internal heat gain due to metabolism of occupants is stated:

$$\dot{Q}_{metabolism} = \sum_k \Phi_{metabolism,k} \tag{3.7}$$

where, k is the number of occupants, $\Phi_{metabolism,k}$ is the mean of metabolic rate of the kth occupant [W]. The mean of metabolic rate of a daily activity was given in the previous chapter.

- The internal heat gain due to electrical appliances is:

$$\dot{Q}_{appliance} = \sum_l P_{appliance,l} \tag{3.8}$$

where, l is the number of electrical appliances, $P_{appliance,l}$ is the power dissipated by the lth electrical appliance [W].

- The free internal heat gain due to a mechanical heat recovery ventilation $\dot{Q}_{recovery}$, is:

$$\dot{Q}_{recovery} = \dot{Q}_{ventilation} \cdot \eta_{recovery} \tag{3.9}$$

where $\dot{Q}_{ventilation}$ is the heat loss by the ventilation equipment (eq.(3.11)), $\eta_{recovery}$ is the re-circulated air rate (from 0 to 1) to recover the thermal energy of air.

- The transmission heat loss through the building envelopes (walls, windows, ceilings, floors, and doors) is:

$$\dot{Q}_{transmission} = H_t (T_{in} - T_{out}) \tag{3.10}$$

where, H_t is the total transmission coefficient of the building across its envelopes (walls, windows, ceilings, floors, doors, roofs) [W/°C]. T_{in} is the indoor temperature of the building [°C], T_{out} is the outdoor temperature of the building [°C].

- The heat loss by a ventilation equipment $\dot{Q}_{ventilation}$, is calculated as below:

$$\dot{Q}_{ventilation} = \rho_{air} c_{p,air} \dot{V}_{ventilation} (T_{in} - T_{out}) \tag{3.11}$$

where ρ_{air}, $c_{p,air}$ and $\dot{V}_{ventilation}$ are respectively the air density [kg/m^3], the specific heat of air [J/(kg·°C)] and the air flow rate [m^3/s] through the ventilation equipment. The heat loss due to

ventilation is simplified as eq.(3.12) with the assumptions, which are ρ_{air}=1.2 [kg/m^3] at 20 [°C] and $c_{p,air}$=1000 [J/(kg·°C)] [131].

$$\dot{Q}_{ventilation} = 0.33 \times N_{change} V_{zone} (T_{in} - T_{out})$$ (3.12)

where N_{change} is the number of air change per hour. It is fixed by designers and determinant to minimize the heat loss by the ventilation. V_{zone} is the volume of the building zone [m^3]. The indoor/outdoor temperature difference depends on the location of the building.

● The heat loss due to infiltration is:

$$\dot{Q}_{infiltration} = \rho_{air} c_{p,air} \dot{V}_{infiltration} (T_{in} - T_{out})$$ (3.13)

where $\dot{V}_{infiltration}$ the air flow rate [m^3/s] due to the infiltration through unsealed surfaces and thermal bridges. The infiltration is the uncontrolled air exchange between the interior and the exterior of a building through air leakage path. According to Sherman and Grimsrud (1980) [132], the air flow rate due to infiltration, which uses the effective air leakage area, is calculated as follows:

$$\dot{V}_{infiltration} = A_{leakage} \sqrt{C_{stack} (T_{in} - T_{out}) + C_{wind} v_{wind}^2}$$ (3.14)

where $A_{leakage}$ is the effective air leakage area [m^2], C_{stack} and C_{wind} are the stack coefficient and wind coefficient, respectively. The values of C_{stack} and C_{wind} are equal to 0.015 and 0.0065 for a one story house. v_{wind} is the local wind speed [m/s].

● The heat loss by hot water consumption is [30]:

$$\dot{Q}_{hotwater} = \rho_{water} c_{p,water} \dot{V}_{escape} (T_{in} - T_{out})$$ (3.15)

where ρ_{water}, $c_{p,water}$ and $\dot{V}_{escape}$ are, respectively the water density [kg/m^3], the specific heat of water [J/(kg·°C)], and the escaped water flow rate [m^3/s] through pipes.

According to the building heat balance equation, the total heat gains are equal to the total heat losses. Hence, obtaining the maximum internal heat gains and minimizing heat losses helps reducing the heating energy consumption of buildings which accounts for more than 40 % of total energy consumption in conventional buildings.

The factors which influence the quantity of heat gains and losses are building location (environment, weather condition and climate), building envelopes, occupants' activities, usage profiles of the electrical appliances, HVAC equipment design, etc. Table 3. 2 lists the dominant factors of each heat flux.

Table 3. 2 Dominant factors of heat gains and losses of a building

	Dominant factors				
	Building Location	Building Envelopes	Occupants' Activities	Usage profile of appliance	Equipment Design
$\dot{Q}_{sun}$	√	√	√	-	-
$\dot{Q}_{metabolism}$	-	-	√	-	-
$\dot{Q}_{appliance}$	-	-	√	√	-
$\dot{Q}_{recovery}$	-	-	-	-	√
$\dot{Q}_{transmission}$	√	√	-	-	-
$\dot{Q}_{ventilation}$	√	-	-	-	√
$\dot{Q}_{infiltration}$	√	√	-	-	-
$\dot{Q}_{hotwater}$	√	-	√	-	-

Amongst heat gains, $\dot{Q}_{metabolism}$ and $\dot{Q}_{appliance}$ are strongly related to the behavior of occupants. Since the production of these heat gains is unpredictable and uncontrollable and since the corresponding quantity is not so much compared to both $\dot{Q}_{sun}$ and $\dot{Q}_{transmission}$ in conventional buildings, such fluxes were not accounted in details. For example, Lubina et al. (2009) [133] conducted on several simulations, considering different occurrences of heat gains due to internal heat sources in link with the occupants' activities like lighting and appliance usage. They found that heat gains which are obtained by such internal heat sources account for 13-24 % of heat losses balance of analyzed flats, which are poorly insulated. At the same time, the solar gain varied from 12 % to 72 % of heat losses of the same flats.

3.2.2 Low Energy Building

Now, the focus is narrowed only on low energy buildings. Figure 3. 2 depicts different heating energy demands of a conventional building and a low energy building. In order to get the same level of thermal comfort and the same indoor temperature, the low energy building needs less heating energy than the conventional building.

In terms of low energy building designs, a high thermal insulation techniques lead to a reduction of heat losses and of heating energy supply. In addition, minimization of the heat losses due to ventilation and infiltration are one of the solutions to design a low energy building [11]. For example, controllable mechanical heat recovery ventilation equipment can be used.
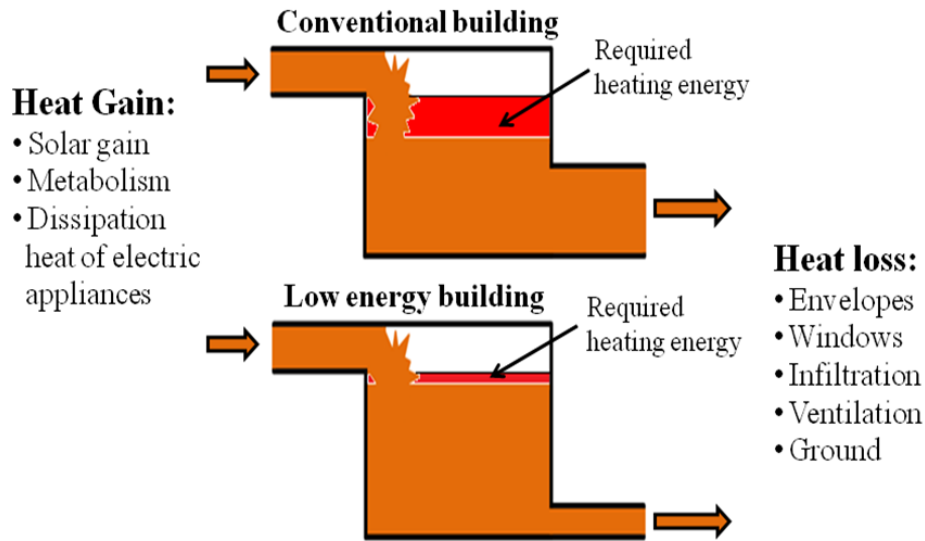
Figure 3. 2 Heat flux in building

Blight et al. (2011) [134] states that one should maximize thermal insulation of buildings, minimize thermal bridges and uncontrolled air exchange in order to achieve low space heating and cooling limits of no more than 15 [kWh/m^2], which is delivered energy. References [135,136,137] additionally prove that improving the quality of materials, and construction methods have significantly reduced the amount of energy demand of the corresponding buildings.

Moreover, several studies have indicated that the behavior of occupants play an increasingly important role in building energy consumption, especially in more energy efficient buildings. It means that the temporal profiles of the occupants' behavior and usage of electrical appliances in low energy buildings have to be considered [134,138,139,140,141]. As one of the relevant investigation, a study carried out by Ferdyn-Grygierek et al. (2011) [142] indicates that the heat gains of internal heat sources is becoming dominant in a low energy building. The investigation shows that the assumed internal heat gains produced by occupants' metabolism, computers, and lighting within a low energy building compensates heating energy losses of the building. Therefore, this building does not require any more heating energy, even though when the outdoor temperature becomes low.

We presented the heat balance of the low energy building and the modeling of its elements. From this principle, we are focusing on the heat balance of a chosen quasi-adiabatic test room in the following subsection. The selected one is a small scale laboratory set-up of a low energy building. This part permits to investigate the thermal influence of electrical appliances in low energy buildings.

3.2.3   Quasi-Adiabatic Test Room

A quasi-adiabatic test room is chosen in this thesis work. It aims to study the thermal impact of the heat flux dissipated by electrical appliances into a low energy building. We

suppose that there is only $\dot{Q}_{appliance}$ as a heat gain of the quasi-adiabatic room. Other heat sources, which are $\dot{Q}_{heater}$, $\dot{Q}_{sun}$, $\dot{Q}_{metabolism}$, $\dot{Q}_{recovery}$, $\dot{Q}_{ventilation}$, $\dot{Q}_{infiltration}$, and $\dot{Q}_{hotwater}$, are not considered.

As a consequence, the heat balance of the quasi-adiabatic test room is derived from eq.(3.2).

$$\dot{Q}_{appliance} = \dot{Q}_{envelope} + \frac{dU_{stored}}{dt} \qquad (3.16)$$

where $\dot{Q}_{envelope}$ is the sum of heat losses through the test room envelopes. The quantity of the stored and lost heat depends on the thermal characteristics of the room.

The next section will describe the chosen quasi-adiabatic test room. In order to thermally characterize the test room, the experimental set-up and the measurement procedures will be introduced.

3.3 EXPERIMENTAL SET-UP AND PROCEDURES

3.3.1 Quasi-Adiabatic Room Description

The quasi-adiabatic test room is located in the University of Cergy-Pontoise, at Neuville, France. This room is one of the well-insulated rooms of the site (Figure 3. 3). It has 9.6 m^2 of floor surface and 2.4 m of height. The wall is made up with polyurethane and stainless steel sheet. It has a door (length: 0.9 m, height: 1.9 m) with the same materials as the wall, and a small window (length: 0.3 m, height: 0.5 m). It has four incandescent lamps (60 W x 2 EA, 75 W x 2 EA) which are positioned on upper side of the walls (x-z plane). An air conditioning system to control the humidity and the temperature of the room is also installed in the room but it was not used. Figure 3. 4 and Figure 3. 5 show the test room and the position of lamps.

3.3.2 Experimental Measurements

3.3.2.1 Temperature Measurement

The test room has twenty K-type thermocouples. These thermocouples are used for measuring the indoor air temperature, the indoor wall surface temperature, the outdoor wall surface temperature, the outdoor temperature, and the surface temperature of any electrical appliance. The standard deviation of the thermocouples is about 0.03 °C at stable conditions. Appendix A describes in details the used thermocouples. The positions of the thermocouples to measure the temperatures within the room are shown in Figure 3. 6.

Quasi-Adiabatic test room

Figure 3. 3 Top view of the building site

(a) Exterior   (b) Interior

Figure 3. 4 Features of the quasi-adiabatic room
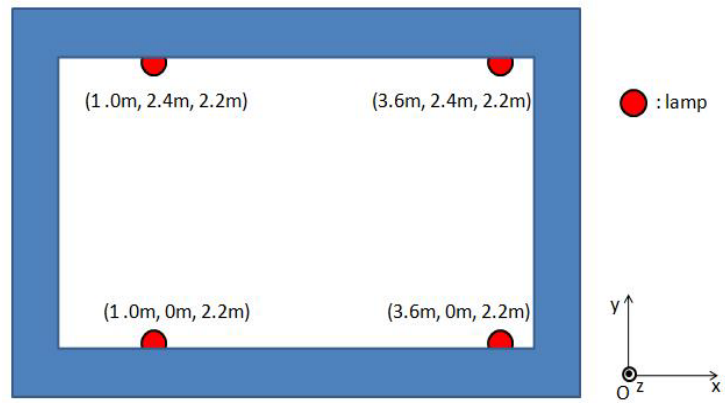
Figure 3. 5 Position of lamp fixtures
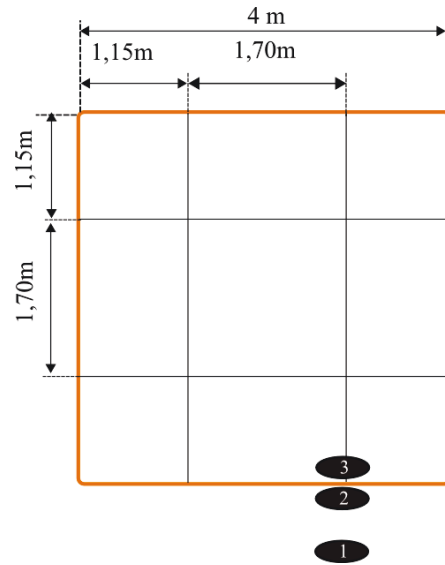
(a) Top view
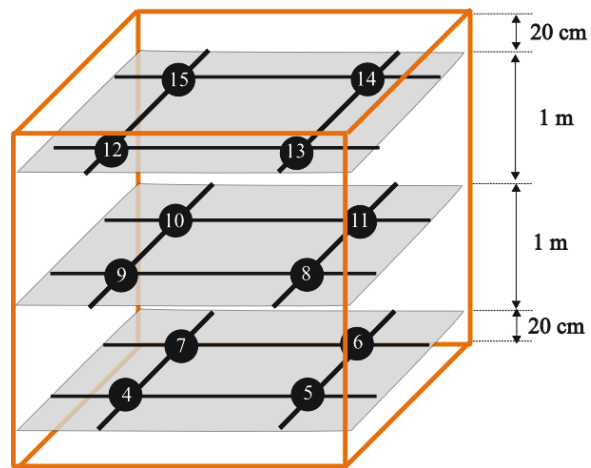
(b) Rear view (thermocouples no. 4~15)
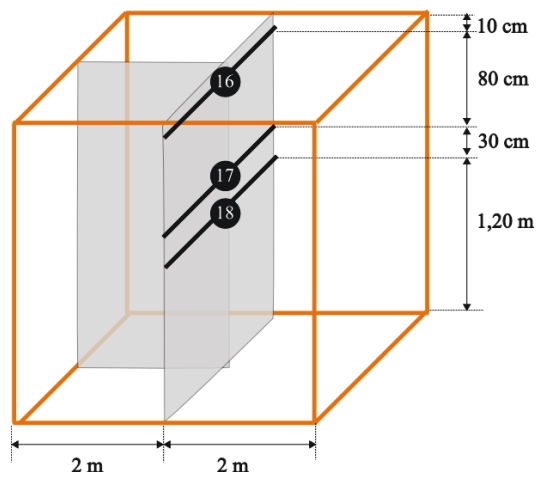
(c) Rear view (thermocouples no. 16~18)

Figure 3. 6 Thermocouples location

We have two outdoor thermocouples to measure the outdoor air temperature $T_e^*(t)$ and the outdoor wall temperature $T_{we}^*(t)$. The superscript symbol '*' indicates that the corresponding quantity is measured. Sixteen thermocouples are used inside the room. One of them is used to measure the indoor wall temperature $T_{wi}^*(t)$. Twelve thermocouples are set on different vertical levels (0.20, 1.20, and 2.20 m from the bottom). For each height, there are four thermocouples on the same plane. Since the room is supposed to be thermally homogeneous, the indoor temperature $T_i^*(t)$ is the average value of the temperature obtained by the twelve thermocouples. More details on the indoor temperature can be found in Appendix B. Besides, three thermocouples are placed on the center of the room at 1.20, 1.50, and 2.30 m in order to observe the stratification of the temperature within the room.

Each thermocouple is connected to a data acquisition device (Aglilent 34970A Data Acquisition/Switch Unit) shown in Figure 3. 7. The device communicates with a data logger software (HP BenchLink Data Logger Version 1.3) of a host computer. It is available to measure and store the temperature data at a certain interval time going from 10^{-2} s to 24 h. In this thesis work, the temperatures are measured each 1 min. It permits to capture short events of an electrical appliance's behavior and as a consequence, its fast thermal dynamics.

Figure 3. 7 Data acquisition device

3.3.2.2 *Power Measurement*

A load profile of an electrical appliance is measured by NZR Standby-Energy-Monitor 16 (NZR SEM 16). This device measures the following values of the electrical appliance: current, voltage, active power, energy consumption, energy costs, and maximal/minimal power during the measurement. A sampling time and a measurement period can be fixed by users. The sampling time is selected among 1, 6, 10, 12, 15, 20, 30, or 60 min; the measurement period can be 1, 7, 30 days, or unlimited period according to the purpose of the measurement. Measurements are transferred to the data reading program (VADEV Distant meter reading system Version 1.0.1) installed in a host computer via an USB interface. All the measurements are synchronized in order to observe the electrical power consumption of an electrical appliance

and its dissipated thermal heat gains at the same time. It permits a temporal analysis of the thermal heat gain of electrical appliances. Moreover, the used sampling period T_S is 1 min.

Figure 3. 8 Electrical power monitoring device (NZR-SEM16)

3.3.3   Experimental Procedures

In order to thermally characterize the test room, the data measurement and the acquisition systems are set-up, as stated above. It needs to supply heat flux to the test room for observing the thermal behavior of the room. As a consequence, four incandescent lamps which have been installed in the test room are selected as the electrical heat source of the room. The total electrical power consumed by the lamps is 270 W. The electrical power is all converted to heat flux by heat transfers, *i.e.* conduction, convection, and radiation.

We selected the incandescent lamp fixtures as a heat source of the room for the following reasons:

- The incandescent lamps consume a constant electrical power and supply a constant heat flux to the test room during the operation. It is considered as a thermal input of the test room.
- The user can easily control the system. It is therefore possible to observe the thermal characteristics of the room during both transient and steady-state.
- There is no additional cost since the lamps have already been installed in the test room.

Figure 3. 9 depicts a flowchart of the experimental procedures. Before starting a new experiment, the test room is opened for a while in order to set the indoor temperature equal to the outdoor temperature. Then, the room is well closed, and the experiment is started. Data acquisition systems are synchronized. Further, four incandescent lamps are turned on at a time. The lamps are kept on for several days until the indoor temperature of the test room becomes stable. After several days, the lamps are turned off. Finally, the measurements are stopped when the indoor/outdoor temperatures are stable.

According to the above experimental procedure, the inputs/outputs of the well-insulated room can be measured. Based on the measurements, the thermal characteristics of the room can then be identified.

```
                    ┌──────────┐
                    │  Start   │
                    └──────────┘
                         │
                         ▼
              ╱─────────────────────╲
             ╱  Indoor temperature   ╲
            ╱   Stabilization and     ╲
            ╲  Data acquisition device╱
             ╲   Synchronization     ╱
              ╲─────────────────────╱
                         │
                         ▼
                  ┌──────────────┐
              ┌──▶│  Lamps ON    │
              │   └──────────────┘
              │          │
              │          ▼
              │   ╱───────────────╲
        no    │  ╱ Indoor temperature╲
              └─◀  is during steady  ╲
                 ╲     state?        ╱
                  ╲───────────────╱
                         │ yes
                         ▼
                  ┌──────────────┐◀──┐
                  │  Lamps OFF   │   │
                  └──────────────┘   │
                         │           │
                         ▼           │
                  ╱───────────────╲  │
                 ╱ Indoor/outdoor  ╲ │  no
                 ╲ temperatures are ╱─┘
                  ╲    stable?     ╱
                   ╲─────────────╱
                         │ yes
                         ▼
              ┌────────────────────────┐
              │ Measurement devices OFF│
              └────────────────────────┘
                         │
                         ▼
                    ┌──────────┐
                    │   End    │
                    └──────────┘
```
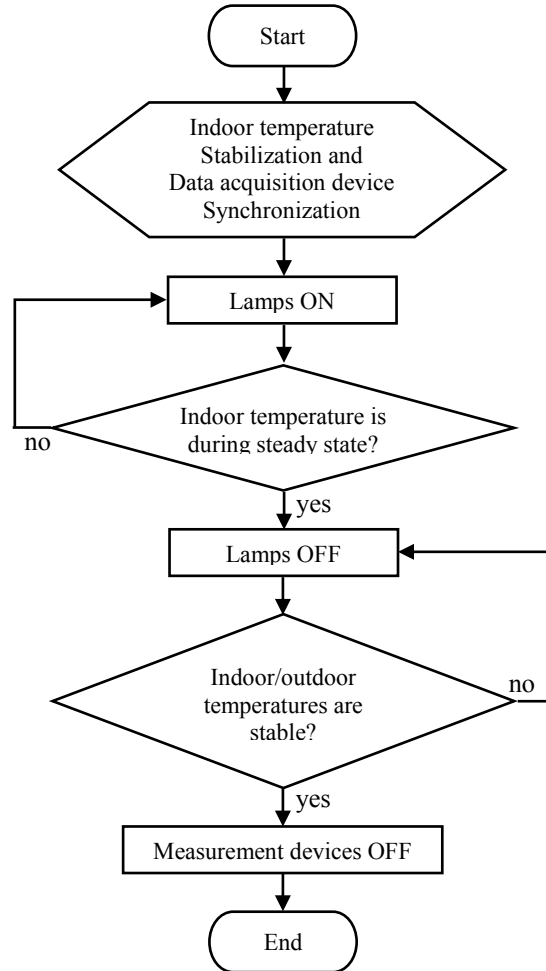
Figure 3. 9 Flowchart of experimental procedure

3.4 THERMAL MODEL OF QUASI-ADIABATIC ROOM

This section presents a methodology for designing thermal models of the well-insulated room and identifying their corresponding thermal parameters. As mentioned above, there are no other heat sources except four incandescent lamps. Based on the first law of thermodynamics, we suggest lumped *RC* parameter circuits by using the thermal-electrical analogy. Then, the parameter identification methods are presented. The thermal parameters are finally estimated from experimental data.

3.4.1 Heat Balance Equation

3.4.1.1 Simple Model

We consider a single zone model with an electrical power source (see Figure 3. 10). The heat balance equation is deduced by the first principle of thermodynamics (eq.(3.1)). It is simplified into eq.(3.16) for a quasi-adiabatic room. It can be also expressed as eq.(3.17). The derivative of the U_{stored} with respect to time is the product of the specific heat capacity, the mass of the room, and the derivative of the indoor temperature.

$$\dot{Q}_{appliance}(t) = \dot{Q}_{envelope}(t) + C_{th}\frac{dT_i(t)}{dt} \tag{3.17}$$

where C_{th} [J/°C] is the global thermal capacitance of the test room and is the product of the specific heat capacity [J/(kg·°C)] and the mass of the room [kg]. T_i is the indoor temperature of the room [°C].

The heat loss through envelopes of the room, $\dot{Q}_{envelope}$ [W] is

$$\dot{Q}_{envelope}(t) = \frac{1}{R_{th}}(T_i(t) - T_e(t)) \tag{3.18}$$

where R_{th} is the global thermal resistance of the room [°C/W], T_e is the exterior temperature of the room.

(a) A single zone model with an electrical power source P

(b) Example of indoor temperature $T(t)$ and electrical power source profile $P(t)$
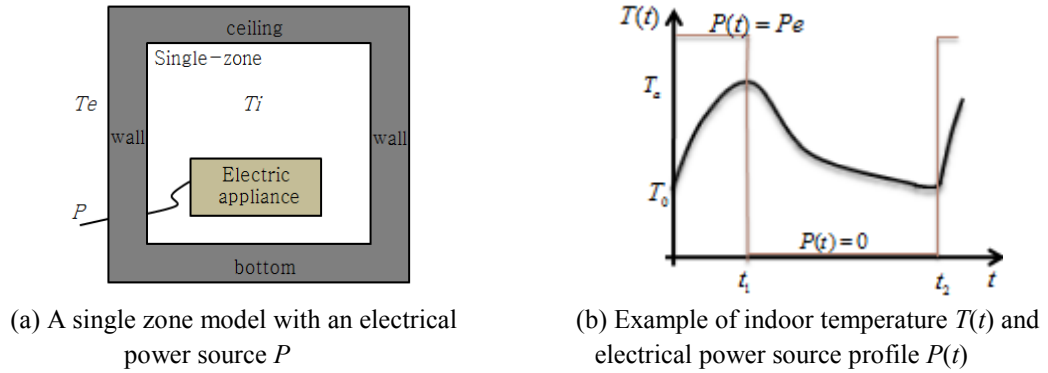
Figure 3. 10 A single zone model and its temperature and supplied power

The indoor temperature can be obtained from eqs.(3.17) - (3.18). It yields eq.(3.19) when $\dot{Q}_{appliance}(t)$ and $T_e(t)$ are constant.

$$T_i(t) = R_{th}\dot{Q}_{appliance}(t) + T_e(t) + (T_0 - T_e(0) - R_{th}\dot{Q}_{appliance}(0))\cdot e^{-t/\tau_{th}} \tag{3.19}$$

The particular case of no heating period is as following when $T_e(t) = T_e(0) =$ constant.

$$T_i(t) = T_e(t) + (T_0 - T_e(0)) \cdot e^{-t/\tau_{th}} \tag{3.20}$$

τ ($= R_{th} \cdot C_{th}$) is the time constant of the room [s], $T_e(0)$ is the initial outdoor air temperature [°C], T_0 is the initial indoor air temperature [°C], and $\dot{Q}_{appliance}(0)$ is the initial power consumption of the appliance [W]. Equation (3.19) shows a general equation of the indoor temperature. Equations (3.19) and (3.20) indicate the indoor air temperature $T_i(t)$ when electrical power source $\dot{Q}_{appliance}(t)$ is enabled and disabled, respectively. The analytical solution is solved in Appendix C.

3.4.1.2 Complex Model

We can develop more complex models of the room using the heat balance equation. As much more elements of a building are modeled, the order, the complexity and the accuracy of the models become higher, but computational efficiency is lower than the case of the simplified building model. The derived heat balance equation for a complex model which consists of m elements is given by eq.(3.21).

$$\begin{aligned} \dot{x} &= Ax + Bu \\ y &= Cx + Du \end{aligned} \tag{3.21}$$

where

$$x = \begin{bmatrix} T_m & T_{m-1} & T_{m-2} & \cdots & T_1 \end{bmatrix}^T \tag{3.22}$$

$$u = \begin{bmatrix} \Phi_n & \Phi_{n-1} & \Phi_{n-2} & \cdots & \Phi_1 & T_0 \end{bmatrix}^T \tag{3.23}$$

$$A = \begin{bmatrix} -\dfrac{1}{R_m C_m} & 0 & 0 & 0 & \cdots & 0 & 0 \\ \dfrac{1}{R_m C_{m-1}} & -\left(\dfrac{1}{R_m} + \dfrac{1}{R_{m-1}}\right)\dfrac{1}{C_{m-1}} & 0 & 0 & \cdots & 0 & 0 \\ 0 & \dfrac{1}{R_{m-1} C_{m-2}} & -\left(\dfrac{1}{R_{m-1}} + \dfrac{1}{R_{m-2}}\right)\dfrac{1}{C_{m-2}} & 0 & \cdots & 0 & 0 \\ \vdots & \vdots & \vdots & \vdots & \ddots & \vdots & \vdots \\ 0 & 0 & 0 & 0 & \cdots & \dfrac{1}{R_2 C_1} & -\left(\dfrac{1}{R_2} + \dfrac{1}{R_1}\right)\dfrac{1}{C_1} \end{bmatrix} \tag{3.24}$$

$$B = \begin{bmatrix} \dfrac{1}{C_m} & 0 & 0 & 0 & \cdots & 0 & \dfrac{1}{R_m C_m} \\[2mm] 0 & \dfrac{1}{C_{m-1}} & 0 & 0 & \cdots & 0 & \dfrac{1}{R_{m-1} C_{m-1}} \\[2mm] 0 & 0 & \dfrac{1}{C_{m-2}} & 0 & \cdots & 0 & \dfrac{1}{R_{m-2} C_{m-2}} \\[2mm] \vdots & \vdots & \vdots & \vdots & \ddots & \vdots & \vdots \\[2mm] 0 & 0 & 0 & 0 & \cdots & \dfrac{1}{C_1} & \dfrac{1}{R_1 C_1} \end{bmatrix} \tag{3.25}$$

where x is the state vector (vector of internal temperature nodes [°C]), u is the input vector (internal heat gains [W] and outdoor temperature [°C]), y is the output vector (measured temperature [°C]). A, B, C and D are the matrices of the model. They depend on thermal resistance R_i [°C/W], and thermal capacitance C_j [J/°C]. The indexes m and n are respectively the number of the temperature nodes and the number of the considered heat sources, respectively.

3.4.2   Equivalent Lumped *RC* Model

From the physical expressions of the quasi-adiabatic room and thermal-electrical analogy, we can develop equivalent lumped *RC* models of the test room in order to analyze its thermal behavior.

Figure 3. 11 illustrates an equivalent *RC* model of a building which corresponds to eq.(3.21). Each building element can be individually modeled by *RC* components and additional heat sources if they exist. The partial models of each element are connected to each other in accordance with their relationship.
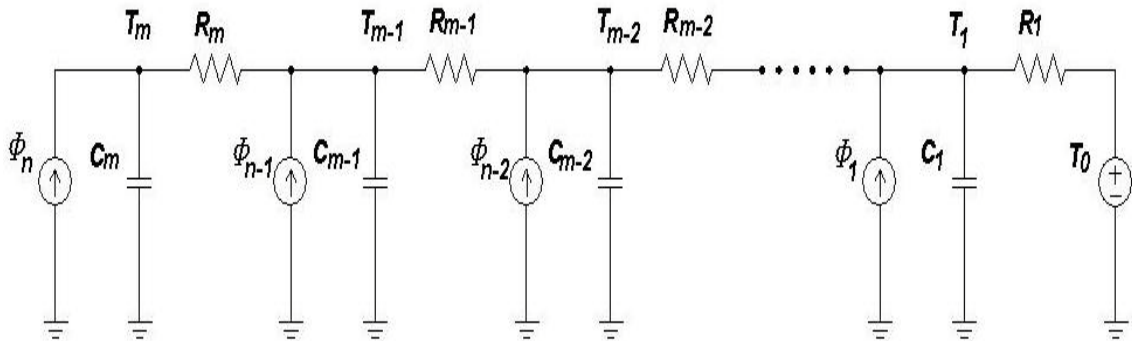
Figure 3. 11 Equivalent *RC* model of a building

Nowadays, simplified or reduced-order lumped *RC* parameter building models are often used owing to their potential advantages, such as reduced computational time, shorter coding, analytical solution of the state equations, and easier verification. In addition, the simplified models can also capture the essential behavior of buildings [63].

There are some researches on reduced-order building models. Fraisse et al. (2002) [64] introduced a study on how to transform a multi-layer wall into a three resistances and four capacities model (3R4C), and aggregated the wall models in order to make a whole building model. They compared its thermal behavior to a real building's one. Reference [101] presents a simplified building model with 2R2C for the internal mass, 3R2C for the external wall, 1R for the window, and 3R2C for the roof. Ghiaus and Hazyuk (2010) [66] proposed a simplified building model using 3R2C for a building zone and 1R for ventilation and infiltration of the building. The model orders ought to be selected according to the purpose of the modeling. These papers show that the proposed reduced order models are able to catch the building dynamics.

Based on the heat balance equation and thermal electrical analogy, we model the room as a first order, a second order, and a third order lumped RC parameter models. Further, we compare them to each other. For each case, the room has only one heat source $\dot{Q}_{appliance}$. This gain is the sum of electrical power supplied to the incandescent lamps as stated in Section 3.3. The following sections present several lumped RC models along with their corresponding assumptions.

3.4.2.1   First Order Lumped RC Model

Figure 3. 12 shows a first order lumped RC (1R1C) parameter model using the thermal-electrical analogy. In this model, we assumed that
- The initial inner and outer building temperatures are the same ($T_i(0)=T_e(0)$).
- The indoor temperature, including the room air temperature, the furniture temperature, and the wall temperature is homogeneous (The model is considered as a well-mixed model).
- The thermal resistance R_{th} and capacitance C_{th} of the test room are global parameters
- There is no additional heat flux from solar radiation, metabolism, infiltration, ventilation, and air leakages by window, door, thermal bridges, or any small hole.
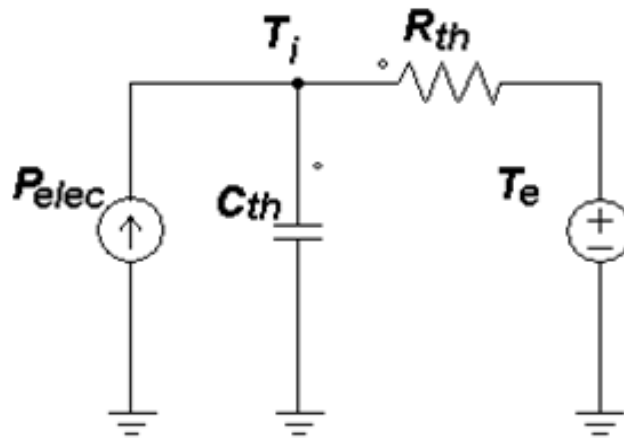
Figure 3. 12 First order lumped RC parameter circuit of building model

3.4.2.2 Second Order Lumped RC Model I

Figure 3. 13 depicts a second order lumped RC ($2R2C$) parameter model using the thermal-electrical analogy. The assumptions that correspond to this model are:

- There are two thermal resistances: R_{i_wi} is the sum of both radiative and convective resistances of the internal wall, R_{wi_e} is the sum of the conductive resistance of the wall and the convective and radiative resistances of the external wall.
- There are two thermal capacitances: C_{i_wi} is the thermal capacitance of internal air mass of the building, C_{wi_e} is the sum of the thermal capacitances of the wall and the external air mass of the building.
- The temperature is uniformed for each node and the initial temperatures are the same ($T_i(0) = T_{wi}(0) = T_e(0)$). T_i is considered as the indoor temperature of the building.
- There is no additional heat flux from solar radiation, metabolism, infiltration, ventilation, and air leakages by window, door, thermal bridges, or any small hole.
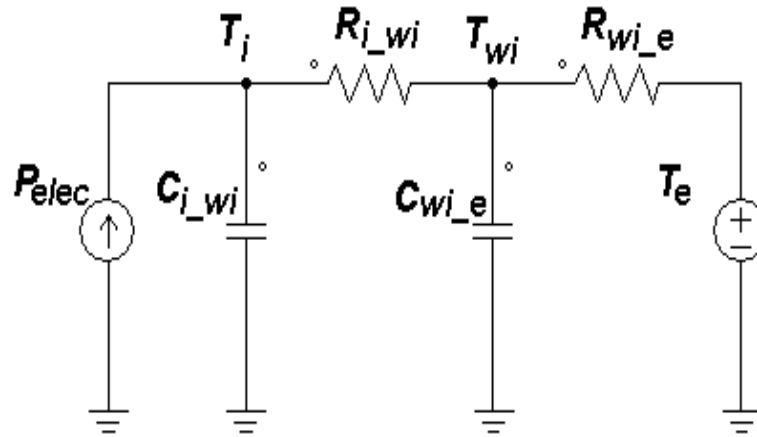
Figure 3. 13 Second order lumped RC parameter circuit of building model I

3.4.2.3 Second Order Lumped RC Model II

Figure 3. 14 shows another second order lumped RC ($2R2C$) parameter model using the thermal-electrical analogy. The assumptions that correspond to the model are:

- There are two thermal resistances: R_{i_w} is the sum of both radiative and convective resistances of the internal wall and the half of the conductive resistance of the wall, R_{w_e} is the sum of the half of the conductive resistance of the wall and the convective and radiative resistances of the external wall.
- There are two thermal capacitances: C_{i_w} is is the sum of the thermal capacitance of internal air mass and the half of the thermal capacitance of the wall, C_{w_e} is the sum of the thermal capacitances of the half of the wall and the external air mass of the building.
- The temperature is uniformed for each node and the initial temperatures are the same ($T_i(0) = T_w(0) = T_e(0)$). T_i is considered as the indoor temperature of the building.

- There is no additional heat flux from solar radiation, metabolism, infiltration, ventilation, and air leakages by window, door, thermal bridges, or any small hole.
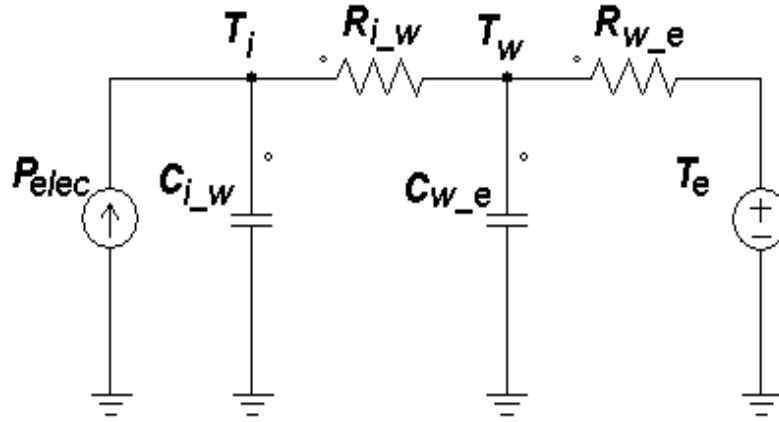
Figure 3. 14 Second order lumped *RC* parameter circuit of building model II

3.4.2.4 Third Order Lumped RC Model

Figure 3. 15 depicts a third order lumped *RC* (3*R*3*C*) parameter model using the thermal-electrical analogy. In this model, we assumed that

- There are three thermal resistances: R_i, R_e are respectively the convective and radiative resistances of the internal/external wall. R_w is the conductive resistance of the wall.
- There are three thermal capacitances: C_i, C_e are the thermal capacitances of internal/external mass of the building. C_w is the thermal capacitance of the wall.
- The temperature is well uniformed for each node and the initial temperatures are the same ($T_i(0) = T_{wi}(0) = T_{we}(0) = T_e(0)$). T_i is considered as the indoor temperature of the building.
- There is no additional heat flux from solar radiation, metabolism, infiltration, ventilation, and air leakages by window, door, thermal bridges, or any small hole.
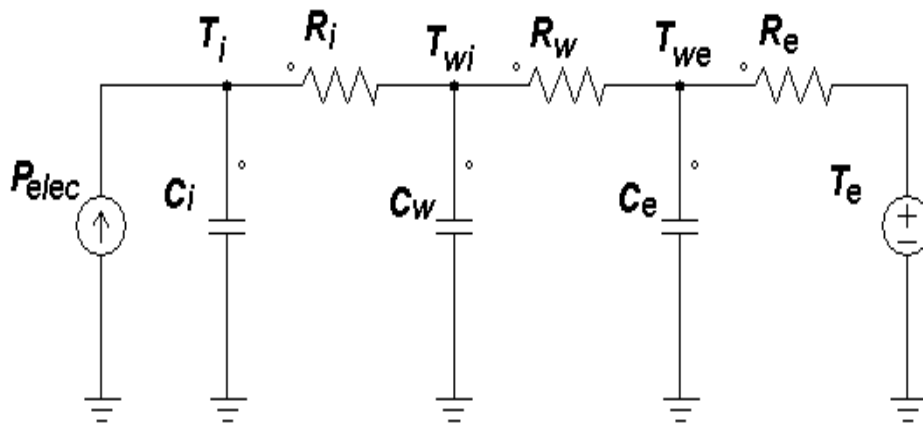
Figure 3. 15 Third order lumped *RC* parameter circuit of building model

In order to describe the thermal behavior of the quasi-adiabatic room, we firstly established the four previously described thermal models of the room. The models are based on the heat balance equation. By using the thermal-electrical analogy, the models were then represented by lumped *RC* circuits. However, the values of the *RC* parameters of the models are unknown. Since the thermal behavior of the room depends on the values of these parameters, they should be estimated. The next section presents the used parameter identification methods.

3.5 PARAMETER IDENTIFICATION OF THE MODEL

3.5.1 Overview

In this section, we describe a procedure to identify thermal parameters of the models of the quasi-adiabatic room which were suggested in the previous section. We first study the parameters of the first order *RC* model and extend the method to the second and the third order models. The identification process is shown in Figure 3. 16. From experimental data, global thermal parameters R_{th} and C_{th} of the first order model are estimated using analytical solution of the heat balance equation. Then, the parameters of the second and third models are identified by optimization process based on the interior-reflective Newton method. The estimated values of global parameters of the first order model R_{th} and C_{th} are used for describing the thermal behavior of the room modeled by the first order model. They are also used for determining the initial values and upper/lower bounds of the thermal parameters of the other models.

The measured data and the thermal parameters that will be estimated are as follows:

- Measured data: heat flux due to lamps $\dot{Q}_{appliance}^*$ (here, $\dot{Q}_{appliance}^*=P_{lamp}^*$), indoor temperature T_i^*, interior wall surface temperature T_{wi}^*, exterior wall surface temperature T_{we}^*, outdoor temperature T_e, and calculated wall temperature T_w^* (which is the average temperature of T_{wi}^* and T_{we}^*).
- Thermal parameters to be estimated: global thermal resistance R_{th}, global thermal capacitance C_{th}, thermal resistances R_{i_wi}, R_{wi_e}, R_{i_w}, R_{w_e}, R_i, R_w, R_e, and thermal capacitances C_{i_wi}, C_{wi_e}, C_{i_w}, C_{w_e}, C_i, C_w, C_e.

The steps of the proposed identification approach are:

- Analytical solution of the heat balance equation in order to obtain the global thermal parameters of the first order model.
- Optimization based on the interior-reflective Newton method in order to identify the thermal parameters of the other thermal models of the test room.
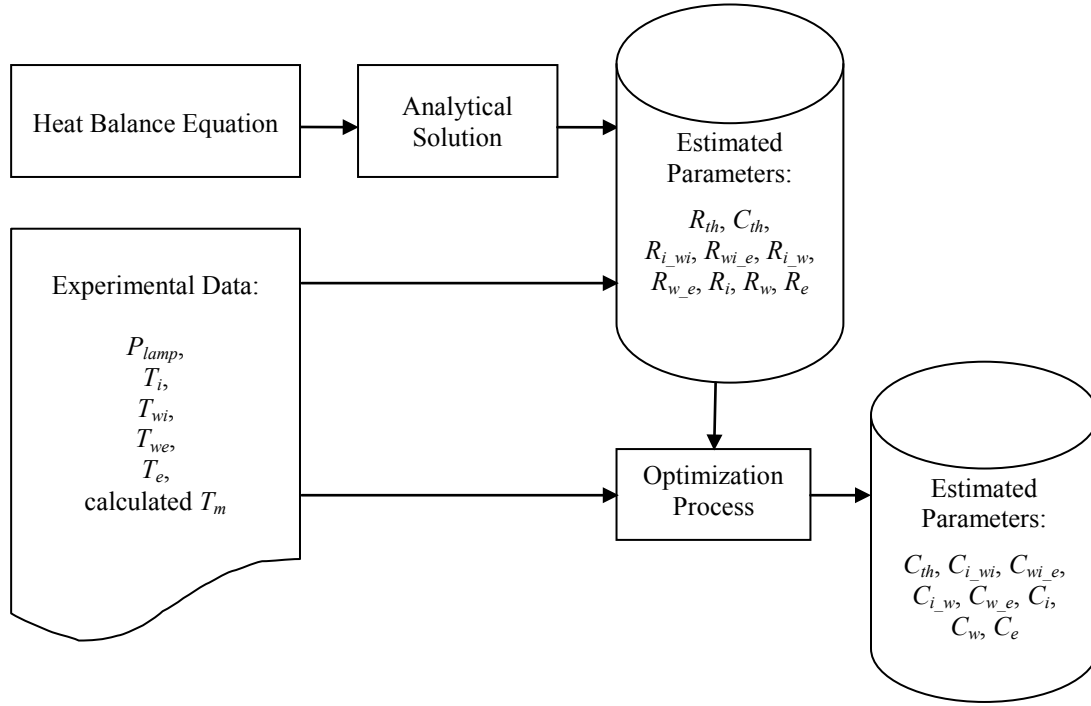
Figure 3. 16 Parameter identification process

3.5.1.1 Analytical Solution

From the heat balance equation, we obtained the analytical solution of the indoor temperature $T_i(t)$ in both cases when the power source is on and when it is off as eqs.(3.19) - (3.20). When the lamps turn on, the dissipated heat flux by lamps is supplied to the room. Consequently, the indoor temperature rises. At steady-state, the global thermal resistance R_{th} is obtained as follows.

$$R_{th} = \frac{T_i^* - T_e^*}{P_{lamp}^*}$$

(3.26)

However, in reality there are little variations on the measured temperature and electrical power consumption. Therefore, we take the averages of the measured $\overline{T_i}^*$, $\overline{T_e}^*$, and $\overline{P_{lamp}}^*$ during steady-state. R_{th} is thus equal to

$$R_{th} \cong \overline{R}_{th} = \frac{\overline{T_i}^* - \overline{T}^*_e}{\overline{P_{lamp}}^*}$$

(3.27)

For the suggested first order model, we considered only a global thermal resistance. However, the global thermal resistance R_{th} is the sum of the internal convective thermal resistance R_i [°C/W], the wall thermal resistance R_w [°C/W], and the external convective thermal resistance R_e [°C/W]. The relation of R_{th}, R_i, R_w, and R_e is given by eq.(3.28).

$$R_{th} = R_i + R_w + R_e \tag{3.28}$$

where

$$R_i = \frac{1}{h_i A}, \quad R_w = \sum_{i=1}^{n} \frac{e_i}{\lambda_i A}, \quad R_e = \frac{1}{h_e A} \tag{3.29}$$

Here, A is the room wall surface [m^2], h_i, h_e are respectively the internal and external convective heat transfer coefficients [W/(m^2·°C)]. λ_i is the ith wall layer thermal conductance [W/(m·°C)], e_i is the ith wall thickness [m], n is the number of the layer.

The thermal resistances of other models R_{i_wi}, R_{wi_e}, R_{i_w}, R_{w_i}, R_i, R_w, and R_e can be in the same way. It gives:

$$R_{th} = R_{i\_wi} + R_{wi\_e} = R_{i\_w} + R_{w\_e} = R_i + R_w + R_e \tag{3.30}$$

Once obtained the global thermal resistance, the global thermal capacitance C_{th} can be identified by searching the time constant of the room. The time constant of the room τ_{th} is the product of R_{th} and C_{th}. We use two methods in order to calculate τ_{th}.

Firstly, we calculate τ_{th} from eq.(3.20) when there is no electrical power in the room.

$$\tau_{th} = \frac{t}{\ln\left(\dfrac{T_{io}^{\ *} - T_{eo}^{\ *}}{T_i^{\ *}(t) - T_e^{\ *}(t)}\right)} \tag{3.31}$$

Equation (3.31) indicates the calculated τ_{th} on the period where the room temperature decreases due to the absence of heat gain. The equation is valid when $T_i^{\ *}$ is superior to $T_e^{\ *}$. For obtaining these above analytical solutions, we must assume that $T_e^{\ *}(t)$ is a constant or its temporal variations are small. However, this assumption can induce errors in reality when $T_e^{\ *}(t)$ changes.

To solve this problem, we use another method for estimating τ_{th} by obtaining an exponential curve which has the smallest difference comparing to the experimentally obtained curve.

From eq.(3.20), the negative exponential curve of the observed $T_i^{\ *}$ is deduced as follows when $T_e^{\ *}$ is constant:

$$e^{-t/\tau_{th}} = \frac{T_i^{\ *}(t) - T_e^{\ *}(t)}{T_{io}^{\ *} - T_{eo}^{\ *}} \tag{3.32}$$

We compare this curve to other negative exponential curves that can be generated by different time constant. The sum of the squared difference S between the measured $y_{measured}$ and the generated curve $y_{generated}$ determined by different τ_{th} is calculated by eq.(3.33).

$$S = \sum_{j=1}^{m} (y_{measured,j} - y_{generated,j})^2 \tag{3.33}$$

where m is the number of data, the $y_{measured,\,j}$ is the jth exponential value obtained by measurements and the $y_{generated,j}$ is the jth generated curve point. We obtain the proper τ_{th} which exponential curve has the least squared difference S. Then C_{th} is deduced from R_{th} and τ_{th}.

3.5.1.2 Optimization Process

The rest of the thermal parameters are estimated by an optimization process. In this study, the subspace trust region solver based on the interior reflective Newton method, which is presented by Coleman and Li (1994) [104], is chosen. This method allows solving nonlinear minimization problems where some of the variables have upper and/or lower bounds. It is available in MATLAB 2010a Optimization Toolbox. The parameters that will be optimized are the thermal capacitances of the two second order models and the third order model. These are C_{i_wi}, C_{wi_e}, C_{i_w}, C_{w_e}, C_i, C_w, and C_e. Moreover, the thermal capacitance of the first order model which is obtained by the analytical solution of the heat balance equation is re-estimated by this optimization process in order to compare the performance of each approach. That is to say that the vector of unknown parameters X consists of C_{th}, C_{i_wi}, C_{wi_e}, C_{i_w}, C_{w_e}, C_i, C_w, and C_e. The objective function J is defined as below [30]:

$$J = \min \frac{\sum_{j=1}^{n} f_j(X)^2}{n} \tag{3.34}$$

$$\text{Subject To:} \quad X_L < X < X_U \tag{3.35}$$

where

$$f_j(X) = y_{measured,j} - y_{predicted,j} \tag{3.36}$$

where n is the number of data, $y_{measured,j}$ is the jth measured value of temperature and $y_{predicted,j}$ is the jth predicted one. X is the vector of unknown parameters, X_L is the lower bound of unknown parameters and X_U is the upper bound of unknown parameters.

3.5.2 Experimental Results

In order to identify the parameters of the suggested models of the room, measurements were carried out during nine days from 11/01/2011 to 21/01/2011. During the first period (6 days), the lamps in the room were turned on in order to supply a constant power of 270 W to the room. They were then turned off during the second period (4 days). The average indoor air temperature T_i^* (the average value of the data obtained by thermocouples no. 4~15), the internal wall surface temperature T_{wi}^* (obtained by thermocouple no. 3), the external wall surface temperature T_{we}^* (obtained by thermocouple no. 2), the calculated wall temperature T_w^* (the average value of T_{wi}^* and T_{we}^*), and the outdoor temperature T_e^* (obtained by thermocouple no. 1) are shown in Figure 3. 17.
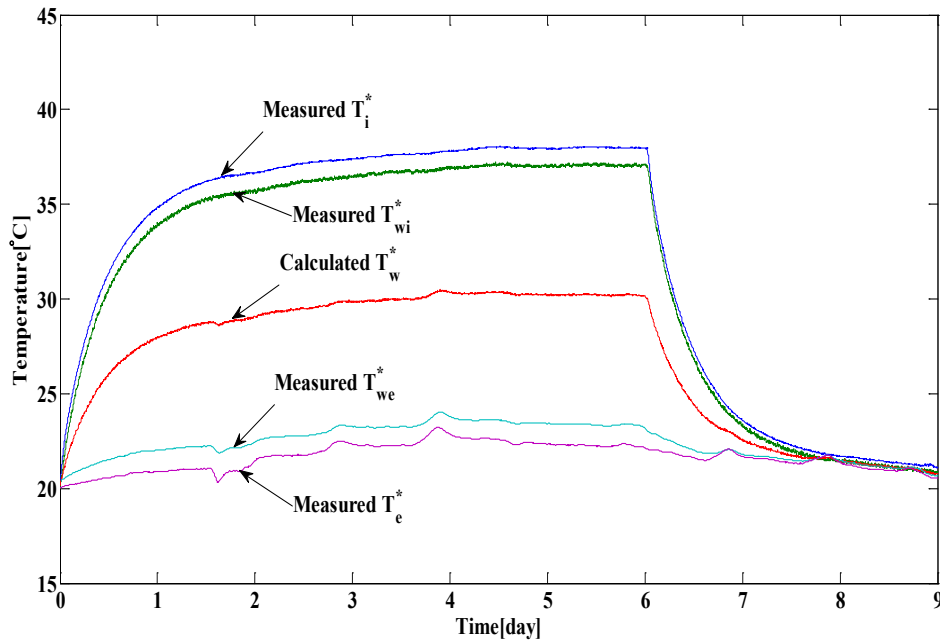
Figure 3. 17 Trends of temperature

The measured temperatures rise during the first period of the measurement. It is due to the heat flux generated by the lamps. Heat is charged within the room until reaching steady state around 38 °C (T_i^*). During steady state, over-charged heat is lost through the envelope of the room. The temperatures T_i^*, T_{wi}^*, T_w^*, T_{we}^* depend on both T_e^* and P_{lamp}^*.

With the help of the measurements, we can deduce the global room thermal resistance R_{th}, and the thermal resistances of other models, R_{i_wi}, R_{wi_e}, R_{i_w}, R_{w_e}, R_i, R_w, and R_e. As discussed in the previous sub-section 3.5.1.1, these thermal resistances are obtained by the data which are measured during two days from 4th to 6th days (during steady-state). Table 3. 3 lists the obtained values of thermal resistances of the selected models.

Table 3. 3 Estimated thermal resistances of the room

1st Order	2nd Order I		2nd Order II		3rd Order		
R_{th}	R_{i_wi}	R_{wi_e}	R_{i_w}	R_{w_e}	R_i	R_w	R_e
$57.8 \cdot 10^{-3}$	$3.4 \cdot 10^{-3}$	$54.4 \cdot 10^{-3}$	$28.6 \cdot 10^{-3}$	$29.2 \cdot 10^{-3}$	$3.4 \cdot 10^{-3}$	$50.4 \cdot 10^{-3}$	$4.0 \cdot 10^{-3}$

unit of R: [°C/W]

The sum of all the thermal resistances for each model is equal to the value of R_{th} of first order model. After the thermal resistances are estimated, τ_{th} is obtained by two methods. The first method is the calculation by eq.(3.31). The second method is the estimation by using eq.(3.32) and eq.(3.33). After that the lamps are turned off, the temperatures T_i^*, T_{wi}^*, T_w^*, T_{we}^* exponentially decrease. From the exponential curve of T_i^* we can estimate the time constant of the room τ_{th} as well as the global thermal room capacitance C_{th}. Table 3. 4 lists the parameters which were carried out by the proposed methods. There is about 9 % of difference between the two estimated values of τ_{th}.

Table 3. 4 Estimated time constant and global thermal capacitance of the room

First method (using eq.(3.31))		Second method (using eqs.(3.32)-(3.33))	
τ_{th} [sec]	C_{th} [kJ/°C]	τ_{th} [sec]	C_{th} [kJ/°C]
4.12×10^4	713	3.78×10^4	654

The obtained values of thermal parameters R_{th} and C_{th} are applied to the first order model of the room. Then the thermal behavior of the room is simulated. The estimated T_i and the measured one are compared to each other. The data which are obtained during the last three days (while the lamps turned off) are selected for the comparison, because they include the information of the time constant of the room. Figure 3. 18 depicts both estimated T_i which are obtained by the two different methods. They have good fitting to the measured value with the coefficient of determination $R^2=0.99$. The black line is the reference. The function y corresponding to the dotted red line indicates the estimated T_i by applying the thermal capacitance obtained with the first method. The function y corresponding to the dotted blue line is the estimated T_i by applying the thermal capacitance obtained with the second method. The used thermal resistance for two cases is the same (57.8×10^{-3} °C/W as listed Table 3. 3).

The unknown parameters C_{i_wi}, C_{wi_e}, C_{i_w}, C_{w_e}, C_i, C_w, and C_e should be bounded in a certain range depending on their physical characteristics. Their lower and upper bounds are chosen based on the global thermal parameter C_{th} which is estimated by the above described process (654 kJ/°C). The initial value of internal thermal capacitance of the test room C_i is obtained by eq.(3.37). The assumed initial values of C_{wi_e}, C_{i_w}, C_{w_e}, and C_w are related to C_{th}. The initial value of C_i is used as initial value of C_{i_wi} and C_e.

$$C_i = \rho_{air} c_{p,air} V_{room} \tag{3.37}$$

where V_{room} is the volume of the test room [m^3]. Knowing that ρ_{air}=1.14 kg/m^3 at 313°C and $c_{p,air}$=1005 J/(kg·°C), the assumed initial value of C_i is fixed to 26396 J/°C.
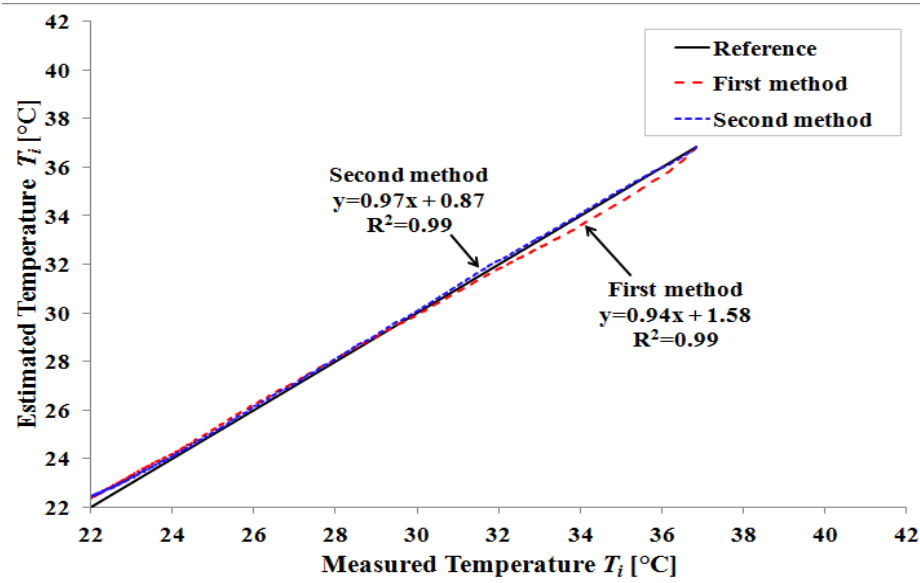
Figure 3. 18 Comparison of the measured indoor temperature and the estimated indoor temperatures

Table 3. 5 lists the used initial values and their lower and upper bounds.

Table 3. 5 Initial guess value and bound value

Model	Parameter	Initial value	Lower bound	Upper bound
1st Order Model	C_{th}	C_{th}	$0.5 \cdot C_{th}$	$5 \cdot C_{th}$
2nd Order Model I	C_{i_wi} C_{wi_e}	C_i C_{th}	$0.8 \cdot C_i$ $0.5 \cdot C_{th}$	$2 \cdot C_i$ $5 \cdot C_{th}$
2nd Order Model II	C_{i_w} C_{w_i}	$C_{th}/2$ $C_{th}/2$	$0.25 \cdot C_{th}$ $0.25 \cdot C_{th}$	$2.5 \cdot C_{th}$ $2.5 \cdot C_{th}$
3rd Order Model	C_i C_w C_e	C_i C_{th} C_i	$0.8 \cdot C_i$ $0.5 \cdot C_{th}$ $0.8 \cdot C_i$	$2 \cdot C_i$ $5 \cdot C_{th}$ $2 \cdot C_i$

Table 3. 6 summarizes the variables obtained with the presented optimization method. The evaluation function of the parameters is the Sum of Squared Errors (*SSE*) which is minimized by the optimization process. According to the *SSE* criterion, the accuracy of the second order model II is the best and the accuracy of the first order model is the worst. The accuracy of two other models are similar.

Table 3. 6 Estimated Parameters

Model	Parameter	Final value	Sum of squared error (SSE) criterion
1st Order Model	C_{th}	623 kJ/°C	723
2nd Order Model I	C_{i_wi}	32 kJ/°C	513
	C_{wi_e}	665 kJ/°C	
2nd Order Model II	C_{i_w}	487 kJ/°C	478
	C_{w_i}	526 kJ/°C	
3rd Order Model	C_i	28 kJ/°C	513
	C_w	670 kJ/°C	
	C_e	31 kJ/°C	

3.6 VALIDATION OF THE MODELS

3.6.1 Simulation Models

In order to validate the proposed parameter identification method, we implemented the obtained models into Matlab/Simulink®. Figure 3. 19 shows the block diagram which contains the quasi-adiabatic test room that we wanted to model. The test room is modeled by four models, as illustrated in Section 3.4.2: First order lumped *RC* model, Second order lumped *RC* model I, Second order lumped *RC* model II, and Third order lumped *RC* model. The common inputs of the models are the measured external temperature T_e^* and the supplied electrical power P_{lamp}^*. The output is the simulated internal temperature of the test room T_i.
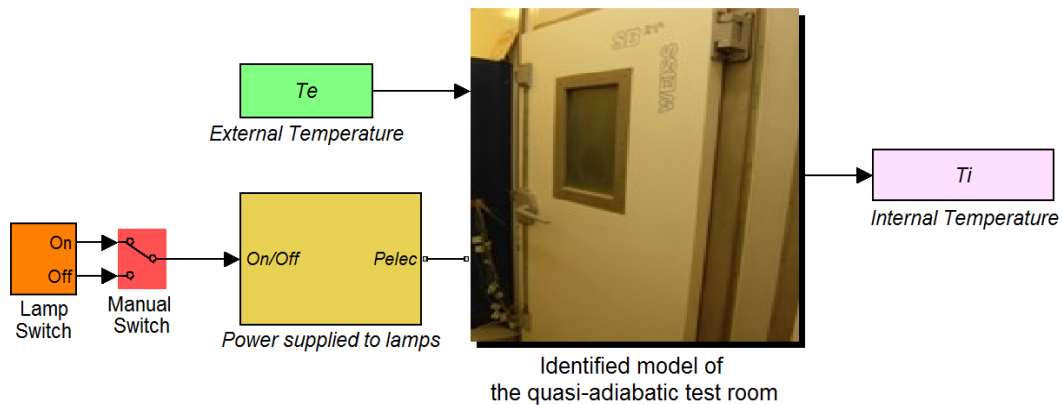
Figure 3. 19 Simulated system

3.6.2 Simulation Results

Based on the proposed models, we simulated the indoor temperature of the room T_i. The conditions of the simulation are the same to the experiment.

Firstly we study the first order model with different global thermal capacitances estimated by different methods. The Absolute Percentage Error (*APE*), Mean Absolute Percentage Error (*MAPE*), and Mean of the sum of Absolute Error (*MAE*) of different models are calculated in order to evaluate the models accuracy as follows:

$$APE = \left| \frac{y_{measured,j} - y_{simulated,j}}{y_{measured,j}} \right| \times 100 [\%] \tag{3.38}$$

$$MAPE = \frac{1}{N} \sum_{j=1}^{N} \left| \frac{y_{measured,j} - y_{simulated,j}}{y_{measured,j}} \right| \times 100 [\%] \tag{3.39}$$

$$MAE = \frac{1}{N} \sum_{j=1}^{N} | y_{measured,j} - y_{simulated,j} | \tag{3.40}$$

where N is the number of data, $y_{measured,j}$ is the jth measured temperature value and $y_{predicted,j}$ is the jth predicted one.

Then, the second order model I, II, and the third order model are evaluated in the same way as the first order model. Finally, the models are compared to each other at the end of this section.

3.6.2.1 First Order Lumped RC Model

We study the first order model with different values of global thermal capacitance. Above, we have already identified the global thermal capacitance in three ways. From the analytical solutions, we obtained the values of C_{th} as 713 kJ/°C, 654 kJ/°C (see Table 3. 4). Moreover, the optimized value obtained by using the interior reflective Newton method is 623 kJ/°C (see Table 3. 6). The value of global thermal resistance R_{th} is 57.8 x10^{-3} °C/W. These estimated thermal parameters are adapted to the first order lumped RC model of the room.

Figure 3. 20 illustrates the comparison of the measurement data and the simulation results. Although estimated curves have different C_{th}, they have a similar behavior. Moreover, they are well fitted to the measured curve. However, as the value of C_{th} is greater, the thermal response of simulated $T_{i,sim}$ is slower especially at transient state. During steady-state, there is no difference among $T_{i,sim}$ because there is no more effect of C_{th} and that R_{th} is the same for three cases. Moreover, we can see that T_e^* influences the simulated $T_{i,sim}$.
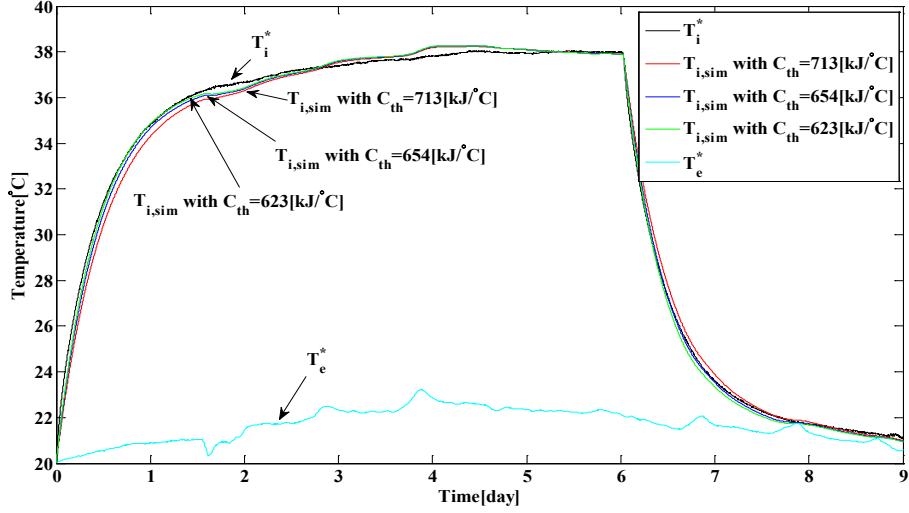
Figure 3. 20 Temperature Evolution of first order model

The *APE* is calculated by eq.(3.38) and is illustrated in Figure 3. 21. This evaluation method is used for verifying the accordance of the model with the different thermal capacitances. Especially at the first day and the sixth day when the operation mode of lamps is changed, the values of *APE* become much bigger than the values during steady-state. The maximum values of the *APE* for the model with C_{th}=713, 654, and 623 kJ/°C are respectively 5.1, 4.1, and 3.7 %. Their corresponding *MAPE* and *MAE* are each 0.96, 0.65, 0.64 % and 0.30, 0.20, 0.19 °C. According to these evaluation values, the simulated $T_{i,sim}$ with C_{th}=623 kJ/°C obtained by interior reflective Newton method has the best matching to the measured T_i^*.
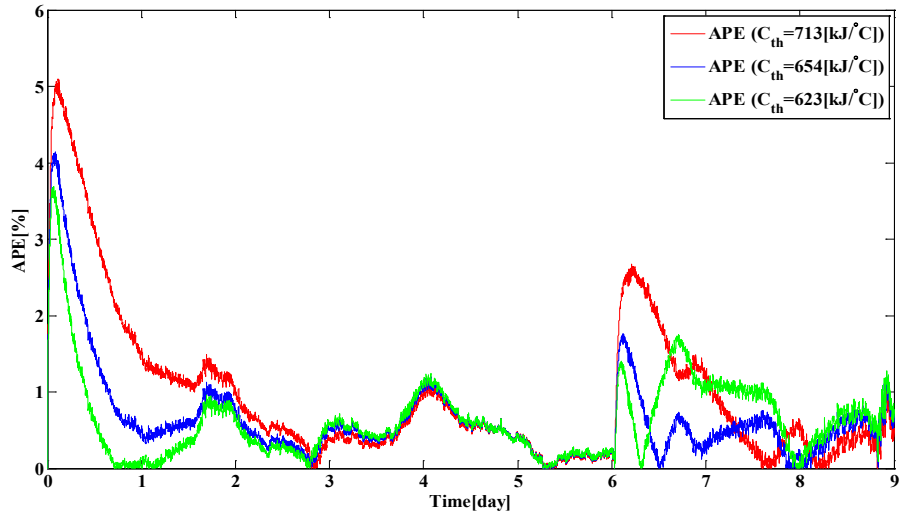
Figure 3. 21 *APE* evolution of first order model

3.6.2.2 Second Order Lumped RC Model I

We study the second order lumped *RC* model I. We obtained its thermal resistances R_{i_wi} and R_{wi_e} by the analytical solution of the heat balance equation during steady-state. The thermal

69

parameters, C_{i_wi} and C_{wi_e} were estimated by the interior reflective Newton method. As indicated Table 3. 3 and Table 3. 6, the values of R_{i_wi}, R_{wi_e}, C_{i_wi} and C_{wi_e} are 3.4 x10^{-3} °C/W, 54.4 x10^{-3} °C/W, 32 kJ/°C, and 665 kJ/°C, respectively.

Figure 3. 22 depicts the comparison of the measurement and the simulation results. The simulated $T_{i,sim}$ has a similar behavior to the measured data, T_i^*. They are well matching to each other at transient-state and steady-state.
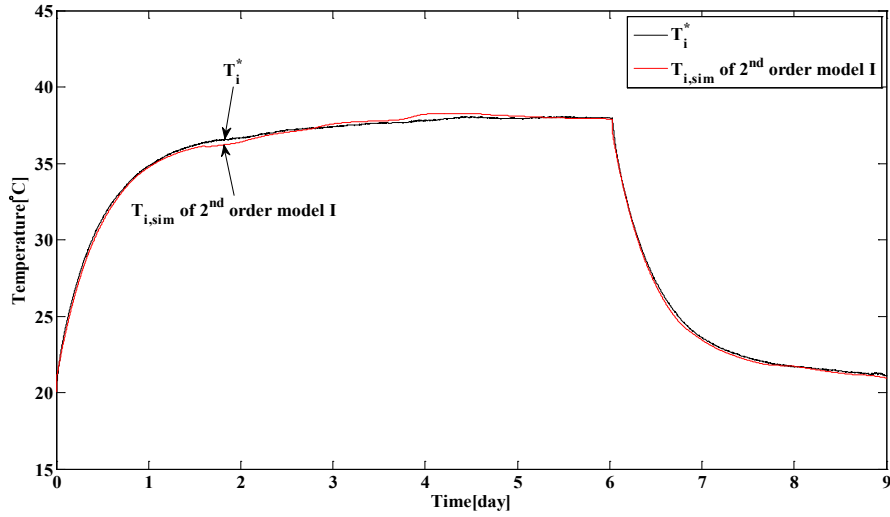
Figure 3. 22 Temperature Evolution of second order model I

Then, the *APE* is calculated and shown in Figure 3. 23. Similar to the first order lumped *RC* model, at the transitions of states, there are relatively bigger errors (see first and sixth day). The maximum *APE* is 2.2 %. The corresponding *MAPE* is 0.55 %. The *MAE* is 0.17 °C.
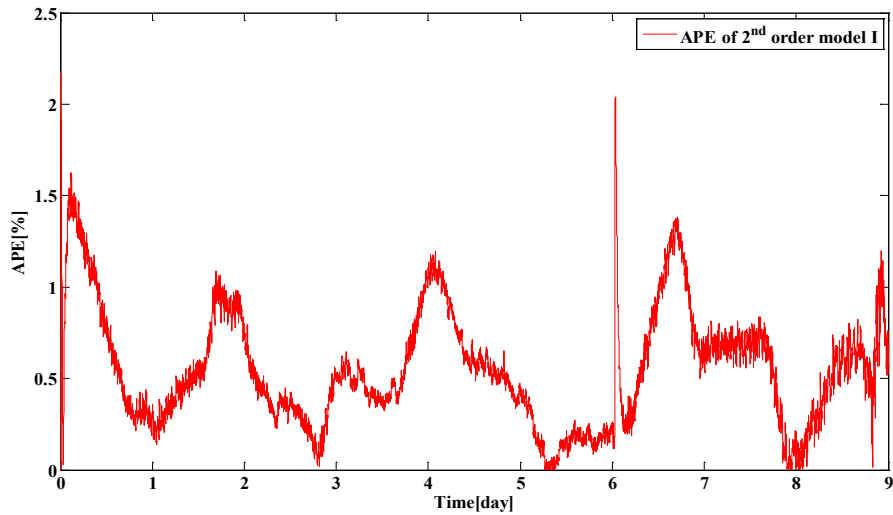
Figure 3. 23 *APE* evolution of second order model I

70

3.6.2.3 Second Order Lumped RC Model II

The second order lumped *RC* model II which was presented in Figure 3. 14 is also conducted on the simulation. The thermal resistances R_{i_w}, R_{w_e} were identified by the analytical solution of the heat balance equation during steady-state. Its thermal parameters C_{i_w} and C_{w_e} were estimated by the interior-reflective Newton method. As shown Table 3. 3 and Table 3. 6, the values of R_{i_w}, R_{w_e}, C_{i_w}, and C_{w_e} are 28.6 x10^{-3} °C/W, 29.2 x10^{-3} °C/W, 487 kJ/°C, and 526 kJ/°C, respectively. These estimated thermal parameters are implemented to the model.

Figure 3. 24 depicts the comparison of the measurement data and the simulation results. The simulated $T_{i,sim}$ has the similar behavior to the measured data, T_i^*. $T_{i,sim}$ is well fitting to T_i^* at transient-state and steady-state.
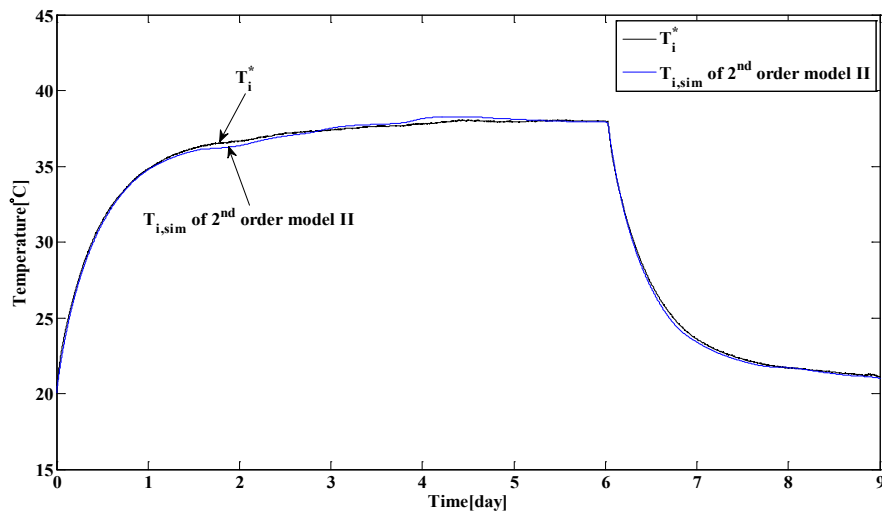
Figure 3. 24 Temperature evolution of second order model II

The *APE* is calculated and shown in Figure 3. 25. Like the first order lumped *RC* model and the second order lumped *RC* model I, there is relatively bigger error at the beginning of the simulation. However, when the lamps are turned off, there is less error comparing to other models. The maximum *APE* and *MAPE* criterion are 2.1 % and 0.53 %, respectively. The *MAE* is 0.17 °C.
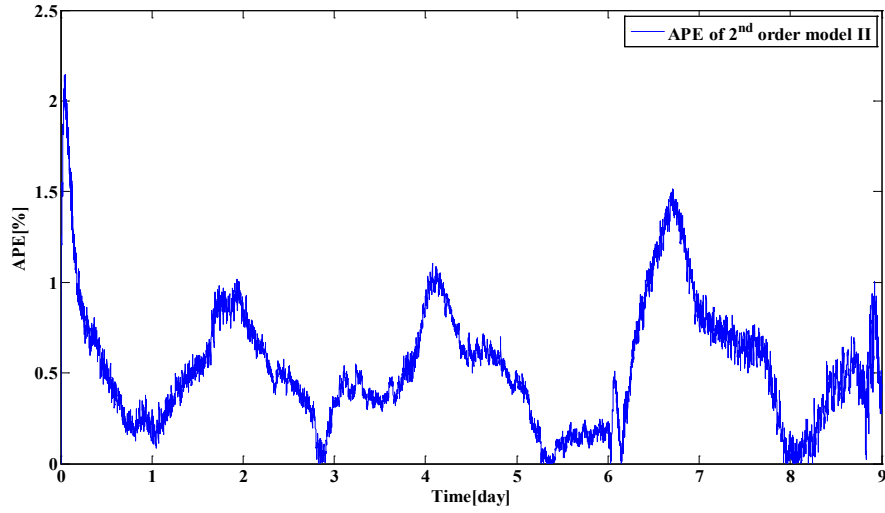
Figure 3. 25 *APE* evolution of second order model II

3.6.2.4 **Third Order Lumped RC Model**

The final model is the third order lumped *RC* model. The thermal resistances of the model R_i, R_w and R_e are determined as 3.4 x10^{-3}, 50.4 x10^{-3}, 4.0 x10^{-3} °C/W by the analytical solution of the heat balance equation during steady-state. The thermal parameters of the model C_i, C_w, and C_e were obtained by the interior-reflective Newton method as following: 28, 670, 31 kJ/°C. These parameters are indicated in Table 3. 3 and Table 3. 6.

Figure 3. 26 shows the comparison of the measured data and the simulation results. The simulated $T_{i,sim}$ has the similar behavior to the measured data T_i^* and is well fitting to T_i^* at both transient-state and steady-state.
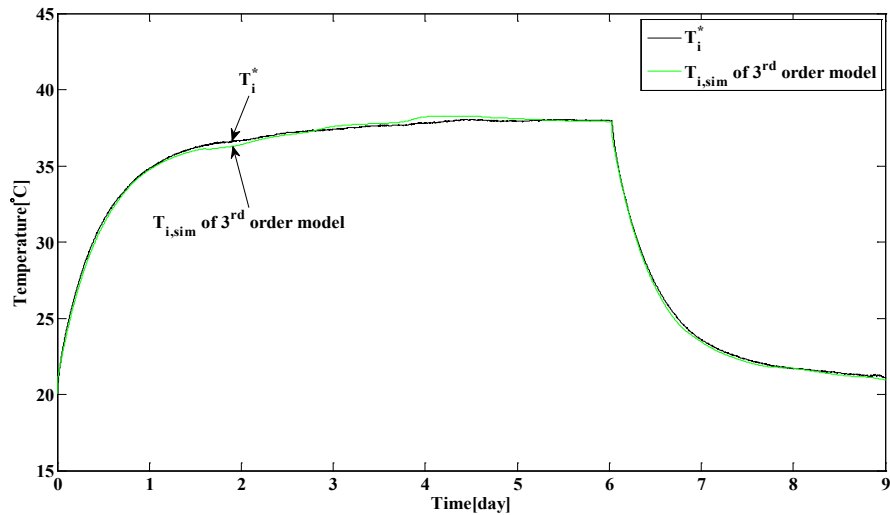
Figure 3. 26 Temperature evolution of third order model

The *APE* is calculated and illustrated in Figure 3. 27. Similar to other models, there is a relatively big error during the beginning of the transient state. The maximum *APE* is 2.2 %. The corresponding *MAPE* and *MAE* are respectively 0.55 % and 0.17 °C.
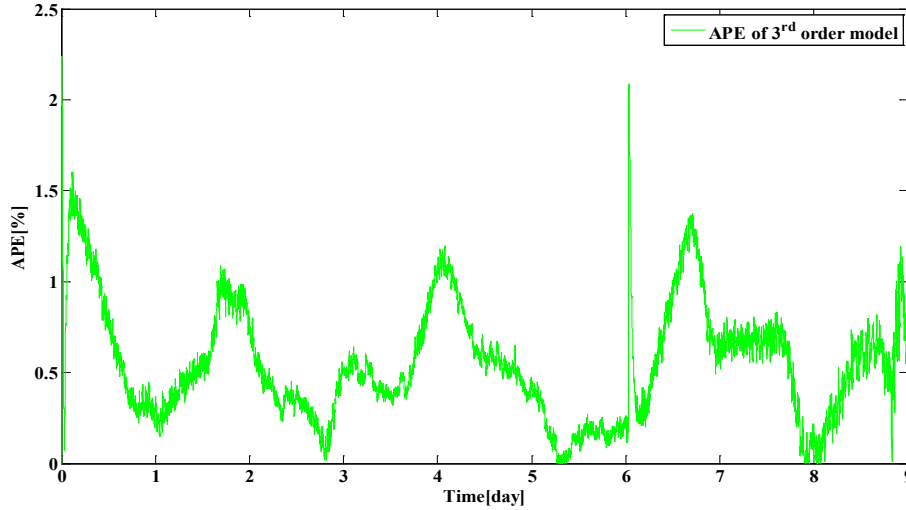
Figure 3. 27 *APE* evolution of third order model

3.6.2.5 Comparison of the Different Models

In order to evaluate the proposed models of the quasi-adiabatic room, the Absolute Percentage Error (*APE*), Mean Absolute Percentage Error (*MAPE*), and Mean of the sum of Absolute Error (*MAE*) of different models were obtained. Table 3. 7 summarizes the calculation results.

Table 3. 7 Evaluation results

Model	maximum *APE* [%]	*MAPE* [%]	*MAE* [°C]
1st Order Model (C_{th} = 713 kJ/°C)	5.1	0.96	0.30
1st Order Model (C_{th} = 654 kJ/°C)	4.1	0.65	0.20
1st Order Model (C_{th} = 623 kJ/°C)	3.7	0.64	0.19
2nd Order Model I	2.2	0.55	0.17
2nd Order Model II	2.1	0.53	0.17
3rd Order Model	2.2	0.55	0.17

Firstly, we compare the evaluation values of the first order models with different C_{th}. According to the obtained results, the model of which parameter was estimated by the interior-reflective Newton Method (with C_{th} = 623 kJ/°C) has better accuracy than the other first order models.

Secondly, we compare the evaluation values of the different order models. The *MAE*s of all the models are less than 0.3 °C. Even, the *MAE* of the well characterized first order model which has 633 kJ/°C of C_{th} is almost similar to the *MAE*s of the 2nd and 3rd order models. Since the envelope of the test room is made by high-insulation materials, its thermal capacitance may be thereby much greater than the internal/external environment's. It means that the thermal capacitance of the envelope is the most important value which has to be exactly estimated among the modeled thermal capacitances. Moreover, at steady-state, all the models have the same thermal behaviors since there is no longer effect of thermal capacitances and that there only exists the influence of the thermal resistances of the envelope. Note that the total thermal resistances of each model are the same. It shows that the first order model with a well estimated C_{th} (here, 623 kJ/°C) can be used to simulate the thermal behavior of the well-insulated room with the advantage of its simplicity. However, considering the maximum *APE* and *MAPE* criteria, the 2nd order models and the 3rd order model are more accurate than the 1st order models. Among the 2nd order models and the 3rd order model, the 2nd order model II has the best accuracy. Even though they were modeled with different orders, C_{i_wi} of the 2nd order model I and C_i of the 3rd order model represent the same component which is the thermal capacitance of internal air mass of the room. The envelope's thermal capacitances of two models are quite similar. Since C_e is relatively small compared to C_w, it can be ignored. For this reason, thermal behavior of the 3rd order model is quite similar to the behavior of the 2nd order model I. However, the 2nd order model II does not separately consider the thermal capacitances of internal/external air mass of the room. Therefore, it leads to reduce the error margin during the state change of the lamps, especially at the beginning of transient-states. While the *APE* during transient-state (6th day) of the 2nd order model I and 3rd order model are about 2.1 %, the *APE* of the 2nd order model II is only 0.5 %. However, even though the performance of the 2nd order model II is better than the others, the 2nd order model I and the 3rd order model can be also useful for the cases where the heat convection of the room is the dominant heat transfer phenomenon. It is because the 2nd order model I and the 3rd order model are distinguishing the heat transfer phenomena of the interior of the room and the envelope.

From this comparison, we can briefly conclude that the 2nd order model II has the best accuracy among the considered models. However, the 2nd order model I has the same accuracy to the 3rd order model and is maybe useful to study the thermal effect of electrical appliances which leads to powerful convection transfer. Between the 2nd order model I and the 3rd order model, the first one is simpler than the second one. We thereby choose the 2nd order models I and II as the building models of the well-insulated room. Thermal models of electrical appliances which will be proposed in the next chapter will be integrated into these two selected building models.

3.7 CONCLUSION

The aim of this chapter was to establish a thermal model for a well-insulated room in order to know the thermal characteristics of the room and describe the thermal behavior of the room. It was the preliminary study to understand the thermal influence of the internal heat gains due to electrical appliances.

To this purpose, the energy balance equations of a conventional building, a low energy building, and a quasi-adiabatic test room were presented. Then, the experimental set-up and procedures for characterizing the test room were presented. A physical model based on the heat balance equation was established. Its equivalent lumped *RC* parameter circuits were also presented using the thermal-electrical analogy. A first order, two second order, and a third order lumped RC parameter models were proposed as the thermal models for the quasi-adiabatic test room. Afterward, the parameter identification procedure was introduced in order to estimate the thermal parameters of the proposed models. The unknown thermal parameters were identified by experimental results and parameter identification methods. Thereafter, the proposed models and their estimated parameters were implemented into Matlab/Simulink®. The thermal behavior of the models was simulated. Finally, the simulation results were compared to the measured data. The evaluation of the models was also achieved. It permits the model selection for the quasi-adiabatic test room. The second order model I and the second order model II were chosen as the thermal models for the quasi-adiabatic room. Briefly, the second order model II is the more accurate model. However, the second order model I is also very accurate and is adapted to describe thermal influence of the electrical appliances which induce a strong convection phenomenon within the room.

The next section will introduce a methodology for designing a generic thermal model of electrical appliances that influences thermal behavior of low energy buildings. Its application will be also presented.

Chapter 4

THERMAL MODELING OF ELECTRICAL APPLIANCES

4.1 INTRODUCTION

Thermal modeling and analysis of building systems have been investigated since 1940s [44,46,47]. Literature introducing different methods to design building systems, including building envelopes, and ventilation/infiltration equipment has been reviewed in the previous chapters. Those investigations help us understanding the thermal behavior of building systems, improving energy efficiency of the systems in order to reach the high thermal comfort of occupants.

There are two factors which influence the thermal behavior and the energy balance of building systems. Firstly, there are deterministic parameters, such as thermal characteristics of building envelopes and sub-systems, geographical and meteorological information of building location. These are quantitatively known at a design level of building constructions. Secondly, there are unpredictable factors, such as occupancy profiles of buildings and usage profiles of building equipment and electrical appliances, which are directly related to the energy consumption of buildings. These are rarely considered or roughly quantified for energy simulation of buildings. These unpredictable factors are one of the reasons causing retrofit errors of building energy simulations [23,24].

The small heat gain differences due to unpredictable factors cause a great error in total for a long-term simulation of energy analysis of a building. The differences influence more the thermal behavior of low energy buildings, zero-energy buildings, and furthermore an energy positive building, which are thermally well-insulated and designed. A more accurate modeling and simulation of heat gains are thus required. As stated before, many researchers have worked

on the modeling of the auxiliary heat gains of buildings, both deterministic and stochastic models of occupant's behavior and lighting usages [38,120,121,122] and metabolic heat by occupants [72,73]. However, there are still only a few researches on modeling of heat gains produced by electrical appliances [19,32]. Roughly estimated load profiles of electrical appliances have been directly quantified as heat gains of electrical appliances in several building simulation tools [58,80]. The rough estimation of heat gains of electrical appliances could be acceptable only if it represents a small portion of the energy of the considered building. However, the number of electrical appliances have increased in both offices and dwelling houses. As a consequence, the thermal modeling of electrical appliances becomes a more important issue for obtaining more reliable and accurate results of the energy simulation of buildings than ever before.

This chapter presents a methodology to establish a thermal model of electrical appliances and to identify its corresponding thermal parameters. In order to present a generic model of all kinds of electrical appliances, we firstly classify electrical appliances into four categories according to thermal and electrical points of view. Based on this classification, a generic thermal model of electrical appliances is established. Then, parameter identification methods for estimating the parameters of the obtained generic model are described in section 4. Afterward, several practical case studies are conducted in order to illustrate the relevance of the proposed model along with the presented identification procedure. Finally, section 7 finally summarizes this chapter.

4.2 CLASSIFICATION OF ELECTRICAL APPLIANCES

As said before, the aim of this chapter is to establish a generic thermal model of electrical appliances. For this purpose, it is necessary to classify electrical appliances regarding their thermodynamic characteristics and their energy conversion types. It is a preliminary study for establishing a generic thermal model of electrical appliances

4.2.1 Types of Thermodynamic Systems

In thermodynamics science, a system is a body which is separated from its surroundings by a boundary. The boundary is a real or imaginary surface between the system and its surroundings. Across the boundary, heat, mass, or work can be exchanged. Based on the interactions through the boundary, three types of thermodynamic systems are defined [143]:

- Isolated System (*IS*),
- Closed System (*CS*),
- Open System (*OS*).

'Isolated System (*IS*)' is a system in which there are no transfers of energy and mass through its boundary. 'Closed System (*CS*)' is a system which has no transfer of mass but which

has energy transfer through its boundary. 'Open System (*OS*)' is a system which permits the mass and energy transfer, across the boundary.

According to the above definitions, each electrical appliance considered as a system, is classified into three types of thermodynamic systems. For the classification, it needs to define first a boundary of an electrical appliance. A boundary of any electrical appliance is defined as the surface of the electrical appliance placed in the building and eventually directly connected to external sub-system.

When the boundary is the surface of an electrical appliance, the surroundings are the outside of the appliance, which is inner space of the building. The energy or/and the mass of electrical appliances are interacted with the inner space of the building. The energy and mass are conserved inside a closed building, only if there is no mass transfer between the interior and the exterior of the building. For the another case, the boundary is not only connection to building envelope but also the surroundings outside of the building. In this case, there exists direct mass transfer (and/or energy) between the electrical appliance and the exterior of the building. Direct mass transfer means that the mass comes in and out of the building through a connection installation, such as a tube. In other words, the boundary for the energy exchange is the surface of the appliance, and the boundary for the mass exchange is the surface of the building.

From these determinations of the boundaries, each electrical appliance which transfers its energy and/or mass is classified as one of the types of thermodynamic systems. However, there is no electrical appliance which is ideally isolated. So, we classify electrical appliances into two different categories: Closed System (*CS*) and Open System (*OS*). Both *CS* and *OS* exchange heat with its surroundings. However, the *OS* additionally exchanges its mass with the surroundings. Almost all electrical appliances only exchange their heat through the boundaries without mass transfer. These are so called *CS*. Here are some examples of *CS*: a refrigerator, a television, a computer, an electric convective heater, a microwave, a hair dryer and so on. Conversely, electrical appliances, which are classified as *OS*, permit the energy and mass transfer, across its boundary. A washing machine and a dish washer are good examples of *OS*. Water is the mass of the appliances. The mass does not remain inside the appliance nor the building. A range hood used for extracting food odors and vapors outside during a cooking process is another example of *OS*. It exchanges the air and the water vapor with its surroundings.

4.2.2 Conversion Types of Electrical Energy

An electrical appliance needs electrical power for its operation. The supplied power into any electrical appliance, $P_{elec}(t)$ [W] is determined by :

$$P_{elec}(t) = V(t) \cdot I(t) \tag{4.1}$$

where $V(t)$ is the voltage [V] and $I(t)$ is the current [A]. Then, the electrical energy of the appliance $E_{elec}(t)$ [J] is expressed by $P_{elec}(t)$ and time t as follows:

$$E_{elec}(t) = \int P_{elec}(t)dt \qquad (4.2)$$

Afterwards, $E_{elec}(t)$ is converted into the other forms of energy, namely, heat and work. According to the conversion types of the electrical energy, electrical appliances are classified in two categories:

- Heating System (*HS*),
- Working System (*WS*).

Basically, all of electrical appliances produce heat due to Joule heating effect. In this procedure, $E_{elec}(t)$ is converted into heat. There are some electrical appliances which function is to heat air or water using Joule heating effect like for example an electric kettle.

Moreover, mechanical equivalent heat is additionally produced by motions of an electrical appliance. For example, a part of $E_{elec}(t)$ is converted into translational or rotational mechanical energy. This mechanical energy is finally converted into heat because there is a mutual interchange between mechanical motion and heat. For example, an electric fan, a refrigerator, and a washing machine generate mechanical equivalent heat as the results of the work of electric motor inside the appliances.

In addition, there is also a part of energy which is converted into acoustic or electromagnetic waves. These forms of energy could also finally be converted into heat. A sound speaker, a radio and a microwave are the examples which produce this kind of heat.

Thus, all the appliances for which $E_{elec}(t)$ is totally converted into heat are called 'Heating Systems (*HS*)'.

However, there are also few appliances whose part of $E_{elec}(t)$ is converted into work, such as comminuting (crushing or grinding) or volume expansion in quasi-adiabatic process. There are some examples, such as an electric grinder and an electric blender. In this case, the final form of the work is not heat. Those appliances, for which final forms of energy are not only heat, but also work, are therefore classified as 'Working systems (*WS*)'.

4.2.3 Categorization

According to the above classifications, electrical appliances can then be categorized into four groups due to their thermodynamic characteristics and energy conversion types:

- Closed-Heating System (*CHS*),
- Closed-Working System (*CWS*),
- Open-Heating System (*OHS*),
- Open-Working System (*OWS*).

Power flux of an electrical appliance regarding the above classification is shown in Figure 4. 1. When electrical power $P_{elec}(t)$ is supplied to an electrical appliance, the power is converted

into several types of power flux according to its own operation and function: the mechanical power $P_{mech}(t)$ [W], the mass flux, and the heat flux across the boundary of the electrical appliance $\dot{Q}_{open}(t)$ and $\dot{Q}_{heat}(t)$ [W]. The characteristics of power fluxes corresponding to each category are detailed in Table 4. 1.
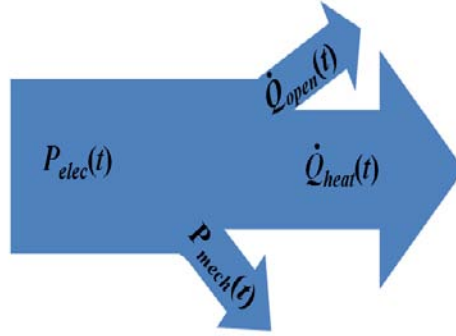
Figure 4. 1 Power flux diagram of an electrical appliance

Table 4. 1 Categories of electrical appliances

	Heating System	Working System
Closed System	$\dot{Q}_{open}(t)=0$, $P_{mech}(t)=0$	$\dot{Q}_{open}(t)=0$, $P_{mech}(t)\neq0$
Open System	$\dot{Q}_{open}(t)\neq0$, $P_{mech}(t)=0$	$\dot{Q}_{open}(t)\neq0$, $P_{mech}(t)\neq0$

$P_{elec}(t)$ of Closed-Heating System (*CHS*) is totally converted into heat flux $\dot{Q}_{heat}(t)$. Therefore, there is neither $\dot{Q}_{open}(t)$ nor $P_{mech}(t)$ in *CHS*. Then $P_{elec}(t)$ of Closed-Working System (*CWS*) is converted into $P_{mech}(t)$ and $\dot{Q}_{heat}(t)$. In *OS*, there is mass flux $\dot{Q}_{open}(t)$ transfers with the exterior of the building. In Open-Heating System (*OHS*), there are $\dot{Q}_{open}(t)$ as well as $\dot{Q}_{heat}(t)$. In Open-Working System (*OWS*), $P_{elec}(t)$ is converted into three types of power fluxes which are $\dot{Q}_{heat}(t)$, $\dot{Q}_{open}(t)$ and $P_{mech}(t)$.

Table 4. 2 shows examples of electrical appliances for each category. The most important difference between *CS* and *OS* is whether the mass flux remains in a building zone or not. Moreover, *HS* and *WS* are distinguished by their energy conversion types. Energy consumed by the electrical appliances which are classified in *CHS* remains in a building zone as a form of heat. The *OHS* appliances convert the supplied power into heat flux, but the flux directly goes outside of the building zone. An electric blender and a grinder, which are *CWS*, convert the electrical energy as forms of comminuting (crushing or grinding) work and heat. The energy remains within a building zone. However, we did not find any example of *OWS*.

As presented above, we classified electrical appliances into four categories: *CHS*, *CWS*, *OHS*, and *OWS*. From this classification, we shall derive a generic thermal model of electrical appliances in the next section.

Table 4. 2 Examples of electrical appliances in categories

	Heating System	Working System
Closed systems	Electric iron, Electric kettle, Electric convective heater, PC, Laptop, Monitor, Video/CD/DVD player, Refrigerator, Electric fan, Hair dryer, Television, Radio, Microwave	Electric blender, Electric grinder
Open Systems	Range hood, Clothes dryer, Washing machine, Dish washer	

4.3 GENERIC THERMAL MODEL OF ELECTRICAL APPLIANCES

This section presents how we establish a generic thermal model of electrical appliances. As mentioned in section 4.1, thermal modeling of electrical appliances becomes an issue of energy simulation of well-insulated buildings, including low energy buildings, zero-energy buildings, and further energy positive buildings. It is helpful to improve accuracy and reliability of thermal analysis of these kinds of buildings with high thermal capacitance/resistance for which even small heat gains can have an influence on the thermal comfort of the inhabitants.

A generic thermal model is deduced by the first law of thermodynamics. The model is then developed by heat and mass transfer phenomena and mechanical operation of electrical appliances. Since the model is generic, it includes the four presented categories of electrical appliances shown in the previous section.

4.3.1 Description of Generic Model

Considering an electrical appliance in a building, we establish a generic thermal model of electrical appliances from the first law of thermodynamics as follows:

$$\Delta U_{ap} = \delta Q_{ap} - \delta W_{ap} \tag{4.3}$$

where, U_{ap}, Q_{ap}, and W_{ap} are respectively the energy [J], the quantity of heat [J] and the work [J] of the electrical appliance. After differentiating U_{ap} with respect to time, eq.(4.3) becomes:

$$\frac{dU_{ap}}{dt} = C_{ap}\frac{dT_{ap}(t)}{dt} = P_{elec}(t) - \dot{Q}_{ap}(t) - \dot{Q}_{ap\_open}(t) - P_{mech}(t) \tag{4.4}$$

where, C_{ap} is the thermal capacitance [J/K] of the electrical appliance, $P_{elec}(t)$ is the input electrical power [W]. $\dot{Q}_{ap}(t)$ and $\dot{Q}_{ap\_open}(t)$ are the heat flux [W] and the corresponding to mass flux [W] generated by the electrical appliance. $P_{mech}(t)$ is the mechanical power [W] of the

appliance. Time-differentiated accumulated heat into the appliance is the sum of power fluxes which are $P_{elec}(t)$, $\dot{Q}_{ap}(t)$, $\dot{Q}_{ap\_open}(t)$, and $P_{mech}(t)$.

Now, we define $\dot{Q}_{ap}(t)$ according to heat transfer phenomena: conduction, convection, and radiation. The heat transfer phenomena of an electrical appliance which is placed on a table in a room are described in Figure 4. 2. The total heat flux of $\dot{Q}_{ap}(t)$ is the sum of the heat flux [W] issued from heat transfers by conduction, convection and radiation as follows:

$$\dot{Q}_{ap}(t) = \dot{Q}_{ap\_cond}(t) + \dot{Q}_{ap\_conv}(t) + \dot{Q}_{ap\_rad}(t) \tag{4.5}$$

where,

$$\dot{Q}_{ap\_cond}(t) = \frac{\lambda_{ap}\kappa S_{ap}}{l_{ap}}(T_{ap}(t) - T_i(t)) \tag{4.6}$$

$$\dot{Q}_{ap\_conv}(t) = h_{ap}(1 - \omega)S_{ap}(T_{ap}(t) - T_i(t)) \tag{4.7}$$

$$\dot{Q}_{ap\_rad}(t) = \varepsilon_{ap}\sigma(1 - \omega)S_{ap}(T_{ap}^{4}(t) - T_i^{4}(t))$$
$$= \varepsilon_{ap}\sigma(1 - \omega)S_{ap}(T_{ap}^{2}(t) + T_i^{2}(t))(T_{ap}(t) + T(t)_i)(T_{ap}(t) - T_i(t)) \tag{4.8}$$
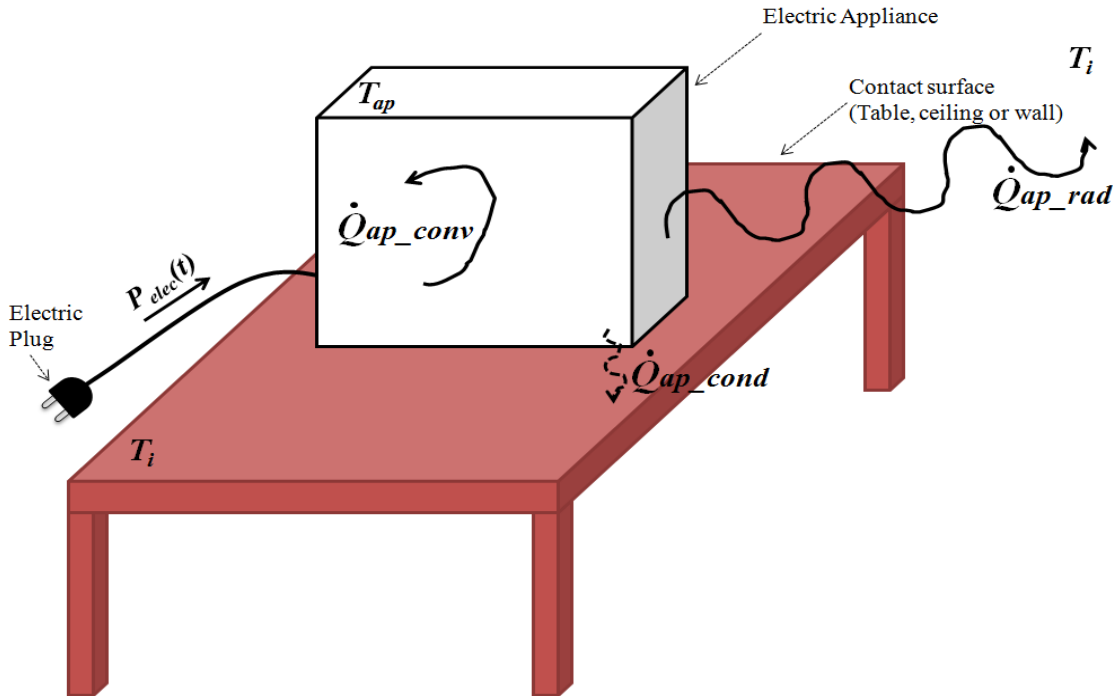
Figure 4. 2 Heat flux by electrical appliance

where, $\dot{Q}$ is the heat flux [W], its indices *ap_cond*, *ap_conv* and *ap_rad* mean respectively conduction, convection, and radiation by appliance. λ_{ap}, l_{ap}, and S_{ap} are the thermal conductivity

[W/m·K], the thickness [m], and the frontier surface area [m^2] of the appliance material, κ is the ratio of contact surface area to surface area of the appliance. h_{ap} is the thermal convective coefficient of air near the appliance [W/m^2·K]. ε_{ap} is the emissivity of the wall, and σ is the Stephan-Boltzman constant whose value is about 5.6704 x 10^{-8} W/m^2·K^4. T_{ap} is the external surface temperature [K] of the appliance. T_i and T_e are the internal and the external temperatures [K] of the room. Depending on these physical properties of electrical appliances, $\dot{Q}_{ap}(t)$ is estimated.

For the simplicity of expressions, eqs.(4.6) - (4.8) would be rewritten as eqs.(4.9) - (4.11).

$$\dot{Q}_{ap\_cond}(t) = \frac{1}{R_{ap\_cond}}(T_{ap}(t) - T_i(t)) \qquad (4.9)$$

$$\dot{Q}_{ap\_conv}(t) = \frac{1}{R_{ap\_conv}}(T_{ap}(t) - T_i(t)) \qquad (4.10)$$

$$\dot{Q}_{ap\_rad}(t) = \frac{1}{R_{ap\_rad}}(T_{ap}(t) - T_i(t)) \qquad (4.11)$$

where R_{ap_cond}, R_{ap_conv}, R_{ap_rad} are the thermal conductive, convective, and radiative resistances [K/W]. They are expressed as follows:

$$R_{ap\_cond} = \frac{l_{ap}}{\lambda_{ap}\omega S_{ap}} \qquad (4.12)$$

$$R_{ap\_conv} = \frac{1}{h_{ap}(1-\omega)S_{ap}} \qquad (4.13)$$

$$R_{ap\_rad} = \frac{1}{\varepsilon_{ap}\sigma(1-\omega)S_{ap}(T_{ap}^{2}(t) + T_i^{2}(t))(T_{ap}(t) + T_i(t))} \qquad (4.14)$$

Then, eq.(4.5) is simplified with R_{ap}, which is the global thermal resistance of the appliance [K/W] :

$$\dot{Q}_{ap}(t) = \frac{1}{R_{ap}}(T_{ap}(t) - T_i(t)) \qquad (4.15)$$

where,

$$\frac{1}{R_{ap}} = \frac{1}{R_{ap\_cond}} + \frac{1}{R_{ap\_conv}} + \frac{1}{R_{ap\_rad}} \qquad (4.16)$$

Here, R_{ap_cond}, R_{ap_conv}, R_{ap_rad} are respectively the conductive, convective and radiative resistances [K/W].

Then, we define $\dot{Q}_{ap\_open}(t)$, the heat flux resulting from mass flux passes in and out of an *OS* electrical appliance.

$$\dot{Q}_{ap\_open}(t) = \frac{1}{R_{ap\_open}}(T_{ap}(t) - \xi T_e(t)) \tag{4.17}$$

where

$$\frac{1}{R_{ap\_open}} = \rho c_p D_{flow} = \rho c_p \int_S v_{flow} dS_{flow} \tag{4.18}$$

where, R_{ap_open} is the equivalent resistance of the mass flux [K/W]. ξ is the ratio between the temperature of external mass T_{e_mass} and the exterior temperature of the building T_e. Then, ρ, c_p, D_{flow}, and v_{flow} are the density [kg/m³], the specific heat [J/(kg·K)], the flow rate [m³/s], and the velocity [m/s] of the mass which goes inside/outside the appliance. S_{flow} is the surface area [m²] of the pipe where the mass goes inside/outside the appliance from/to the exterior of the building.

As following, we define $P_{mech}(t)$, the mechanical power of an electrical appliance which is classified as *WS*:

$$P_{mech}(t) = \eta \cdot P_{elec}(t) \tag{4.19}$$

where, η is the efficiency of mechanical part of the electrical appliance.

From above eqs.(4.5) - (4.19), the mathematical form of generic thermal model is finally deduced as follows:

$$C_{ap}\frac{dT_{ap}(t)}{dt} = (1-\eta) \cdot P_{elec}(t) - \frac{1}{R_{ap}}(T_{ap}(t) - T_i(t)) - \frac{1}{R_{ap\_open}}(T_{ap}(t) - \xi T_e(t)) \tag{4.20}$$

Depending on the categories of electrical appliances, the ranges of thermal parameters are differently defined. The next sub-section states how to adapt this generic thermal model to each category of electrical appliances.

4.3.2 Detailed Models for Each Category

According to the classification method of electrical appliances, which was presented in Section 4.2, there are four categories of electrical appliances: *CHS*, *CWS*, *OHS*, and *OWS*. Table 4. 3 shows the range of determined thermal parameters R_{ap_open} and η of an electrical appliance according to the respective categories. If a system is closed (*CS*) which means that the mass flux of the electrical appliance equals to zero then, the value of R_{ap_open} is considered as infinity. If a system is opened (*OS*), R_{ap_open} has a value which is less than infinity. In addition, in the cases of *HS*, η of the electrical appliance equals to zero. Conversely, η of *WS* is greater than zero but less than one.

Table 4. 3 Range of thermal Parameters according to the categories

	Heating System	Working System
Closed Systems	$R_{ap\_open} = \infty, \eta = 0$	$R_{ap\_open} = \infty, 0 < \eta < 1$
Open Systems	$0 < R_{ap\_open} < \infty, \eta = 0$	$0 < R_{ap\_open} < \infty, 0 < \eta < 1$

Table 4. 4 summarizes the mathematical expressions of each category of electrical appliances deduced from the established generic thermal model. The parameters of each model R_{ap}, C_{ap}, R_{ap_open} are directly calculated when the physical properties and characteristics of electrical appliances are exactly known.

Table 4. 4 Physical models of the thermal systems

	Model Equation
Closed-Heating Systems	$C_{ap} \dfrac{dT_{ap}(t)}{dt} = P_{elec}(t) - \dfrac{1}{R_{ap}}(T_{ap}(t) - T_i(t))$
Closed-Working Systems	$C_{ap} \dfrac{dT_{ap}(t)}{dt} = (1-\eta) \cdot P_{elec}(t) - \dfrac{1}{R_{ap}}(T_{ap}(t) - T_i(t))$
Open-Heating Systems	$C_{ap} \dfrac{dT_{ap}(t)}{dt} = P_{elec}(t) - \dfrac{1}{R_{ap}}(T_{ap}(t) - T_i(t)) - \dfrac{1}{R_{ap\_open}}(T_{ap}(t) - \xi T_e(t))$
Open-Working Systems	$C_{ap} \dfrac{dT_{ap}(t)}{dt} = (1-\eta) \cdot P_{elec}(t) - \dfrac{1}{R_{ap}}(T_{ap}(t) - T_i(t)) - \dfrac{1}{R_{ap\_open}}(T_{ap}(t) - \xi T_e(t))$

However, since the physical properties of each component of electrical appliances are rarely known, it is difficult to obtain the exact values of these parameters. Moreover, even if the physical properties and characteristics of each component of electrical appliances are known, the values of parameters of the model can evolve because of the heat, the age related-degradations and the environment. These unknown parameters cause unfitted results of simulations and analysis of thermal behaviors of electrical appliances and buildings. In order to avoid these problems, identification process is required. The following section presents the used parameter identification procedure.

4.4 PARAMETER IDENTIFICATION OF THE MODEL

Preliminary identification studies and relative literatures have been reviewed in Chapter 2. The reviews were especially focused on building systems. The presented models of electrical appliances in this chapter are of grey-box types. The parameters of the models are depending on the physical properties of electrical appliances, but are not known in details. In addition, this model needs measured input and output data, which provide empirical information of the system behavior.

In this section, we firstly review a parametric identification method using several representative parametric models which are deduced by mathematical relations between measured input and output data of a system. These models include un-controllable noises. Once establishing parametric models and estimating their parameters, we compare them to the presented physical principle-based model to obtain equivalent parameters of each model. However, the model developed by physical principles is expressed in continuous-time domain while the model derived by experiments is described in discrete-time domain. Therefore, we describe in sequence the conversion of a deterministic model in continuous-time into a stochastic model in discrete-time. Thereafter, the relations between the parametric models and the physical principle-based models are described and the parameters of the proposed model of electrical appliances are finally obtained.

4.4.1 Parametric Identification Method

4.4.1.1 Description of Parametric Identification Method

The parametric identification method is used in order to estimate the parameters of a black-box model which has neither prior information nor interaction between a model structure and input/output data of a system. Despite of the absence of physical information of the system, its dynamic behaviors can be predicted by investigating a relationship of predefined parametric models and measured input/output data of the system that we want to model. Methods that identify parameters of a model with minimized prediction error are called "Prediction Error Methods (*PEM*)" [144].

In order to formulate these methods, we suppose that $y[k]$, the measured output at instant $t=k$ and that there is complete knowledge on the past measured output. The predicted output at $t=k+1$ is denoted $\hat{y}[k+1|k]$, which is also called "one-step ahead prediction" of y. $\hat{y}[k+1|k]$ means that $\hat{y}[k+1]$ depends on $y[k]$. The prediction error $\varepsilon[k+1|k]$, between the measured output $y[k+1]$ and the predicted one, is given by

$$\varepsilon[k+1|k] = y[k+1] - \hat{y}[k+1|k] \qquad (4.21)$$

If the model is good, its prediction error has to be small for large sequences of samples ($k=1\sim N$). In order to prevent compensation of positive and negative errors, the square of the error is used. An appropriate loss function J_N is then,

$$J_N = \frac{1}{N}\sum_{k=1}^{N}\varepsilon^2[k|k-1] \qquad (4.22)$$

The model which minimizes the loss function is thus the best model. The parameters of a model structure are collected in a parameter vector θ. The optimal set of parameters of the best model is expressed by $\hat{\theta}_N$. Prediction Error Methods are searching the optimal model for which

$\hat{\theta}_N$ minimizes eq. (4.22). This approach is based on the least square method. Several parametric model structures that fit this approach are stated below.

4.4.1.2 Description of Parametric Model Structures

Parametric model provides a compact form of models which uses predefined polynomials, $A(q)$, $B(q)$, $C(q)$, $D(q)$, or $F(q)$ of the shift operator q. Measured input/output data are available for parameter identification. It is assumed that the input data is a deterministic signal. However, this signal is noisy due to measurement noise. [145].

The general form of the models is given (See also Figure 4.3) [144]:

$$A(q) \times y[k] = \frac{B(q)}{F(q)} x[k] + \frac{C(q)}{D(q)} e[k]$$

(4.23)

where $y[k]$, $x[k]$ are respectively the output and the input of system. $e[k]$ is the stochastic error of the system. The error accounts for a white noise, which has a normal distribution, a zero mean, and a constant covariance.
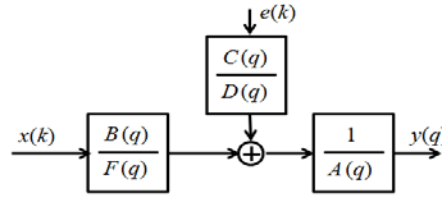
Figure 4. 3 Block diagram of general form of parametric model

The polynomials of the model structures are defined as:

$$A(q) = 1 + a_1 q^{-1} + a_2 q^{-2} + \cdots + a_{n_a} q^{-n_a}$$

(4.24)

$$B(q) = b_1 q^{-1} + b_2 q^{-2} + \cdots + b_{n_b} q^{-n_b}$$

(4.25)

$$C(q) = 1 + c_1 q^{-1} + c_2 q^{-2} + \cdots + c_{n_c} q^{-n_c}$$

(4.26)

$$D(q) = 1 + d_1 q^{-1} + d_2 q^{-2} + \cdots + d_{n_d} q^{-n_d}$$

(4.27)

$$F(q) = 1 + f_1 q^{-1} + f_2 q^{-2} + \cdots + f_{n_f} q^{-n_f}$$

(4.28)

where a_i, b_i, c_i, d_i, and f_i are the ith constant coefficients of the corresponding polynomial. n_a, n_b, n_c, n_d, and n_f are the order of the respective polynomials.

By selecting one or more polynomials, the different model structures are obtained. There are several predefined parametric models: Auto-Regressive with eXogenous input (*ARX*) model, Auto-Regressive Moving Average with eXogenous input (*ARMAX*) model, Output Error (*OE*)

model, and Box-Jenkins (*BJ*) model. More details on parametric models can be found in [146,147,148]. Auto-Regressive with eXogenous input (*ARX*) model is described by eq. (4.29). There is an input excitation and a noise term. The transfer functions of the output/input and the output/noise have the same dynamics because they have the same set of poles. Despite there is no flexibility for the choice of the noise transfer function, this model is frequently used for its simplicity. The solution is always unique and satisfies the global minimum of the least square loss function.

$$A(q) \times y[k] = B(q) \times x[k] + e[k] \tag{4.29}$$

$$y[k] = [(1 - A(q)) \times y[k] + B(q)x[k]] + e[k] \tag{4.30}$$

Using eqs. (4.29) - (4.30), the model output $\hat{y}[k]$, the optimal parameter vector $\hat{\theta}_k$ and the regression vector $\phi[k]$ are given as below:

$$\hat{y}[k] = [(1 - A(q)) \times y[k] + B(q)x[k]] = \phi_k^T \hat{\theta}_k \tag{4.31}$$

$$\hat{\theta}_k = [a_1 \quad \cdots \quad a_{n_a} \quad b_1 \quad \cdots \quad b_{n_b}]^T \tag{4.32}$$

$$\phi_k^T[k] = [-y[k-1] \quad \cdots \quad y[k-n_a] \quad x[k-1] \quad \cdots \quad x[k-n_b]] \tag{4.33}$$

Auto-Regressive Moving Average with eXogenous input (*ARMAX*) model is structured by eq.(4.34). Although disturbances of the model is filtered by the polynomial $A(q)$, it has a more flexible noise transfer function due to polynomial $C(q)$. This model is widely used in the presence of uncertain dynamics.

$$A(q)y[k] = B(q)x[k] + C(q)e[k] \tag{4.34}$$

$$y[k] = [(1 - A(q))y[k] + B(q)x[k]] + C(q)e[k] \tag{4.35}$$

Using eqs. (4.34) - (4.35), the *ARMAX* prediction model output $\hat{y}[k]$, the optimal parameter vector $\hat{\theta}_k$, and the regression vector $\phi[k]$ are as below:

$$\hat{\theta}_k = [a_1 \quad \cdots \quad a_{n_a} \quad b_1 \quad \cdots \quad b_{n_b} \quad c_1 \quad \cdots \quad c_{n_c}]^T \tag{4.36}$$

$$\phi_k^T[k|\theta] = [-y[k-1] \quad \cdots \quad -y[k-n_a] \quad x[k-1] \quad \cdots \quad u[k-n_b] \quad \varepsilon[k-1|\theta] \quad \cdots \quad \varepsilon[k-n_c|\theta]] \tag{4.37}$$

$$\hat{y}[k|\theta] = [(1 - A(q))y[k] + B(q)x[k]] + (C(q)-1)\varepsilon[k|\theta] = \phi_k^T[k|\theta]\hat{\theta}_k \tag{4.38}$$

Output Error (*OE*) model assumes that there is only uncertainty of an additive white noise which is typically measurement noise. The model structure is expressed by

$$F(q)w[k] = B(q)x[k] \tag{4.39}$$

$$w[k] = (1 - F(q))w[k] + B(q)x[k] \tag{4.40}$$

$$y[k] = w[k] + e[k] = (1 - F(q))w[k] + B(q)x[k] + e[k] \tag{4.41}$$

The output of the prediction model $\hat{y}[k]$, the optimal parameter set $\hat{\theta}_k$, and the regression vector $\phi[k]$ are as follows:

$$\hat{y}[k] = (1 - F)w[k] + B(q)x[k] = \phi_k^T[k \mid \theta]\hat{\theta}_k \tag{4.42}$$

$$\hat{\theta}_k = [b_1 \quad \cdots \quad b_{n_a} \quad f_1 \quad \cdots \quad f_{n_f} \quad]^T \tag{4.43}$$

$$\phi_k^T[k \mid \theta] = [x[k-1] \quad \cdots \quad x[k-n_b] \quad -w[k-1] \quad \cdots \quad -w[k-n_f]] \tag{4.44}$$

The basic equation for Box-Jenkins (*BJ*) model is given by eq.(4.45). This model gives a better flexibility to handle disturbances with its polynomials $C(q)$ and $D(q)$.

$$y[k] = \frac{B(q)}{F(q)}x[k] + \frac{C(q)}{D(q)}e[k] \tag{4.45}$$

$$w[k] = (1 - F(q))w[k] + B(q)x[k] \tag{4.46}$$

$$v[k] = (1 - F(q))w[k] + B(q)x[k] - y[k] \tag{4.47}$$

The prediction model $\hat{y}[k]$ follows from eqs.(4.45) - (4.47).

$$\hat{y}[k \mid \theta] = D(q)v[k] + C(q)y[k] \tag{4.48}$$

$$\hat{y}[k \mid \theta] = v[k] + (D(q) - 1)v[k] + (C(q) - 1)\varepsilon[k \mid \theta] + y[k] \tag{4.49}$$

$$\hat{y}[k \mid \theta] = w[k] + (D(q) - 1)v[k] + (C(q) - 1)\varepsilon[k \mid \theta] \tag{4.50}$$

$$\hat{y}[k \mid \theta] = Bx[k] + (C(q) - 1)\varepsilon[k \mid \theta] + (D(q) - 1)v[k] + (1 - F(q)) = \phi_k^T[k \mid \theta]\hat{\theta}_k \tag{4.51}$$

Then, the optimal parameter set $\hat{\theta}_k$ and the regression vector $\phi[k]$ are as below:

$$\hat{\theta}_k = [b_1 \quad \cdots \quad b_{n_b} \quad c_1 \quad \cdots \quad c_{n_c} \quad d_1 \quad \cdots \quad d_{n_d} \quad f_1 \quad \cdots \quad f_{n_f}]^T \tag{4.52}$$

$$\phi_k^T[k \mid \theta] = [x[k-1] \quad \cdots \quad x[k-n_b] \quad \varepsilon[k-1] \quad \cdots \quad \varepsilon[k-n_c]$$
$$v[k-1] \quad \cdots \quad v[k-n_d] \quad -w[k-1] \quad \cdots \quad -w[k-n_f]] \tag{4.53}$$

Table 4. 5 briefly indicates the different model structures and selection of the polynomials of each structure. A '1' denotes that the polynomial is fixed as 1, and a '√' denotes that it can be freely chosen.

The main difference among the presented structures is the way to model disturbances. The disturbances of the *ARX* and the *ARMAX* models have the same poles. The disturbances of the *OE* and *BJ* models are separately modeled from the plant model. The *OE* model does not

include any polynomial in noise process. The *BJ* model has a free numerator and a free denominator polynomials. These models are useful when measurement noise is dominant.

Table 4. 5 Different model and selection of polynomials

	$A(q)$	$B(q)$	$C(q)$	$D(q)$	$F(q)$
ARX	√	√	1	1	1
ARMAX	√	√	√	1	1
OE	1	√	1	1	√
BJ	1	√	√	√	√

1: fixed as 1, √: chosen freely

We have been presented several structures of empirical models. The obtained parameters of these models have no direct physical meaning. These parameters are only considering a relation between the input and the output of the system to be modeled. The following sub-section presents a reformulation of the physically governed equation into a stochastic differential equation in discrete-time domain. The objective of this matching process is finding out the relations between the empirical models and the physical prior based-model proposed in Section 4.3 in order to estimate the parameters of the system which can be physically interpreted.

4.4.2 Reformulation of Physically Governed Equation

4.4.2.1 Stochastic Differential Equation

A lumped continuous-time state space models is described as follows [149]:

$$\frac{dx}{dt} = f(x,u,t,\theta) \tag{4.54}$$

where *f* is the function of appropriate dimension. The model variables are classified as follows: *u* is the vector of independent variables (input), *x* is the vector of dependent variables described by differential equations (states), *t* is the time, and θ is the vector of possibly unknown parameters.

We develop this structure into a linear stochastic form with an additional noise term. The noise term represents measurement noise and/or input noise. Using this term, the deviation between real measurements and simulations can be described. The framework of linear stochastic differential equations in continuous-time is described as follows [107,150]:

$$\frac{dx}{dt} = f(x,u,t,\theta) + \frac{d\omega(t)}{dt} \tag{4.55}$$

91

where $\omega(t)$ is a stochastic Wiener process. It is assumed to be a stochastic process with independent incremental deviation.

In the general linear case, if only a linear combination of the states is measured, the measured or recorded variables are written as follows:

$$y = g(x,u,t,\theta)dt + e(t) \tag{4.56}$$

where g is a function of appropriate dimension, $e(t)$ is the measurement error. It accounts for a white noise, which has a normal distribution, a zero mean, and a constant covariance.

In our case, the structure of the generic model in continuous-time domain is established as shown in eq. (4.20). The structure can be derived into a linear stochastic form, which includes a random noise process, as stated above. As using the noise term, the deviation between real measurements and simulation results can be compensated. The model is expressed by the linear stochastic differential form as follows:

$$C_{ap}\frac{dT_{ap}(t)}{dt} = (1-\eta)\cdot P_{elec}(t) - \frac{1}{R_{ap}}(T_{ap}(t) - T_i(t)) - \frac{1}{R_{ap\_open}}(T_{ap}(t) - \xi T_e(t)) + e(t) \tag{4.57}$$

where $e(t)$ is once again the stochastic process which is assumed to be a zero mean white noise.

4.4.2.2 Difference Equation in Discrete-Time Domain

To identify the parameters of a model, time series of the input and the output of the system are required. They are measured in practice in discrete-time. In order to match the measurement results and the observed variables of the model, the continuous-time model needs to be discretized. To do this discretization, several methods are available: Euler, Tustin. Here, the Euler method was used for its simplicity. This choice is justified because of the great difference between the sampling period and the dynamics of the studied systems. With this method, the derivative term is approximated as follows

$$\frac{dx}{dt} = \frac{x[(k+1)T_S] - x[kT_S]}{T_S} \tag{4.58}$$

where k is the kth sampling instant, T_S is the sampling period.

Equation. (4.57) is then discretized by Euler method as follows:

$$T_{ap}[k] - \left(1 - \frac{T_S}{R_{ap}C_{ap}} - \frac{T_S}{R_{ap\_open}C_{ap}}\right)T_{ap}[k-1]$$

$$= \frac{T_S(1-\eta)}{C_{ap}}P_{elec}[k-1] + \frac{T_S}{R_{ap}C_{ap}}T_i[k-1] + \frac{T_S\xi}{R_{ap\_open}C_{ap}}T_e[k-1] + e[k] \tag{4.59}$$

Equation (4.59) is also expressed as below, using the delay shift operator q^{-1}, in order to match the equation with the parametric model's one.

$$\left\{1-\left(1-\frac{T_S}{R_{ap}C_{ap}}-\frac{T_S}{R_{ap\_open}C_{ap}}\right)q^{-1}\right\}T_{ap}[k]$$

$$=\frac{T_S(1-\eta)}{C_{ap}}q^{-1}P_{elec}[k]+\frac{T_S}{R_{ap}C_{ap}}q^{-1}T_i[k]+\frac{T_S\xi}{R_{ap\_open}C_{ap}}q^{-1}T_e[k]+e[k] \qquad (4.60)$$

Equation (4.60) shows a Multi-Input Single-Output (*MISO*) model which has three inputs $P_{elec}[k]$, $T_i[k]$ and $T_e[k]$, and one output $T_{ap}[k]$. This model now corresponds to the presented linear parametric models. The next sub-section shows their correspondences and the way to convert parameters estimated by the parametric models to the parameters of the physics prior based-model.

4.4.3 Correspondence to Parametric Models

4.4.3.1 Corresponding Model Structures

We develop here the *MISO* parametric models which has a *3*-dimensional input vector and a single output. The dimensions of input and output vectors are the same of eq.(4.60). The corresponding parametric models of the generic model of electrical appliances given by eq. (4.60) are shown below.

ARX model:
$$A(q)T_{ap}{}^*[k]=\begin{bmatrix} B_1(q) & B_2(q) & B_3(q)\end{bmatrix}\cdot\begin{bmatrix} T_i^*[k] \\ T_e^*[k] \\ P_{elec}{}^*[k]\end{bmatrix}+e[k] \qquad (4.61)$$

ARMAX model:
$$A(q)T_{ap}{}^*[k]=\begin{bmatrix} B_1(q) & B_2(q) & B_3(q)\end{bmatrix}\cdot\begin{bmatrix} T_i^*[k] \\ T_e^*[k] \\ P_{elec}{}^*[k]\end{bmatrix}+C(q)e[k] \qquad (4.62)$$

OE model:
$$T_{ap}{}^*[k]=\begin{bmatrix} \dfrac{B_1(q)}{F_1(q)} & \dfrac{B_2(q)}{F_2(q)} & \dfrac{B_3(q)}{F_3(q)}\end{bmatrix}\cdot\begin{bmatrix} T_i^*[k] \\ T_e^*[k] \\ P_{elec}{}^*[k]\end{bmatrix}+e[k] \qquad (4.63)$$

BJ model:
$$T_{ap}{}^*[k]=\begin{bmatrix} \dfrac{B_1(q)}{F_1(q)} & \dfrac{B_2(q)}{F_2(q)} & \dfrac{B_3(q)}{F_3(q)}\end{bmatrix}\cdot\begin{bmatrix} T_i^*[k] \\ T_e^*[k] \\ P_{elec}{}^*[k]\end{bmatrix}+\dfrac{C(q)}{D(q)}e[k] \qquad (4.64)$$

where * means the measured quantities. $A(q)$, $B_1(q)$, $B_2(q)$, $B_3(q)$, $C(q)$, $D(q)$, $F_1(q)$, $F_2(q)$, and $F_3(q)$ are polynomials in the shift operator q, defined as

$$A(q) = 1 + a_1 q^{-1} \tag{4.65}$$

$$B_i(q) = b_{i1} q^{-1} \tag{4.66}$$

$$C(q) = 1 + c_1 q^{-1} \tag{4.67}$$

$$D(q) = 1 + d_1 q^{-1} \tag{4.68}$$

$$F_i(q) = 1 + f_{i1} q^{-1} \tag{4.69}$$

where the subscript i is the number of the inputs (i=1~3). a_1, b_{i1}, c_1, d_1, and f_1 are the parameters to be estimated.

The parameter vector θ to be identified, the regression vector $\phi[k]$, and the output of the prediction model $\hat{T}_{ap}[k|\theta]$ are as follows.

ARX
$$\theta = \begin{bmatrix} a_1 & b_{11} & b_{21} & b_{31} \end{bmatrix}^T$$

$$\phi[k] = \begin{bmatrix} -T_{ap}^*[k-1] & T_i^*[k-1] & T_e^*[k-1] & P_{elec}^*[k-1] \end{bmatrix}^T \tag{4.70}$$

$$\hat{T}_{ap}^*[k|\theta] = \theta^T \phi[k] = \phi^T[k]\theta$$

ARMAX
$$\theta = \begin{bmatrix} a_1 & b_{11} & b_{21} & b_{31} & c_1 \end{bmatrix}^T$$

$$\phi[k|\theta] = \begin{bmatrix} -T_{ap}^*[k-1] & T_i^*[k-1] & T_e^*[k-1] & P_{elec}^*[k-1] & \varepsilon[k-1|\theta] \end{bmatrix}^T \tag{4.71}$$

$$\hat{T}_{ap}^*[k|\theta] = \theta^T \phi[k|\theta] = \phi^T[k|\theta]\theta$$

OE
$$\theta = \begin{bmatrix} b_{11} & b_{21} & b_{31} & f_{11} & f_{21} & f_{31} \end{bmatrix}^T$$

$$\phi[k|\theta] = \begin{bmatrix} T_i^*[k-1] & T_e^*[k-1] & P_{elec}^*[k-1] & -w_1[k-1] & -w_2[k-1] & -w_3[k-1] \end{bmatrix} \tag{4.72}$$

$$\hat{T}_{ap}^*[k|\theta] = \theta^T \phi[k|\theta] = \phi^T[k|\theta]\theta$$

BJ
$$\theta = \begin{bmatrix} b_{11} & b_{21} & b_{31} & c_1 & d_1 & f_{11} & f_{21} & f_{31} \end{bmatrix}^T$$

$$\phi[k|\theta] = \begin{bmatrix} T_i^*[k-1] & T_e^*[k-1] & P_{elec}^*[k-1] & \varepsilon[k-1|\theta] & v[k-1] \\ & -w_1[k-1] & -w_2[k-1] & -w_3[k-1] \end{bmatrix} \tag{4.73}$$

$$\hat{T}_{ap}^*[k|\theta] = \theta^T \phi[k|\theta] = \phi^T[k|\theta]\theta$$

In order to search the optimal parameter vector $\hat{\theta}_N$, the least square method is used. $J_N(\theta)$ is the criterion to be minimized.

$$\hat{\theta}_N = \arg\min J_N[\theta] \tag{4.74}$$

$$J_N(\theta) = \frac{1}{N}\sum_{k=1}^{N} \varepsilon^2[k \mid k-1, \theta] \tag{4.75}$$

where

$$\varepsilon[k \mid k-1, \theta] = T_{ap}^{*}[k] - \hat{T}_{ap}[k \mid k-1, \theta] \tag{4.76}$$

$\varepsilon[k \mid k-1, \theta]$ is the prediction error between the measured output $T_{ap}^{*}[k]$ and the predicted one $\hat{T}_{ap}[k \mid k-1, \theta]$ for the kth sample.

All the identification procedure was carried out with the help of the Matlab® System Identification Toolbox. Finally, by comparing the physically governed model (eq.(4.60)) with the identified parameters of the above presented parametric models, the equality of the parameters can be derived.

4.4.3.2 Physical Interpretation of Parameters

Among the presented parametric models, *ARX* and *ARMAX* models have a good matching with eq. (4.60). However, *OE* and *BJ* models have different poles depending on the considered transfer function, ($B_1(q)/F_1(q)$, $B_2(q)/F_2(q)$, and $B_3(q)/F_3(q)$). Therefore, in the following we only consider the *ARX* and *ARMAX*. After estimating the optimal parameters of the presented *ARX* and *ARMAX* parametric models, we can then deduce the parameters of the physically governed model. The unknown parameters of eq. (4.26) are then obtained by comparing eq. (4.60) with the parameters of *ARX* and *ARMAX* models described by eq. (4.61) and eq. (4.62). It yields

$$a_1 = -1 + \frac{T_S}{R_{ap}C_{ap}} + \frac{T_S}{R_{ap\_open}C_{ap}} \tag{4.77}$$

$$b_{11} = \frac{T_S(1-\eta)}{C_{ap}} \tag{4.78}$$

$$b_{21} = \frac{T_S}{R_{ap}C_{ap}} \tag{4.79}$$

$$b_{31} = \frac{T_S}{R_{ap\_open}C_{ap}} \tag{4.80}$$

Once establishing the thermal model of an electrical appliance and obtained its physical parameters, we can then integrate the model into a well-insulated building model. The following section shows the coupled model of an electrical appliance and a well-insulated building.

4.5 COUPLED MODEL WITH A WELL-INSULATED BUILDING MODEL

One of the main objectives of thermal modeling of electrical appliances is to investigate thermal effect of heat gain of electrical appliances in buildings. The quantity of heat gains of electrical appliances in a building increase as the variety of electrical appliance becomes widespread and their usages become more frequent in human life. Moreover, the heat gain becomes more and more significant in energy efficient building. From these backgrounds, we present a coupled model of an electrical appliance and a well-insulated building in order to study their mutual thermal behaviors.

4.5.1 Physically Governed Model

The proposed generic thermal model of electrical appliances is now connected to a well-insulated building model. The used building model is based on the heat balance equation which was presented in Chapter 3. In previous chapter, it was assumed that the electrical power of an electrical appliance is instantaneously transferred as a form of heat to the space where it has been placed. However, in this chapter, the heat flux supplied by an electrical appliance was modeled more accurately, including its own dynamics. The heat balance equation is now

$$\frac{dU_{in}(t)}{dt} = \dot{Q}_{appliance}(t) - \dot{Q}_{envelope}(t) \tag{4.81}$$

where U_{in} is the energy [J] supplied to the building, $\dot{Q}_{appliance}$ is the heat flux [W] dissipated by the electrical appliance and $\dot{Q}_{envelope}$ is the heat flux [W] which is transferred through the building envelope, due to the difference of T_i and T_e.

The time-differentiated energy of an electrical appliance was shown in eq. (4.20). The formula of $\dot{Q}_{envelope}$ was expressed as eq. (3.18) in the previous chapter. From these expressions, eq. (4.81) which is a mathematical form of the coupled model of an electrical appliance and a well-insulated building is then deduced as:

$$C_{th}\frac{dT_i(t)}{dt} = \frac{1}{R_{ap}}(T_{ap}(t) - T_i(t)) - \frac{1}{R_{th}}(T_i(t) - T_e(t))$$

$$= (1-\eta)\cdot P_{elec}(t) - C_{ap}\frac{dT_{ap}(t)}{dt} - \frac{1}{R_{ap\_open}}(T_{ap}(t) - \xi T_e(t)) - \frac{1}{R_{th}}(T_i(t) - T_e(t)) \tag{4.82}$$

The thermal behavior of an electrical appliance, a building, and their mutual interactions are depending on both the initial conditions of the temperatures: $T_{ap}(0)$, $T_i(0)$, $T_e(0)$ and the

parameters of the model: R_{ap}, C_{ap}, R_{th}, C_{th}, R_{ap_open}, η, and ξ. The parameters are obtained by the physical properties of each electrical appliance and of the building. However, if their physical properties are not exactly known, they can be estimated by identification (see section 4.4).

4.5.2   Equivalent *RC* Model

From the above principles, we can develop an equivalent lumped *RC* circuit of the generic thermal model of electrical appliances which is integrated into a building model. This model is to predict the indoor temperature of the building $T_i(t)$ and the heat flux $\dot{Q}_{ap}(t)$ generated by an electrical appliance. We can use the analogy between thermal model and electrical circuit which was presented in Section 3.4.

According to the thermal-electrical analogy, an electrical heat source in a thermal model corresponds to a current source in an electrical circuit. Temperature potentials in thermal model can be expressed by their equivalent voltages in electrical circuit. Moreover, a thermal capacitance and a thermal resistance are equivalent to an electrical capacitance and an electrical resistance. Using this analogy, a coupled model of an electrical appliance and a well-insulated building expressed by eq.(4.20) and eq.(4.82).

The proposed scheme is shown Figure 4. 4. The assumptions of the coupled model are the followings:

- The initial temperatures of the electrical appliance, the inner and outer building are the same ($T_{ap}(0)=T_i(0)=T_e(0)$).
- The temperature of electrical appliance is homogeneous.
- The indoor temperature is homogeneous.
- The thermal resistance and the thermal capacitance of the electrical appliances are the global parameters.
- The thermal resistance and the thermal capacitance of the building models are the global parameters.
- There is no additional heat flux from solar radiation, metabolism, infiltration, ventilation and air leakages by window, door, thermal bridges or any small hole.
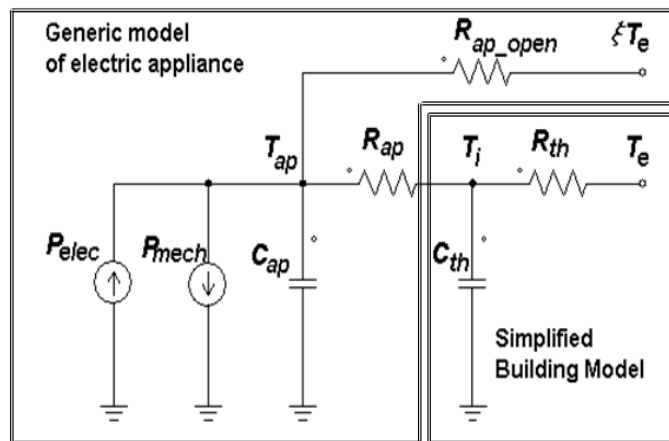
Figure 4. 4 Thermal-electrical equivalent circuit of a coupled model

The proposed coupled model consists of two parts: a generic model of the electrical appliance and a simplified building model. Once electrical power is supplied to the electrical appliance, it is converted into a mechanical power if the appliance is a working system, and a heat flux. A certain quantity of the heat flux is then accumulated in the appliance depending on the thermal capacity of the appliance. The rest of the heat flux goes through two ways: R_{ap_open} and R_{ap}. If the appliance is a *CS*, R_{ap_open} is infinity. It means that in the case of *CS*, all the heat flux passes through R_{ap}.

Moreover, it is of possible to replace the simplified first-order lumped *RC* model of a well insulated building model by the second or third order models as introduced in section 3.4.2.

4.6 CASE STUDY

In this section we present the application to practical cases of the proposed generic thermal model of electrical appliances. Five Closed-Heating Systems (*CHS*) are chosen: a monitor, a computer, a refrigerator, a portable electric convection heater, and a microwave.

4.6.1 Description of Experiment

The selected electrical appliances were tested in a well-insulated room. The thermal characteristics of the room were already identified in Chapter 3. The estimated global thermal parameters of the test room are equal to R_{th}=57.8 x10^{-3} °C/W, C_{th}=623 kJ/°C. The characteristics of the second order models and the third order model of the room are also detailed in section 3.5.2.

In this room, we measure the following data of each electrical appliance: $T_{ap}^{*}(t)$, $T_{i}^{*}(t)$, $T_{wi}^{*}(t)$, $T_{we}^{*}(t)$, $T_{e}^{*}(t)$, and $P_{elec}^{*}(t)$. To measure each temperature, twenty K-type thermocouples were installed inside and outside of the room. Two thermocouples are positioned beyond the electrical appliance in order to measure $T_{ap}^{*}(t)$ for each experiment. Eighteen thermocouples are positioned for measuring $T_{i}^{*}(t)$, $T_{wi}^{*}(t)$, $T_{we}^{*}(t)$, and $T_{e}^{*}(t)$ as mentioned in Chapter 3. At the same time a power metering device is connected to the tested electrical appliance to measure $P_{elec}^{*}(t)$ of the appliance. The data is measured each minute and is stored into a host computer. All the measurements are synchronized. The details of the room and measurement instruments are given in Chapter 3.

4.6.2 Description of the Method

Since the selected electrical appliances belong to the Closed-Heating System category, the values of R_{ap_open} and η is already known ($R_{ap\_open} = \infty$, $\eta = 0$). Thus, we gather $P_{elec}^{*}(t)$, $T_{ap}^{*}(t)$, and $T_{i}^{*}(t)$ among all of the measured data for each electrical appliance in order to estimate the thermal parameters R_{ap} and C_{ap}. With these experimental data, we establish Multi-Input Single-

Output (*MISO*) parametric models, namely, *ARX* and *ARMAX* structures for each electrical appliance. Then, we identify the optimal parameter vector, which minimizes the criterion defined by eq. (4.22). After that, we convert the estimated parameters into R_{ap}, C_{ap}, τ_{ap} by using the following relations between the parametric models and the physical principle based-model parameters. These relations are derived from eqs. (4.77) - (4.80).

$$R_{ap} = \frac{b_{11}}{b_{21}} \tag{4.83}$$

$$C_{ap} = \frac{T_S}{b_{11}} \tag{4.84}$$

$$\tau_{ap} = \frac{T_S}{a_{11}+1} \tag{4.85}$$

where τ_{ap} is the time constant of the electrical appliance [s]. T_S is the sampling time, that is fixed to 60s. Using the estimated parameters R_{ap} and C_{ap}, we can then simulate $T_{ap}(t)$ and compare it to its corresponding measurement $T_{ap}^{*}(t)$ in order to validate the thermal model of each appliance.

After establishing the model and identifying its parameters, each modeled electrical appliance is integrated into a well-insulated building model in order to observe its thermal behavior within the building. The second order lumped *RC* models I and II are selected to represent the building.

We then compare the internal temperature of the building in which there are three models for each electrical appliance. The first two models are the models that have been modeled by the above procedure. These models have the parameters which were identified with the help of the *ARX* and *ARMAX* models. The third one is the simplified model which was used in Chapter 3. It means that the third model includes no other thermal characteristics of the electrical appliance, than, its consumed electrical power which is directly injected to the building model. This comparative study investigates the interest of modeling accurately electrical appliances. It helps to reply to the question whether there is a certain benefit of the thermal modeling of electrical appliance when performing building energy simulations.

4.6.3 Evaluation of Models

After structuring the model and identifying its parameters, it is integrated in the well-insulated building model. It aims to observe its thermal behavior within the building. The measured value and the simulated value of the temperature T_{ap} are then compared. In order to evaluate the accuracy of the obtained models of each electrical appliance, the Mean of the sum of Absolute Error (*MAE*) and Mean of the sum of Square Errors (*MSE*), and Mean Absolute Percentage relative Error (*MAPE*) are taken [108]:

$$MAE = \frac{1}{N} \sum_{k=1}^{N} | T_{ap}^{*}[k] - T_{ap}[k] | \tag{4.86}$$

$$MSE = \frac{1}{N}\sum_{k=1}^{N}[T_{ap}^{*}[k] - T_{ap}[k]]^2 \qquad (4.87)$$

$$MAPE = \frac{1}{N}\sum_{j=1}^{N}\left|\frac{T_{ap}^{*}[k] - T_{ap}[k]}{T_{ap}^{*}[k]}\right| \times 100[\%] \qquad (4.88)$$

These evaluation terms are also used for T_i in order to evaluate the integrating models.

4.6.4   Results of Parameter Estimation

In this sub-section, we identify two parameters R_{ap} and C_{ap} of the thermal models of several electrical appliances. The selected electrical appliances are a monitor, a computer, a refrigerator, a portable electric convection heater, and a microwave as indicated above. The model parameters are estimated by using the proposed identification methods.

4.6.4.1   Monitor Case

The experiment for a thermal characterization of a monitor was carried out during six days. Before starting the measurement, a monitor was placed in the well-insulated room in order to have the same initial temperature with the room initial temperature. After starting the experiment, the monitor was kept on during the first four days. Then, it was turned off during rest of the experiment.

Among the measured data, $P_{elec}^{*}(t)$, $T_{ap}^{*}(t)$, and $T_i^{*}(t)$ were used for estimating the thermal parameters of the monitor. By using proposed parameter estimation method, the parameters of *ARX* and *ARMAX* models were obtained. According to the relation between the *ARX* and *ARMAX* parametric models and the physical model of *CHS*, the parameters of the monitor R_{ap}, C_{ap}, and τ_{ap} were identified. Table 4. 6 lists the results. Even though the values of R_{ap}, C_{ap} estimated by *ARX* and *ARMAX* model are different, their time constants τ_{ap} are similar.

Table 4. 6 Estimated thermal parameters of a monitor

Observed Variable	Parametric Model	Name	R_{ap} [°C/W]	C_{ap} [kJ/°C]	τ_{ap} [s]
T_{ap}	*ARX*	*sim1*	2.5 x10⁻³	36.7	92
	ARMAX	*sim2*	4.7 x10⁻³	19.5	92

Based on these obtained parameters of *ARX* and *ARMAX* models, the temperatures of the monitor T_{ap} were separately simulated and were compared to the measured one. Figure 4. 5 describes the results of T_{ap}: T_{ap}^{*} is the measured one, $T_{ap,sim1}$ and $T_{ap,sim2}$ are the simulation results corresponding to the *ARX* and *ARMAX* models.
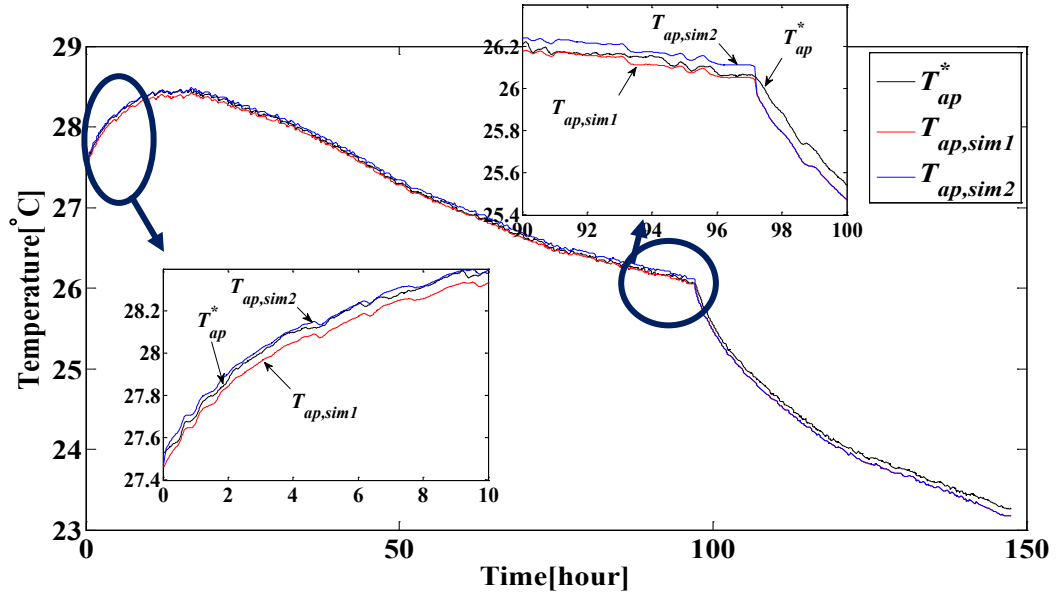
Figure 4. 5 Measured and simulated temperatures of a monitor T_{ap}

The three curves of T_{ap} globally tend to decrease. It is due to a drop of the external temperature during the experiment. However, regardless of this falling behavior, the simulated $T_{ap,sim1}$ and $T_{ap,sim2}$ have a good matching with the measured one during both at transient and at steady-state.

Table 4. 7 presents the evaluation results of the models. The mean of the sum of absolute error (*MAE*) of each model is less than 0.05 °C. The difference of the *MAE* of each model is about 0.003 °C. After the monitor is turned off, the curves of $T_{ap,sim1}$ and $T_{ap,sim2}$ are identical to each other since their time constants which show their thermal characteristics are equal. Therefore, the difference of the *MAE*s of these models is mainly caused by R_{ap}. We can observe that $T_{ap,sim2}$ is just a little greater than T_{ap}^* during steady-state. It means that R_{ap} of *ARMAX* model is a little over-estimated. However, the error is negligible. In addition the *MAPE* of each model is less than 0.2 %. From these evaluation results, it is shown that the parameters estimated by both parametric models are well-estimated.

Table 4. 7 Results of model evaluation by T_{ap}

Observed Variable	Parametric Model	Name	Evaluation		
			MAE [°C]	*MSE* [°C^2]	*MAPE* [%]
T_{ap}	*ARX*	sim1	0.043	0.003	0.167
	ARMAX	sim2	0.046	0.003	0.178

Figure 4. 6 illustrates the measured $P_{elec}^*(t)$ and simulated $\dot{Q}_{ap}(t)$ of the monitor. The legends $\Phi_{ap,sim1}$ and $\Phi_{ap,sim2}$ indicate $\dot{Q}_{ap}$ simulated by *ARX* and *ARMAX* models. P_{elec}^* is almost constant during the operation of the monitor. $\Phi_{ap,sim1}$ and $\Phi_{ap,sim2}$ follow P_{elec}^* with small variations in time. It is attributed to the heat capacity of the monitor and the temperature

difference, as given eq.(4.20). Although there are such variations, the total quantity of electrical energy is conserved as the total thermal energy. The calculated total electrical energy consumption of the monitor during the measurement period is 9.49 MJ. The simulated total thermal energy of the *sim1* and *sim2* are each 9.65 and 9.58 MJ. The ratios of the electrical energy and the thermal energy are about 1.02 and 1.01, respectively.
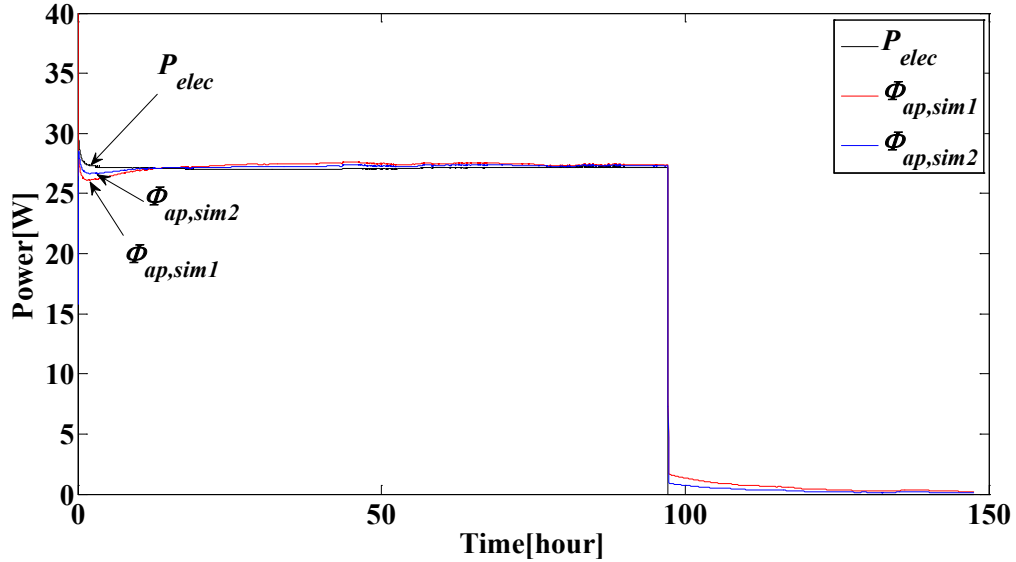
Figure 4. 6 Load profile P_{elec}^* and simulated heat fluxes $\Phi_{ap,sim1}$, $\Phi_{ap,sim2}$ of a monitor

The characterized models of the monitor are then integrated into different building models (2*R*2*C*). The first model is the 2nd order lumped *RC* model I (*model I*) and the second model is the 2nd order lumped *RC* model II (*model II*). The details of these models were presented in Chapter 3. Finally, apart from the identified parametric models of the monitor, the basic model of the monitor (no dynamics) is also tested.

Figure 4. 7 illustrates the three curves of T_i of *model I*. Among three curves, T_i^* is the measured one, $T_{i,sim1}$, $T_{i,sim2}$ are the simulated temperatures of which model parameters were identified by *ARX* and *ARMAX* models, and $T_{i,sim3}$ is the simulated temperature from the basic model of the monitor. In the same way, Figure 4. 8 depicts the three curves of T_i of *model II*. T_i^* is the measured one, $T_{i,sim4}$, $T_{i,sim5}$ are the simulated temperatures whose model parameters were identified by *ARX* and *ARMAX* models, and $T_{i,sim6}$ is the simulated temperature from the basic model of the monitor.

The behavior of measured and simulated T_i of *model I* and *model II* is globally similar to the behavior of T_{ap}^*. Table 4. 8 lists the evaluation values of each model integrated into the *model I* and *model II* of the building. Their global *MAE*s are less than 0.15 °C. As the accuracy of T_{ap} simulated by *ARX* model is better than the accuracy of T_{ap} simulated by *ARMAX* model, T_i simulated by *ARX* model has the best accuracy. Comparing the results of *model I* and *model II*, *model II* has the better accuracy than *model I*. This result is similar to what was already obtained in Chapter 3.
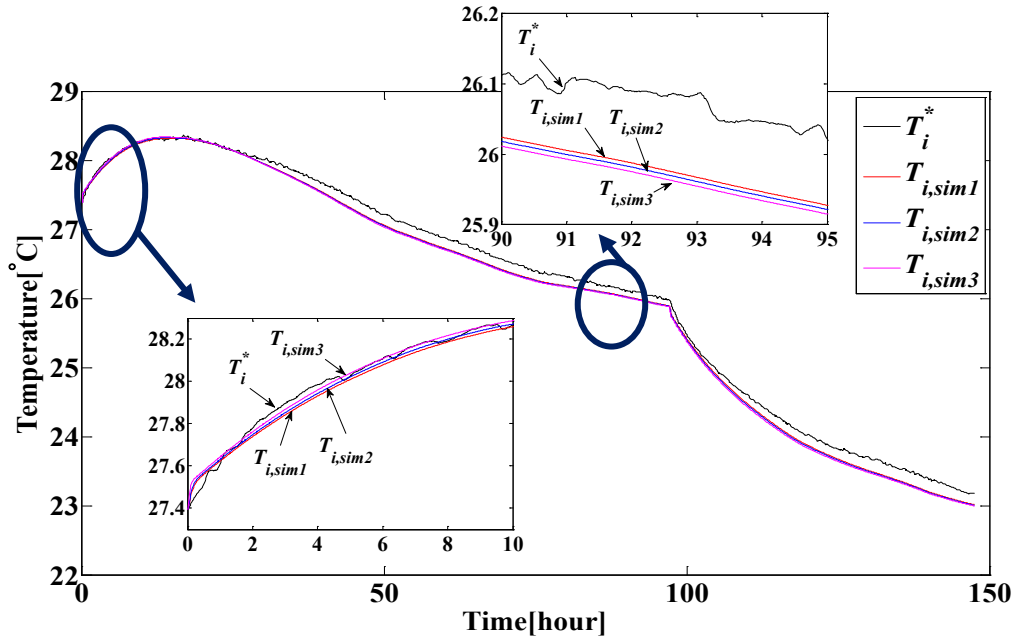
Figure 4. 7 Comparison of measured and simulated temperatures T_i (*Model I*)
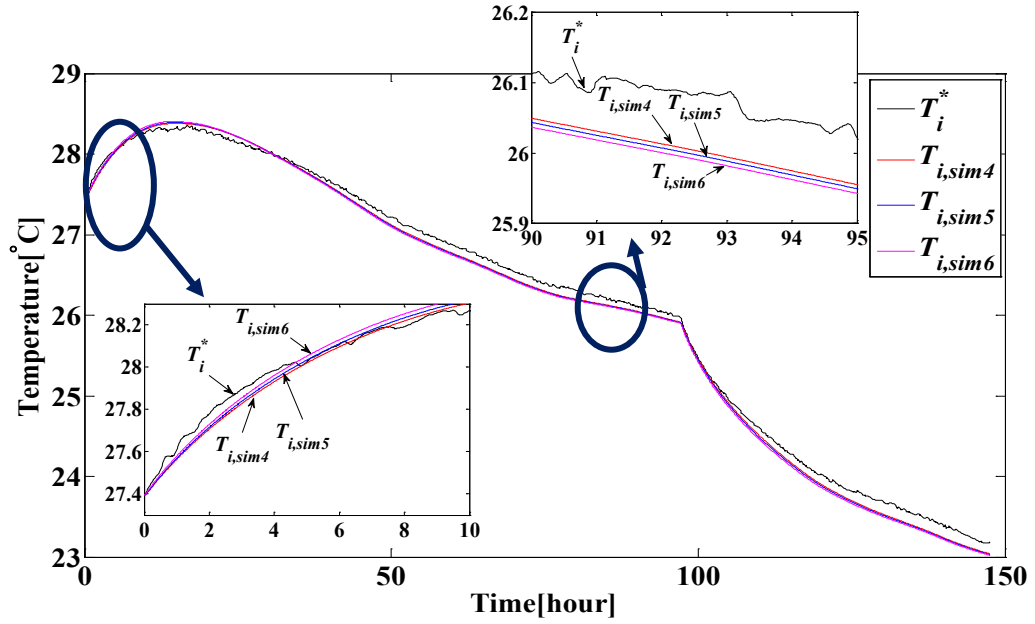
Figure 4. 8 Comparison of measured and simulated temperatures T_i (*Model II*)

The differences of *MAE* among three models into each building model are about 0.02 °C. Although we modeled a thermal model of a monitor with some efforts, there are no big differences of thermal influences of the modeled ones and un-modeled one (basic model with no dynamics) This can be explained by the small thermal time constant and the small power consumption of the monitor.

Table 4. 8 Results of model evaluation by T_i

Observed Variable	Building Model	Parametric Model	Name	Evaluation		
				MAE [°C]	*MSE* [°C^2]	*MAPE* [%]
T_i	Model I	*ARX*	*sim1*	**0.11**	**0.015**	**0.43**
		ARMAX	*sim2*	0.12	0.018	0.47
		none	*sim3*	0.13	0.021	0. 51
	Model II	*ARX*	*sim4*	**0.08**	**0.009**	**0. 33**
		ARMAX	*sim5*	0.09	0.010	0. 37
		none	*sim6*	0.10	0.013	0. 41

4.6.4.2 Computer Case

The experiment for a thermal characterization of a computer was carried out during ten days. Before starting the experiment, a computer was placed in the well-insulated room for having a condition which is $T_{ap}{}^*(0)=T_i{}^*(0)$. During the first five days (about 127 h), the computer was turned on. Then, it was turned off for rest of the experiment.

$P_{elec}{}^*$(t), $T_{ap}{}^*$(t), and $T_i{}^*$(t) were used for estimating the thermal parameters of the computer, among the measured data. By using proposed parameter estimation method, the parameters of *ARX* and *ARMAX* models were obtained. The parameters of physical model of the computer, R_{ap}, C_{ap} and τ_{ap} were calculated by eqs.(4.83)-(4.85). Table 4. 9 shows the values of each estimated parameter. The values of the parameters identified by *ARX* model are less than the values of the parameters of *ARMAX* model. τ_{ap} of *ARX* model is about a quarter of τ_{ap} of *ARMAX* model.

Table 4. 9 Estimated thermal parameters of a computer

Observed Variable	Parametric Model	Name	R_{ap} [°C /W]	C_{ap} [kJ/°C]	τ_{ap} [s]
T_{ap}	*ARX*	*sim1*	2.8 x10^{-3}	13.74	39
	ARMAX	*sim2*	3.7 x10^{-3}	45.25	167

Based on these estimated physical parameters of the models, T_{ap} is simulated and compared with the measured one. Figure 4. 9 illustrates three curves of T_{ap}: $T_{ap}{}^*$ is the measured one. $T_{ap,sim1}$ and $T_{ap,sim2}$ are the simulated ones.

The measured and simulated curves of T_{ap} have increased. Once again, it is due to the external temperature. Apart from this behavior, the simulated T_{ap} match quite well with the measurement for both transient and steady-states. The evaluation results are listed in Table 4. 10. The performance of the model of which parameter was estimated by *ARMAX* model is better than another model.
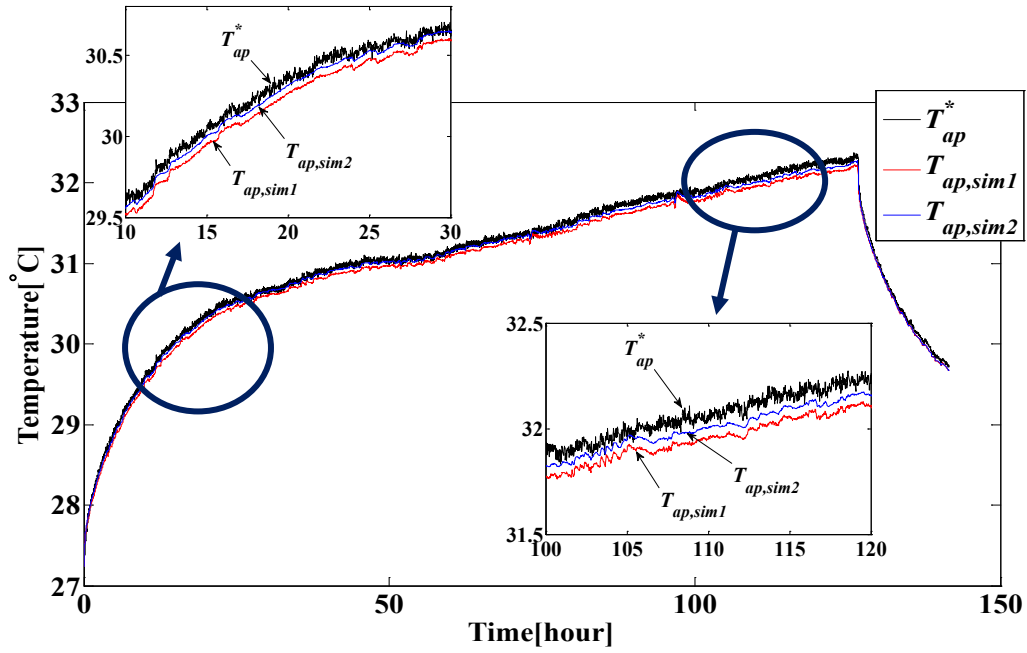
Figure 4. 9 Measured and simulated temperatures T_{ap} of a computer

However, the *MAE*s of two models are even less than 0.05 °C. It shows that the parameters obtained by the proposed method are well-estimated.

Table 4. 10 Results of model evaluation by T_{ap}

Observed Variable	Parametric Model	Name	Evaluation		
			MAE [°C]	*MSE* [°C^2]	*MAPE* [%]
T_{ap}	*ARX*	*sim1*	0.088	0.009	0.28
	ARMAX	*sim2*	**0.044**	**0.003**	**0.14**

The measured $P_{elec}{}^*(t)$ and simulated $\dot{Q}_{ap}(t)$ of the computer are shown in Figure 4. 10. The legends $\Phi_{ap,sim1}$ and $\Phi_{ap,sim2}$ indicate $\dot{Q}_{ap}$ simulated by *ARX* and *ARMAX* models, respectively. $P_{elec}{}^*$ is almost constant during the operation of the computer. $\Phi_{ap,sim1}$ and $\Phi_{ap,sim2}$ follow $P_{elec}{}^*$ with small variations in time. However, at the beginning of transient state (Off→On), the quantity of heat flux, $\Phi_{ap,sim1}$ and $\Phi_{ap,sim2}$ are less than $P_{elec}{}^*$. The dissipated heat of the computer is stored in the computer due to its thermal capacity. In other hands, at the beginning of another transient-state (On→Off), the quantity of heat flux, $\Phi_{ap,sim1}$ and $\Phi_{ap,sim2}$ are more than $P_{elec}{}^*$. The stored heat of the computer flows to the room at this moment. Even though there are such variations, the total electrical energy is conserved as the total thermal energy. The calculated total electrical energy consumption of the monitor during the measurement period is 26.05 MJ. The simulated total thermal energy of *ARX* and *ARMAX* models are 26.02 and 25.94 MJ, respectively. The ratios of the electrical energy and the thermal energy are both about 0.99.
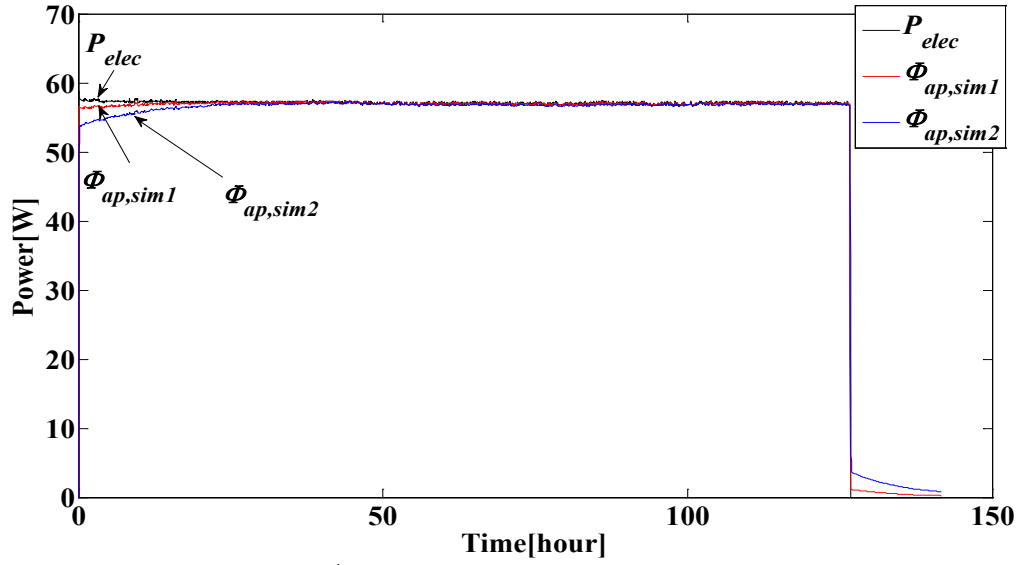
Figure 4. 10 Load profile $P_{elec}{}^*$ and simulated heat fluxes $\Phi_{ap,sim1}$, $\Phi_{ap,sim2}$ of a computer

The models of the computer are then integrated into the building models, *model I* and *model II*. In addition, an un-modeled computer model (basic model with no dynamics) is also integrated into the building models for comparison. The results are as follows. Figure 4. 11 depicts four curves of T_i of *model I*: the measured temperature ($T_i{}^*$), the simulated ones ($T_{i,sim1}$ and $T_{i,sim2}$) that model parameters were identified by *ARX* and *ARMAX* models, and $T_{i,sim3}$ simulated from the un-modeled computer model.
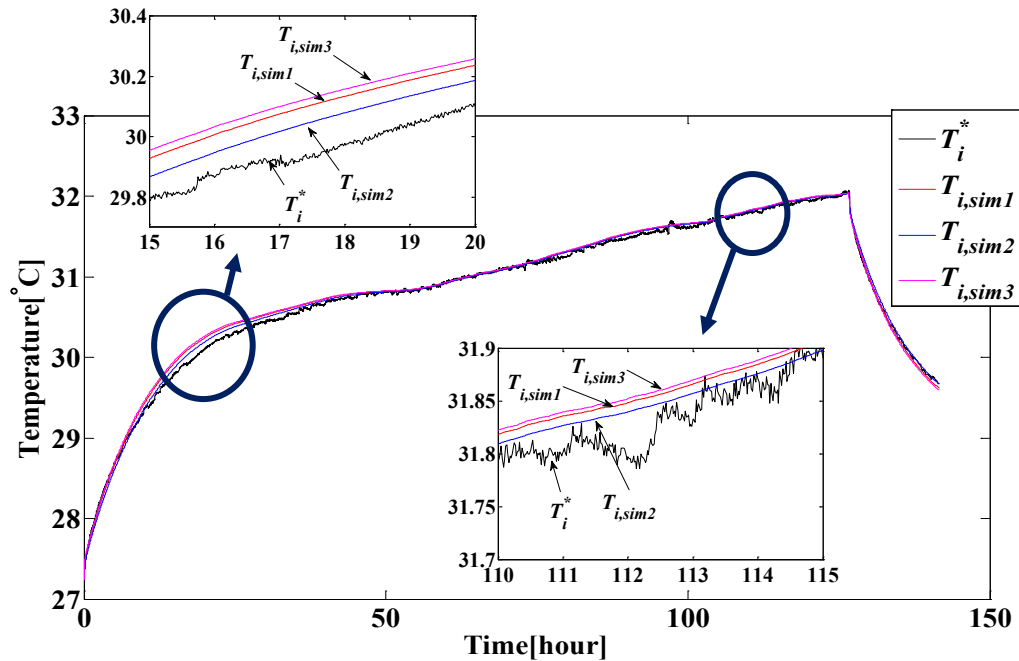
Figure 4. 11 Comparison of measured and simulated temperatures T_i (*Model I*)

Figure 4. 12 shows T_i of *model II*: the measured temperature (T_i^*), the simulated ones ($T_{i,sim4}$ and $T_{i,sim5}$) whose model parameters were identified by *ARX* and *ARMAX* models, and $T_{i,sim6}$ simulated from the un-modeled computer model. The global rising tendency of T_i is due to the same reason of the behavior of T_{ap}. For each model, we observe that T_i simulated by *sim2* and *sim5* are more closer to the measured one both for transient and steady state conditions.
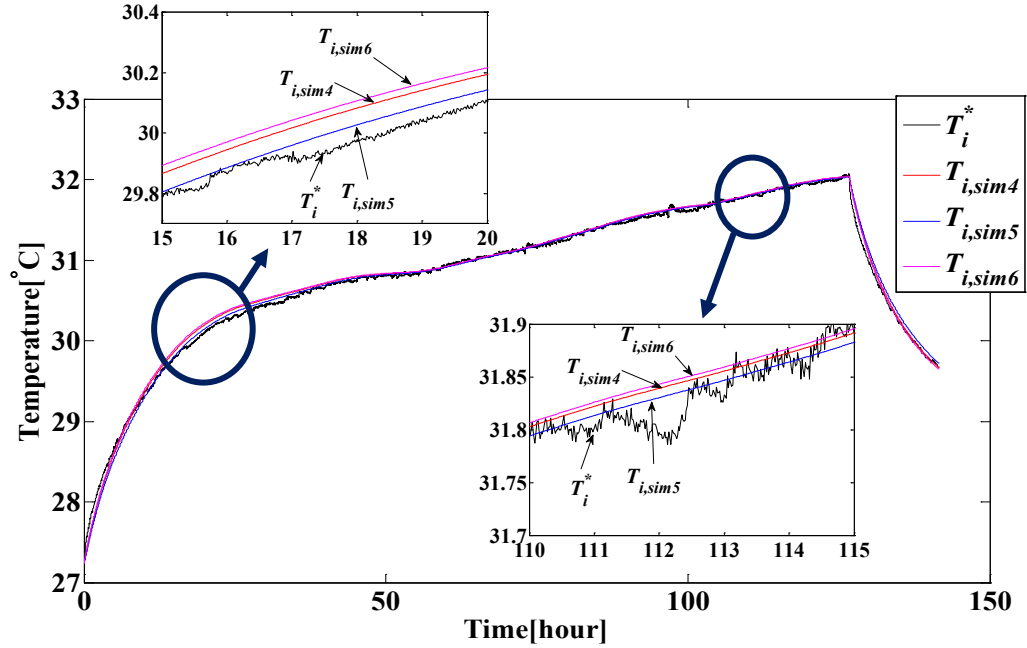
Figure 4. 12 Comparison of measured and simulated temperatures T_i (*Model II*)

Table 4. 11 lists their evaluation values. The *MAE*s are less than 0.06 °C for each model. Like the thermal model of the monitor, there is a very small difference of thermal influences of the modeled ones and un-modeled one, on the thermal behavior of the building. However, the modeled ones are more performing than the un-modeled one. Like that the accuracy of T_{ap} simulated by *ARMAX* model is better than the accuracy of T_{ap} simulated by *ARX*, T_i simulated by *ARMAX* model is more accurate. Comparing the building models, *model II* has a better accuracy than *model I*.

Table 4. 11 Results of model evaluation by T_i

Observed Variable	Building Model	Parametric Model	Name	Evaluation		
				MAE [°C]	*MSE* [°C²]	*MAPE* [%]
T_i	Model I	*ARX*	*sim1*	0.05	0.004	0.15
		ARMAX	*sim2*	**0.04**	**0.003**	**0.13**
		none	*sim3*	0.05	0.005	0.18
	Model II	*ARX*	*sim4*	0.04	0.003	0.14
		ARMAX	*sim5*	**0.04**	**0.003**	**0.13**
		none	*sim6*	0.05	0.004	0.15

4.6.4.3 Refrigerator Case

The experiment for a thermal characterization of a refrigerator was carried out during a week. Before starting the experiment, a refrigerator was placed in the well-insulated room. It aims to be having the same initial temperatures of the refrigerator and the room, as $T_{ap}^{*}(0)=T_i^{*}(0)$. During the first five days (about 118 h) of the experiment, the refrigerator was working. Then, it was stopped for rest of the experiment.

The refrigerator operates only while its inner temperature is within a certain range. The temperature range can be fixed by the user. The temperature range of the refrigerator for the experiment is from -2 to 3 °C. It means, the refrigerator stops operating when its inner temperature is under -2 °C. Then, the refrigerator restarts operating when its inner temperature is reached at 3 °C.

Among the measured data, $P_{elec}^{*}(t)$, $T_{ap}^{*}(t)$, and $T_i^{*}(t)$ were used for estimating the thermal parameters of the refrigerator. By using proposed parameter estimation method, the parameters of *ARX* and *ARMAX* models were obtained. According to the relation between *ARX*, *ARMAX* models and the physical model of the *CHS*, R_{ap}, C_{ap}, and τ_{ap} of the refrigerator were identified as listed in Table 4. 12. The values of the parameters estimated by the *ARX* model are less important than the values of the parameters of *ARMAX* model. τ_{ap} of *ARX* model is the half of τ_{ap} of *ARMAX* model.

Table 4. 12 Estimated thermal parameters of a refrigerator

Observed Variable	Parametric Model	Name	R_{ap} [°C /W]	C_{ap} [kJ/°C]	τ_{ap} [s]
T_{ap}	*ARX*	*sim1*	$10.9 \cdot 10^{-3}$	61.8	673
	ARMAX	*sim2*	$12.9 \cdot 10^{-3}$	90.8	1172

By using these estimated physical parameters converted by the coefficients of *ARX* and *ARMAX* model structures, the temperature of the refrigerator T_{ap} was simulated and was compared with the measured one. Figure 4. 13 illustrates the results of T_{ap}: T_{ap}^{*} is the measured temperature, $T_{ap,sim1}$ and $T_{ap,sim2}$ are the simulated temperatures (*ARX* and *ARMAX* models).

We can observe that there are two kinds of thermal dynamics: the dynamics of the refrigerator and the dynamics of the building. The small temperature-rises and drops are due to the dynamics of the refrigerator while the global temperature rising during first 50 h is mainly attributed by the dynamics of the building. However, we analyze only the dynamics of the refrigerator in this case, since the thermal characteristics of the building has been already discussed in Chapter 3.
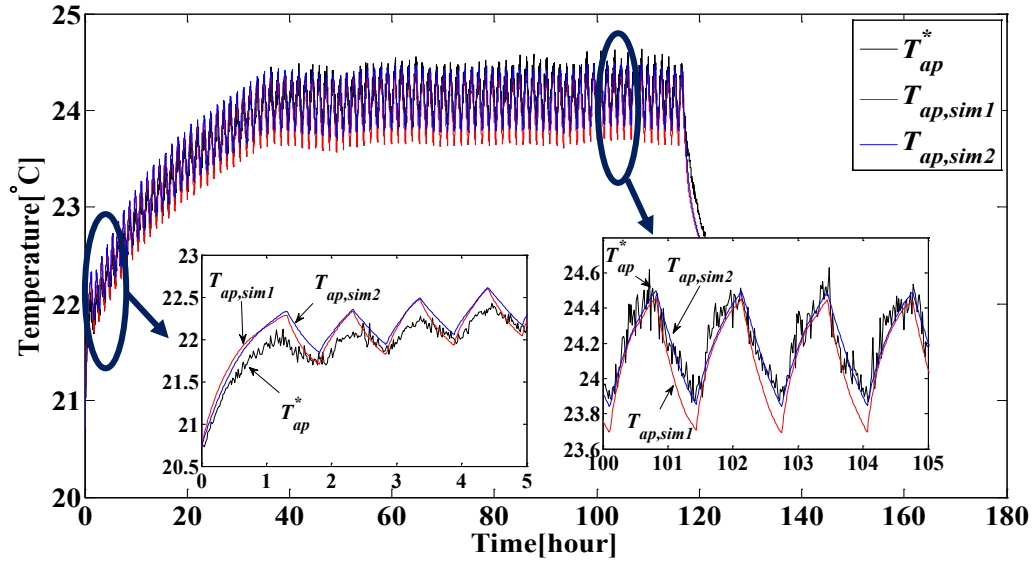
Figure 4. 13 Measured and simulated temperatures T_{ap} of a refrigerator

$T_{ap,sim1}$ and $T_{ap,sim2}$ are well following the temperature-rises and drops of T_{ap}^{*}. However, the thermal response of model '*sim1*' of which parameters were estimated by *ARX* model is faster than the model '*sim2*' because of the smaller time constant. These two models were evaluated in terms of *MAE*, *MSE*, and *MAPE*, as given by eqs.(4.86) - (4.88).

Table 4. 13 present the results of the model evaluation. *MAE*s of each model is around 0.1 °C. Moreover, *MAPE*s are less than 0.5 %. It shows that the parameters of both parametric models were well-estimated. Furthermore, we can see that *ARMAX* model is more accurate than *ARX* model. Indeed, the ARMAX model is more efficient in this case because it allows to partially compensate the effect of neglected internal dynamics of the refrigerator thermal system that are due to the automatic regulation of its inside temperature.

Table 4. 13 Results of model evaluation by T_{ap}

Observed Variable	Parametric Model	Name	Evaluation		
			MAE [°C]	*MSE* [°C^2]	*MAPE* [%]
T_{ap}	*ARX*	*sim1*	0.10	0.017	0.47
	ARMAX	*sim2*	**0.08**	**0.011**	**0.37**

Figure 4. 14 shows the measured $P_{elec}^{*}(t)$ and simulated $\dot{Q}_{ap}(t)$ of the refrigerator. The legends $\Phi_{ap,sim1}$ and $\Phi_{ap,sim2}$ indicate $\dot{Q}_{ap}$ simulated by the models whose parameters were estimated by *ARX* and *ARMAX* models. P_{elec}^{*} is supplied to the refrigerator with a cyclic form which respects the operation of the refrigerator as mentioned above. It is observed that there are heat charge and discharge of the refrigerator. When the electrical power is supplied to the refrigerator during its operation period, the converted heat is stored in the refrigerator. On the contrary, after the operation is stopped, the stored heat flows to the room. It is explained by the heat capacity of the refrigerator and the temperature difference, as given eq.(4.20). Despite of the different forms of the heat fluxes $\Phi_{ap,sim1}$, $\Phi_{ap,sim2}$, and the electrical power P_{elec}, total thermal

energies and total electrical energy are almost the same. The total thermal energy of the models '*sim1*' and '*sim2*' are respectively 18.430 and 18.429 MJ, while the calculated total electrical energy consumed by the refrigerator is about 18.431 MJ. The ratios between the electrical energy and the thermal energy are about 1, for both cases.
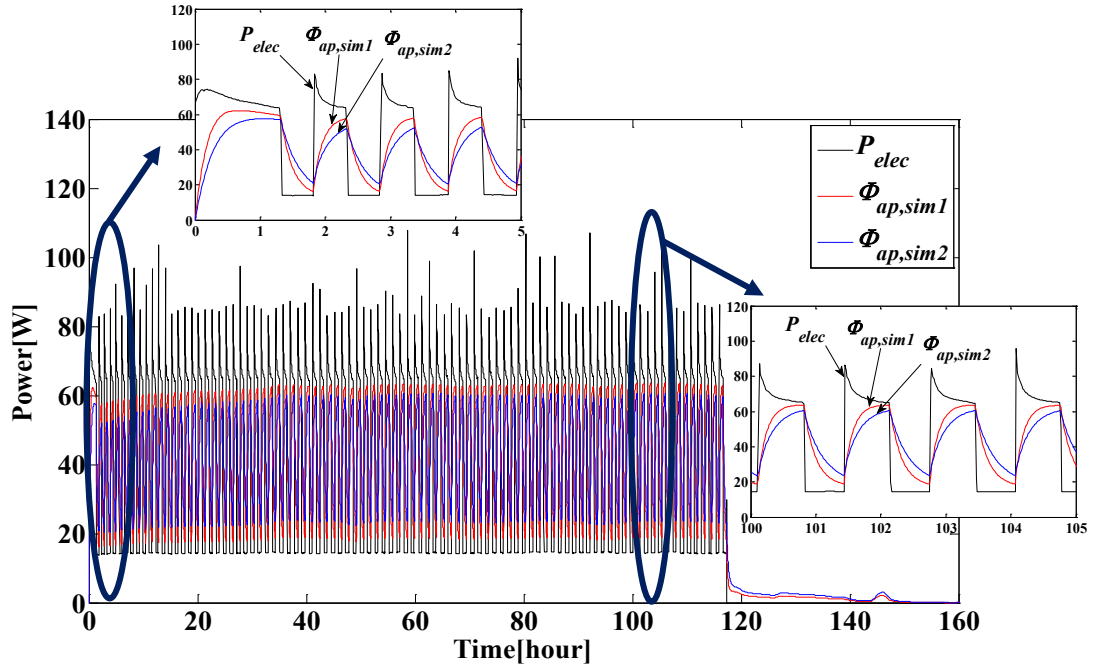
Figure 4. 14 Load profile P_{elec}^{*} and simulated heat fluxes $\Phi_{ap,sim1}$, $\Phi_{ap,sim2}$ of a refrigerator

The characterized models of the refrigerator are then integrated into the building models, *model I* and *model II*. In addition, an un-modeled refrigerator model (without dynamics) is also integrated for comparison purpose. Figure 4. 15 describes four curves of T_i of *model I*: the measured temperature (T_i^{*}), the simulated ones ($T_{i,sim1}$ and $T_{i,sim2}$) that model parameters were identified by *ARX* and *ARMAX* models, and $T_{i,sim3}$ simulated from the un-modeled refrigerator model.

Along the same way, Figure 4. 16 depicts the three curves of T_i of *model II*. T_i^{*} is the measured one, $T_{i,sim4}$, $T_{i,sim5}$ are the simulated temperatures of which model parameters were identified by *ARX* and *ARMAX* models, and $T_{i,sim6}$ is the simulated temperature from the un-modeled one.

Comparing to the simulation results of T_i of model *I* and model *II*, we can see that there is an important phenomenon. The *model I* which has the indoor air convective resistance is more performing to estimate T_i than *model II*. It is obvious that the convection of indoor air is the dominant heat transfer phenomenon in this case. Conversely, for the lamp, the monitor, and the computer, it is unnecessary to consider the indoor air convective resistance.
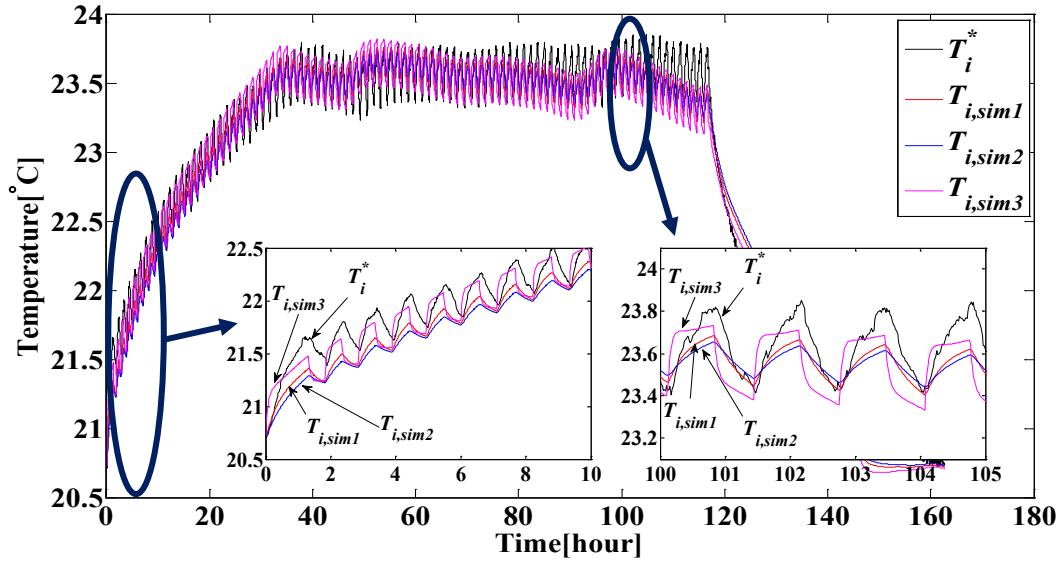
Figure 4. 15 Comparison of measured and simulated temperatures T_i (*Model I*)
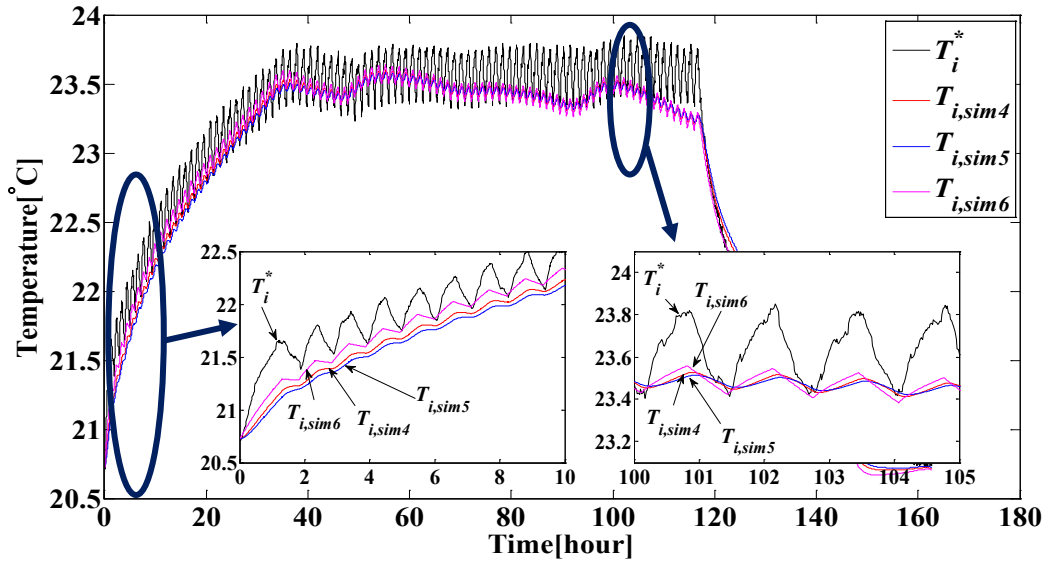
Figure 4. 16 Comparison of measured and simulated temperatures T_i (*Model II*)

The evaluation results of the models are listed in Table 4. 14. It states that $T_{i,sim1}$ simulated by *ARX* model in the building *model I* is the closest to the measured T_i^*. $T_{i,sim2}$ is then the next. The temperature response of the un-modeled refrigerator model is too rapid because it does not consider the thermal dynamics of the refrigerator. For the building *model II*, the un-modeled refrigerator model has the best performance to estimate T_i than other parametric models. But the building *model II* cannot catch the heat convection of indoor air. Even though thermal characteristics of an electrical appliance are well estimated, it does not ensure that the model makes a good estimation of thermal behavior of a building.

111

Table 4. 14 Results of model evaluation by T_i

Observed Variable	Building Model	Parametric Model	Name	Evaluation		
				MAE [°C]	*MSE* [°C²]	*MAPE* [%]
T_i	Model I	ARX	sim1	**0.10**	**0.015**	**0.43**
		ARMAX	sim2	0.11	0.019	0.49
		none	sim3	0.12	0.024	0.55
	Model II	ARX	sim4	0.15	0.032	0.64
		ARMAX	sim5	0.16	0.037	0.69
		none	sim6	0.13	0.026	0.57

4.6.4.4 Electric Heater Case

The experiment for a thermal characterization of a portable electric convection heater was carried out during a week. The used heater is small and portable. It heats the zone mainly by convection and radiation. Before starting the experiment, the heater was placed in the well-insulated room in order to have the same initial temperatures between the heater and the room $T_{ap}^*(0)=T_i^*(0)$. During the first three days (about 72 h) of the experiment, the heater is operating. Then it is off for rest of the experiment.

The electric heater used for this experiment has a bimetal sensor. It aims to control the operation of the heater by itself. Experimentally, the heater works in the following temperature range, from 37 to 57 °C. This temperature range is able to be changed by user's preference.

Among all of the measured data, $P_{elec}^*(t)$, $T_{ap}^*(t)$, and $T_i^*(t)$ were only selected for estimating the thermal parameters of the heater. By using proposed parameter estimation method, the parameters of *ARX* and *ARMAX* models were obtained. According to the relation between *ARX* model and physical model, and between *ARMAX* model and physical model, R_{ap}, C_{ap} and τ_{ap} of the heater were identified as listed in Table 4. 15. The value of τ_{ap} of the *ARMAX* model is about 110 % of the τ_{ap} which was estimated by *ARX* model.

Table 4. 15 Estimated thermal parameters of a portable electric convection heater

Observed Variable	Parametric Model	Name	R_{ap} [°C /W]	C_{ap} [kJ/°C]	τ_{ap} [s]
T_{ap}	ARX	sim1	$16.4 \cdot 10^{-3}$	7.65	125
	ARMAX	sim2	$15.8 \cdot 10^{-3}$	8.67	137

By using these estimated physical parameters, the temperature of the heater T_{ap} was simulated and was compared with the measured one. Figure 4.17 depicts three curves of T_{ap}: T_{ap}^* is the measured temperature, $T_{ap,sim1}$ and $T_{ap,sim2}$ are the simulated temperatures of which

model parameters were identified by *ARX* and *ARMAX* models. It is observed that there are two kinds of thermal dynamics, like in the case of the refrigerator. The first one is the dynamics of the electric heater and the second one is the dynamics of the building. The small temperature-rises and drops are due to the dynamics of the heater internal regulation. The global temperature increase is mainly due to the dynamics of the building. The well estimated thermal characteristics of the heater leads good-fitness of T_{ap}. After the electric heater is switched on, the heater starts transferring heat fluxes, converted by Joule effect in order to heat the room for getting a certain range of temperatures.
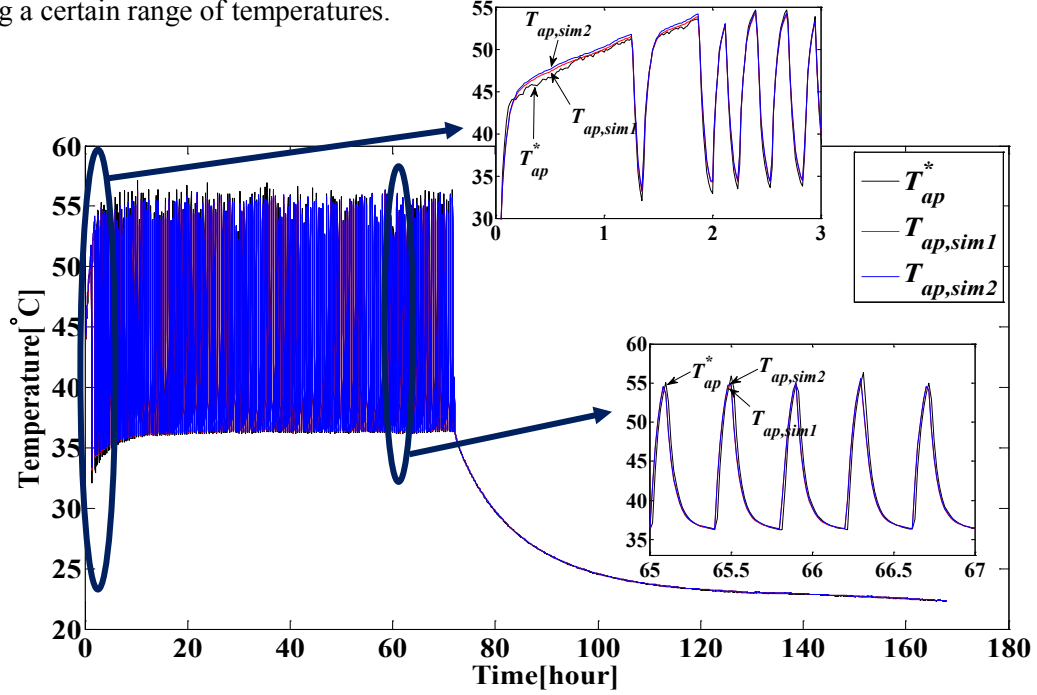
Figure 4. 17 Measured and simulated temperatures T_{ap} of an electric heater

$T_{ap,sim1}$ and $T_{ap,sim2}$ are well following the temperature-rises and drops of $T_{ap}{}^*$. These two models are evaluated by *MAE*, *MSE*, and *RMSE* criteria. Table 4. 16 presents the results of the model evaluation. According to each evaluation term, the model '*sim1*' is more accurate than the model '*sim2*'with a very small difference. *MAE*s and *MAPE*s of the simulated T_{ap} of two models are both less than 0.3 °C and 0.65 %.

Table 4. 16 Results of model evaluation by T_{ap}

Observed Variable	Parametric Model	Name	Evaluation		
			MAE [°C]	*MSE* [°C^2]	*MAPE* [%]
T_{ap}	*ARX*	*sim1*	**0.25**	**0.42**	**0.61**
	ARMAX	*sim2*	0.26	0.42	0.63

The measured $P_{elec}{}^*$(t) and simulated $\dot{Q}_{ap}$(t) of the heater are shown in Figure 4. 18. The legends $\Phi_{ap,sim1}$ and $\Phi_{ap,sim2}$ indicate $\dot{Q}_{ap}$ simulated by the models of which parameters were estimated by *ARX* and *ARMAX* models. $P_{elec}{}^*$ is supplied to the electric heater with a cyclic form with a respect to the operation of the heater as mentioned above. The estimated τ_{ap} of the heater leads that the forms of $\Phi_{ap,sim1}$ and $\Phi_{ap,sim2}$ are not exactly the same to the form of $P_{elec}{}^*$. In this

113

case where the maximum electrical power is about 1000 W, it is obvious that the heat flux impact more the thermal behavior of the building.

Despite of the different forms of the heat fluxes $\Phi_{ap,sim1}$, $\Phi_{ap,sim2}$, and the electrical power P_{elec}^{*}, total thermal energies and total electrical energy are almost the same. The total thermal energy of the models '$sim1$' and '$sim2$' are both about 68.53 MJ, while the calculated total electrical energy consumed by the heater is about 68.528 MJ. The ratios between the electrical energy and the thermal energy are about 1 for both cases.
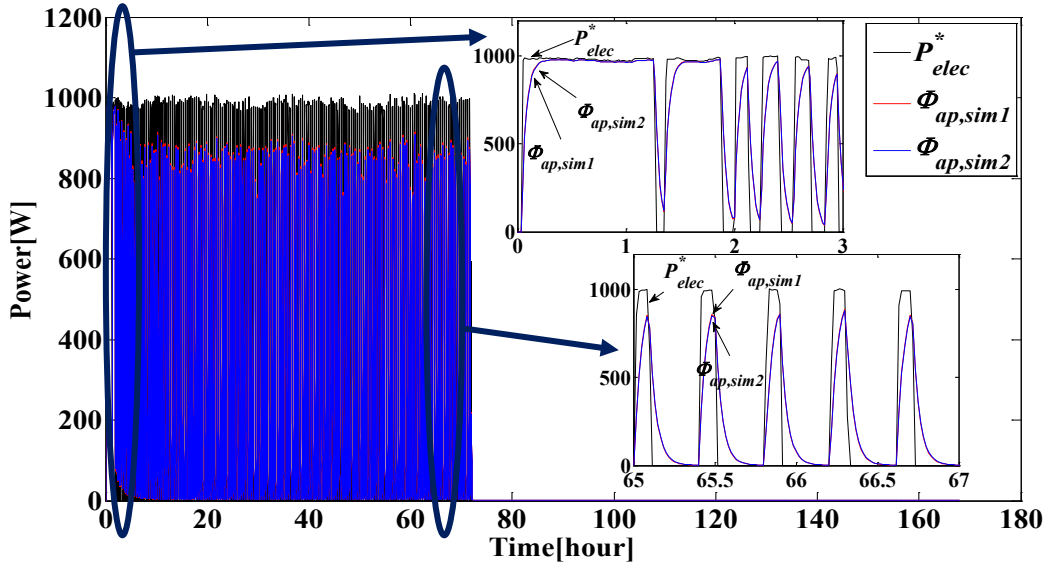
Figure 4. 18 Load profile P_{elec}^{*} and simulated heat fluxes $\Phi_{ap,sim1}$, $\Phi_{ap,sim2}$ of a portable electric convection heater

The characterized models of the electric heater are then integrated into the building models, *model I* and *model II*. In addition, an un-modeled heater model (basic model without dynamics) is also integrated into the building models for comparison purpose. Figure 4. 19 describes the four curves of T_i of *model I*: the measured temperature (T_i^{*}), the simulated ones ($T_{i,sim1}$ and $T_{i,sim2}$) that model parameters were identified by *ARX* and *ARMAX* models, and $T_{i,sim3}$ simulated from the un-modeled refrigerator model. In the same way, Figure 4. 20 depicts the three curves of T_i of *model II*. T_i^{*} is the measured one, $T_{i,sim4}$, $T_{i,sim5}$ are the simulated temperatures of which model parameters were identified by *ARX* and *ARMAX* models, and $T_{i,sim6}$ is the simulated temperature from the un-modeled one.

The simulated T_i of *model I* and *model II* are following the measured one T_i^{*}. However, they do not exactly catch up the amplitudes of temperature-rises and drops of T_i^{*}. Comparing to the simulation results of T_i of model *I* and model *II*, we can see that there is an important phenomenon. The *model I* which has the indoor air convective resistance is more performing to estimate T_i than *model II*. It is known that the dominant heat transfer phenomenon of the electric convection heater is convection. Therefore, the convection of indoor air has to be considered in this case. Like for the case of the refrigerator, *model I* is more accurate than *model II*.
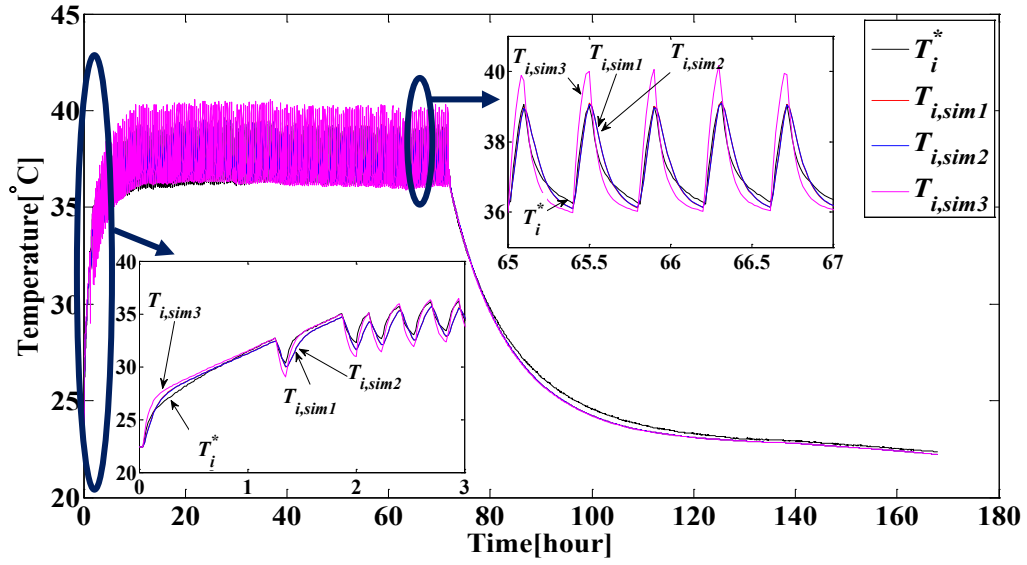
Figure 4. 19 Comparison of measured and simulated temperatures T_i (*Model I*)
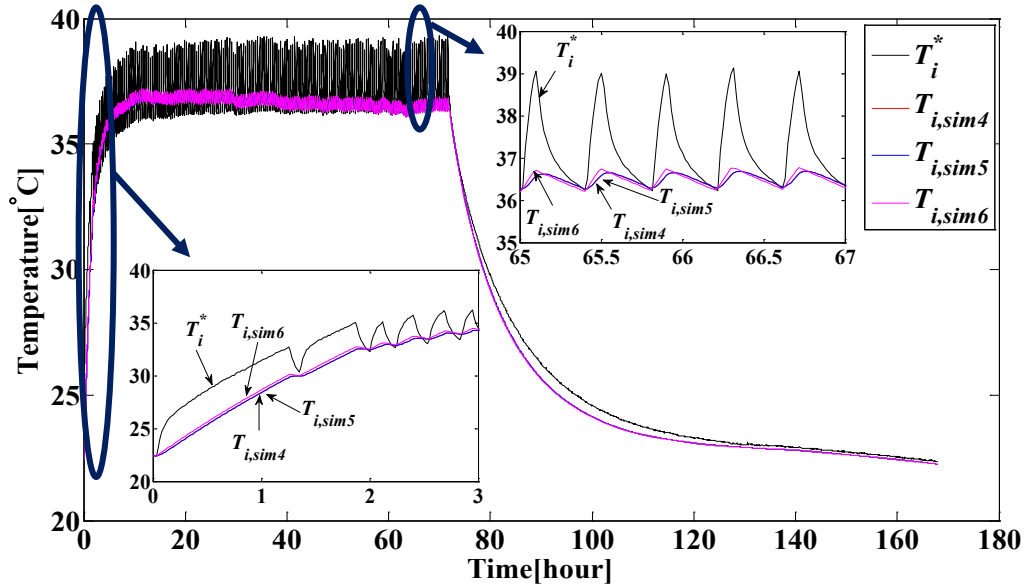
Figure 4. 20 Comparison of measured and simulated temperatures T_i (*Model II*)

The models were then evaluated by *MAE*, *MSE*, and *RMSE* criteria. Table 4. 17 shows the results of model evaluation by T_i. It shows that $T_{i,sim1}$ simulated by *ARX* model in the building *model I* is the closest to the measured T_i^*. $T_{i,sim2}$ is then the next. The temperature response of the un-modeled electrical heater model is too fast since the thermal dynamics of the heater were eliminated in this model. For the building *model II*, the un-modeled heater model has the best performance to estimate T_i than other parametric models, but as said before, the building *model II* cannot catch the heat convection of indoor air.

115

Table 4. 17 Results of model evaluation by T_i

Observed Variable	Building Model	Parametric Model	Name	Evaluation		
				MAE [°C]	MSE [°C^2]	MAPE [%]
T_i	Model I	ARX	sim1	**0.28**	**0.138**	**0.90**
		ARMAX	sim2	0.28	0.140	0.91
		none	sim3	0.29	0.168	0.95
	Model II	ARX	sim4	0.46	0.532	1.45
		ARMAX	sim5	0.47	0.533	1.45
		none	sim6	0.45	0.488	1.43

4.6.4.5 Microwave Case

The experiment for a thermal characterization of a microwave was carried out during about two days. Before starting the experiment, a microwave was placed in the well-insulated room for having a condition which is $T_{ap}^*(0)=T_i^*(0)$. During the first thirty minutes, the microwave was working on. For the rest of the experiment, it was switched off. Since it is difficult to keep the microwave working on for a long time, we just conducted the experiment during 30 minutes.

Among the measured data, $P_{elec}^*(t)$, $T_{ap}^*(t)$, and $T_i^*(t)$ were used for estimating the thermal parameters of the microwave. By using proposed parameter estimation methods, the parameters of ARX and ARMAX models were obtained. Although the parameters were obtained from different parametric models, the estimated parameters are almost the same. The parameters of physical model of the microwave, R_{ap}, C_{ap}, and τ_{ap} are listed in Table 4. 18.

Table 4. 18 Estimated thermal parameters of a microwave

Observed Variable	Parametric Model	Name	R_{ap} [°C /W]	C_{ap} [kJ/°C]	τ_{ap} [s]
T_{ap}	ARX	sim1	$1.3\cdot10^{-3}$	94.2	122
	ARMAX	sim2	$1.3\cdot10^{-3}$	94.1	122

Based on these estimated physical parameters, the temperature of the microwave T_{ap} was simulated and was compared with the measured one. Figure 4. 21 describes three curves of T_{ap}: T_{ap}^* is the measured temperature, $T_{ap,sim1}$ and $T_{ap,sim2}$ are the simulated temperatures of which model parameters were identified by ARX and ARMAX models.

During the first 30 min., the microwave was operating according to user's programming. During its operation, T_{ap}^* rises. Then, after the operation was stopped, T_{ap}^* decreased. These temperature-rise and drop result from heat flux converted by electrical power supplied to the microwave. Since the thermal parameters of each model of the microwave are almost the same,

the simulated temperature T_{ap} of *sim1* and *sim2* are also very similar. It leads the same thermal behavior for both models.
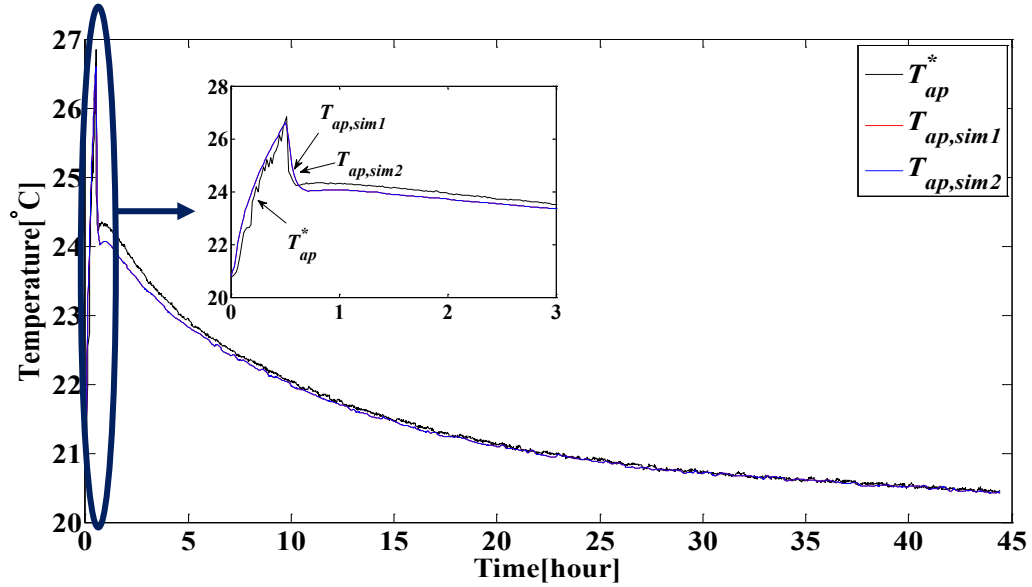
Figure 4. 21 Measured and simulated temperatures T_{ap} of a microwave

The models of which parameters were obtained by *ARX* and *ARMAX* models are evaluated as following on Table 4. 19. Since there is no difference between the parameters estimated by two different parametric models, the evaluation values of *MAE*, *MSE*, and *RMSE* are also the same. The values which are between brackets are the terms that were calculated during operation 0.5 h. Despite of the short time of the experiment, T_{ap} is well estimated with a *MAE* equal to 0.05 °C for whole period and equal to 0.45 °C for the operating period.

Table 4. 19 Results of model evaluation by T_{ap}

Observed Variable	Parametric Model	Name	Evaluation		
			MAE [°C]	*MSE* [°C^2]	*MAPE* [%]
T_{ap}	*ARX*	*sim1*	0.051 (0.45)	0.010 (0.30)	0.23 (1.94)
	ARMAX	*sim2*	0.051 (0.45)	0.010 (0.30)	0.23 (1.94)

(value) : Obtained value when *N* is 30, that corresponds the operation time of the microwave.

The measured $P_{elec}{}^*$(t) and simulated $\dot{Q}_{ap}$(t) of the microwave are described in Figure 4. 22. The legends $\Phi_{ap,sim1}$ and $\Phi_{ap,sim2}$ indicate $\dot{Q}_{ap}$ simulated by *ARX* and *ARMAX* models. Even though the experiment was conducted during about 45 [h], the figure depicts only the first three hours. Since the operation time of the microwave was short against the whole experimental time, we eliminate the rest of data in this case. Because of the significant C_{ap}, the $\Phi_{ap,sim1}$ and $\Phi_{ap,sim2}$ do not capture quickly $P_{elec}{}^*$ in a short time. Although the profiles of $\Phi_{ap,sim1}$ and $\Phi_{ap,sim2}$ are not exactly the same form compared to $P_{elec}{}^*$, the total energy is almost the same. The calculated total electrical energy consumption of the microwave during the experiment is 2.14 MJ. The

simulated total thermal energies of the sim1 and sim2 are the same as 2.16 MJ. The ratios between the electrical energy and the thermal energy are about 1.01 for both cases.
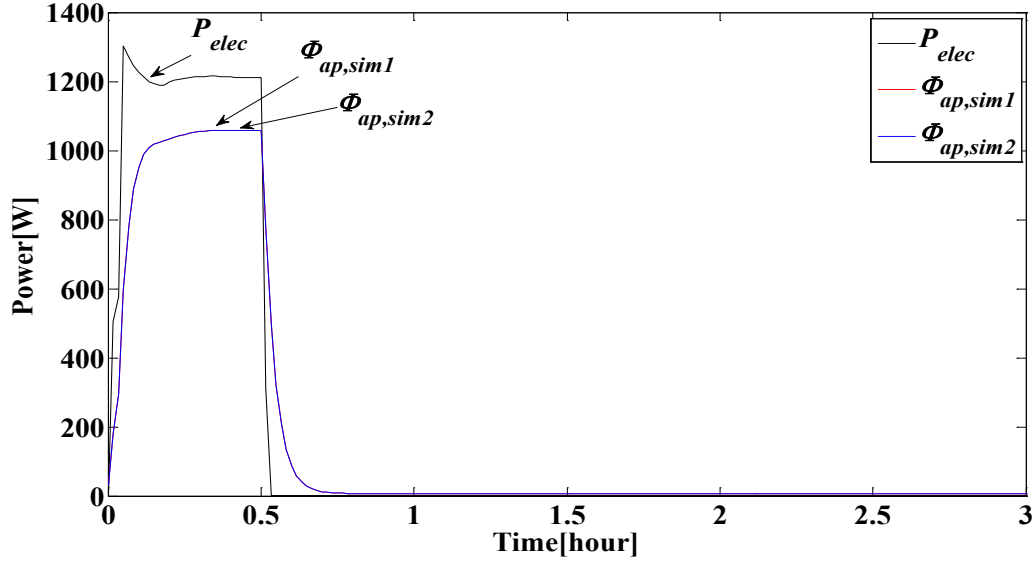
Figure 4. 22 Load profile of computer P_{elec} and simulated heat fluxes $\Phi_{ap,sim1}$, $\Phi_{ap,sim2}$ of a microwave

The characterized models of the microwave are then integrated into the building models, *model I* and *model II*. In addition, an un-modeled microwave model is also integrated into the building models. Figure 4. 23 describes four curves of T_i of *model I*: the measured temperature (T_i^*), the simulated ones ($T_{i,sim1}$ and $T_{i,sim2}$) that model parameters were identified by *ARX* and *ARMAX* models, and $T_{i,sim3}$ simulated from the un-modeled microwave model.
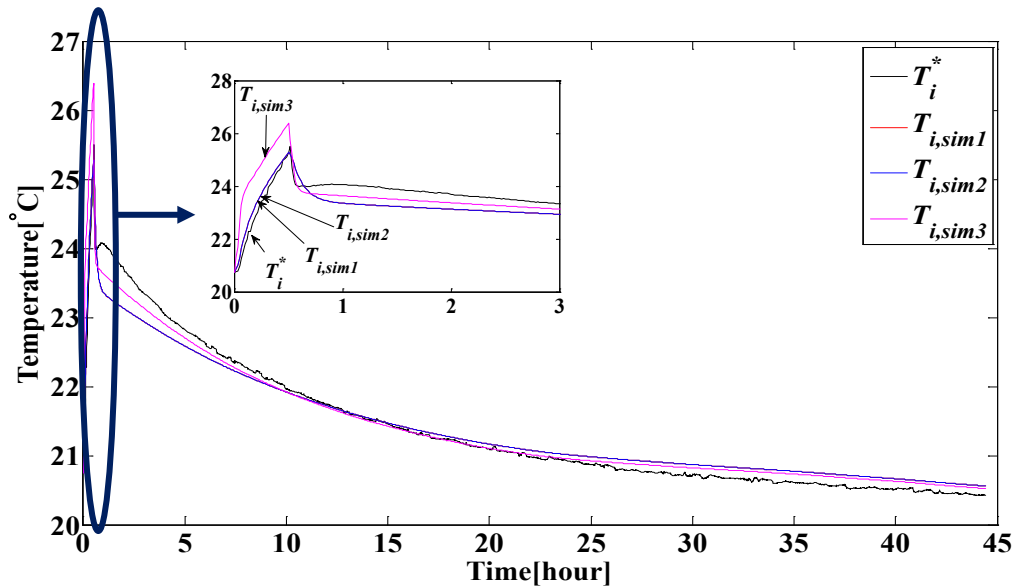
Figure 4. 23 Comparison of measured and simulated temperatures T_i (*Model I*)

In the same way, Figure 4. 24 depicts the three curves of T_i of *model II*. T_i^* is the measured one, $T_{i,sim4}$, $T_{i,sim5}$ are the simulated temperatures whose model parameters were identified by *ARX* and *ARMAX* models, and $T_{i,sim6}$ is the simulated temperature from the un-modeled one.
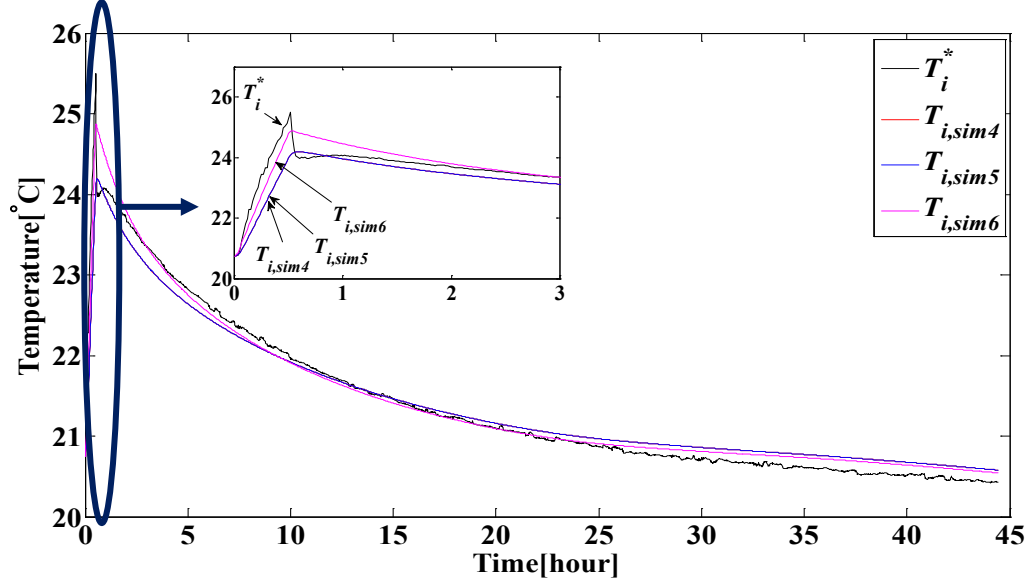
Figure 4. 24 Comparison of measured and simulated temperatures T_i (*Model II*)

Similar to the cases of the refrigerator and the electric heater, the simulated T_i in building model I are much more closed to the measured one, than the simulated T_i in building model II. For the cases where the injected power is important, we can see that convection becomes the more effective heat transfer phenomenon.

Considering the period while the microwave operates, the performances of the models which contain the thermal dynamics of the microwave are much better than the un-modeled one's. Regarding the model II, the un-modeled microwave model is always better performed considering that the microwave which consumes great electrical power about 1200 W, it has to be thermally modeled with accuracy in order to analyze its thermal effect on the building.

Table 4. 20 Results of model evaluation by T_i

Observed Variable	Building Model	Parametric Model	Name	Evaluation		
				MAE [°C]	*MSE* [°C²]	*MAPE* [%]
T_i	Model I	*ARX*	*sim1*	0.15 (0.26)	0.04 (0.09)	0.68 (1.12)
		ARMAX	*sim2*	0.15 (0.26)	0.04 (0.09)	0.68 (1.12)
		none	*sim3*	0.11 (1.37)	0.04 (2.06)	0.50 (5.80)
	Model II	*ARX*	*sim4*	0.13 (0.91)	0.03 (1.03)	0.59 (3.82)
		ARMAX	*sim5*	0.13 (0.91)	0.03 (1.03)	0.59 (3.82)
		none	*sim6*	0.09 (0.43)	0.02 (0.23)	0.40 (1.82)

(value): *N* is 30, that is the operation time of the microwave.

4.6.5 Discussions

In this chapter, we showed several applications of the thermal modeling of electrical appliances in order to illustrate the relevance of the proposed model along with the identification procedure. The electrical appliances which are in *CHS* category were selected in practice. The selected ones are a monitor, a computer, a refrigerator, a portable electric convection heater, and a microwave. These electrical appliances are widely used in dwelling houses.

We firstly estimated thermal parameters of each appliance by using the relation between the *ARX* model and the physical model of *CHS*, and between the *ARMAX* and the physical model of *CHS*. Based on the estimated values, we simulated $T_{ap,sim1}$ and $T_{ap,sim2}$ and compared them to the measured one, $T_{ap}{}^*$. From this comparison, we observed that:

- The simulated T_{ap} is globally well fitted to the measured one. It shows us that the proposed parameter estimation method and the proposed model of electrical appliances, especially for *CHS,* are well obtained.

- The impact factors on thermal modeling of electrical appliances are time constant, and amplitude of P_{elec} of the electrical appliances:

    - ✓ The time constants estimated by *ARX* and *ARMAX* models of the monitor and the microwave are exactly the same. It leads the same forms of $T_{ap,sim1}$ and $T_{ap,sim2}$ for each appliance.
    - ✓ With different time constants, $T_{ap,sim1}$ and $T_{ap,sim2}$ were differently simulated. The computer, the refrigerator, and the electric heater are in this case.
    - ✓ On the case where the supplied P_{elec} is significant, the impact of the time constant on the thermal behaviors of the electrical appliances is greater. Although the estimated time constants are very similar to each other in the range of 10 % of differences, there are significant differences on simulated T_{ap}. The electric heater is in this case. P_{elec} of the heater is about 1000 W.

Then, we integrated the models of each electrical appliance into the well-insulated building model. We compared the T_i simulated by the models (*sim1*, *sim2*) derived from the *ARX* model and the *ARMAX* model, the T_i derived from the basic model which contains no thermal dynamics of the electrical appliance to the measured $T_i{}^*$. From this comparison, we found that,

- The thermal behavior of the building is better described when the injected heat flux of the appliance is modeled by a thermal model of the electrical appliance.

- Although the performances of the dynamic models are better than the basic model, there is not a big difference on the thermal behavior of the room if the injected power is small (i.e. thermal models of the monitor and the computer).

- Thermal modeling of electrical appliances is strongly demanding for the following cases:

  ✓ The time constant of the electrical appliance is important because the heat flux injected inside the building strongly depends on the time constant of the electrical appliances and may impact the comfort of the inhabitant.
  ✓ P_{elec} of the appliance is greater than at least equal to 1000 W. In the cases of the portable heater and of the microwave, which both consume around 1000 W during their operation time, the simulated T_i. derived from '*sim1*' and '*sim2*' match quite well the corresponding measurement T_i^*.

Regarding the methods for estimating the parameters, we did not find significant differences between the *ARX* and the *ARMAX* models. Both models globally well estimated the parameters. However, ARMAX approach was considered as more relevant when internal dynamics are neglected like in the case of inner temperature regulation (refrigerator).

4.7 CONCLUSION

In this chapter, we presented a methodology to establish a thermal dynamic model of electrical appliances and to identify the corresponding parameters of the model. In order to provide a generic model of all types of electrical appliances, we firstly classified electrical appliances into four categories according to thermal and electrical points of view. Based on this classification, a generic thermal model of electrical appliances was obtained. Then, parameter identification methods for estimating parameters of the generic model were described, using grey-box modeling approach. After that, we presented several practical cases of the proposed generic thermal model of electrical appliances in order to validate our approach. The proposed work provided detailed information on the thermal behavior of electrical appliances. Quantitative studies on T_{ap} and heat fluxes generated by electrical appliances were achieved. Moreover, a comparison between the obtained thermal dynamic models of electrical appliances and the standard basic model which does not include dynamics was also conducted. It helped to understand the thermal influence of the heat gains of electrical appliances on thermal behaviors of buildings. Especially, it provides the preliminary information for thermal analysis of the impact of electrical appliances on a well-insulated building.

The experimental protocol and the identification procedure were optimized to identify the appliance thermal properties. As the thermal behavior is coupled to the room properties, we reach the question of the accuracy of the reduced model when not including the convective phenomenon or all other non-linear aspect.

Chapter 5

SIMULATION OF COUPLED MODEL
OF
A BUILDING AND ELECTRICAL APPLIANCES

5.1 INTRODUCTION

Building simulation tools have been developed and upgraded for improving energy performance of buildings. Before constructing a building, engineers can simulate its thermal behavior and environmental condition, design its heating/cooling equipment, and assess its energy performance and inhabitant's thermal comfort [110,111].

An overview and several comparative studies of building simulation tools were reviewed in Chapter 2. Among the most representative simulation tools, such as ESP-r, TRNSYS, EnergyPlus, PLEIADE[18][151,152], and SIMBAD, we chose SIMBAD simulation tool for this thesis work.

We remind that the advantages of a building simulation by SIMBAD are:
- Hierarchy design of building system;
- Configuration in graphical interfaces;
- Component's design linked to m-files;
- Facilities to adapt a building system in an interface of Matlab/Simulink;
- Co-simulation with the other softwares which are compatible with Matlab/Simulink;
- Possibility of control of building sub-systems;
- Intra-hour simulation, etc.

---

[18] PLEIADE: Passive Low Energy Innovative Architectural Design

In the previous chapter, we focused on modeling of electrical appliances from the thermal point of view. We established a generic thermal model of electrical appliances and identified thermal parameters of several electrical appliances based on experimental protocol in the actual study. The presented model was developed and validated within a model of a well-insulated room with a Matlab/Simulink interface. In this chapter 5, we integrate the proposed electrical appliances thermal model into a building model developed in SIMBAD simulation tool. It aims to observe thermal influence of electrical appliances within a low energy building.

To this purpose, this chapter first describes a building model that we have chosen. Then basic information of thermal behavior of the building is given according to different operations of HVAC systems. After that, several types of electrical appliances are integrated into the building model. Then, the thermal behavior and the heating energy consumption of the building are determined and analyzed during winter and summer periods. According to scheduling of electrical appliances, we extract and analyze the energy demand change of the considered building. In sequence, thermal discomfort owing to usages of electrical appliances during a summer period is also studied at the end of this chapter. Finally, main conclusions are given.

5.2 DESCRIPTION OF BUILDING

In order to study thermal influence of electrical appliances within a low energy building, we select an individual residential building model which was developed and validated by the French Technical Research Center for Building (CSTB) on a real building. It is one of the reference dwelling houses in France and is used for assessment of building energy performance. The details of the considered building are given in references [66,153]. Table 5. 1 lists physical dimensions of each room of the reference building. Figure 5. 1, Figure 5. 2 and Figure 5. 3 show the blueprint of the considered building. It is a two floor house, which consists of a living room, a kitchen, three rooms, and a bathroom on the first floor, and an attic on the second floor. The surface and the volume of the living places are 100.86 m^2 and 252.15 m^3, respectively. The surface and the volume of the attic are 100.86 m^2 and 137.84 m^3, respectively.

Table 5. 1 Physical dimensions of each zone of the reference building

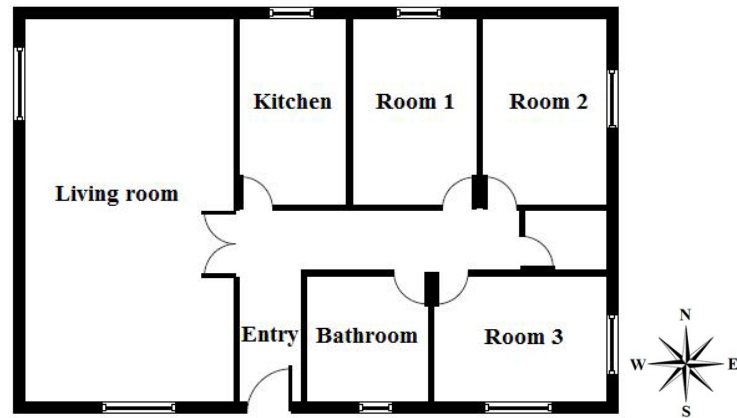| Zone	Height [m]	Surface [m^2]	Volume [m^3]	Window	
				Direction	Surface [m^2]
Living room		36.90	92.25	West	2.80
				South	2.90
Kitchen		9.52	23.79	North	1.04
Room 1		10.94	27.34	North	1.08
Room 2		11.14	27.84	East	1.94
Room 3	2.5	10.50	26.25	East	1.94
				South	2.58
Bathroom		7.42	18.55	South	0.44
Entry		14.45	36.13	-	-
Attic		100.86	137.84	-	-

Figure 5. 1 A blueprint of the reference house (First floor)
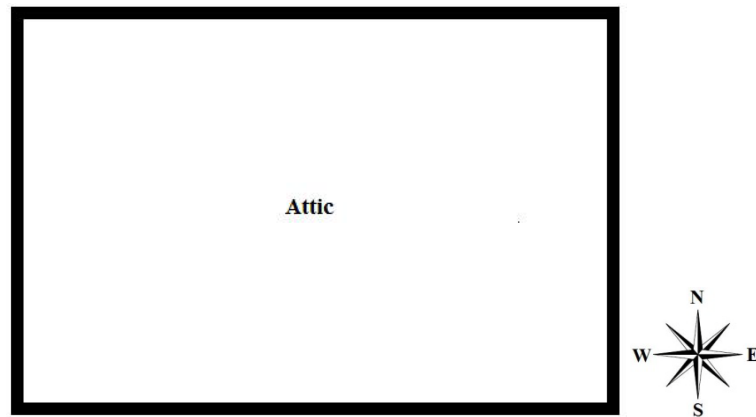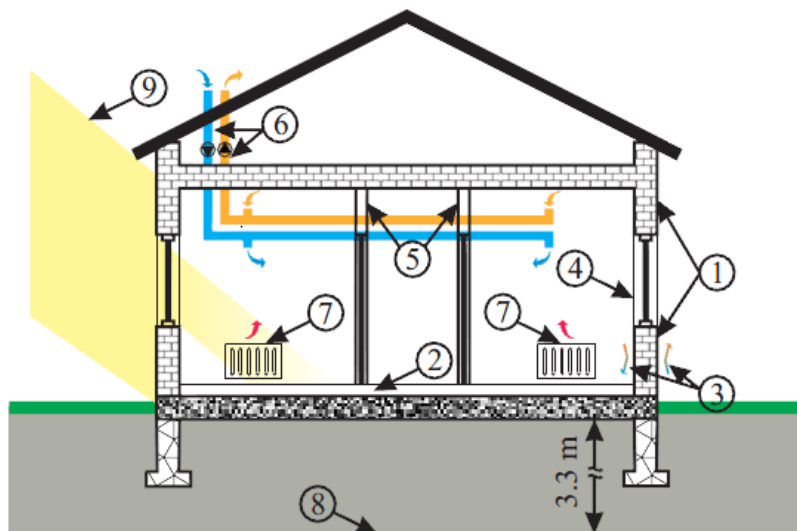

Figure 5. 2 A blueprint of the reference house (Second floor)

1: Building envelope, 2: Floor, 3: Convective heat transfer, 4: Windows,
5: Internal walls, 6: Ventilation, 7: Water radiators, 8: Ground 9: Solar radiation

Figure 5. 3 A sectional view of the reference house [153]

The exterior wall of the building is made of plasterboards, extruded polystyrenes, and solid concrete blocks. The partition of each zone is made of plaster boards. Between the plaster boards, it is filled with air. The ground floor has three layers of tiles, solid concrete blocks, and extruded polystyrenes. The upper floor is made of Glass wools, wood joists, and plasterboards. Table 5. 2 lists the detail of the materials of the building.

Table 5. 2 Properties of wall materials of the reference building

Name	Number of layers	Material	Thick-ness [m]	Density [kg/m³]	Specific heat [J/(kg·°C)]	Thermal conductivity [W/(m·°C)]
Exterior wall	3	Plasterboard	0.01	850	800	0.35
		Extruded polystyrene	0.10	35	1200	0.033
		Solid concrete	0.2	2300	920	1.75
Partition		Plasterboard	0.01	850	800	0.35
		Air	0.03	1.24	1006	0.025[19]
		Plasterboard	0.01	850	800	0.35
Ground floor		Tile	0.01	800	850	1.30
		Solid Concrete	0.20	2300	920	1.75
		Extruded polystyrene	0.15	35	1200	0.033
Upper floor	2	Glass wool , wood joists	0.135	100	980	0.045
		Plasterboard	0.01	850	800	0.35
Roof	1	Tile	0.02	1700	1000	0.66

The envelopes of the building are modeled using a simplified wall model. The simplified model assumes that

- Each material of the envelopes is uniformly distributed on the entire surface, and its thermo-physical properties are constant in time,
- Heat conduction through the envelope is one-dimensional and perpendicular to the envelope surface,
- Convective heat transfer on both sides of the envelope is approximated by Newton law: where the exchange coefficient h is constant and independent of the wind velocity,
- The surface temperatures of all the walls are close enough to neglect the radiative heat transfer balance between the walls,
- Windows do not store heat and they are not part of the massive wall.

---

[19] It will be considered without inner convection

An equivalent electrical circuit of the simplified model of the envelope is illustrated in Figure 5. 4. The total thermal resistance R_t in series and the thermal capacitances C_1, C_2 of the model are calculated as follows.

$$R_t = \sum_{i=1}^{n} R_i = \sum_{i=1}^{n} \frac{e_i}{\lambda_i A} \tag{5.1}$$

$$C_t = \sum_{i=1}^{n} \rho_i \times C_{p,i} \times V_i \tag{5.2}$$

$$C_1 = \sum_{i=1}^{n} \rho_i \times C_{p,i} \times V_i \times \left(1 - \frac{1}{2}\frac{R_i + R_{i-1}}{R_t}\right) \tag{5.3}$$

$$C_2 = C_t - C_1 \tag{5.4}$$

where λ_i and e_i are the wall layer thermal conductance [W/(m·°C)] and thickness [m] of the ith layer material, n is the total number of the layer, and A is the room surface [m^2]. ρ_i is the density [kg/m^3], $C_{p,i}$ is the specific heat [J/(kg·°C)], and V_i is the volume [m^3] of the ith wall.
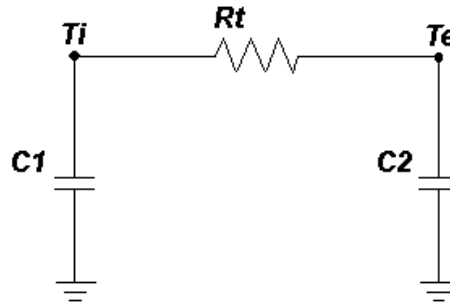
Figure 5. 4 An equivalent circuit of the simplified model of a wall

The assumptions of the indoor and outdoor environment of the building are as follows.

- The used weather and geographic data are based on the data of Paris, in France.
- Indoor temperature is homogeneous in each zone. There are small variations of temperature between each room.
- The attic is not heated by any radiator and its temperature is closed to the outdoor air temperature.
- The solar radiation incident on each surface of the envelope varies from moment to moment depending on its geographic location (latitude and longitude of the place), orientation, season, day of year, time of day, and atmosphere [154].
- The solar radiation falling on the roof has no visible impact on the internal thermal mass.
- The solar radiation passing through the windows can vary depending on the blind positions. From May to September, the blinds are operating during a daytime (10:00-18:00).

- The used ventilation equipment is a controlled mechanical ventilation single flow system. When this equipment is activated, air flow due to the ventilation and infiltration is constant and its given flow rate is 0.0384 kg/s (0.44 Vol/h).

In order to reach the BBC[20] label, renewable energy systems (a photovoltaic or a hydraulic system) are as usual integrated to the building, as additional equipment of the building.

5.3 THERMAL BEHAVIOR OF BUILDING

In order to observe the global thermal behavior of the selected building, we conducted on several simulations using SIMBAD toolbox. In Chapter 3, we have already reviewed the factors, which influence the building thermal conditions, such as a solar radiation, weather, a building structure, occupants' behavior, and operations of HVAC systems.

Among these factors, the climate and the structure are determined at the level of a building design and its construction. On the contrary, the behavior of occupants including their presence/absence, their activities, and their usages of electrical appliances is stochastic by nature. Thus, in order to study only the thermal behavior of the building, we thereby do not consider the behavior of occupants. Instead, we will build different thermal conditions of the building by changing the operation of HVAC systems including ventilation equipment and heaters during the simulations. The HVAC systems are easily controllable and are mostly used to maintain comfortable indoor thermal conditions of the building.

Table 5. 3 lists the different operating conditions of HVAC systems that we considered in this study to the purpose of the characterization of the thermal behavior of the selected building in order to underline the weight of energy consumption. For all the preliminary cases, we do not take account of any occupants' behavior. The following sub-sections show how the building thermally behaves in accordance with the operation of the HVAC systems of the building.

Table 5. 3 Different operating conditions of HVAC system

	Space heating								Ventil-ation
	Living room	Kit-chen	Room1	Room2	Room3	Bath-room	Entry	Attic	
Case A	0	0	0	0	0	0	0	0	0
Case B	0	0	0	0	0	0	0	0	1
Case C	1	0	0	0	0	0	0	0	0
Case D	1	0	0	0	0	0	0	0	1
Case E	1	1	1	1	1	1	1	0	0
Case F	1	1	1	1	1	1	1	0	1

(1: Active, 0: Inactive)

---

[20] BBC: (fr) Bâtiment de Basse Consommation, (en) Low Energy Building

5.3.1 Case A (Without heating/Without ventilation)

We first obtained temperature profiles of each zone of the building in natural discharge condition without occupancy. In this case, both the space heating and the ventilation are inactivated. It aims to know thermal characteristics of the building without any artificial thermal influence due to an active heater, or ventilation equipment. This kind of the situation occurs when occupants leave the house for a vacation, or move out to another place.

Figure 5. 5 shows the obtained temperature profiles. The initial temperature of the building was set to 20°C. The indoor temperature of each zone globally decreases during the first two weeks. It follows the outdoor temperature of the building. The decreasing curve has the global tendency of the negative exponential curve which implies thermal characteristics of the building, namely, the time constant of the building.
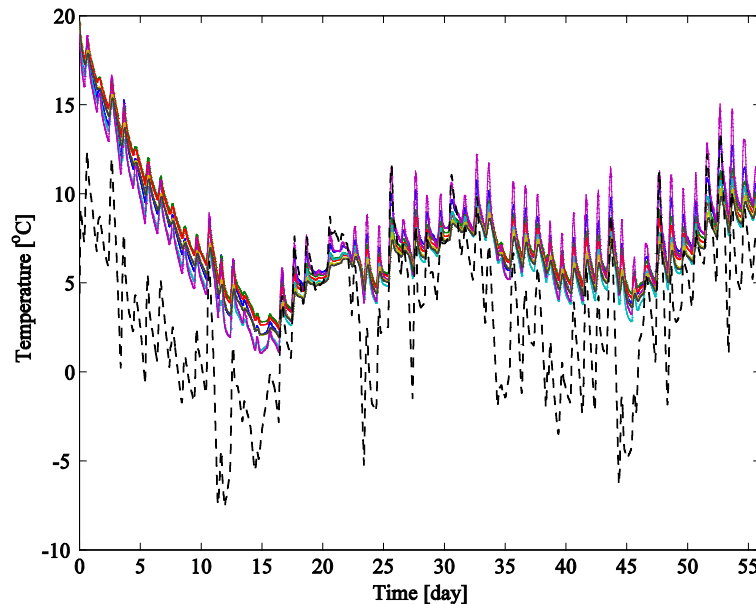

Figure 5. 5 Obtained temperature profiles of each zone of the building for a winter period in Case A (Blue line: Living room, Green: Kitchen, Red: Room 1, Aquamarine: Room2, Purple: Room3, Olive: Bathroom, Black: Entry, Black point: Exterior)

After a while, the house becomes thermally stable and the temperature difference between indoor and outdoor temperature decreases. However, since the building structure has thermal resistances and heat capacities, the indoor temperature cannot be exactly the same to the outdoor temperature. Moreover, when there are strong solar radiations during a daytime, both indoor and outdoor temperatures raise up. The room 3 is much influenced by the outdoor temperature and solar radiations because of its south-east orientations.

Each zone of the building has its own thermal and structural characteristics, such as localization, orientation, heat capacity, thermal resistance, a number of windows, etc, so that, there are also differences of the temperature between the different zones. Moreover, we can observe that there is a thermal delay of indoor temperature opposite to the outdoor temperature.

A zoomed figure of the temperature is shown in Figure 5. 6. The observed thermal delay is mainly due to global time constant of the building and is about 2.5 h in this case.
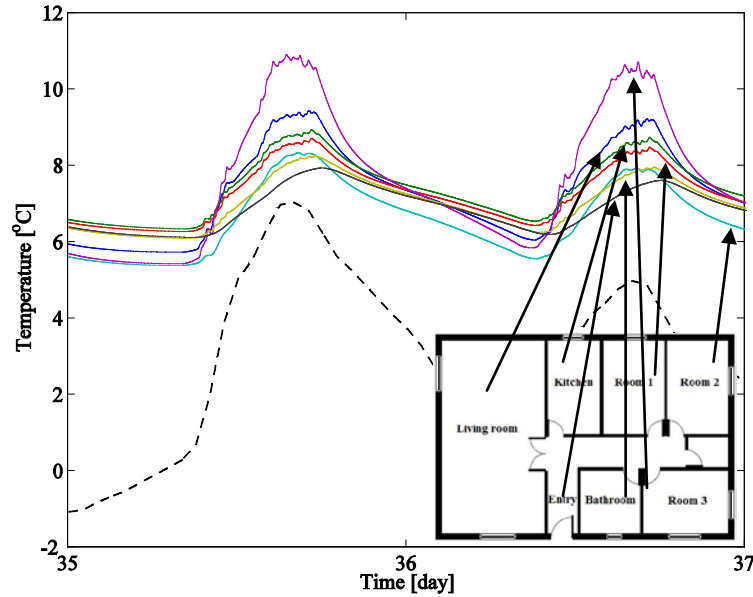

Figure 5. 6 Obtained temperature profiles of each zone of the building (Case A) for two days

5.3.2 Case B (Without heating/With ventilation)

In the previous Case A, the ventilation system was off. However, for the Case B, the ventilation system was maintained active during the simulation period in order to underline the effect of an open system. The other conditions, such as the weather, the structure of the building, the occupancy, and the operation of heaters, are the same as previously presented in Case A. This simulation aims to observe the thermal role of the ventilation system in the building. On account of the function of the ventilation system, indoor and outdoor air of the building is exchanged. Then, acceptable indoor air quality can be maintained.

From the simulation, we obtained the temperature profiles of the building as shown in Figure 5. 7. Its global tendency is similar to Case A. However, during the air exchange process (open system), fresh air enters in the building from the exterior, and indoor polluted warm air goes out. As a consequence, the building loses more its thermal energy. Therefore indoor temperature falls down more to Case A (See Figure 5. 8). This phenomenon is due to the equivalent thermal resistance of ventilation which causes that the total thermal resistance of the building decreases during the ventilation process. The calculated global thermal resistance of the reference building without ventilation is 11.5 x10^{-3} °C/W. The value with the considered ventilation system is 2.1 x10^{-3} °C/W which corresponds to 20 % of surface heat loses.
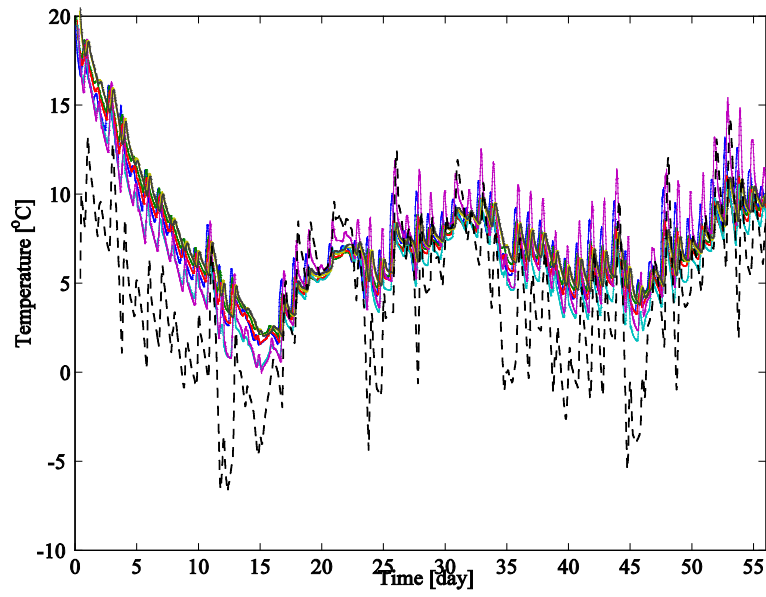
Figure 5. 7 Obtained temperature profiles of the different building zones in Case B
(Blue line: Living room, Green: Kitchen, Red: Room 1, Aquamarine: Room2, Purple: Room3, Olive:
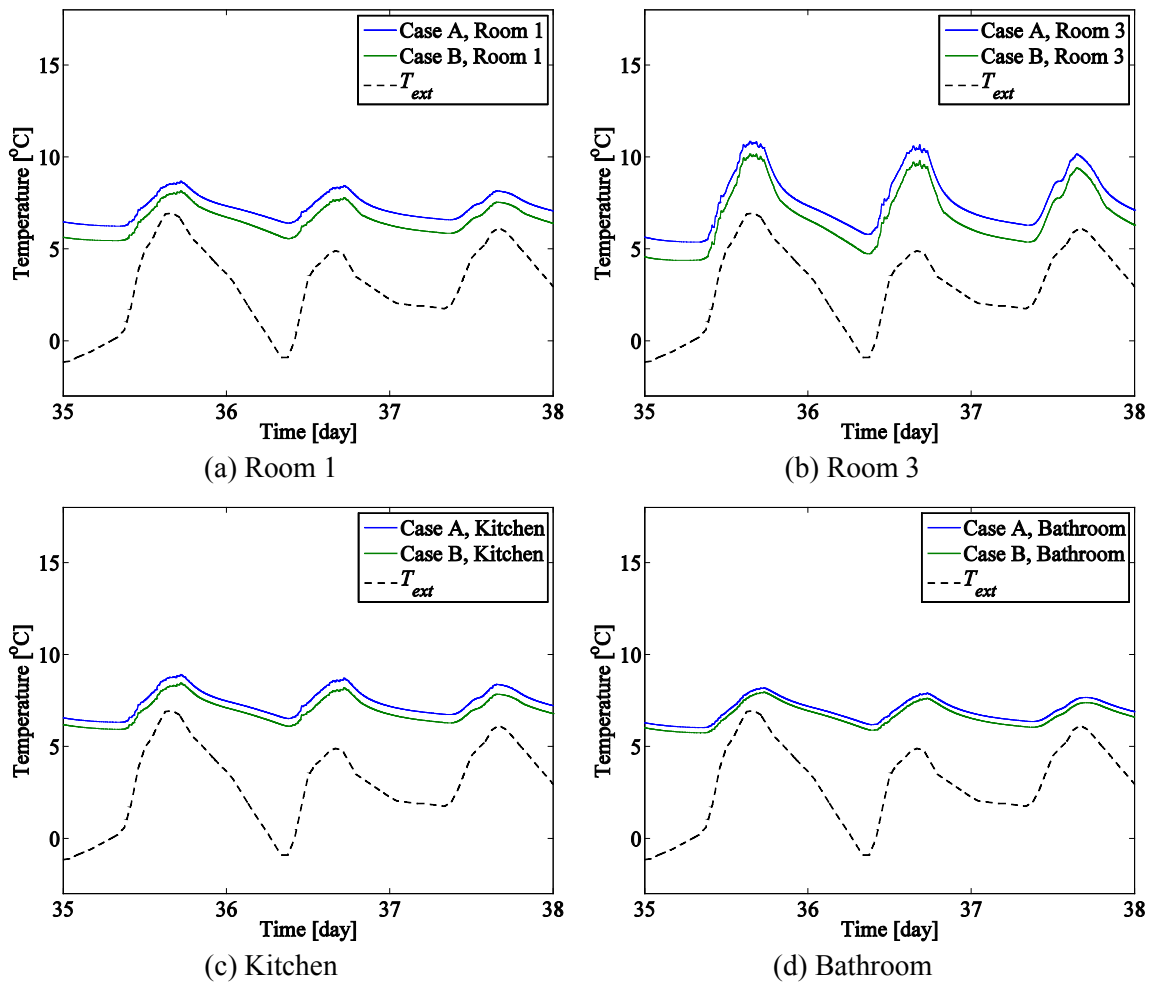Bathroom, Black: Entry, Black point: Exterior)

(a) Room 1

(b) Room 3

(c) Kitchen

(d) Bathroom

Figure 5. 8 Obtained temperature profiles of several zones of the building

131

The previous two analyzed cases clearly illustrate the possible temperature differences between the different zones. These results pay attention to the inaccuracy approach if we consider the building model as a mono-zone, instead of a multi-zone. We are then focusing on non-equilibrated heating between the different zones. It permits to check the thermal heterogeneity on the considered system.

5.3.3   Case C (Local heating for a living room/Without ventilation)

In Case C, we simulated temperature profiles of the building of which living room is heated by an electrical convective heater. However, the ventilation system does not operate in the living room. Moreover, the other living spaces are neither heated, nor ventilated. The temperature reference was set to 19 °C (regulated between 18-20 °C) during daytime from 07:00 to 22:00. Then, it was set to 17 °C (regulated between 16-18 °C) during night from 22:00 to 07:00.

In practical cases, it is needed to differently control the temperature of building zones for the thermal comfort of occupants and the energy saving of buildings. If the building model is designed as a multi-zone model, the thermal interaction between each zone should not be too strong and then heterogeneity of temperature profiles of each zone can be observed. However, if there is not a big temperature difference between rooms even if the temperature of each zone is differently controlled, the building model can be considered as a mono-zone model. Moreover, the above kinds of control might not be useful in the mono-zone. To know whether there is temperature heterogeneity of each zone of the building model, the present case, i.e. named C, was studied.

The obtained temperature profiles are illustrated in Figure 5. 9. The temperature of the living room follows quite well its reference. It is higher than the temperature of adjacent spaces. As a consequence, heat of the living room is lost through the exterior envelopes and the interior partition of the building.

The temperature of the room 2 and the room 3 is the lowest because it is easy to lose their heat through the exterior envelopes of which surface is bigger than other sides'. We also underline that the room 3 exhibits the important temperature fluctuation from coldest (due to external surface area) to warmest during mid-day as consequence of efficient solar radiation captured through the south-oriented window. Nevertheless, this result corresponds to partitioned area (closed doors) but the reality will be less pronounced due to convective nonlinearities and the resulting convective flow from the induced temperature differences.
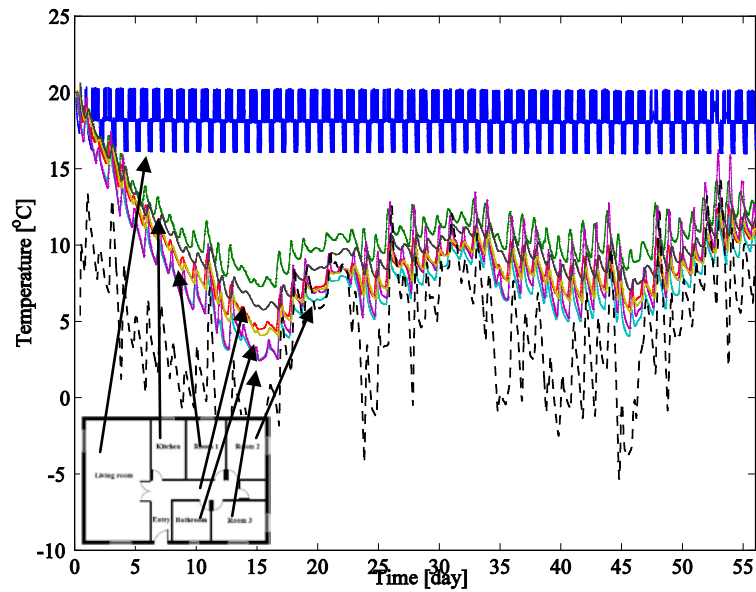
Figure 5. 9 Obtained temperature profiles of the different zones of the building (Case C)

The average[21] and the maximum/minimum temperatures of each zone and the outdoor temperature during the winter period are shown in Figure 5. 10. There are the differences of the temperatures, around 10 degrees between the heated zone and other sub-zones and 5 degrees between the non heated area. Since there is such temperature heterogeneity on the considered building, i.e. between the zones, we must consider this building as a multi-zone. Moreover, we know that the ventilation equipment was not activated and that the space heating of sub-zones are less coupled in this case.

Figure 5. 10 Obtained temperature profiles of each zone of the building (Case C)

---

[21] The average value on the considered simulation period

5.3.4 Case D (Local heating for a living room/With ventilation)

Under the same condition of heaters of Case C, we conducted on another simulation with ventilation (Case D). Figure 5. 11 shows the temperature profiles of each zone of the building. The temperature of the living room follows the reference temperature like Case C. Comparing to the temperatures obtained in Case C, the temperature of the other zones is descending for the same reason of the Case B.
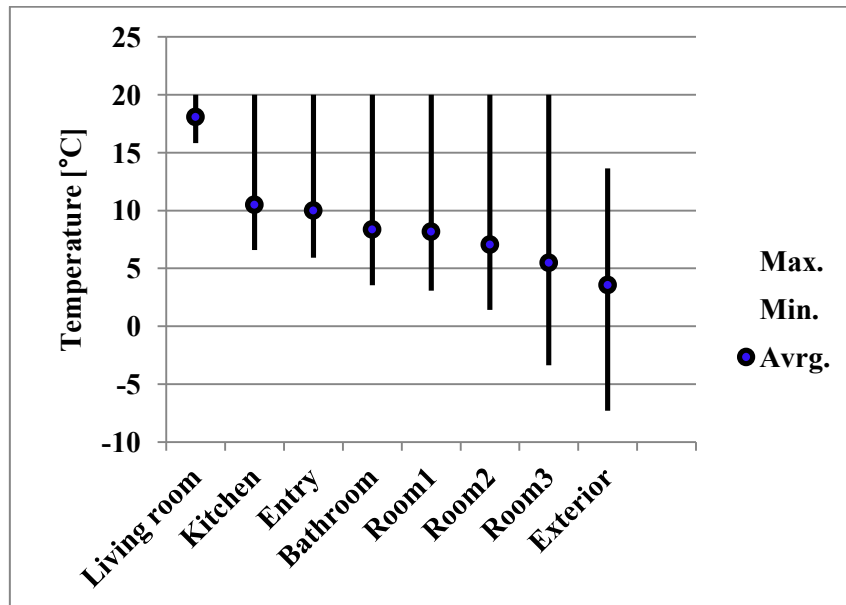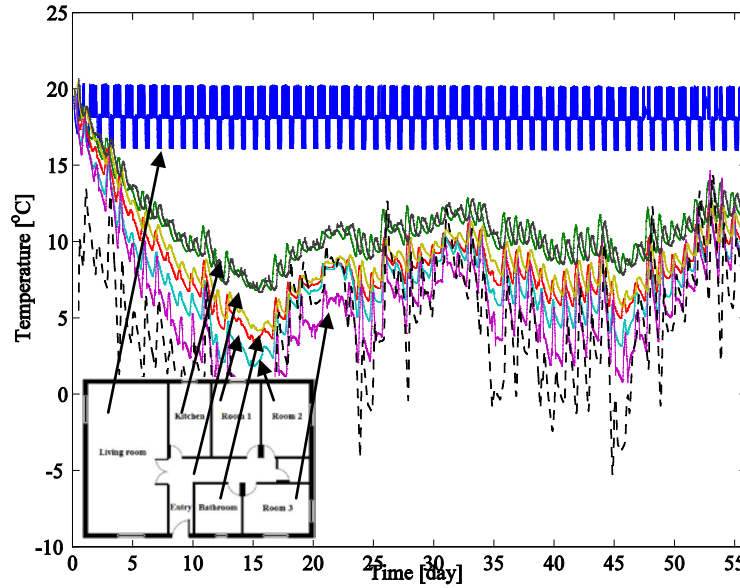

Figure 5. 11 Obtained temperature profiles of the different zones of the building (Case D)

Figure 5. 12 depicts a comparison of the temperature profiles of the room 1, the room 3, the kitchen, and the bathroom obtained by Case C and Case D. As stated above, for all the zones, the indoor temperature which was simulated without ventilation (Case C) is higher than the results obtained by Case D for the same reason of Case B. However, the differences of the temperature within the kitchen and the bathroom are smaller than the differences within room 1 and room 3. It is explained by air flows within the building by the ventilation system. While the ventilation system operates, fresh cold air enters through the living room, the room 1, the room 2, and the room 3 and makes the temperature of these rooms decreasing. Then, the indoor air moves to the kitchen, the bathroom, and the entry because of the differences of the temperature and the air pressure, and escapes to the exterior of the building. As a result, the kitchen and the bathroom are less influenced by cold air which directly enters into the rooms.

(a) Room 1   (b) Room 3

(c) Kitchen   (d) Bathroom
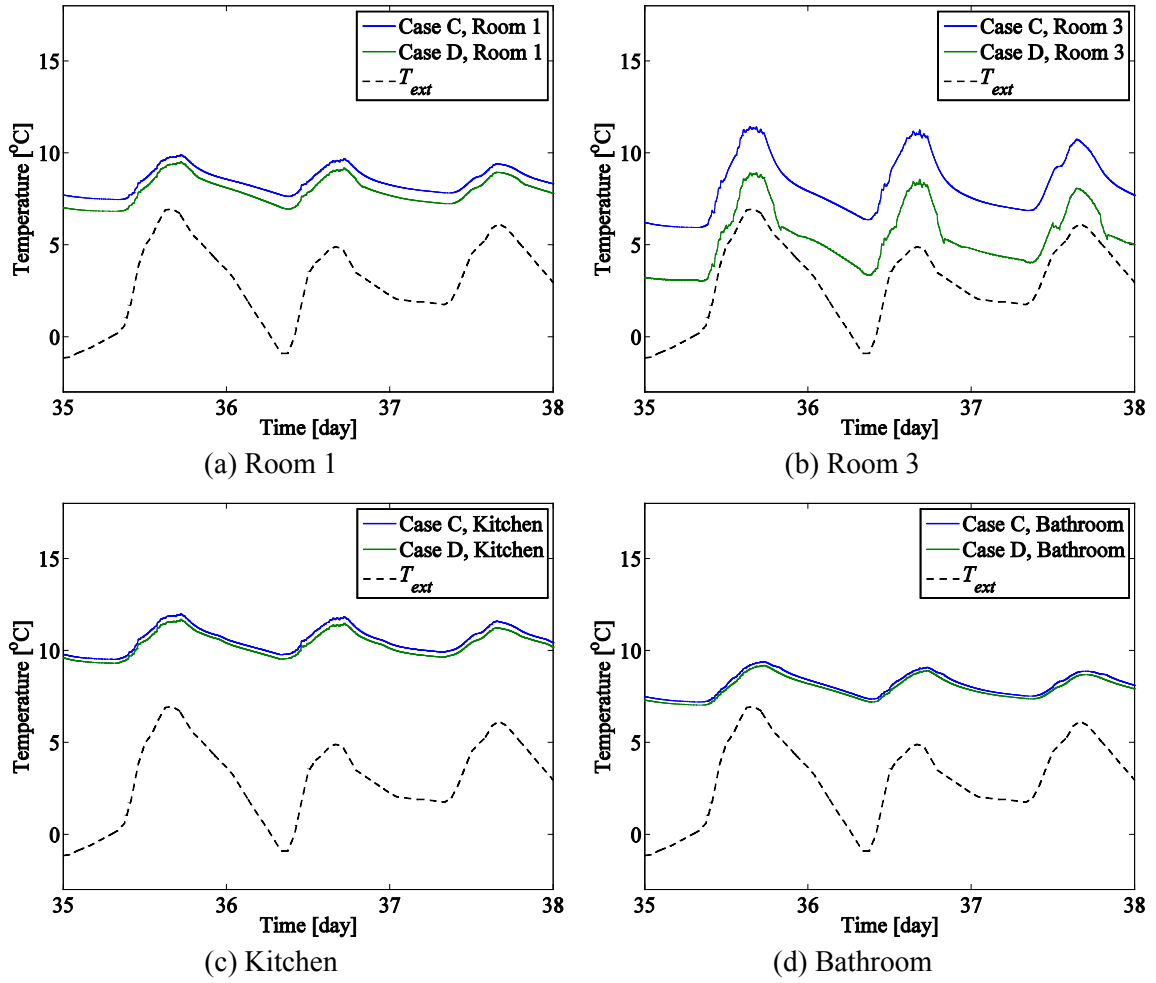
Figure 5. 12 Obtained temperature profiles of several zones of the building

We also compared the electrical power profiles of the heater which is placed in the living room for Case C and Case D. In order to maintain the reference temperature within the living room, it is obvious that the electrical power in Case D is more frequently supplied to the heater than in Case C according to the need of heating. Figure 5. 13 shows daily power profiles of the heater in the living room for Case C and Case D. During the simulation period, the accumulated energy used by the heaters in Case C and Case D is respectively 3.29 and 3.37 GJ. The difference of the used energy comes from the heat loss generated via the ventilation and the infiltration in Case D.
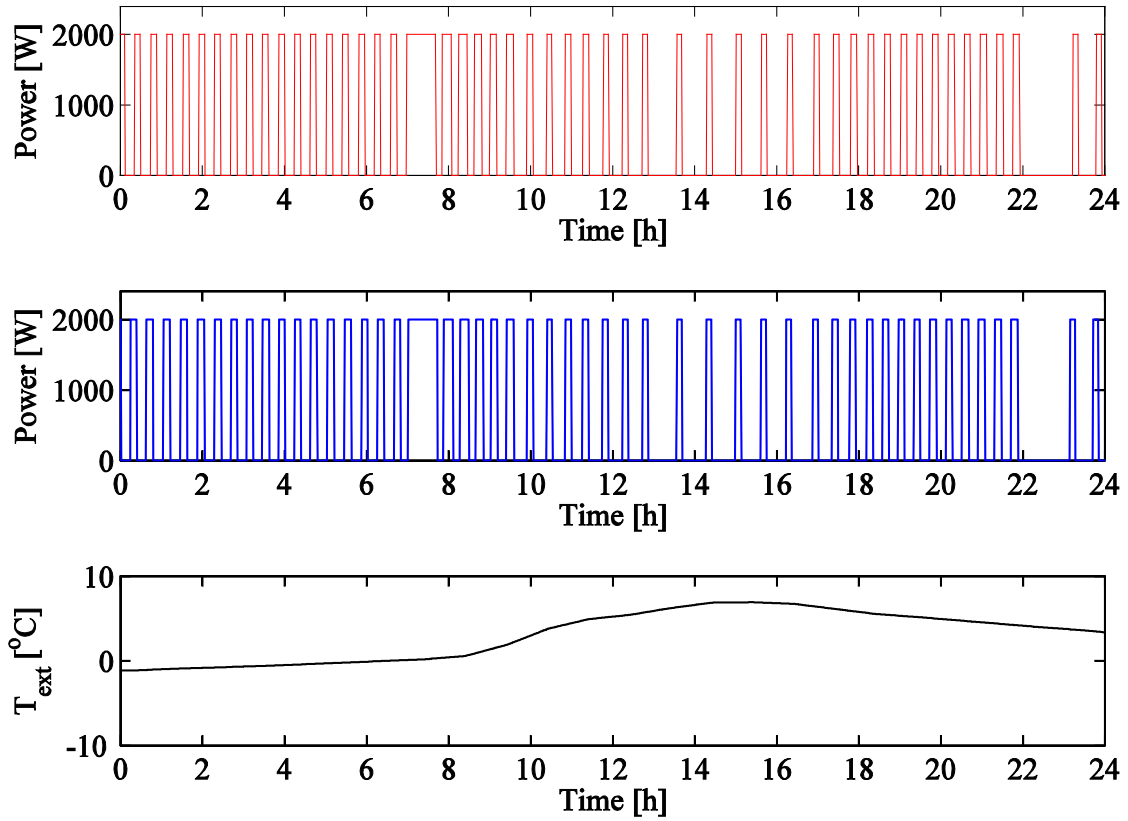
Figure 5. 13 An example of daily power profiles of the heater in the living room for Case C (Red line) and Case D (Blue line) and daily exterior temperature

5.3.5 Case E (With heating/Without ventilation) / Case F (With heating/With ventilation)

In the previous cases (Case C and Case D), we analyzed the building under a local heating condition. Now, we consider a global heating condition. The first floor of the building is totally heated, as if it is all occupied. Heaters operated according to the set temperature which is the same to the reference temperature of the living room. However, in Case E, there is no ventilation. Vice versa, in Case F, the ventilation system is activated in order to reach the required goal of Indoor Air Quality (IAQ).

From the simulations, we obtained the indoor temperature for the both cases. Despite of the variations of the outdoor temperature, the indoor temperature of each room is following the reference temperature in both cases. However, in order to keep the same range of the reference temperature within each zone, it is expected that the heating energy demand increases more in Case F than in Case E. Figure 5. 14 illustrates the accumulated heating energy use of the heater which is placed in the living room for Case E and Case F. The final values of the accumulated energy used by the heaters of the living room for both Case E and Case F are respectively 2.73 and 3.05 GJ. It is also related to the thermal resistance of the building with/without the equivalent thermal resistance of the ventilation in parallel.
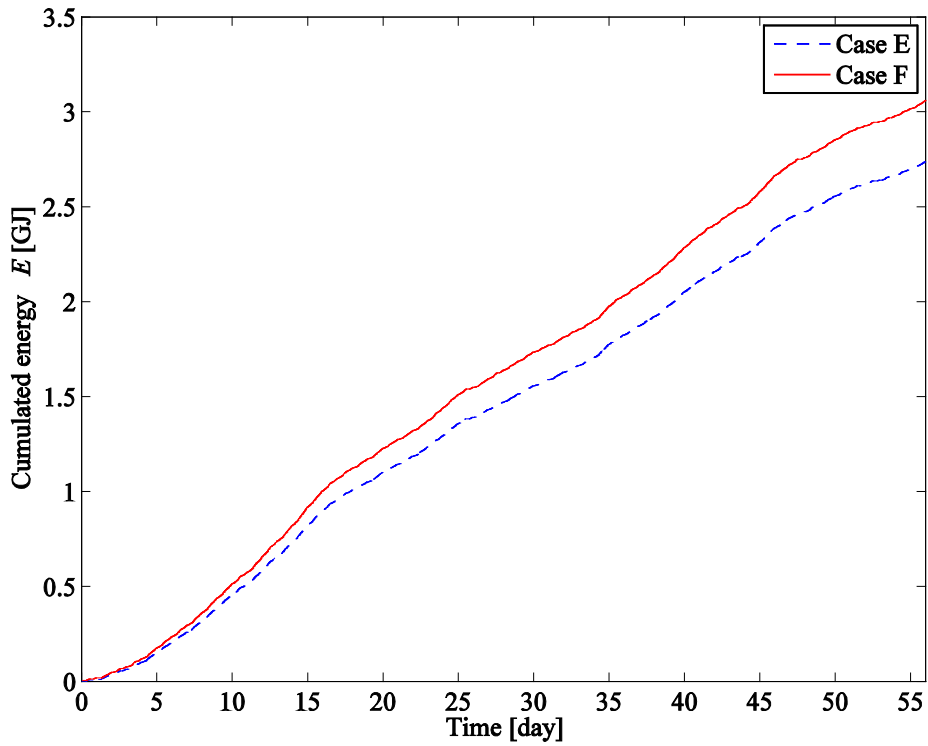
Figure 5. 14 accumulated heating energy use of the heater for Case E and Case F

In this section we have observed the thermal behavior of the selected building especially during a winter period. As considering the different operating conditions of the HVAC system, we could analyze the thermal characteristics of the building, in terms of thermal resistance, thermal delay, time constant, temperature heterogeneity between each zone, and energy demand of the living room. The next section deals with the thermal influence of electrical appliances within the same building.

5.4 INTEGRATION OF ELECTRICAL APPLIANCES

As aforementioned in Chapter 4, an electrical appliance within a building operates as an internal heat source of the building. It means that the appliance influences the thermal behavior of the building. Moreover, this influence depends on the power consumption profile and the time constant of the appliance. In order to study the thermal effect of different electrical appliances within a building, we integrate several kinds of electrical appliances into the selected building model.

As stated above, the chosen building model is preliminarily characterized as a multi-zone model. To the purpose of the study, the electrical appliances were selected and placed in the living room.

The reason why the living room was selected for this study is as follows:

✓ The living room is the most occupied place within residential buildings.
✓ Various electrical appliances are used in a living room.

Generally, the size and the type of houses and the number of person per family are different. However, the used electrical household appliances for each family are statistically globally similar. For example, a refrigerator, a television, a telephone, a computer, an electric iron, and a washing machine are the common electrical appliances for a normal household. Appendix D lists the representative electrical household appliances and their electrical power consumption. Among them, the appliances which are typically used in a living room of a residential building list Table 5. 4. According to the table, we selected different electrical appliances of which power consumption levels are 200, 600, 1200 W to study. In order to check the thermal dynamic effect of these appliances, we also explore several time constant values, as 60, 120, 600, 1200 sec. As a result, twelve models which represent the different electrical appliances were studied for this investigation in total. Each of the selected electrical appliances was placed in the living room of the building model for each simulation. Table 5. 5 lists the code of the studied models of the electrical appliances. The code case is '**EP***X***TC***Y*(Electrical Power *X* and Time Constant *Y*)', where *X*, *Y* are the values of the electrical power consumption and the time constant of an electrical appliance, respectively. For example, a code '**EP***200***TC***60*' means that the appliance consumes 200 W of electrical power, and that its time constant is 60 sec.

However, most of electrical appliances are consuming electrical power, even while they do not operate. It means that small quantity of standby power is supplied to maintain the appliance when it is plugged in. According to KERI[22], the average number of electrical appliances used in a household in Korea is 23.9. Among these appliances, 74.5 % of electrical appliances are consuming standby power. It accounts for 6.1 % of yearly total power consumption of a household and it represents about 209 kWh in Korea. The institute reported that the greatest standby power consumer is a television set-top box which consumes 12.3 W of standby power. In sequence, a modem (6 W), a standing air-conditioner (5.8 W), a boiler (5.8 W), an audio speaker (5.6 W), a home theater (5.1 W), a video (4.9 W), an audio component (4.4 W), a Wi-fi router (4.0 W), a DVD player (3.7 W), a rice cooker (3.5 W), and a microwave (2.2 W) are following [155]. Therefore, we should consider these standby electrical appliances which are always turned on. We fixed the standby power consumption at 20 W for each zone of the house in this study.

---

[22] Korea Electrotechnology Researching Institute

Table 5. 4 Examples of power consumption of household electrical appliances

Function	Item	Power consumption [W]	Average time per day in use [h]
Cleaner	Air purifier	5	< 12
	Humidifier	280	< 12
	Vacuum cleaner	1000	< 0.5
Entertainment	Blu-ray player	20	< 2
	Digital picture frame	10	< 0.5
	DVD player	10	< 2
	Mp3 speakers	20	< 2
	Audio component	100	< 5
	Sub-woofer	200	< 5
Office	Cell phone charger	3	< 2
	Computer	80	< 3
	Computer speaker	4	< 2
	Cordless phone	2	24
	Inkjet printer	8	< 0.2
	Laser printer	20	< 0.2
	Monitor	33	< 3
	Scanner	40	<0.2
	Wi-fi router	7	24
Television	Projection TV (65 inch)	210	< 5
	LED TV (46 inch)	110	< 5
	LCD TV (42 inch)	100	< 5
	Plasma TV (42 inch)	100	< 5
Television boxes	PVR	900	< 1
	Satellite	80	< 5
	Set-top box	24	24
Video games console	Nintendo Wii	20	< 2
	Play station 3	200	< 2
	Xbox 360	180	< 2

Table 5. 5 Code of the models of electrical appliances with different values of the electrical power consumption and the time constant

		Time Constant [s]			
		60	120	600	1200
Electrical Power Consumption [W]	200	EP*200* TC*60*	EP*200* TC*120*	EP*200* TC*60*	EP*200* TC*1200*
	600	EP*600* TC*60*	EP*600* TC*120*	EP*600* TC*60*	EP*600* TC*1200*
	1200	EP*1200* TC*60*	EP*1200* TC*120*	EP*1200* TC*60*	EP*1200* TC*1200*

Moreover, we set additional 300 W of constant power within the kitchen and the bathroom according to their occupancy. Table 5. 6 lists the considered input power consumption data of each zone of the building model.

Table 5. 6 Input power of each zone of the building model

Zone	Power consumption of a Tested Appliance [W]	Stand-by Power consumption [W]	Additional Power consumption [W]
Living room	Various (See Table 5.5)	20	-
Kitchen	-		300
Room 1	-		-
Room 2	-		-
Room 3	-		-
Bathroom	-		300
Entry	-		-
Attic	-		-

The overall layout of usage of the electrical appliances within the building is illustrated in Figure 5. 15 based on block diagrams. The block *A* sets the profiles of electrical appliances of which function depends on the occupancy. The block *B* sets the profiles of standby appliances which are always 'ON'.

The electrical appliances are operating according to their occupation profiles. The tested appliances in the living room and the appliances in the kitchen and the bathroom are occupied from 6:30 to 8:30, from 12:00 to 14:00, and from 18:00 to 23:00. The occupancy profile and the usage profiles of the electrical appliances are shown in Figure 5. 16 and Figure 5. 17, respectively.
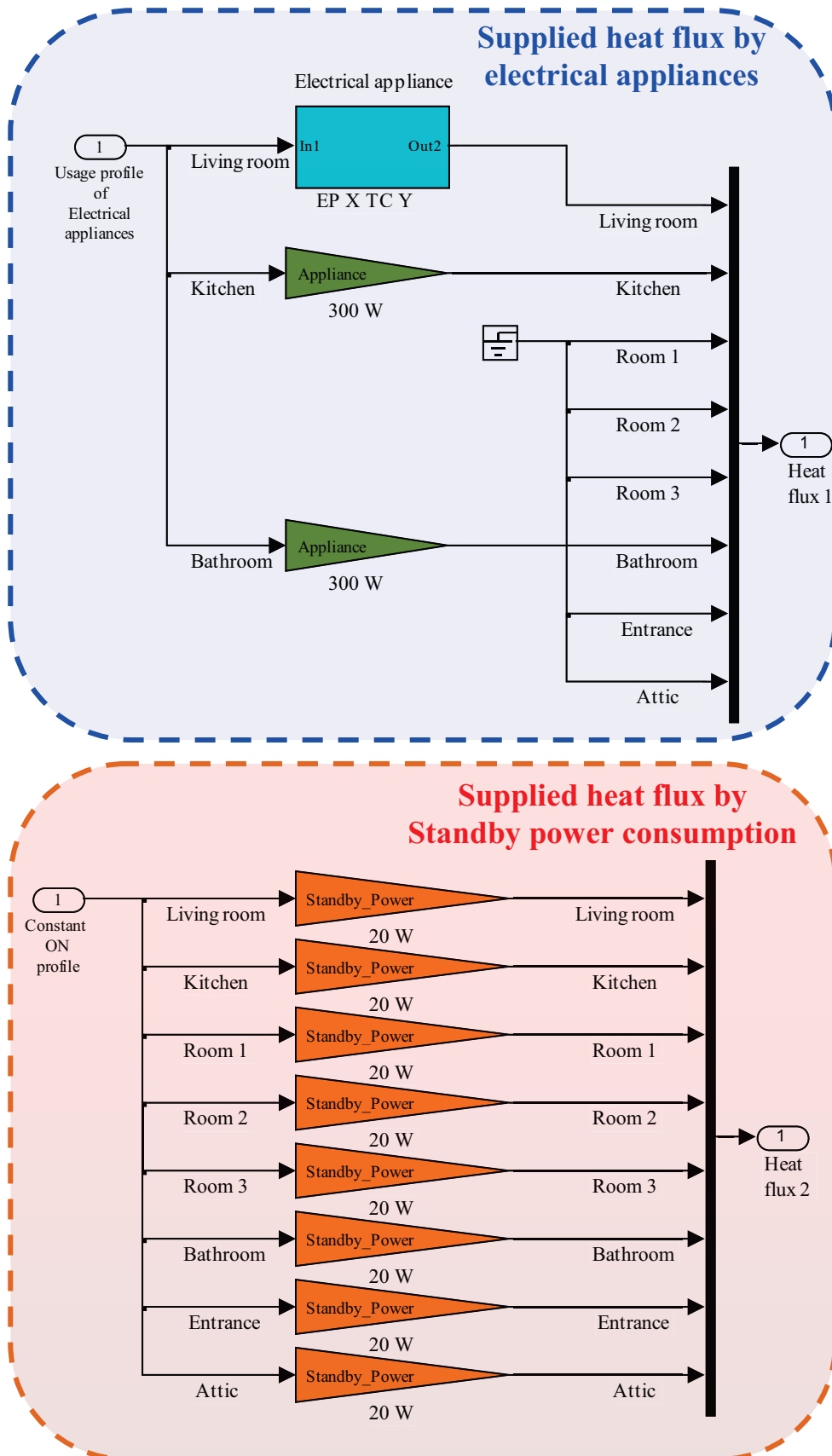
Figure 5. 15 The overall layout of usage of the appliances within the building model
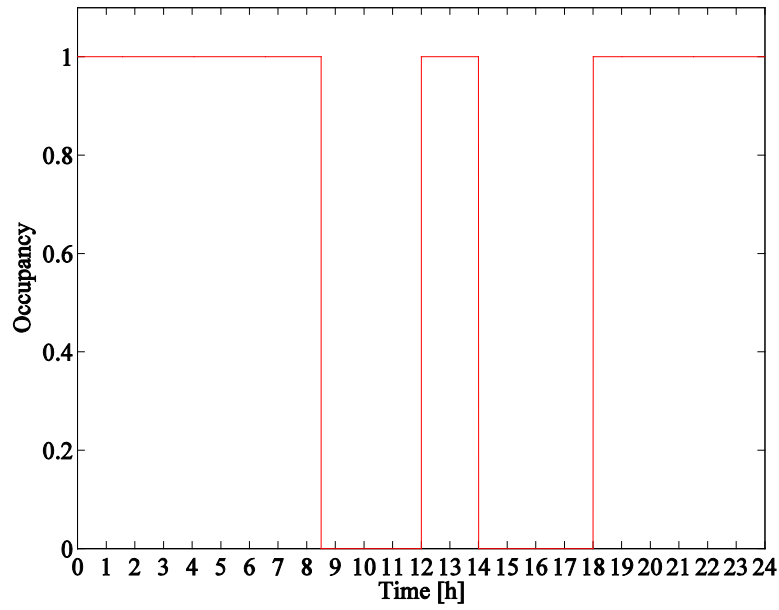
Figure 5. 16 A profile of occupancy
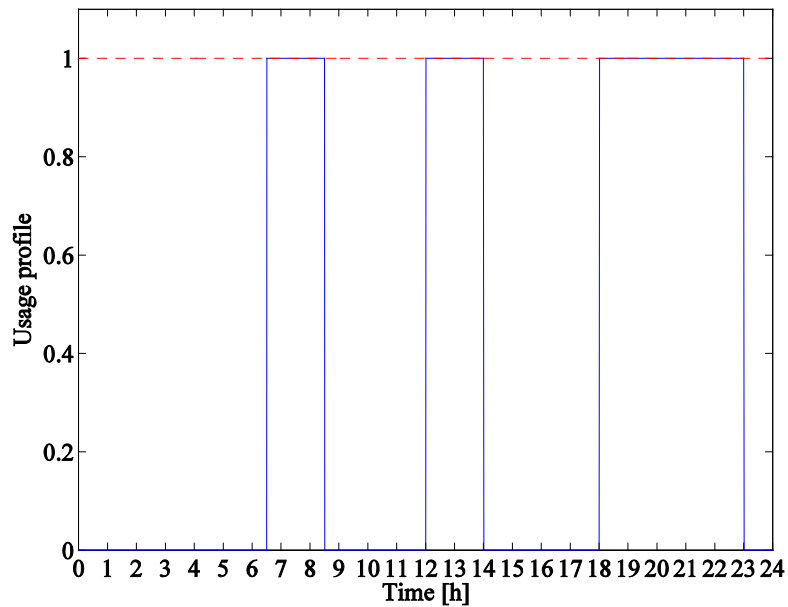
Figure 5. 17 Usage profiles of the appliances (Blue line: Electrical appliances, Red point: Standby power use)

For the thermal comfort of habitants of the building, electrical convective heaters, which consume 2000 W of electrical power, were also placed in all the living places except the attic. The heaters are operating for obtaining a reference temperature of the zones. There are four modes of the heater: Comfort, Sleep, Eco, and Stop. Comfort mode sets the temperature to 18~20 °C, Sleep mode sets the temperature to 16~18 °C, Eco mode sets the temperature to 10~12 °C, and Stop mode makes the heater stop operating. Table 5. 7 lists the setting profiles of the heater.

Table 5. 7 Setting profile of the heater

Mode	Temperature Regulated ±1[°C]	Usage Time
Comfort	19	05:00 - 08:30 11:30 - 13:30 17:00 - 23:00
Sleep	17	23:00 - 05:00
Eco	11	08:30 - 11:30 13:30 – 17:00

Based on the above condition and schedule, we conducted on two kinds of the simulations in order to study the thermal influence of electrical appliances:

- Case 1: Simulations regardless of usage of electrical appliances
- Case 2: Simulations including usage of electrical appliances

5.4.1 Analysis of the Simulation Case 1

Heating energy demand of a building depends on the energy balance of the building. For the simulations Case 1, there are heat gains due to solar radiation and heat loss through the envelopes of the building. We obtained the heating energy demand of the living room by calculating the energy consumption of the heater placed in the living room ($E_{1,heater}$). During a winter period from January to February (8 weeks), the heater of the living room consumes 2.92 GJ for a space heating. Thanks to the operation of the heater, the living room temperature is regulated to its reference value as shown in Figure 5. 18.
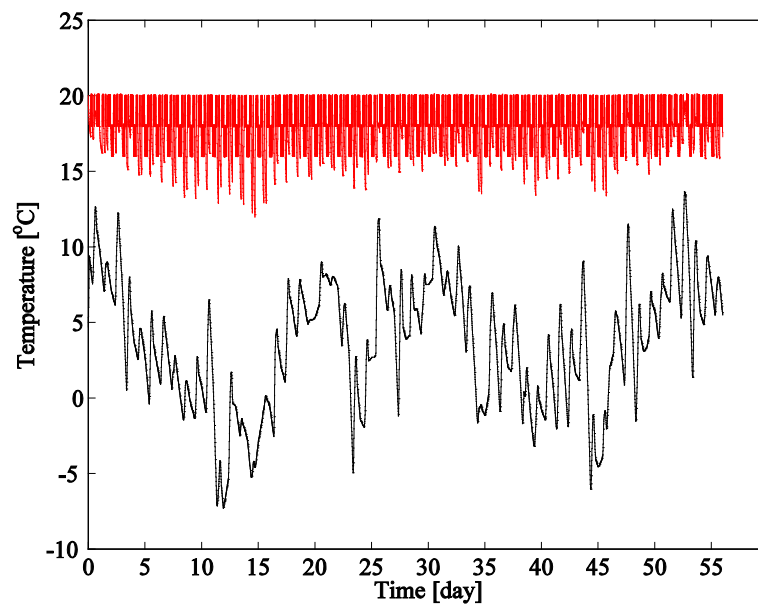

Figure 5. 18 Indoor temperature of the living room (red line) and outdoor temperature of the house (black point)

143

An example of daily indoor temperature of the living room and power consumption of the heater is also illustrated in Figure 5. 19. The heater operates for maintaining the reference temperature to the purpose of the occupant's thermal comfort. It compensates for the heat loss of the building.
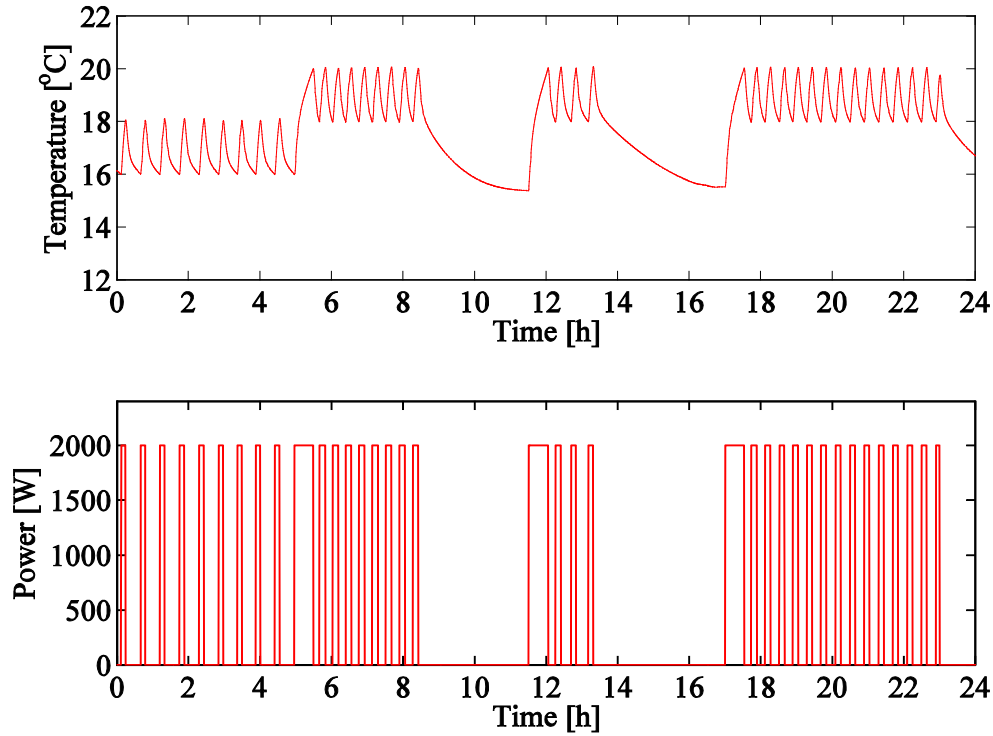

Figure 5. 19 An example of daily indoor temperature of the living room and power consumption of the heater

5.4.2   Analysis of the Simulation Case 2

Regarding the usage of electrical appliances, we conducted on 12 simulations for analyzing thermal influence of different types of electrical appliances. We simulated the indoor temperature and the space heating energy use of the heater within the living room of the house. The heater operated in order to maintain the reference temperature in the living room. Figure 5. 20 shows examples of daily temperature profiles in the living room for both Case 1 and Case 2.

Figure 5. 20 (a) shows the temperature profiles while electrical appliances which consume 200 W of power (EP*200*TC*60*, EP*200*TC*120*, EP*200*TC*600*, EP*200*TC*1200*) were placed one by one in the living room for each simulation. In the same way, Figure 5. 20 (b) and (c) show the temperature profiles when electrical appliances which consume 600, and 1200 W of electrical power, respectively. However, in reality it is seldom to use an electrical appliance which consumes a high power such as 1200 W every day, regularly. Therefore the example in Figure 5. 20 (c) can be just illustrative for a special case, or show the power consumption of a set of electrical appliances used in the living room.
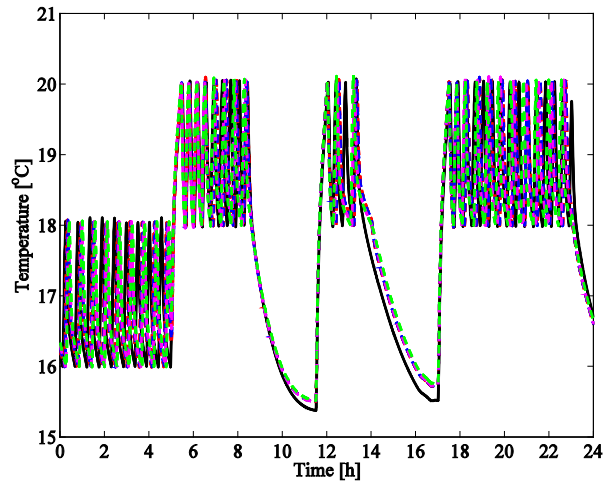
(a) EP*200*
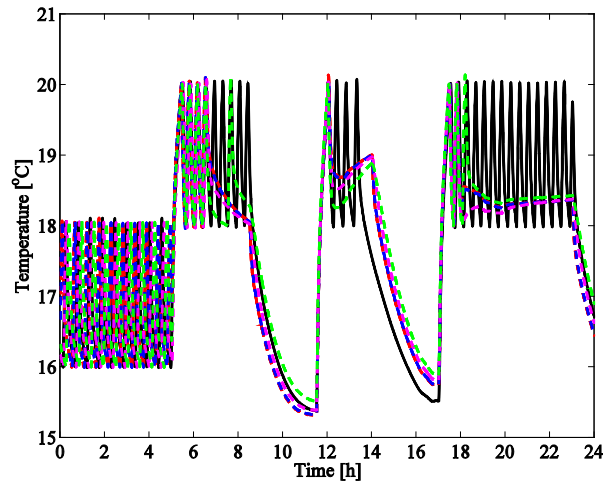
(b) EP*600*
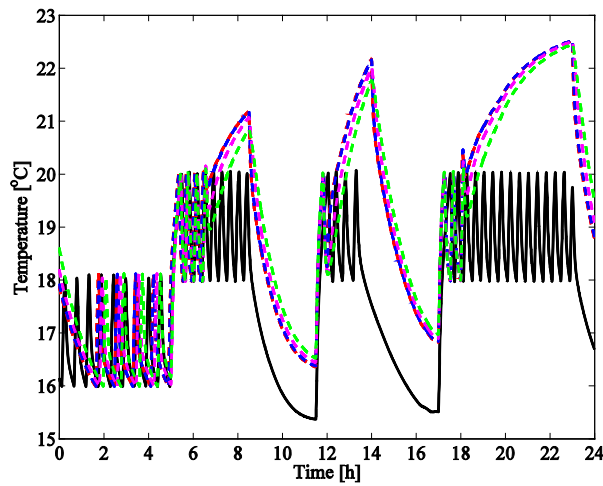
(c) EP*1200*

Figure 5. 20 Comparison of indoor temperature of the living room
((-): Case 1, (--): Case 2 (TC*60*), (--): Case 2 (TC*120*), (--): Case 2 (TC*600*),
(--): Case 2 (TC*1200*))

In each figure, there are five curves which show thermal impact of the time constant of electrical appliances. We can see that the heater operates significantly less when an electrical appliance is used. It is due to the heat gain of the electrical appliance. Moreover, as discussed in Chapter 4, the time constant of the electrical appliance which consumes more power, impacts the thermal behavior of the zone. The corresponding power profiles are shown in Figure 5. 21.

The profile of the heat flux induced by an electrical appliance is determined by its electrical power consumption profile and its time constant. We already mentioned that the space heating energy consumed by the heater decreases as a higher power is consumed by an electrical appliance. As comparing the profiles of the indoor temperature and the power consumption of electrical appliances within the living room, it is obvious that a bigger heat flux of an appliance compensate for the need of the heater. However, a significant heat gain can also lead overheating and can cause the energy waste.

The corresponding heat flux of an electrical appliance $\Phi_{ap}(t)$ can be obtained as follows

$$\phi_{ap}(t) = \phi_{ap,Active}(t) + \phi_{ap,Inactive}(t) \tag{5.5}$$

$$\phi_{ap,Active}(t) = P_{elec} \cdot (1 - e^{-t/\tau}) \qquad \text{(active)} \tag{5.6}$$

$$\phi_{ap,Inactive}(t) = P_{elec} \cdot e^{-t/\tau} \qquad \text{(inactive)} \tag{5.7}$$

where $\Phi_{ap,Active}$ and $\Phi_{ap,Inactive}$ are respectively the heat fluxes [W] while the electrical appliance is activated and inactivated. P_{elec} is the available supplied electrical power [W]. The corresponding heating energy due to the electrical appliance is

$$
\begin{aligned}
\int_{t_0}^{t_2} \phi_{ap}(t)dt &= \int_{t_0}^{t_1} \phi_{ap,Active}(t)dt + \int_{t_1}^{t_2} \phi_{ap,Inactive}(t)dt \\
&= \int_{t_0}^{t_1} P_{elec} \cdot (1 - e^{-t/\tau})dt + \int_{t_1}^{t_2} P_{elec} \cdot e^{-t/\tau} dt \\
&= P_{elec} \cdot (-t_0 + t_1 - \tau \cdot (e^{-t_0/\tau} - e^{-t_1/\tau})) + P_{elec} \cdot \tau \cdot (t_1 e^{-t_1/\tau} - t_2 e^{-t_2/\tau}) \\
&= P_{elec} \cdot (-t_0 + t_1) - (P_{elec} \cdot \tau \cdot (e^{-t_0/\tau} - e^{-t_1/\tau})) + P_{elec} \cdot \tau \cdot (t_1 e^{-t_1/\tau} - t_2 e^{-t_2/\tau})
\end{aligned}
\tag{5.8}
$$

where t_0 is initial time when the appliance is activated, t_1 is the moment when the appliance is inactivated, and t_2 is the moment when the heat flux is not available any more. From Eq. (5.8), we can know the effect of thermal characteristics of electrical appliances according to its power consumption level. Moreover, we can obtain the stored energy within the electrical appliance which will be used after the appliance becomes inactivated. The calculated stored energy according to the time constant of the appliance versus its operating time is shown in Figure 5. 22.
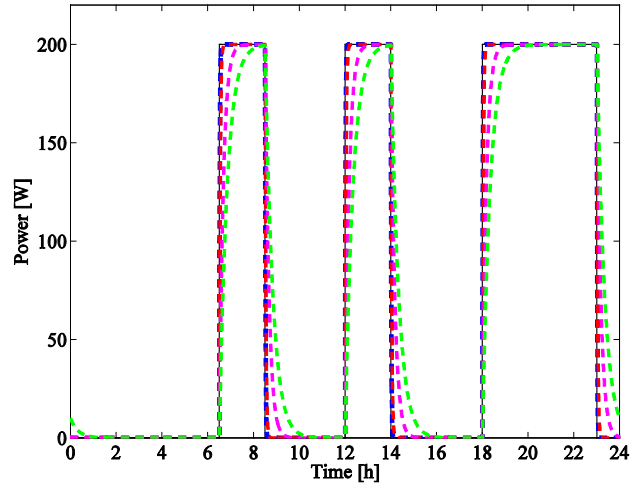
(a) EP*200*
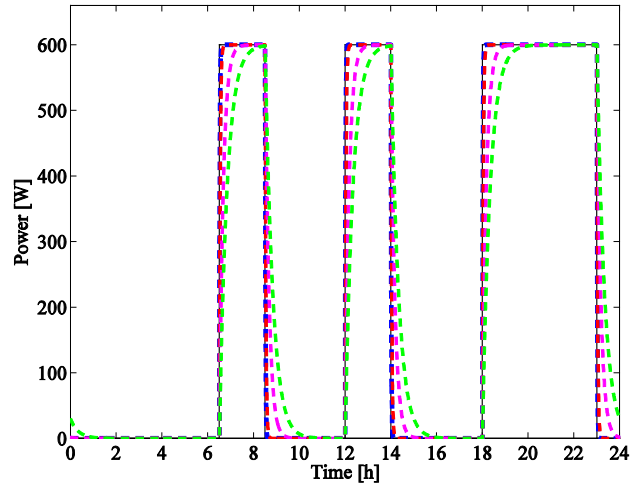
(b) EP*600*
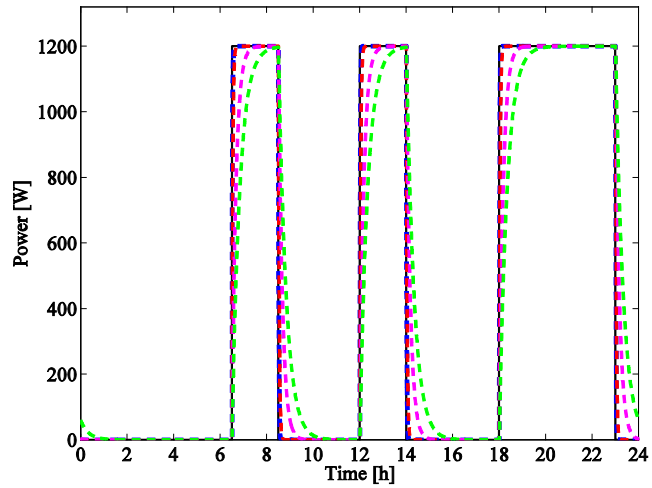
(c) EP*1200*

Figure 5. 21 Comparison of power profiles of electrical appliances
((-): Electrical power, (--):TC60, (--):TC120, (--):TC600, (--):TC1200)
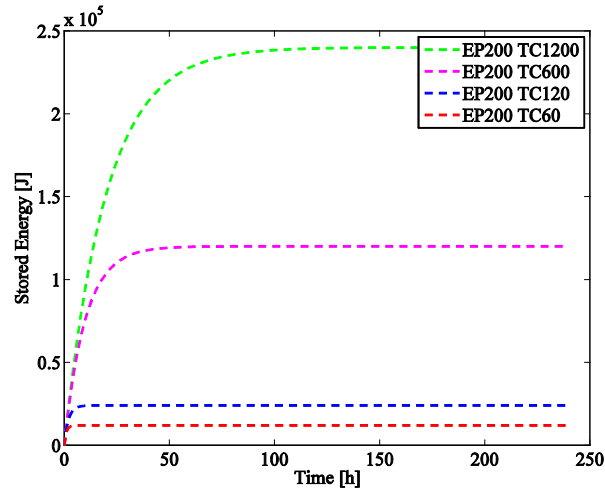
(a) EP*200*
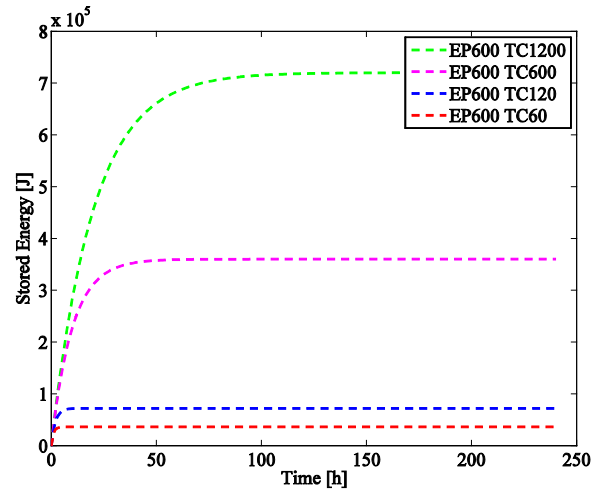
(b) EP*600*
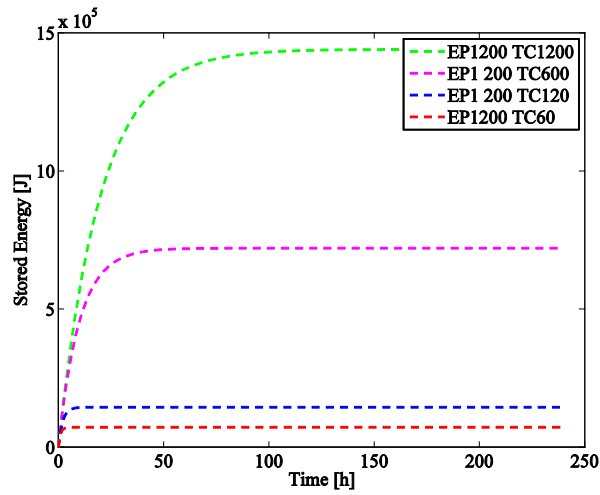
(c) EP*1200*

Figure 5. 22 Comparison of stored energy within different electrical appliances

Accordingly, we calculated the quantities of the accumulated energy use of the heater ($E_{2,heater}$) and the accumulated energy use of the selected electrical appliances ($E_{2,appliance}$). These are illustrated in Figure 5. 23.

The accumulated energy of the electrical heater is reduced when a higher power is supplied to an electrical appliance (substitution). The heating energy used by the heater with respect to the use of different electrical appliances which consume 200, 600, 1200 W is about 525, 145, 45 % of the energy used by electrical appliances.

However, it is interesting to note that the quantities of the accumulated heating energy are almost the same with about 2 % of the difference among them when the power consumption of the electrical appliance is by 600 W. Therefore, the thermal comfort of the living room can be maintained despite a reduction of the heat flux. The heat flux induced by 2000 W of the electrical power supplied to the heater easily overpasses the need of heat for maintaining the reference temperature of the room.


	EP200 TC60	EP200 TC120	EP200 TC600	EP200 TC1200	EP600 TC60	EP600 TC120	EP600 TC600	EP600 TC1200	EP1200 TC60	EP1200 TC120	EP1200 TC600	EP1200 TC1200
■ E2,heater [GJ]	2.412	2.414	2.42	2.426	1.703	1.705	1.713	1.723	1.038	1.039	1.041	1.036
■ E2,appliance [GJ]	0.46	0.46	0.46	0.46	1.185	1.185	1.185	1.185	2.274	2.274	2.274	2.274
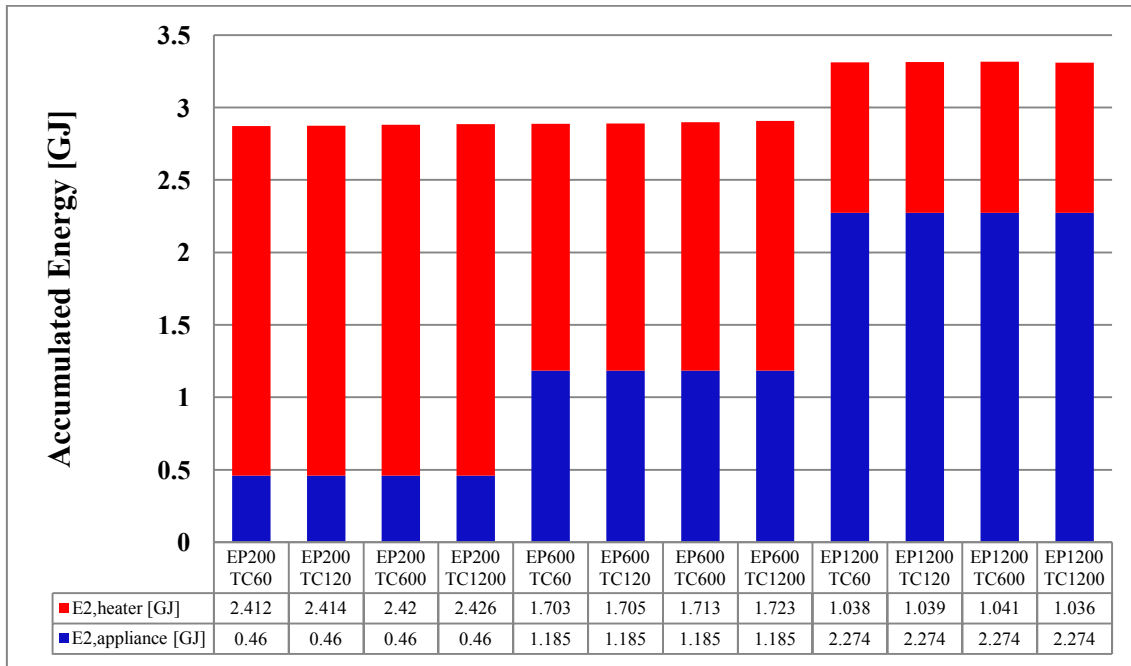
Figure 5. 23 Accumulated energy use of a heater and electrical appliances

To analyze the impact of the time constant of the appliances, we compared the accumulated energy used by the heater in another way. Figure 5. 24 shows the accumulated energy used by the heater when a different electrical appliance is placed in the living room. Except in the case of EP*1200*TC*1200*, a smaller time constant makes the consumed energy use of the heater decrease. The appliance which has the shortest time constant can compensate for the lack of space heating energy quasi instantaneously.

However, as the time constant is becoming larger, more time is needed to convert the electrical power to heat. Therefore, the heating energy demand cannot be sufficiently compensated by the electrical appliance in a given amount of time. Moreover, when the converted heat is slowly supplied to the living room because of the large time constant, it may

cause unwanted overheating problem within the living room as in the 1200W case. However, the slowly supplied heat can also compensate for the heating energy use of the heater when the heat lasts to the next usage period of the heater. As the supplied power and the time constant are larger, the heat lasts longer and slower. The case of the appliance EP*1200*TC*1200* is a good example of this trend. In this case, the heating energy used by the heater is less than any other cases for which smaller time constant is applied.

(a) EP*200*   (b) EP*600*   (c) EP*1200*
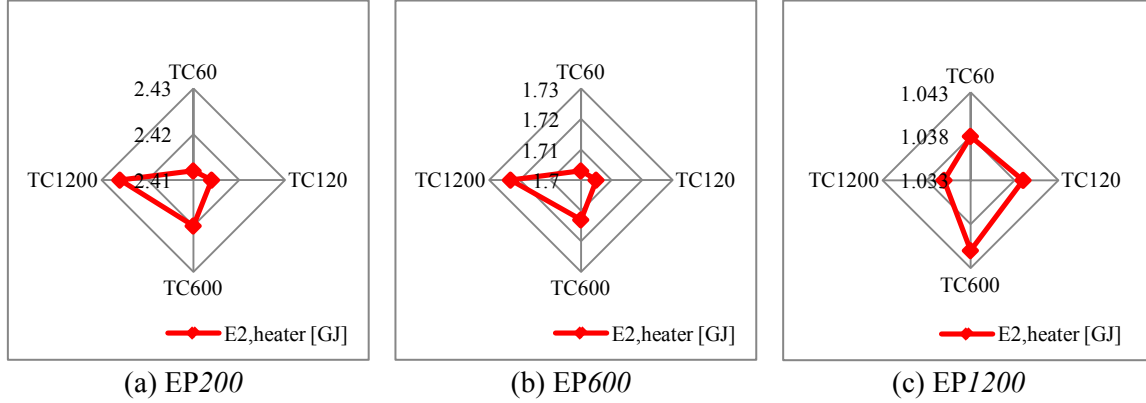
Figure 5. 24 Accumulated energy of the heater for a winter period

5.4.3   Comparison of Case 1 and Case 2

As comparing the results of the simulations Case 1 (without electrical appliances) and Case 2 (with electrical appliances), we found that the heating energy use of the heater in Case 1 ($E_{1,heater}$) is more important than the heating energy use of the heater in Case 2 ($E_{2,heater}$). It shows that the usage of electrical appliances influences the thermal condition of the building and that the heat dissipated by electrical appliances can compensate for the need of space heating energy. In addition, it is interesting that $E_{2,total}$ (the sum of $E_{2,appliance}$ and $E_{2,heater}$) is even less than $E_{1,heater}$ when the used electrical appliance consumes 200 or 600 W. It shows that even a smaller heat flux of electrical appliances is useful to maintain the reference temperature within the building. However, when the used electrical appliance consumes 1200 W, $E_{2,total}$ is bigger than $E_{1,heater}$. In this case, the heat gain of the appliance leads overheating of the living room.

Figure 5. 25 shows examples of the comparison of the energy used in Case 1 and Case 2. Figure 5. 25 (a) shows the case where $E_{1,heater}$ is superior to the sum of $E_{2,heater}$ and $E_{2,appliance}$ ($E_{2,total}$). Figure 5. 25(b) shows the case where $E_{1,heater}$ is inferior to $E_{2,total}$. The difference between $E_{2,total}$ and $E_{1,heater}$ represents the heating energy waste or overheating problem of the living room.

Figure 5. 26 shows examples of the temperature profiles corresponding to Figure 5. 25. In Figure 5. 26 (b), we can observe the overheating problem within the living room due to the additional heat flux of the electrical appliance which consumes 1200 W of electrical power.
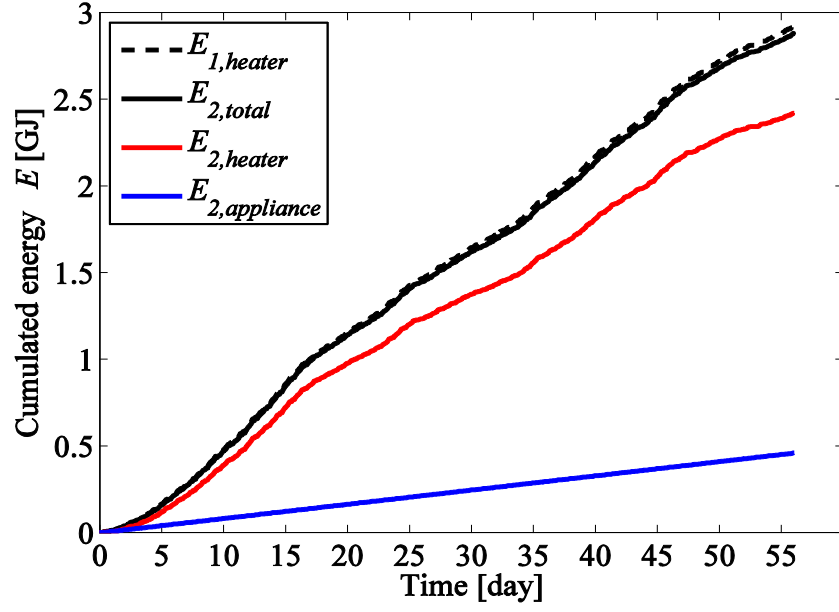
(a) $E_{1,heater} > E_{2,total}$ (EP200TC1200)
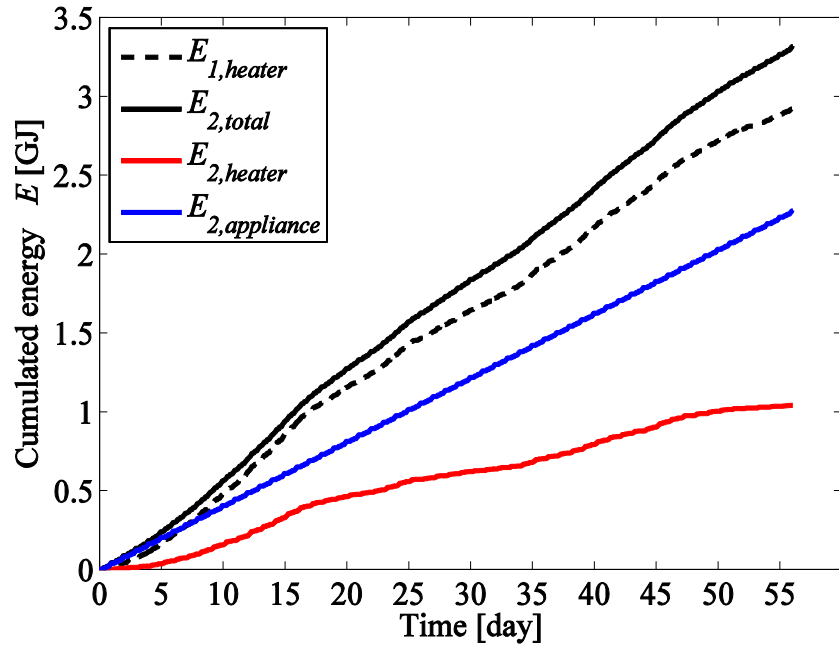
(b) $E_{1,heater} < E_{2,total}$ (EP1200TC1200)

Figure 5. 25 Accumulated energy use of a heater and electrical appliances in the living room
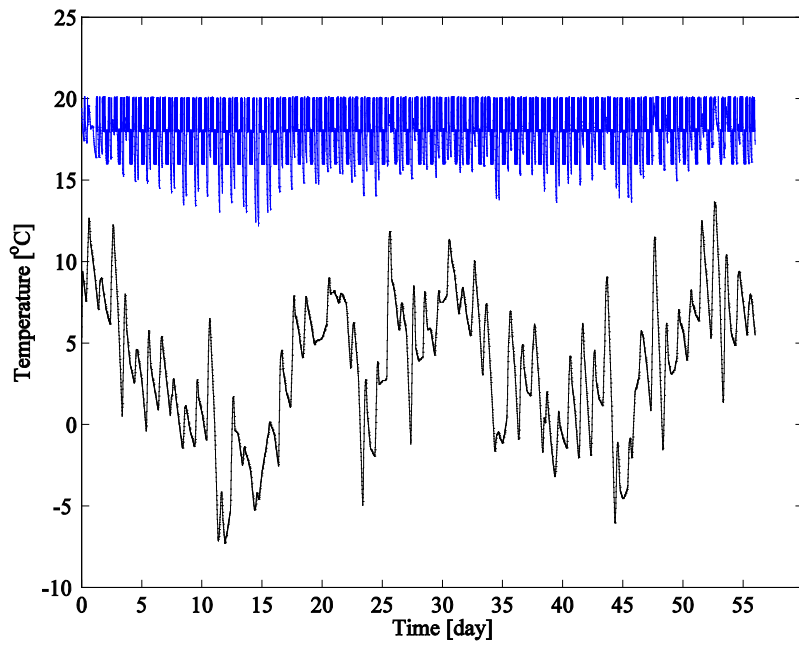
(a) EP*200*TC*1200*
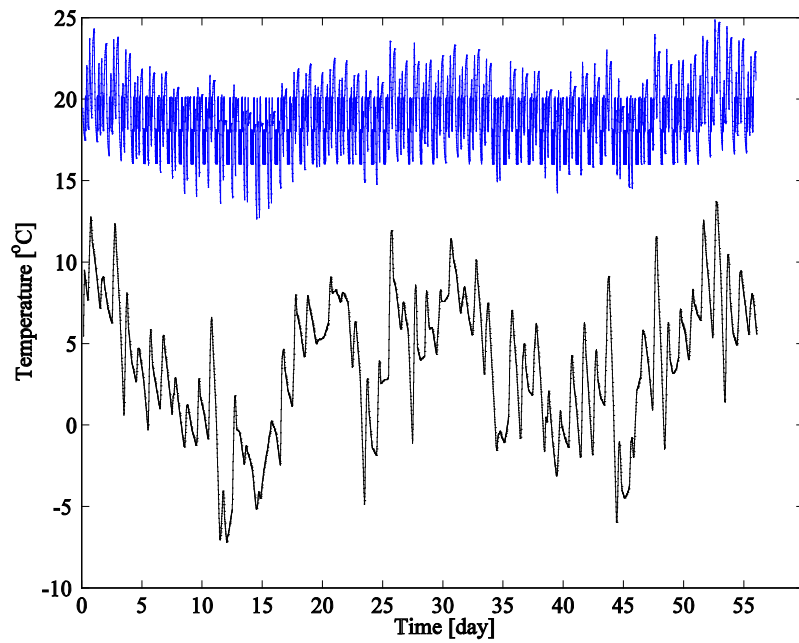
(b) EP*1200*TC*1200*

Figure 5. 26 Examples of the temperature profiles corresponding to Figure 5. 25

We studied above the thermal effect of electrical appliances within a building during a winter period, from the energetic aspect. The next section presents the thermal influence of electrical appliances within a building during a summer period.

5.5 THERMAL COMFORT DURING A SUMMER PERIOD

In the summer period, the heat gain of electrical appliances is considered as a disturbance that may impact the thermal comfort of the occupants of the building. In order to study the thermal influence of electrical appliances during a summer period, we conducted on the simulations from July to August (8 weeks).

Here are the chosen assumptions,

- ✓ A summer period from July to August (8 weeks) is selected for this study.
- ✓ Blinds are operating during daytime (10:00-18:00).
- ✓ There is no heater any more, but the ventilation equipment is activated.

Under these conditions, we achieved two kinds of the simulations:

- ■ Case 1: Simulations without electrical appliances (reference case)
- ■ Case 2: Simulations including the usage of electrical appliances

The only difference between two cases is whether there is the usage of electrical appliances or not. Case 1 is a comparative case of Case 2. The following lists the conditions and appliances' use:

- ✓ Two groups of electrical appliances are chosen depending on the time constant and power consumption: first group (EP*200*TC*600*, EP*600*TC*600*, and EP*1200*TC*600*) second group (EP*600*TC*60*, EP*600*TC*120*, EP*600*TC*600*, and EP*600*TC*1200*).
- ✓ The profile of occupancy is the same as the previous study carried out during a winter period.
- ✓ The usage profiles of the selected electrical appliances are the same as the previous study carried out during a winter period.

In order to introduce the thermal discomfort, we calculated a Thermal Discomfort Rate (**TDR**) [%]:

$$TDR[\%] = \frac{D_{discomfort}}{D_{appliance}} \times 100 \tag{5.9}$$

where $D_{discomfort}$ [sec] is the duration while the indoor temperature exceeds 26 °C, and $D_{appliance}$ [sec] is the duration while the electrical appliances are used.

5.5.1 Analysis of the Simulation Case 1

We first conducted on the simulation without consideration of the use of electrical appliances. Thermal conditions of the building are influenced by solar radiations, ventilation, and weather. Indoor temperature does not oscillate largely comparing to the exterior

temperature of the building, because of the building thermal inertia. Moreover, the installed blinds alleviate the influence of the solar radiation during a daytime. Figure 5. 27 shows the obtained temperature profiles.
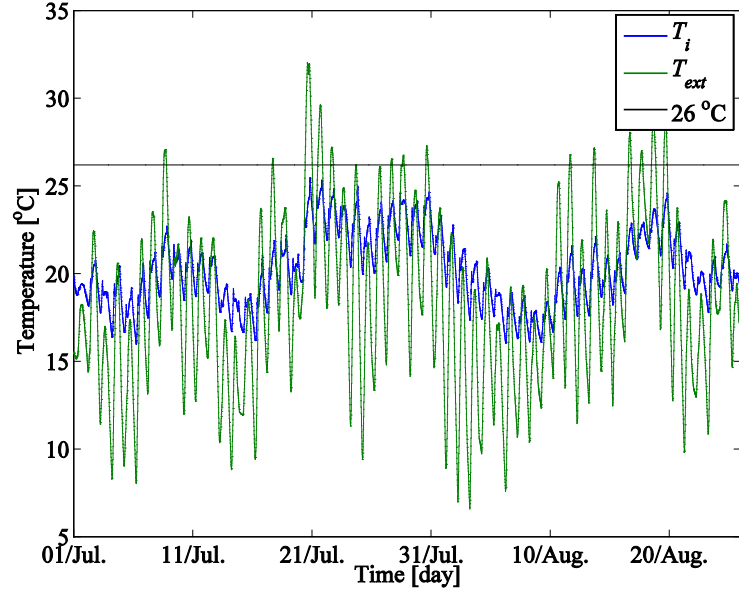
(a) Whole period
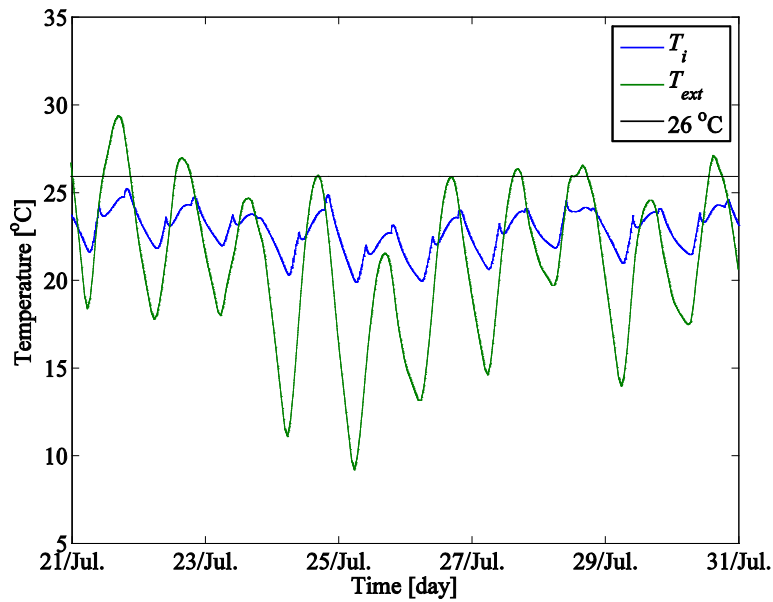
(b) Ten days

Figure 5. 27 Temperature during a summer period (Case 1)

The indoor temperature of the living room oscillates versus time between 15.9 and 25.4 °C while the exterior temperature oscillates versus time between 6.5 and 31.8 °C during the considered period. Even though the exterior temperature overpasses from time to time 26 °C, that is considered as the boundary temperature for thermal comfort, the indoor temperature never exceeds the boundary temperature. It means that the thermal comfort in the living room is preserved.

5.5.2 Analysis of the Simulation Case 2

We then conducted on simulations which integrate the use of electrical appliances. As mentioned above, we considered two groups of electrical appliances:

The first group includes EP*200*TC*600*, EP*600*TC*600*, and EP*1200*TC*600*. The appliances in this group have a similar time constant equal to 600 sec and different levels of power consumption. The simulation results of the indoor temperature of the living room influenced by the heat gain of these appliances are illustrated in Figure 5. 28. As expected, we can observe that the indoor temperature increases according to the use of the electrical appliances. The more electrical power is consumed, the more indoor temperature increases. In Case 1, the indoor temperature never exceeded the limit of 26 °C. However, in Case 2, this limit is regularly overpassed.

The obtained values of **TDR** corresponding to EP*200*TC*600*, EP*600*TC*600*, EP*1200*TC*600* are respectively 12 %, 76 %, 186 %. It is obvious that a higher power leads to more thermal discomfort for the occupants.
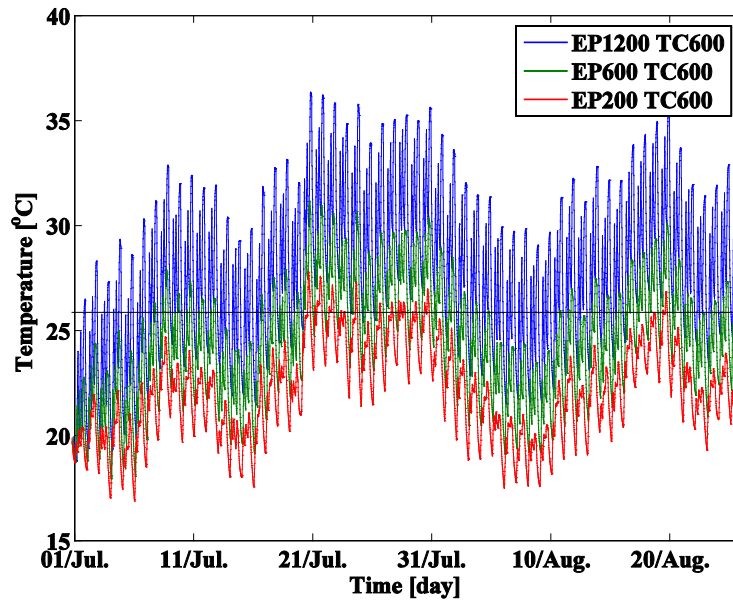
(a) Whole period
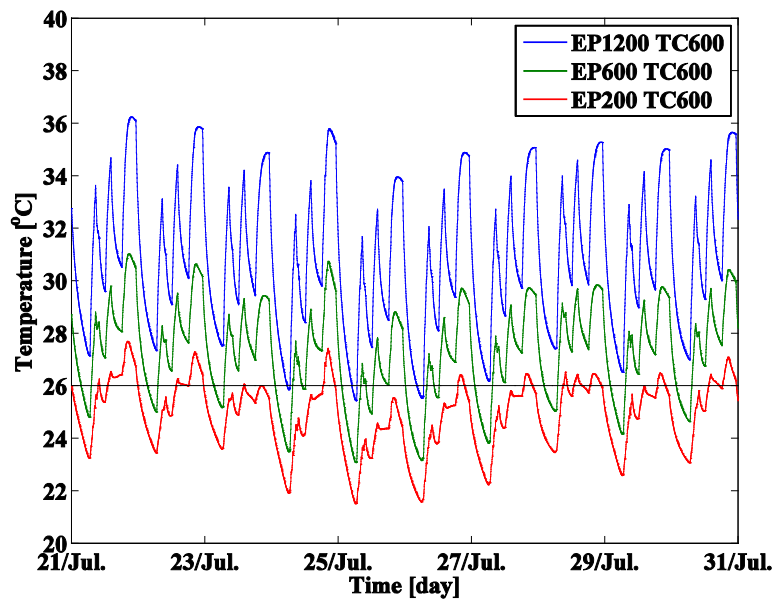
(b) Ten days

Figure 5. 28 Temperature during a summer period (Case 2, TC*600*)

The second set of simulations concerns the following cases: EP*600*TC*60*, EP*600*TC*120*, EP*600*TC*600*, and EP*600*TC*1200*. The appliances in this group have the same level of power consumption of 600 W, but different values of time constant. The simulation results of the indoor temperature within the living room is shown in Figure 5. 29.
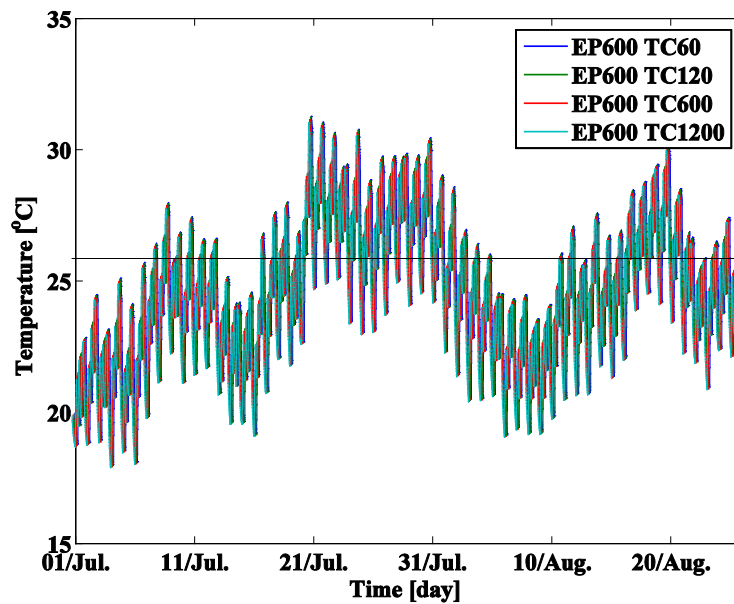
(a) Whole period
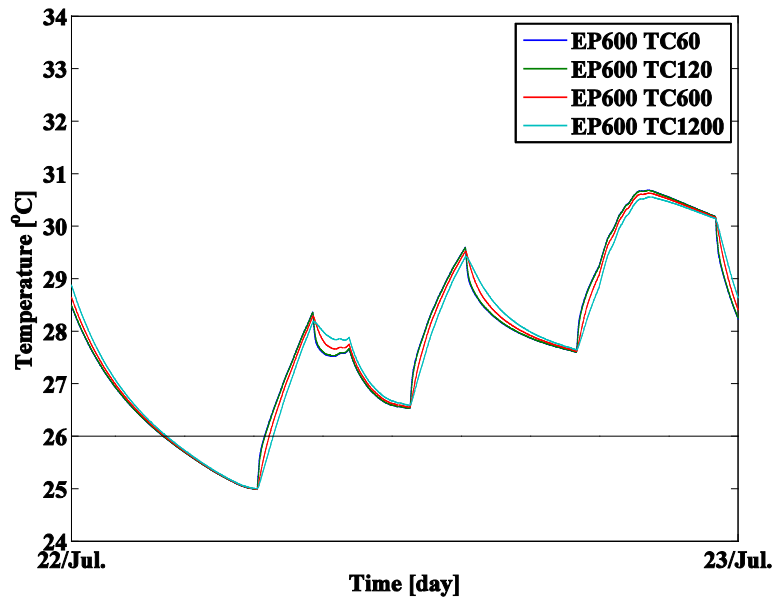
(b) One day

Figure 5. 29 Temperature during a summer period (Case 2, EP*600*)

The simulated indoor temperature of each case has the similar behaviors. Thus, the impact of the thermal time constant of the appliances on the comfort of the inhabitants is not very important.

We also calculated the discomfort rate, *TDR* in order to evaluate the thermal discomfort due to the usage of electrical appliances which have different values of the time constant. The obtained values of *TDR* for the following cases (EP*600*TC*60*, EP*600*TC*120*, EP*600*TC*600*, and EP*600*TC*1200*) are 76.3 %, 76.2 %, 75.8 %, and 75.7 %, respectively.

5.6 CONCLUSION

The objective of this chapter was to present thermal influence of electrical appliances within a low energy building. The previously proposed thermal model of electrical appliances was integrated into a residential building model which was developed and validated by the French Technical Research Center. The assessment was achieved by using SIMBAD simulation tool.

The conventional method to calculate the internal heat gain of electrical appliances in a building simulation considers only the usage profiles of electrical appliances and their supplied power levels. However, in this study, we additionally took account of the thermal characteristics of the electrical appliances. It aims to obtain more accurate results of the simulation, especially within a low energy building which is well insulated and where the thermal influence of electrical appliances can not be ignored.

We first described a residential building model. Then the basic information of the thermal behaviors and characteristics of the building was given according to the different operations of

157

HVAC systems. After that, several types of electrical appliances were integrated into the building model, and the thermal behavior was observed during a winter period. The energy demand change of the considered building was also extracted and analyzed. In addition, thermal discomfort due to the use of electrical appliances during a summer period was also presented.

Consequently, this chapter has provided quantitative results on the thermal effect of electrical appliances within a building. Moreover, it has led to observe the thermal dynamics of both the electrical appliances and the building. Based on the given results, we will further study the method to manage the heating energy demand of a building according to the use of electrical appliances.

GENERAL CONCLUSION

This dissertation brought out the interest of the internal heat gains obtained by solar energy, human metabolism, and heat dissipation of electrical appliances within a low energy building. Since the low energy building is thermally well-insulated, the quantity of unwanted heat losses through its structure and its envelopes is limited. As a consequence, the thermal influence of the internal heat gains impacts significantly the thermal behavior of the low energy building, especially in summer or winter period.

Considering a standard building, the heat flux dissipated by electrical appliances is too small to compensate the heat losses of the building. Moreover, thermal dynamics of the appliances are too fast comparing those of the building itself. Because of the negligible impact of the appliances within a standard building, it has been therefore statically modeled in building energy simulation tools (by the supplied electrical power and the usage profile of electrical appliances). Comparing to the quantity of investigations on the solar irradiation modeling, on both deterministic and stochastic models of occupant's behavior, on lighting/equipment usages, and on metabolic heat, only few works are dedicated to the dynamic modeling of heat gain of electrical appliances.

However, in a low energy building for which insulation is reinforced, the heat gains of electrical appliances may more impact the thermal behavior of the building. Despite of increasing more energy-efficient appliances, their power densities have been increasing too, as well as the use of the various appliances along with the increase of the quality of human life. In addition, intra-hour simulations are required for more accurate building thermal analysis and control strategy of the building equipment in order to achieve a higher energy efficiency of the building system and a higher thermal comfort of occupants. Accordingly, this dissertation deeply focused on the thermal dynamic modeling of electrical appliances, which becomes an emerging issue for the above given reasons and for obtaining reliable results of thermal analysis of low energy buildings.

The issues and their scientific solutions linked to this thesis work were brought out by reviewing the state-of-the-art literature. In order to ensure and to quantify the thermal influence

of electrical appliances within a low energy building, it needs to thermally model a well-insulated building and the corresponding electrical appliances. Therefore, the possible methodologies for thermal modeling of building systems were firstly presented. From several introduced thermal modeling approaches, we selected the thermal network modeling approach because of its simplicity and its accuracy to combine both the heat source and the structure of the building. Secondly, the parameter identification methods suitable to the models of building systems were studied. A number of examples were introduced. Thirdly, several references of comparative studies on the simulation tools were given and the uncertain factors of simulation tools were discussed. It permitted to select a building energy simulation tool, SIMBAD.

Then the thermal model representing a well-insulated room was established, by using the thermal network method. The building was modeled for the aim of thermal characterization of electrical appliances. Based on the energy balance equation and the thermal-electrical analogy, a first order, two second order, and a third order lumped *RC* parameter circuits were proposed.

Thereafter, the thermal parameters of the model components were estimated from experimental results and parameter identification methods. Global thermal parameters of the first order model were identified by solving the analytical solution derived by the energy balance equation. However, the limitation of the analytical solution required a numerical study. Therefore, the parameters of this model as well as the other models were also estimated by using the interior-reflective Newton method. Thereafter, the proposed models and their estimated parameters were implemented into Matlab/Simulink. The thermal behaviors of the models were simulated and compared to the measured data. The evaluation of the models was also achieved.

As a result, the second order model I and the second order model II were chosen as the thermal models for the well-insulated room. The second order model II was considered as the most accurate model. However, the second order model I was also considered as very accurate and adapted to describe the thermal influence of the electrical appliances which induce a strong convection phenomenon within the room.

Along with this, the thermal model of electrical appliances were modeled and thermally characterized within the developed thermal models of the well-insulated room. In order to present a generic model of all kinds of electrical appliances, electrical appliances were classified into four categories according to thermal and electrical points of view: Closed-Heating System (*CHS*), Closed-Working System (*CWS*), Open-Heating System (*OHS*) and Open-Working System (*OWS*).

Based on this classification, a generic thermal model of electrical appliances was deduced from the energy balance equation and was also represented by its equivalent lumped RC parameters. In order to estimate the parameters of the obtained generic model, linear parametric models, namely, *ARX* and *ARMAX* models were introduced. Thereafter, the relations between the parametric models and the physical principle-based models were described and the parameters of the proposed model of electrical appliances were obtained.

Then, the cases of a monitor, a computer, a portable heater, a refrigerator and a microwave, which are commonly used within dwellings, were studied in order to illustrate the proposed approach. The matching between the measurements on the actual systems and the results of simulations based on the identified generic model of the appliance validate the proposed approach.

As a result, the temperature of each appliance T_{ap} simulated by ARX and $ARMAX$ models was globally well fitted to the measured one. Moreover, the results showed that the impact factors on thermal modeling of electrical appliances are the time constant, and the amplitude of P_{elec} of the electrical appliances.

As comparing thermal influence of the proposed dynamic thermal model of electrical appliances with the standard static model, it yielded that the thermal behavior of the building was better described when the injected heat flux of the appliance was modeled by a dynamic thermal model.

Regarding the methods for estimating the parameters, we did not find significant differences between the ARX and the $ARMAX$ models. Both models globally well estimated the parameters. However, $ARMAX$ approach was considered as more relevant when internal dynamics were neglected like in the case of inner temperature regulation (refrigerator).

After modeling the thermal model of electrical appliances, the model was integrated into a building simulation tool in order to observe its thermal influence within a low energy building. To this purpose, an individual residential building model which was developed and validated on a real building by the French Technical Research Center for Building was chosen and was physically described. Then, basic information of thermal behavior of the building was given according to different operations of HVAC systems. After that, several differently characterized electrical appliances were integrated into the building model, and thermal behavior and heating energy uses of the building were observed during a winter period. According to characteristics of electrical appliances, the energy demand of the considered building was changed. The differences were extracted and analyzed. In sequence, thermal discomfort owing to the use of electrical appliances during a summer period was also studied.

Consequently, this coupled model especially provided quantitative results of the thermal effect of electrical appliances within a low energy building. Moreover, it led to observe thermal dynamics of both the electrical appliances and the building and persuaded the necessity of thermal dynamic modeling of electrical appliances for energy management of low energy buildings and thermal comfort of inhabitants.

The results of this thesis work are listed as above. Nevertheless, several questions are still open:

■ Comparison of the building model: In order to validate the models of a well-insulated building, we have only used Matlab/Simulink®. However, it requires comparing the results of the modeling and the obtained values of parameters by using other building simulation tools, such as TRNSYS and EnergyPlus. Moreover, it further needs to apply different electrical power

signals with different frequency to the room model in order to more exactly evaluate the different order models.

■ Accuracy of the model of electrical appliance: This study simply took into account the global parameters of the thermal model of electrical appliances. According to the supplied electrical power, the physical properties and structures of the appliance, the properties of the coupled building model, dominant heat transfer phenomenon of an electrical appliance can be modified. It may lead the different value of thermal constant of electrical appliance. Therefore, the proposed experimental protocol and the identification procedure may not be available for all range of electrical appliances.

■ Validation for various types of electrical appliances: The considered appliances within the present study are without phase change or within a situation where the latent heat part could be neglected. Moreover, the case studies to validate the proposed thermal model of electrical appliances and identification method only concerned the appliances which are classified as a *CHS*. Therefore, a further study should include the appliances of which latent heat is important and the other types of appliances classified as a *CWS*, *OHS*, and/or *OWS*.

■ Usage profiles of electrical appliances: The deterministic usage profiles of electrical appliances were used in this study. Since the thermal effect of the appliances depends on their operating time as well as their electrical power consumption and their time constant, more relevant usage profiles of electrical appliances related to the occupant's behavior are required. Therefore, the stochastic models of the occupant's behavior and the usage profiles of electrical appliances have to be further developed and applied to the building energy simulations.

■ Definition of thermal comfort: This study limits the temperature for thermal comfort of occupants in summer below 26 °C. However, thermal comfort is not measurable and depends on each individual. It needs to define thermal comfort more flexible and evaluate it within different regions and conditions. Moreover, a computational fluid dynamics method can be used for obtaining temperature profile within a building according to the usage of electrical appliances and the behavior of occupants.

As addressing the listed issues, it is also required to apply the presented work to further researches. As stated on the context of this thesis, thermal modeling of electrical appliances helps to simulate energy performance of low energy building with higher accuracy. According to thermal characteristics and load profiles of an electrical appliance, a heat flux dissipation profile can be obtained and is used for predicting thermal behavior of buildings and their heating demand. Moreover, as developing smart metering technology, the operating state of a specific electrical appliance could be informed in real-time. Once a load profile of any electrical appliance is detected and predicted, the thermal influence of the electrical appliance can be estimated. From this information, the building heating/cooling system can be controlled with the aims of a lower energy consumption and a higher thermal comfort of the building. In addition, if we know the heat flux of electrical appliances, the usage profiles of each electrical appliance can then be optimized in order to get better performances of the building.

APPENDIX A

THERMOCOUPLES

A.1   Principle of Thermocouples

When two dissimilar metals are joined, current flows from one junction at higher temperature to another junction at lower temperature. The Electromotive Force (EMF) driving the current calls a thermoelectric EMF and the phenomenon is known as thermoelectric effect or Seeback effect.

A thermocouple is a thermoelectric element which measures temperature using Seeback effect. It consists of two dissimilar metals which are joined together at one end. The end is called the measurement junction or hot end. The other end is connected to a voltmeter and known as the reference junction or cold end. A temperature difference between the measurement ($T_{measurement}$) and reference junction ($T_{reference}$), an EMF is produced which is approximately proportional to the junctions temperature differential. The EMF generated by the temperature differential of joined dissimilar metals a and b is expressed by:

$$EMF \propto (T_{measurement} - T_{reference}) = S_{ab}(T_{measurement} - T_{reference}) \qquad (A.1)$$

where S_{ab} is the relative Seeback coefficient of two dissimilar metals a and b.

A.2   Features of Thermocouples

Thermocouples have the following features in comparison with other thermometers:

1. They can respond quickly and the measurement is stable by direct contact with the measuring object.
2. They measure over a wide range of temperature from -270 to 2,300 °C.
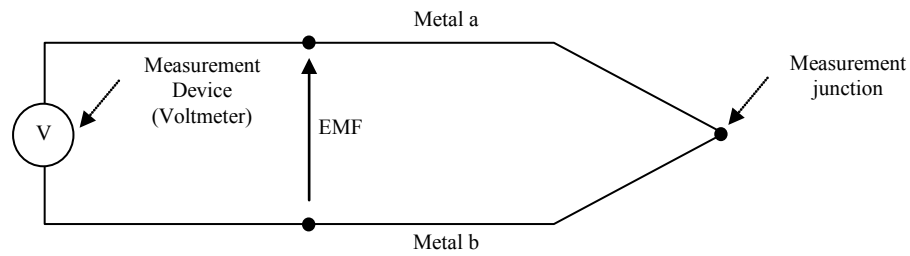
163

Figure A. 1 Principle test arrangement of the thermocouple

3. They can measure temperature of specific spot or small space.
4. Since temperature is detected by means of EMF generated, measurement, adjustment, amplification, control, conversion and other data processing are easy.
5. They are less expensive and have better interchangeability than other temperature sensors.
6. They are manufactured in a wide range of probes and packages.
7. The common types comply with international standards.

A.3   Different types of thermocouples

There are hundreds of types of thermocouples. Most of them are manufactured from metals, but some are made of semiconductors and graphite/ceramic materials. Thermocouples are normally manufactured in accordance with the international standards. The characteristics of thermocouples which are defined by International Electrotechnical Commission (IEC)-Pub584-2 are listed as below:

A.4   Accuracy of Thermocouples

Thermocouples can be used to measure absolute temperatures to 0.5 °C accuracy. With laboratory calibration, this can be improved to 0.2 °C. The maximum permitted errors for various common thermocouples comply with IEC 584-2. The data available for the specific temperature range of 0~200 °C is shown as below:

A.5   Used Thermocouples

The selected thermocouple in this thesis work is a K-type thermocouple. The K-type thermocouple consists of nickel alloys called Chromel (90 % Nickel and 10 % Chromium) and Alumel (95 % Nickel, 2 % Manganese, 2 % Aluminium and 1 % Silicon). The sensitivity of the K-type thermocouple is approximately 41μV/°C.

Temperatures of boiled water were measured by twenty K-type thermocouples. While the water had been cooling, the measurement had been also kept going on. The measurement was conducted during three days and the data were acquired each 30 sec. It is to observe the temperature variations of each thermocouple in large range of the temperature variations. The results and the average value are shown in Figure A. 2. The zoom-up figures of Figure A. 2 are

illustrated in Figure A. 3 - Figure A. 6. It is observed that the boiled water is cooling during about 10000 sec. Then the temperatures are stable at near of 21.5 °C.

Table A. 1 Characteristics of different types of thermocouples

Type	Material		Range	Notes
	Positive part	Negative part		
K	Chromel [90 % Nickel/ 10 % Chromium]	Alumel [95 % Nickel/ 2 % Mn/ 2 % Al]	-200 to 1100°C	Most common type, general purpose
J	99.5 % Iron	Constantan [55 % Copper/ 4 5% Nickel]	-20 to 200 °C	Iron rusts at low temperature, oxidization at high temperature
T	100 % Copper	Constantan [55 % Copper/ 45 % Nickel]	-250 to 350 °C	Low temperature, cryogenic uses
E	Chromel [90 % Nickel/ 10 % Chromium]	Constantan [55 % Copper/ 45 % Nickel]	0 to 800 °C	High EMF, suitable for vacuum
R	87 % Platinum/ 13 % Rhodium	100 % Platinum	0 to 1500 °C	Stable, high temperature, low oxidation, easily contaminated
S	90 % Platinum/ 10 % Rhodium	100 % Platinum	0 to 1550 °C	Similar to R type
B	70 % Platinum/ 30 % Rhodium	94 % Platinum/ 6 % Rhodium	50 to 1650 °C	Similar to R type, Can use Coppper-Copper compensating cable
N	Nicrosil [84 % Nickel/ 14.2 % Chromium/ 1.45 % Silicon]	Nisil [95 % Nickel/ 4.4 % Silicon/ 0.15 % Magnesium]	650 to 1260 °C	

Table A. 2 Thermocouple accuracy by type and temperature

Temperature	K	J	T	E	R	S	B	N
0 °C	1.5	1.5	0.5	1.7	1.0	1.0	-	1.5
200 °C	1.5	1.5	0.8	1.7	1.0	1.0	-	1.5

*unit: [°C]
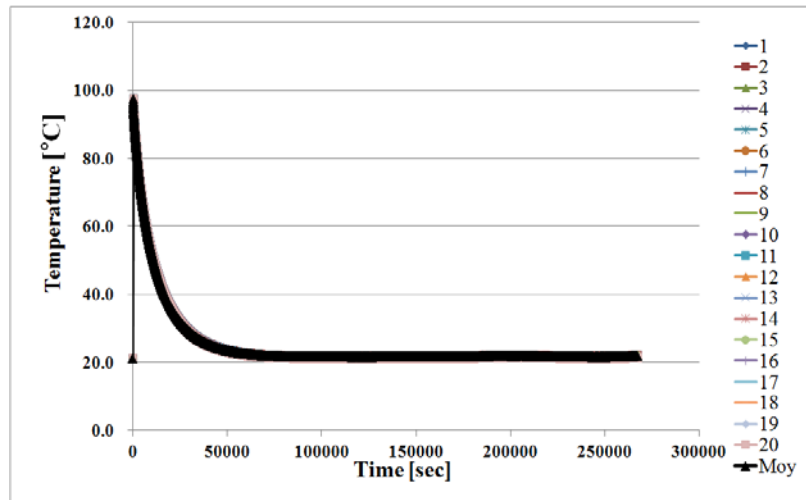
Figure A. 2 Temperature of boiled water measured by twenty K-type thermocouples
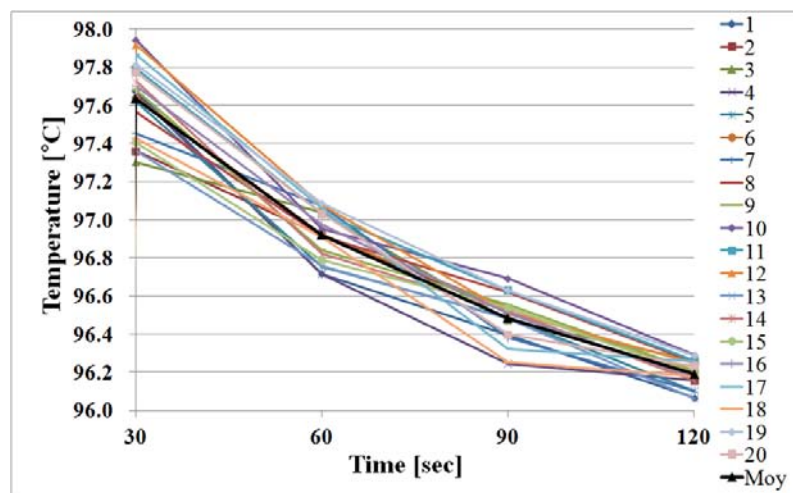
Figure A. 3 Temperature of boiled water measured by twenty K-type thermocouples
(Time range 1)
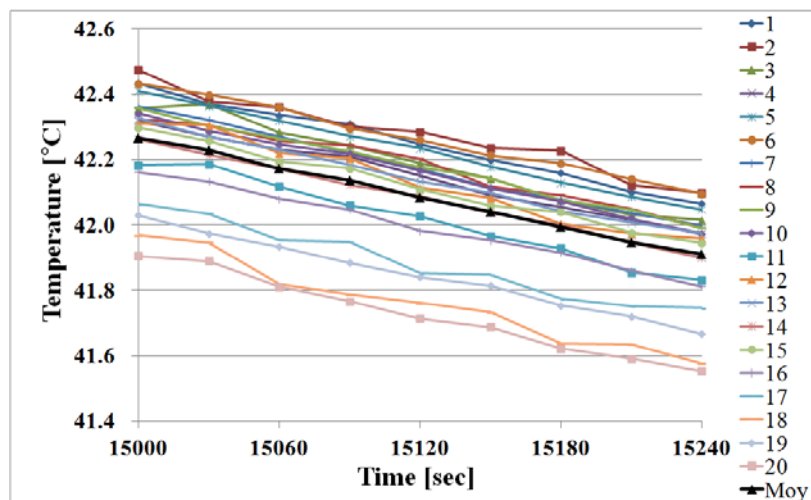
Figure A. 4 Temperature of boiled water measured by twenty K-type thermocouples
(Time range 2)
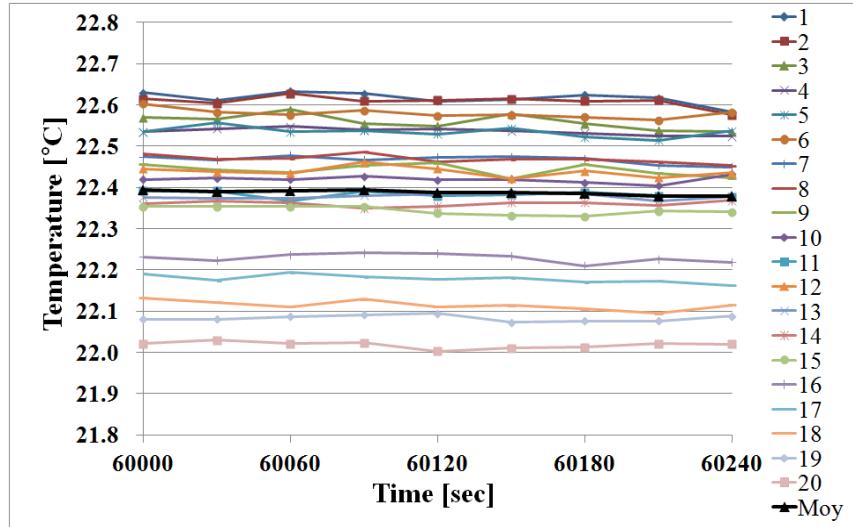
Figure A. 5 Temperature of boiled water measured by twenty K-type thermocouples (Time range 3)
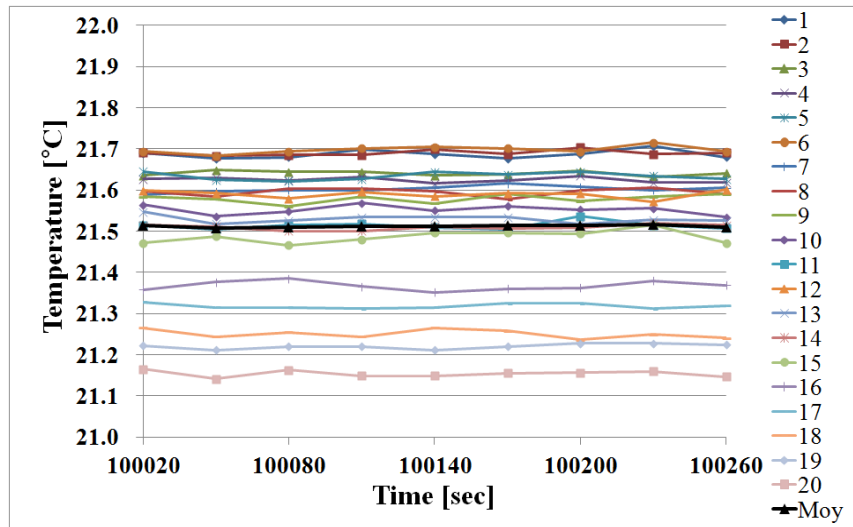
Figure A. 6 Temperature of boiled water measured by twenty K-type thermocouples (Time range 4)

Figure A. 7 depicts the standard deviations versus time axis. The standard deviations among the thermocouples at each time during the whole measurement period are less than 0.3 °C. At the permanent state from 100000 sec, the standard deviations are less than 0.04 °C.

167
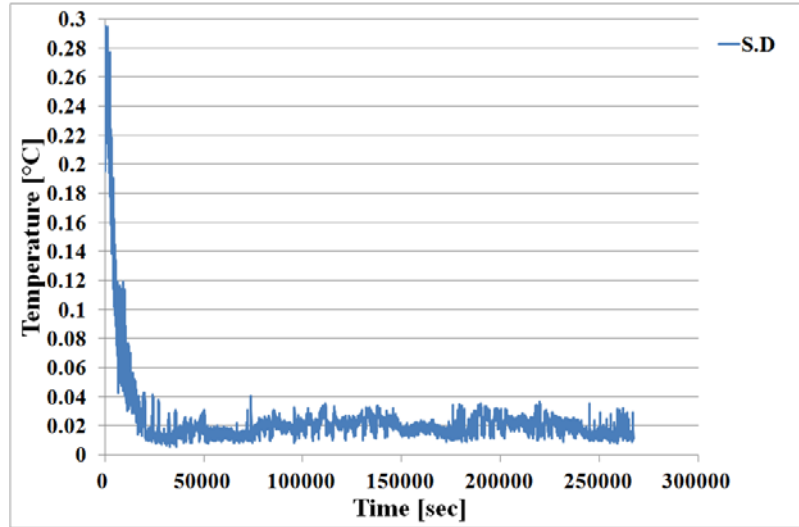
Figure A. 7 Standard deviation of twenty K-type thermocouples

Figure A. 8 depicts the zoom up figure of the previous figure in the range of the time while the measured temperatures are from 21.5 to 60 °C (The maximum measured temperature of this thesis work on the heater is about 60 °C). As the measured temperature is bigger, the standard deviation is bigger. Smaller than 54.5 °C (at t=9000 sec), the standard deviations are less than 0.05 °C. Moreover, smaller than 40.0 °C (at t=16590 sec), the standard deviations are less than 0.045 °C.
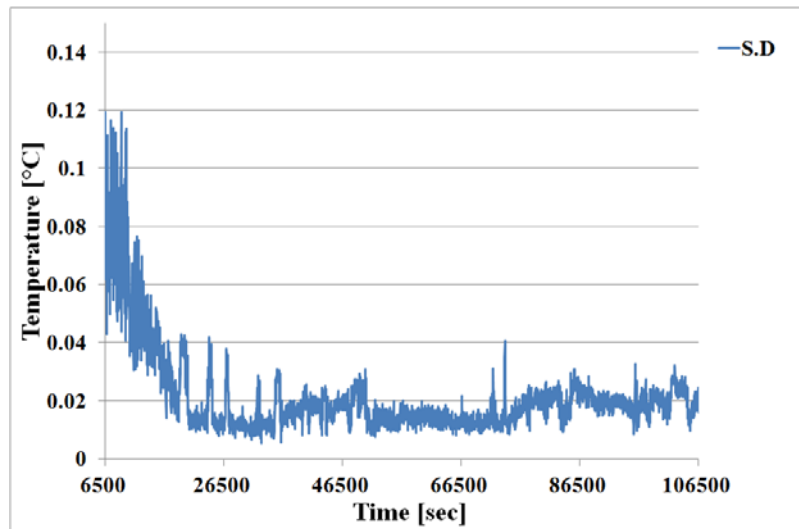
Figure A. 8 Standard deviation of twenty K-type thermocouples (Zoom-up)

The uncertainty of the temperature measurement is also caused by other factors such as the accuracy of voltage measurement of the data logger, composition of the thermocouple alloys and local changes of the alloys at the junction.

APPENDIX B

INDOOR TEMPERATURE

B.1 Definition

In this thesis, we define that the indoor temperature is the temperature of surroundings inside a building (or a room). It calls the ambient temperature or the interior temperature (T_i, T_{in}). Its antonyms are the outdoor temperature and the exterior temperature (T_{ext}, T_e) which mean the temperature outside the building (see Figure B. 1).
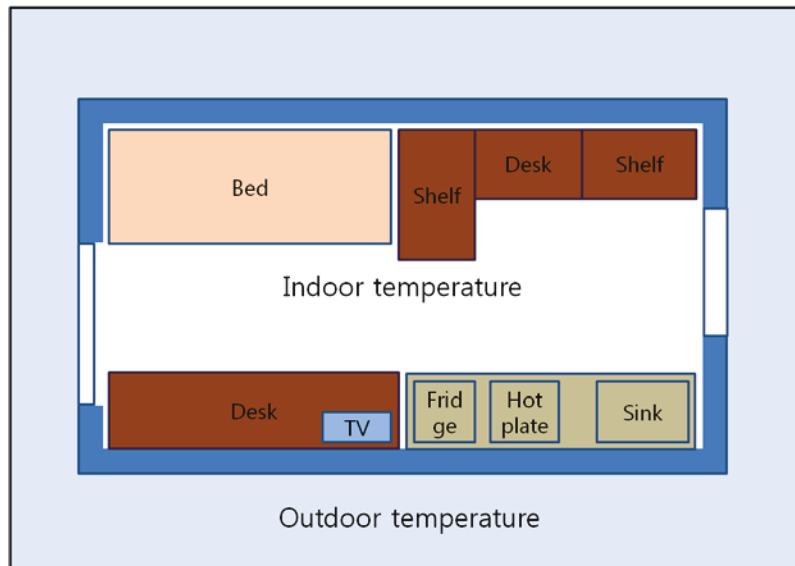
Figure B. 1 Indoor temperature and Outdoor temperature

B.2   Indoor temperature of well-mixed model

Indoor temperature is different at each part of a building caused by air flow, heat transfer, occupant's movement, placement of furniture, materials, etc. According to Riederer(2002)[23], the temperature models of a building zone exist with three different levels of complexity: well-mixed model, zonal model, and computational fluid dynamics (CFD) model.

The indoor temperature of the well-mixed model is represented by one air node. It means the temperature is homogeneous throughout the whole air volume in the zone. This model is used to study the energy use in buildings and control problems[24]. The zonal model is based on solving the pressure field to predict airflow and temperatures in large indoor spaces[25]. In the zonal method, the room is subdivided into a number of volumes or cells in which temperature and density are assumed to be homogeneous, while pressure varies hydrostatically. Mass and thermal energy balances are applied to each cell, with air treated as an ideal gas. CFD model is used to solve the Reynolds Averaged Navier-Stockes equations with turbulence modeling using two equations for the transport of turbulent kinetic energy and its dissipation rate in order to predict airflow, temperature or pollutant concentration distributions in a building zone[26].

In this thesis work, we only focus on the variation of the indoor temperature. The details in air flow or pressure are not important. There is no additional turbulent energy by occupants. We need a simple model to describe whole indoor temperature. Therefore we assume that the tested quasi-adiabatic room is a well-mixed model. The indoor temperature of the whole volume of the room is assumed homogeneous. We take the average temperature of the room as the indoor temperature of the room. The well-mixed model is based on the energy balance equation. The temporal and spatial variations of the energy is expressed by

$$(\rho c_p)_i \frac{\partial T_i}{\partial t} = \lambda_i \cdot \nabla(\nabla T_i) \tag{B.1}$$

where ρ and c_p are the density [kg/m³] and the specific heat [J/kg·K] of the air in the room, λ_i is the thermal conductivity [W/K] of the room envelope, and T_i is the indoor temperature of the room [K].

Equation (B.1) is derived on the volume V [m³] as below:

[23] P. Riederer, D. Marchio, J.C. Visier, A. Husaunndee, R. Lahrech, "Room thermal modelling adapted to the test of HVAC control systems", Building and Environment, Vol.37(8–9), 2002, pp.777-790.

[24] P. Riederer, D. Marchio, J.C. Visier, "Influence of sensor position in building thermal control: criteria for zone models", Energy and Buildings, Volume 34(8), 2002, pp.785-798.

[25] E.Wurtz, J.M. Nataf, F.W. Winkelmann, "Two- and Three-Dimensional Natural and Mixed Convection Simulation Using Modular Zonal Models in Buildings", International Journal of Heat and Mass Transfer, Vol. 42, 1999, pp.923-940.

[26] L. Mora, A.J. Gadgil, E. Wurtz, C. Inard, "Comparing zonal and CFD model predictions of indoor airflows under mixed convection conditions to experimental data", Third European Conference on Energy Performance and Indoor Climate in Buildings, Lyon, France, 10.2002, pp.1-6.

$$\int_V (\rho c_p)_i \frac{\partial T_i}{\partial t} dV = \int_V \lambda_i \cdot \nabla(\nabla T_i) dV \qquad (B.2)$$

The sum of the temperature variations in a very small volume is the sum of the energy flux goes in/out through the small volume. Then the sum of the average temperature variations of the room is the sum of the energy flux goes in/out through the room as described below.

$$(\rho c_p V)_i \frac{\partial \overline{T_i}}{\partial t} = \int_S \lambda_i \cdot \nabla T_i \times dS \qquad (B.3)$$

$$(\rho c_p V)_i \frac{\partial \overline{T_i}}{\partial t} = \int_{S_{in}} \lambda_i \cdot \nabla T_i \times dS_{in} + \int_{S_{out}} \lambda_i \cdot \nabla T_i \times dS_{out} \qquad (B.4)$$

where $\overline{T_i}$ is the average temperature of the room [K], S is the surface [m^2]. The first one of the right term is the heat flux injected in the room. Here, it is the electric power of an electric appliance. The second one of the right tem is the heat loss through the room envelopes.

$$(\rho c_p V)_i \frac{\partial \overline{T_i}}{\partial t} = P_{elec}(t) + \int_{\Sigma_{out}} \lambda_i \cdot \nabla T_i \times dS_{out} \qquad (B.5)$$

APPENDIX C

ANALYTICAL SOLUTION OF INDOOR TEMPERATURE

Equations (3.17) - (3.18) are deduced as below:

$$C_{th}\frac{dT_i(t)}{dt} = \dot{Q}_{appliance}(t) - \frac{1}{R_{th}}(T_i(t) - T_e(t)) \tag{C.1}$$

The general solution of eq.(C.1) is expressed by

$$T_i(t) = A \cdot e^{-t/\tau_{th}} \tag{C.2}$$

where τ_{th} is the thermal time constant of the room which is the product of global thermal resistance and capacitance [sec].

The particular solution of eq.(C.1) is derived as follows if $\dot{Q}_{appliance}(t)$ and $T_e(t)$ are constant:

$$C_{th}(A'e^{-t/\tau_{th}} - \frac{A}{\tau}e^{-t/\tau_{th}}) + \frac{A}{R_{th}}e^{-t/\tau_{th}} = \dot{Q}_{appliance}(t) + \frac{1}{R_{th}}T_e(t) \tag{C.3}$$

$$(A'e^{-t/\tau_{th}} - \frac{A}{\tau}e^{-t/\tau_{th}}) + \frac{A}{\tau_{th}}e^{-t/\tau} = \frac{\dot{Q}_{appliance}(t)}{C_{th}} + \frac{1}{\tau_{th}}T_e(t) \tag{C.4}$$

$$A'e^{-t/\tau_{th}} = \frac{1}{\tau_{th}}(R_{th} \cdot \dot{Q}_{appliance}(t) + T_e(t)) \tag{C.5}$$

$$A' = \frac{1}{\tau_{th}}(R_{th} \cdot \dot{Q}_{appliance}(t) + T_e(t))e^{t/\tau_{th}} \tag{C.6}$$

$$A = (R_{th} \cdot \dot{Q}_{appliance}(t) + T_e(t))e^{t/\tau_{th}} + B \tag{C.7}$$

Consequently,

$$T_i(t) = ((R_{th} \cdot \dot{Q}_{appliance}(t) + T_e(t))e^{t/\tau_{th}} + B) \cdot e^{-t/\tau_{th}} \tag{C.8}$$

The coefficient B is determined by using the initial condition of temperature, that is

$$T_0 = T_i(t=0) = T_e(t=0) = \text{constant} \tag{C.9}$$

Then, T_i at t=0 is given by

$$T_i(t=0) = T_0 = (R_{th} \cdot \dot{Q}_{appliance}(0) + T_e(0)) + B \tag{C.10}$$

Therefore,

$$B = T_0 - (R_{th} \cdot \dot{Q}_{appliance}(0) + T_e(0)) \tag{C.11}$$

As a result, the analytical solution of eq.(C.1) is defined as follows:

$$T_i(t) = R_{th}\dot{Q}_{appliance}(t) + T_e(t) + (T_0 - T_e(0) - R_{th}\dot{Q}_{appliance}(0)) \cdot e^{-t/\tau_{th}} \tag{C.12}$$

The particular case of no heating regime is given by:

$$T_i(t) = T_e(t) + (T_0 - T_e(0)) \cdot e^{-t/\tau_{th}} \tag{C.13}$$

APPENDIX D

TYPICAL POWER CONSUMPTION OF VARIOUS HOME APPLIANCES

Place	Item	Power consumption [W]	Average time per day in use [h]
Bathroom	Curling iron	35	< 0.5
	Flat iron	350	< 0.5
	Hair dryer	1000	< 0.5
	Shaver (charging)	3	< 0.5
	Tooth brush (charging)	2	< 0.5
Bedroom	Alarm clock	5	< 0.5
	Electric blanket	200	< 2
Kitchen	Blender (conter-top)	700	< 0.5
	Blender (hand-held)	200	< 0.5
	Bread maker	700	< 0.5
	Coffee maker (12-14 cup)	1000	< 0.5
	Corn popper	1200	< 0.5
	Deep fryer	1500	< 0.5
	Dishwasher	1200	< 2
	Electric mixer	350	< 0.5

Place	Item	Power consumption [W]	Average time per day in use [h]
Kitchen	Freezer	500-800	24
	Garbage disposal	1000	< 2
	Kettle (1.2-1.8 litres)	1500	< 0.5
	Microwave	1400	< 1
	Oven	1800	< 1
	Refrigerator/Freezer	600	24
	Toaster (2 slice)	1000	< 0.5
	Toaster (4 slice)	1500	< 0.5
Laundry	Cloth dryer	2100	< 2
	Iron	1500	< 0.5
	Steamer	1500	< 0.5
	Washing machine (Top load 1997)	2200	<2
	Washing machine (Top load 2010)	945	< 2
	Washing machine (Energy star 2010)	380	< 2
Lighting	Compact Fluorescent light bulb	15-40	< 12
	Fluorescent tube lighting	15~75	< 12
	Halogen lighting	50-150	< 12
	Incandescent light bulb	60-150	< 12
Living room	Air purifier	5	< 12
	Audio component	100	< 5
	Blu-ray player	20	< 2
	Cell phone charger	3	< 2
	Computer	80	< 3
	Computer speaker	4	< 2
	Cordless phone	2	24
	Digital picture frame	10	< 0.5
	DVD player	10	< 2
	Humidifier	280	< 12
	Inkjet printer	8	< 0.2
	Laser printer	20	< 0.2

Place	Item	Power consumption [W]	Average time per day in use [h]
Living room	LCD TV (42 inch)	100	< 5
	LED TV (46 inch)	110	< 5
	Monitor	33	< 3
	Mp3 speakers	20	< 2
	Nintendo Wii	20	< 2
	Plasma TV (42 inch)	100	< 5
	Play station 3	200	< 2
	Projection TV (65 inch)	210	< 5
	PVR	900	< 1
	Satellite	80	< 5
	Scanner	40	<0.2
	Set-top box	24	24
	Sub-woofer	200	< 5
	Vacuum cleaner	1000	< 0.5
	Wi-fi router	7	24
	Xbox 360	180	< 2
	Cloth dryer	2100	< 1
	Iron	1500	< 0.5
	Steamer	1500	< 0.5

PUBLICATIONS

- International Journal

- **H.Park**, M.Ruellan, N.Martaj, R.Bennacer, E.Monmasson, "Generic Thermal Model of Electrical Appliances In Thermal building: Application to the Case of a Refrigerator", International Journal of Energy and Buildings(SCIE), Accepted.

- International Conference

- **H.Park**, M.Ruellan, N.Martaj, R.Bennacer, E.Monmasson, "Generic Thermal Model of Electric Appliances Integrated in Low Energy Building", in Proc. IEEE IECON 2012, Montréal, Canada, pp.3318-3323.
- **H.Park**, M.Ruellan, A.Bouvet, E.Monmasson, R.Bennacer, "Thermal Parameter Identification of Simplified Building Model with Electric Appliance", in Proc. IEEE EPQU 2011, Lisbon, Portugal, pp, 1-6, 2011

-Domestic Conference

- **H.Park**, M.Ruellan, A.Bouvet, H.Ben Hamid, B.Multon, R.Bennacer, "Modelisation methodology of temporal heat gain of domestic appliance in residential building (Original version : Méthodologie de modélisation des apports temporels de chaleur dus aux appareils électriques dans un bâtiment résidentiel)", IBPSA France, 11.2010. CD version.

REFERENCES

[1] European Commission, "Communication from the Commission to the European Council and the European Parliament-An Energy Policy for Europe", 2007.

[2] World Business Council for Sustainable Development, "Transforming the Market: Energy Efficiency in Buildings", 2009, pp.16.

[3]Trevor Houser, "Policy Brief August 2009, The economics of energy efficiency in buildings", Peterson Institute for International Economics, 2009, pp.2.

[4] International Energy Agency, "Energy Technology Perspectives 2010-Scenario&Strategies to 2050", OECD/IEA, 2010, pp.211.

[5] International Energy Agency, "Energy Efficiency Series-Summary of Country Reports Submitted to the Energy Efficiency Working Party", 2010.

[6] EU Energy Performance of Buildings Directive CA Energy performance of building, "Implementing the Energy Performance of Buildings Directive-Featuring Country Reports 2010", 2010.

[7] Official Journal of the European Union, "DIRECTIVE 2010/31/EU of the European Parliament and of the Council of 19 May 2010 on the energy performance of buildings", June 2010

[8] http://www.breeams.org

[9] http://www.leed.net

[10] http://www.ibec.or.jp/CASBEE/index.htm

[11] http:// www.passiv.de

[12] http://www.minergie.ch

[13] http://www.effinergie.org

[14] G.Krigsvoll, M.Fumo, R.Morbiducci, "National and International Standardization (International Organization for Standardization and European Committee for Standardization) Relevant for Sustainability in Construction", Sustainability, vol.2, February 2010, pp.3777-3791.

[15] CSTB, "Description and comparison of internatioal evaluation and/or certification of environmental quality (Original version : Déscription et comparaison des méthodes internationales d'évaluation et/ou de certification de la qualité environnementale) ", 2007.

[16] Low energy buildings in Europe: Current state of play, definitions and best practice", 2009.

[17] Ad-hoc Industrial Advisory Group, "Energy-Efficient Buildings PPP, Multi-Annual roadmap and longer term strategy 2011", European Commission, 2011.

[18] http://www.beodom.com/en/education/entries/using-thermal-inertia-for-better-comfort-and - heat-savings

[19] H. Park, M. Ruellan, A. Bouvet, B. Multon, H. BenAhmed, R. Bennacer, "Modelisation methodology of temporal heat gain of domestic appliance in residential building (Original version : Méthodologie de modélisation des apports temporels de chaleur dus aux appareils électriques dans un bâtiment résidentiel) ", IBPSA France conference, 11.2010. CD version.

[20] D.B. Crawley, L.K. Lawrie, "What next for building energy simulation-A glimpse of the future", IBPSA proceedings, 1997, (http://www.ibpsa.org/proceedings/BS1997/BS97_P092.pdf)

[21] U.S. Department of energy, Energy efficiency and renewable energy, (http://apps1. eere.energy.gov/buildings/tools_directory)

[22] E. Wurtz, "DYNASIMUL : Projet ANR-06-PBAT-004-01", Rapport scientifique final, 08.2010.

[23] B. Peuportier, "Benchmarking of thermal simulation tools (Original version: Bancs d'essai de logiciels de simulation thermique)", Proceedings of Journée Thématique SFT-IBPSA, 03.2005..

[24] B. Polly, N. Kruis, D. Roberts, Assessing and improving the accuracy of energy analysis for residential buildings, U.S. Department of energy, 07.2011 (http://www.nrel.gov/docs/fy11osti/50865.pdf).

[25] J. Neymark, R. Judkoff , U.S. International Energy Agency Building Energy Simulation Test and Diagnostic Method (IEA BESTEST), Technical Report NREL/TP-550-43827, National Renewable Energy Laboratory, 09.2008 (http://www.nrel.gov/docs/fy08osti /43827.pdf).

[26] Peter Loutzenhiser, Heinrich Manz, Gregory Maxwell, "Empirical Validations of Shading/Daylighting/Load Interactions in Building Energy Simulation Tools", A Report for the International Energy Agency's SHC Task 34/ ECBCS Annex 43 Project C, 08.2007(http://www.ecbcs.org/docs/Annex_43_Task34-Empirical_Validations.pdf).

[27] Robert H. Henninger, Michael J. Witte, EnergyPlus Testing with IEA BESTEST In-Depth Ground Coupled Heat Transfer Tests Related to Slab-on-Grade Construction, EnergyPlus Version 7.0.0.036, U.S. Department of Energy, 11. 2011(http://apps1.eere.energy.gov/ buildings/energyplus/pdfs/energyplus_slab-on-grade_tests.pdf).

[28] J. Neymark, R. Judkoff , International Energy Agency Building Energy Simulation Test and Diagnostic Method for Heating, Ventilating, and Air-Conditioning Equipment Models (HVAC BESTEST), Technical Report NREL/TP-550-30152, National Renewable Energy Laboratory, 01.2002 (http://www.nrel.gov/docs/fy02osti/30152.pdf).

[29]J. Neymark, R. Judkoff , International Energy Agency Building Energy Simulation Test and Diagnostic Method (IEA BESTEST), In-Depth Diagnostic Cases for Ground Coupled Heat Transfer Related to Slab-On-Grade Construction, Technical Report NREL/TP-550-43388, National Renewable Energy Laboratory, 09.2008 (http://www.nrel.gov/docs/fy08osti/43388.pdf)

[30] Bing Dong, Integrated building heating, cooling and ventilation control, Carnegie Mellon University, Ph.D. Thesis, 2010

[31] A. Bhatia, "Cooling Load Calculations and Principles", Course No. M06-004, CED engineering.com

[32] McDonald, A.T. Friskney, S.H. Ulrich, D.J., Thermal model of the dishwasher heater in air, IEEE Transactions on Industry Applications, Volume 25, Issue 6, November/December 1989, pp.1176-1180.

[33] H. Park, M. Ruellan, A. Bouvet, E. Monmasson, R. Bennacer, "Thermal parameter identification of simplified building model with electrical appliance", in Proc. IEEE EPQU, pp.1-6, 2011.

[34] International Energy Agency, "Worldwide Trends in Energy Use and Efficiency, Key Insights from IEA Indicator Analysis", OECD/IEA, 2008, pp.46-50.

[35] K.J. Kontoleon, M. C. A. Torres, "Modelling Building Envelopes in order to assess and improve their Thermal Performance", 2nd PALENC Conference, 09.2007, pp.565-569.

[36] J.L.M. Hensen, "Simulation for performance based building and systems design: some issues and solution directions", Proc. of 6th International Conference on Design and Decision Support Systems in Architecture and Urban Planning,2 002, pp.186-199.

[37] M.L. Gennusa et al., "A model for managing and evaluating solar radiation for indoor thermal comfort", Solar Energy, Vol.81(5), 2007, pp.594-606.

[38] J. Page et al. "A generalised stochastic model for the simulation of occupant presence", Energy and Buildings, Vol.40, 2008, pp.83–98.

[39] P. Tuomaalaa, K. Piiraa, M. Vuolleb, "A rational method for the distribution of nodes in modelling of transient heat conduction in plane slabs", Building and Environment, Vol.35(5), July 2000, pp.397–406

[40] F. Pierce, Energy Conservation Modeling, April 27th 2011, (presentation power point file) http://www.nrel.gov/applying_technologies/state_local_activities/pdfs/tap_webinar_20110427_ energy_conservation_modeling.pdf

[41] M.S. Al-Homoud, "Computer-aided building energy analysis techniques", Building and Environment, Vol. 36(4), May 2001, pp.421-433.

[42] S. Wang, Y. Chen, "Transient heat flow calculation for multilayer constructions using a frequency-domain regression method", Building and Environment, Vol.38, 2003, pp.45-61.

[43] D.G. Stephenson, "Periodic Heat Flow in Walls and Roofs", National Research Council of Canada, Division of Building Research, Report number of 131, 1957. (http://www.nrccnrc.gc.ca/obj/irc/doc/ pubs/ir/r132/r132.pdf)

[44] C.O. Mackey, L.T. Wright Jr., "Periodic heat flow – homogeneous walls or roofs", Trans. ASHVE, Vol.50, 1944, pp.293-312.

[45] C.O. Mackey, L.T. Wright Jr., "Periodic heat flow – composite walls or roofs", Trans. ASHVE, Vol.50, 1946, pp.283-296.

[46] A.H. Van Gorcum, "Theoretical considerations on the conduction of fluctuating heat flow", Applied Scientific Research, Vol.42, 1951, pp.272-280.

[47] G.P. Mitlas, D.G. Stephenson, "Cooling Load Calculations by Thermal Response Factor Method", Amarican Society of Heating, and Air-Conditioning Engineering, Vol.74, 1967.

[48] G.P. Mitlas, D.G. Stephenson, "Room Thermal Response Factors", Amarican Society of Heating, and Air-Conditioning Engineering, Vol.74, 1967.

[49] Lawrence Berkeley Laboratory, "DOE-2 Engineering Manual Version 2.1C", Lawrence Berkeley Laboratory, Berkeley, 1982.

[50] X.Xu, S.Wang, "A simplified dynamic model for existing buildings usting CTF and thermal network models", International Journal of Thermal Sciences, Vol.47, 2008, pp.1249-1262.

[51] I.R. Maestre, P. R. Cubillas, L. Pérez-Lombard, "Transient heat conduction in multi-layer walls: An efficient strategy for Laplace's method", Energy and Buildings, Vol.42(4), 2010, pp.541-546. (http://www.sciencedirect.com/science/article/pii/S0378778809002722)

[52] D.C. Hittle, "Calculating building heating and cooling loads using the frequency response of
multilayered slabs", Ph.D. Thesis, University of Illinois at Urbana-Champaign, 1979.

[53] Y. Jiang, "State-space method for the calculation of air-conditioning loads and the simulation of thermal behavior of the room," ASHRAE Transactions.Vol.88(2), 1982, pp.122-138.

[54] Y.M. Chen, S.W. Wang, "Transient Heat Flow Calculation for Multi-layer Constructions Using Frequency-Domain Regression Method", Building and Environment, Vol.38(1), 2003, pp.45-61.

[55] J. Wang, S. Wang, X. Xu, Y. Chen, "Short time step heat flow calculation of building constructions based on frequency-domain regression method", International Journal of Thermal Sciences, Vol.48(12), 2009, pp.2355-2364.

[56] X. Li, Y. Chen, J. D. Spitler, D. Fisher, "Relationship between Accuracy of Heat Conduction Calculation and Material Properties of Building Slabs", Proceedings of Building Simulation, 2007, pp. 140-147.(http://www.ibpsa.org/proceedings/BS2007/p045_final.pdf)

[57] C. Park, D.R. Clark, G.E. Kelly, "HVACSIM+ building systems and equipment simulation program: building loads calculation", NBSIR 86-3331, National Bureau of Standards, February 1986.

[58] S.A. Klein et al., "TRNSYS 16 –A TRaNsient SYstem Simulation program", Solar Energy Laboratory, University of Wisconsin-Madison, Madison, USA, User Manual, 2004.

[59] D.C. Hittle, "Building loads analysis and system thermodynamic (BLAST) programs. Version 2.0: Users Manual", Technical Report E-153, US Army Construction Engineering Research Laboratory (USACERL), Champaign, IL, 1979.

[60] D.B. Crawley, L. K. Lawrie, C. O. Pedersen, F. C. Winkelmann, "EnergyPlus: energy simulation program", ASHRAE Journal, Vol.42(4), 2000, pp.49-56. (http://apps1.eere.energy.gov/buildings/ energy-plus/pdfs/bibliography/ashrae_journal_0400.pdf)

[61] J.J. Roux, Proposition de modèle simplifiés pour l'étude du comportement thermique des bâtiment . INSA de Lyon, Thèse de Doctorat, 1984.

[62] M.J. Ren, J.A. Wright, "A ventilated slab thermal storage system model", Building and Environment, Vol.33(1), January 1998, pp. 43–52.

[63] M.M. Gouda, S. Danaher, C.P. Underwood, "Building thermal model reduction using nonlinear constrained optimization", Building and Environment, Vol.37(12), December 2002, pp.1255–1265.

[64] G. Fraisse, C. Viardot, O. Lafabrie, G. Achard, "Development of a simplified and accurate building model based on electrical analogy", Energy and Buildings, Vol.34(10), November 2002, pp.1017–1031.

[65] G. Parnis, "Building thermal modeling using electric circuit simulation", Master Thesis, University of New South Wales, 2012.

[66] C. Ghiaus, I. Hazyuk , "Calculation of optimal thermal load of intermittently heated buildings", Energy and Buildings, Vol.42(8), August 2010, pp.1248-1258.

[67] I. Hazyuk, C. Ghiaus, D. Penhouet , "Optimal temperature control of intermittently heated buildings using Model Predictive Control: Part I – Building modeling, Building and Environment", Vol.51, May 2012, pp.379-387.

[68] B.E. Psiloglou, H.D. Kambezidis, "Estimation of the ground albedo for the Athens area, Greece", Journal of Atmospheric and Solar-Terrestrial Physics, Vol.71, Issues 8–9, June 2009, pp.943-954.

[69] B.Y.H. Liu, R.C. Jordan, "The long term average performance of flat plate solar energy collectors", Solar Energy, Vol.7, 1963, pp. 53–74.

[70] M. García-Sanz, "A reduced model of central heating systems as a realistic scenario for analyzing control strategies", Applied Mathematical Modelling, Vol.21(9), September 1997, pp.535–545.

[71] P. Bacher, H. Madsen, "Identifying suitable models for the heat dynamics of buildings", Energy and Buildings, Vol.43(7), July 2011, pp. 1511–1522.

[72] D.Brunt, "Some physical aspects of the heat balance of the human body", The proceedings of the physical society, Vol.59, Part 5, September 1947, pp.713-726.

[73] G. Havenith, I. Holmér, K. Parsons, "Personal factors in thermal comfort assessment: clothing properties and metabolic heat production", Energy and Buildings, Vol.34, 2002, pp.581-591.

[74] ISO 8996, "Ergonomics of the thermal environments-determination of metabolic heat production", ISO, Geneva, 1989.

[75] ISO 7730, "Ergonomics of the thermal environment — Analytical determination and interpretation of thermal comfort using calculation of the PMV and PPD indices and local thermal comfort criteria", third edition, ISO, Geneva, 2005.

[76] S. Seo, W.K. Choi, "TRNSYS16 and multi-zone building", Iljinsa, 2009, pp.180.

[77] F. Thellier, F. Monchoux, M. Bonnis-Sassi, B. Lartigue, "Modeling additional solar constraints on a human being inside a room", Solar Energy, Vol.82, 2008, pp.290-301.

[78] A. Husaunndee et al., "SIMBAD: A simulation toolbox for the design and test of HVAC control systems", Proceedings of the 5th international IBPSA conference, Prague, Czech Republic, pp.269-276.

[79] Roberto Z. Freire, Gustavo H.C. Oliveira, Nathan Mendes, "Development of regression equations for predicting energy and hygrothermal performance of buildings", Energy and Buildings, Vol.40, 2008, pp. 810-820.

[80] Energy System Research Unit, "The ESP-r System for Building Energy Simulation", University of Strathclyde, Glasgow, UK, Version 10 Series, 2002.

[81] D.B. Crawley et al., "Energyplus: new cabable and linked", in Proc. of the SimBuild 2004 Conference IBPSA-USA, Boulder, Colorado, USA, 2004.

[82] N. Mendes, R.C.L.F. Oliveira, G.H. Santos, "A whole-building hygrothermal simulation program", in Proc. of the Eighth Building Simulation Conference (IBPSA'03), Eindhoven, Netherlands, Vol.1, 2003, pp. 863–870.

[83] J. Kosny, A.M. Syed, "Interactive Internet-Based Building Envelope Materials Database for Whole-Building Energy Simulation Programs", ASHRAE Thermal IX Conference Clearwater Beach, FL December, 2004.

[84] S.M. Bambrook, A.B. Sproul, D. Jacob, "Design optimization for a low energy home in Sydney", Energy and Buildings, Vol.43, 2011, pp.1702-1711.

[85] G. Zemella, D. de March, M. Borrotti, I. Poli, "Optimised design of energy efficient building façades via evolutionary neural networks", Energy and Buildings, Vol.43, 2011, pp.3297-3302.

[86] B. Givoni, "Effectiveness of mass and night ventilation in lowering the indoor daytime temperatures. Part I: 1993 experimental periods", Energy and Buildings, Vol.28(1), 08.1998, pp.25-32.

[87] E. Krüger, B. Givoni, "Predicting thermal performance in occupied dwellings", Energy and Buildings, Vol.36(3), 03.2004, pp.301-307.

[88] X. Fang, T. Yang, "Regression methodology for sensitivity analysis of solar heating walls", Applied Thermal Engineering, Vol.28, 2008, pp.2289-2294.

[89] T. Catalina, J. Virgone, E. Blanco, "Development and validation of regression models to predict monthly heating demand for residential buildings", Energy and Buildings, Vol.40, 2008, pp.1825-1832.

[90] H. U. Frausto, J. G. Pieters, J.M. Deltour, "Modelling Greenhouse Temperature by means of Auto Regressive Models", Biosystems Engineering, Vol.84(2), 02.2003, pp.147-157.

[91]G.J. Ríos-Moreno, R. Castañeda-Miranda, V.M. Hernández-Guzmán, G. Herrera-Ruiz, "Modelling temperature in intelligent buildings by means of autoregressive models", Automation in construction, Vol.16(5), 2007, pp.713-722.

[92] G. Mustafaraj, J. Chen, G. Lowry, "Development of room temperature and relative humidity linear parametric models for an open office using BMS data", Energy and Buildings, Vol.42, 2010, pp.348-356.

[93] A. Mechaqrane, M. Zouak, "A comparison of linear and neural network ARX models applied to a prediction of the indoor temperature of a building", Neural Computing & Applications, Vol.13(1), 2004, pp.32-37.

[94] S. L. Patil, H. J., Tantau, V. M., Salokhe, "Modelling of tropical greenhouse temperature by auto regressive and neural network models", Biosystems Engineering, Vol.99, 2008, pp.423-431.

[95] T. Lu, M. Viljanen, "Prediction of indoor temperature and relative humidity using neural network models: model comparison", Neural Computing & Applications, Vol.18(4), 03.2009, pp.345-357.

[96] H. Madsen, J. Holst, "Estimation of continuous-time models for the heat dynamic of a building", Energy and Buildings, Vol.22, 1995, pp.67-79.

[97] M. Cucumo, A. De Rosa, V. Ferraro, D. Kaliakatsos, V. Marinelli, "A method for the experimental evaluation in situ of the wall conductance", Energy and Buildings, Vol.38, No.3, 2006, pp.238-244.

[98] C. Penga, Z. Wu, "In situ measuring and evaluating the thermal resistance of building construction", Energy and Buildings, Vol.40, No.11, 2008, pp.2076-2082.

[99] S.E.G. Jayamaha, N. E. Wijeysundera, S. K. Chou, "Measurement of the heat transfer coefficient for walls", Building and Environment, Vol.31, No.5, 1996, pp.399-407.

[100] C. Luo, B. Moghtaderi, S. Hands, A. Page, Determining the thermal capacitance, conductivity and the convective heat transfer coefficient of a brick wall by annually monitored temperatures and total heat fluxes, Energy and Buildings, Vol.43, No.2-3, 2011, pp.379-385.

[101] S. Wang, X. Xu, "Simplified building model for transient thermal performance estimation using GA-based parameter identification", International Journal of Thermal Sciences, Vol.45, 2006, pp.419-432.

[102] Y. Zhang, V.I. Hanby, "Model-Based Control of Renewable Energy Systems in Buildings", HVAC&R Research, Vol.12(3a), 07.2006, pp.739-760.

[103] J.A. Crabb, N.Murdoch, J.M.Penman, "A simplified thermal response model", Building Services Engineering Research and Technology, Vol.8(1), 02.1987, pp. 13-19.

[104] T.F. Coleman, L. Yuying, "On the convergence of interior-reflective Newton methods for nonlinear minimization subject to bounds", Mathematical Programming, Vol.67, 1994, pp.189-224.

[105] G. Platt, J. Li, R. Li, G. Poulton, G. James, J. Wall, "Adaptive HVAC zone modeling for sustainable buildings", Energy and Buildings, Vol.42(4), 04.2010, pp.412-421.

[106] M. J. Jiménez, H. Madsen, "Models for describing the thermal characteristics of building components", Building and Environment, Vol.41, 2008, pp.152-12.

[107] M. J. Jiménez, H. Madsen, K.K. Andersen, "Identification of the main thermal characteristics of building components using MATLAB", Building and Environment, Vol.43, 2008, pp.170-180.

[108] S. Wu, J.Q. Sun, "A physics-based linear parametric model of room temperature in office buildings", Buildings and Environment, Vol.50, 2012, pp.1-9.

[109] J.A. Clarke, "Energy Simulation in Building Design", 2nd Edition Butterwiorth-Heinemann, Oxford, 2001.

[110] T. Hong, S.K.Chou, T.Y. Bong, "Building simulation: an overview of developments and information sources", Building and Environment, Vol.35, 2000, pp.347-361.

[111] D.B. Crawley et al. "Contrasting the capabilities of building energy performance simulation programs", Building and Environment, Vol.43(4), 2008, pp.661-673.

[112] M.D. Doyle, "Investigation of Dynamic and Steady State Calculation Methodologies for Determination of Building Energy Performance", Ms. Thesis, Dublin Institute of Technology, 07.2008.

in the context of the EPBD

[113] EnergyPlus Energy Simulation Software (http://apps1.eere.energy.gov/buildings)

[114] D.B. Crawley et al., "EnergyPlus: creating a new-generation building energy simulation program", Energy and Buildings, Vol.33(4), 04.2001, pp.319-331.

[115] H.Vaezi-Nejad et al., "Real time simulation of a building with electrical heating system or fan coil air conditioning system", CLIMA 2000, BRUXELLES, pp.1-13.

[116] C.A, Roulet "prEN-ISO 13790 – A Simplified Method to Assess the Annual Heating Energy Use in Buildings", ASHRAE Transactions, Vol.108, pp911-918, 2002.

[117] CEN, "EN ISO 13790, Thermal performance of buildings - Calculation of energy use for space heating", Geneva, 2004.

[118] F Karlsson, P. Rohdin, M.L. Persson, "Measured and predicted energy demands of a low energy building, Building Services Engineering Research and Technology, Vol.38(3), 2007, pp 223-235.

[119] S.M.A. Bekkouche et al., "Introduction to control of solar gain and internal temperatures by thermal insulation, proper orientation and eaves", Energy and Buildings, Vol.43(9), 09.2011, pp.2414-2421.

[120] B. Abushakra et al., "Compilation of diversity factors and schedules for energy and cooling load calculations", Report RP-1093, American Society of Heating, Refrigerating and Air-Conditioning Engineers, 2001.

[121] D. Wang, C.C. Federspiel, F. Rubinstein, "Modeling occupancy in single person offices", Energy and Buildings, Vol.37, 2005, pp.121–126.

[122] I. Richardson et al., Domestic lighting: A high-resolution energy demand model, Energy and Buildings, Vol.41, 2009, pp.781–789.

[123] J. Dieckmann, "Improving humidity control with Energy Recovery Ventilation", ASHRAE Journal, 08.2008, pp.38-45.

[124] Caleb Management Services, "Based on Assessment of Potential for the Saving of Carbon Dioxide Emissions in European Building Stock", EuroACE, 05.1998, pp. 1-18.

[125] Passive House Institute Darmstadt, "Active for more comfort: The Passive House", International Passive House Association, 2010, pp.1-39.

[126] G.G.J. Achterbosch, P.P.G. de Jong, C.E. Krist-Spit, S.F. van der Meulen, J. Verberne, "The development of a convenient thermal dynamic building model", Energy and Buildings, vol. 8, 1985, pp. 183-196.

[127] G. Hudson, C.P. Underwood, "A simple building modeling procedure for Matlab/ Simulink", Proceedings of Building Simulation, International IBPSA conference, 1999, pp.777-783.

[128] N. Mendes, G. H. C. Oliveira, H. X. de Araujo, "Building thermal performance analysis by using Matlab/Simulink", Proceedings of Building Simulation, International IBPSA conference, 2001, pp. 473-480.

[129] http://www.ce.utexas.edu/bmeb/energybalance.cfm

[130] N. Morel, E. Gnansounou, "Energétique du bâtiment", Ecole Polytechniaue Fédérale de Lausanne, Lecture note, 09.2008, pp.84.

[131] F. Hall, "Building Services and Equipment", Pearson Education, 3rd edition, Vol.1, Ch.4, 2012.

[132] M.H. Sherman, D.T. Grimsrud, "Measurement of infiltration using fan pressurization and weather data", First Symposium of the air infiltration centre on instrumentation and measurement techniques", Windsor, England, 1980.

[133] P. Lubina, M.B. Nantka, "Internal heat gains in relation to the dynamics of buildings heat requirements", Journal of Architecture Civil engineering Environment, The Silesian University of Technology, vol.2(1), 2009, pp. 137-142.

[134] T. Blight, D.A. Coley, "Modeling occupant behaviors in passivhaus buildings: Bridging the energy gap", CIBSE Technical Symposium, DeMonfort University, Leicester, UK, 09.2011, pp.1-13.

[135] S. Leth-Petersen, M. Togeby, "Demand for space heating in apartment blocks: measuring effect of policy measures aiming at reducing energy consumption", Energy Economics, vol.23, 2001, pp.387-403.

[136] H. Jeeninga, M. Uyterlinde, J. Uitzinger, "Energy Use of Energy Efficient Residences", Report, ECN and IVAM, Pelten, 2001.

[137] M. Beerepoot, N. Beerepoot., "Government regulations as an impetus for innovations-Evidence for energy performance regulation in the dutch residential building sector", Energy Policy, vol.35, 2007, pp.4812-4825.

[138] G. Wood, M. Newborough, "Dynamic energy-consumption indicators for domestic appliances: environment, behaviour and design", Energy and Buildings, vol.35(8), 2003, pp. 821-841.

[139] G. Branco, B. Lachal, P. Gallinelli, W. Weber, "Predicted versus observed heat consumption of a low energy multifamily complex in Switzerland based on long term experimental data", Energy and Buildings, vol.36, 2004, pp. 543–555.

[140] R.V. Andersen, J. Toftum, K. K. Andersen, B.W. Olessen, "Survey of occupant behaviour and control of indoor environment in Danish dwellings", Energy and Buildings, vol.41, 2009, pp. 1–16.

[141] Z.M. Gill, M.J. Tierney, I.M. Pegg, N. Allan, "Measured energy and water performance of an aspiring low energy/carbon affordable housing site in the UK", Energy and Buildings, vol.43(1), 2011, pp. 117-125.

[142] J. Ferdyn-Grygierek, A. Baranowski, "Energy demand in the office buildings for various internal heat gains", Architecture Civil engineering Environment, The Silesian University of Technology, vol.4(2), 2011, pp.89-93.

[143] P. Perrot, "A to Z of Thermodynamics", Oxford University Press. ISBN 0-19-856552-6, 1998.

[144] P. P. J. van den Bosch, A. C. van der Klauw, "Modeling, Identification and Simulation of Dynamical Systems", CRC Press, 1994, Ch. 2, 4.

[145] J.K.van Thiel, "An optimal Kalman filter derived without prior noise and parameter knowledge", Eindhoven University of Technology, WFW Report, 1994.

[146] National Instruments, "Selecting a Model Structure in the System Identification Process", Tutorial, 06.2010.

[147] T.M. Laleg, M.Sorine, Q.Zhqng, "Input Impedance of the Arterial System Using Parametric Models", ICES, 05.2006, Algérie.

[148] E.Ali, "Identification of a liquid phase chemical reactor", King Saud University, Final Research Report No.42/425, 2004.

[149] T.A. Johansen, B.A. Foss, "Operating regime based process modeling and identification", Computers Chemical Engineering,Vol.21(2), 1997, pp. 159-176.

[150] N.R. Kristensen, H. Madsen, S.B. Jørgensen, "A method for systematic improvement of stochastic grey-box models", Computers Chemical Engineering,Vol.28, 2004, pp.1431-1449.

[151] http://www.dep.mines-paristech.fr/Recherche/Centres/CES/ETB/

[152] A. Guiavarch et al., "Intégration d'un modèle simplifié de matériau à changement de phase dans une plate-forme d'aide à la conception énergétique de bâtiments", IBPSA France 2008, Lyon, France, 6-7 novembre 2008, paper 28, (http://ibpsa.fr/jdownloads/Conferences_et _Congres/ IBPSA_ France/2008_ conferenceIBPSA/ guiavarch_alain-bs08-_intgration_dun _modle_simplifi_de_ma.pdf).

[153] I. Hazyuk, "Dynamical optimisation of renewable energy flux in buildings", Ph.D. Thesis, INSA de Lyon and Universitatea Tehnică din Cluj-Napoca , 2011.

[154] P. Gevorkian, "Solar Power in Building Design-The engineer's complete design resource", Mc Graw Hill, Ch.4, 2008.

[155] Korea Electrotechnology Researching Institute (www.keri.re.kr)